

1972

# Carrier generation using pulse width modulation

Frederick Herbert Raab  
*Iowa State University*

Follow this and additional works at: <https://lib.dr.iastate.edu/rtd>

 Part of the [Electrical and Electronics Commons](#)

## Recommended Citation

Raab, Frederick Herbert, "Carrier generation using pulse width modulation " (1972). *Retrospective Theses and Dissertations*. 5226.  
<https://lib.dr.iastate.edu/rtd/5226>

This Dissertation is brought to you for free and open access by the Iowa State University Capstones, Theses and Dissertations at Iowa State University Digital Repository. It has been accepted for inclusion in Retrospective Theses and Dissertations by an authorized administrator of Iowa State University Digital Repository. For more information, please contact [digirep@iastate.edu](mailto:digirep@iastate.edu).

## INFORMATION TO USERS

This dissertation was produced from a microfilm copy of the original document. While the most advanced technological means to photograph and reproduce this document have been used, the quality is heavily dependent upon the quality of the original submitted.

The following explanation of techniques is provided to help you understand markings or patterns which may appear on this reproduction.

1. The sign or "target" for pages apparently lacking from the document photographed is "Missing Page(s)". If it was possible to obtain the missing page(s) or section, they are spliced into the film along with adjacent pages. This may have necessitated cutting thru an image and duplicating adjacent pages to insure you complete continuity.
2. When an image on the film is obliterated with a large round black mark, it is an indication that the photographer suspected that the copy may have moved during exposure and thus cause a blurred image. You will find a good image of the page in the adjacent frame.
3. When a map, drawing or chart, etc., was part of the material being photographed the photographer followed a definite method in "sectioning" the material. It is customary to begin photoing at the upper left hand corner of a large sheet and to continue photoing from left to right in equal sections with a small overlap. If necessary, sectioning is continued again — beginning below the first row and continuing on until complete.
4. The majority of users indicate that the textual content is of greatest value, however, a somewhat higher quality reproduction could be made from "photographs" if essential to the understanding of the dissertation. Silver prints of "photographs" may be ordered at additional charge by writing the Order Department, giving the catalog number, title, author and specific pages you wish reproduced.

### **University Microfilms**

300 North Zeeb Road  
Ann Arbor, Michigan 48106

A Xerox Education Company

72-20,000

RAAB, Frederick Herbert, 1946-  
CARRIER GENERATION USING PULSE WIDTH MODULATION.

Iowa State University, Ph.D., 1972  
Engineering, electrical

University Microfilms, A XEROX Company , Ann Arbor, Michigan

Carrier generation using  
pulse width modulation

by

Frederick Herbert Raab

A Dissertation Submitted to the  
Graduate Faculty in Partial Fulfillment of  
The Requirements of the Degree of  
DOCTOR OF PHILOSOPHY

Major Subject: Electrical Engineering

Approved:

Signature was redacted for privacy.

In Charge of Major Work

Signature was redacted for privacy.

For the Major Department

Signature was redacted for privacy.

For the Graduate College

Iowa State University  
Ames, Iowa

1972

PLEASE NOTE:

Some pages may have

indistinct print.

Filmed as received.

University Microfilms, A Xerox Education Company

## TABLE OF CONTENTS

	Page
I. INTRODUCTION	1
II. TYPES AND EFFICIENCIES OF AMPLIFIERS	8
A. Conventional Amplifiers	8
B. Switching Amplifiers	17
III. BASIC IMPLEMENTATION	34
IV. BASIC SPECTRAL ANALYSIS	46
V. BASIC SPECTRUM OF A CLASS D RF AMPLIFIER	54
A. Bipolar PWM	55
B. Monopolar PWM	67
C. Saturation Voltage	73
VI. PULSE TIMING DISTORTION	80
A. Pulse Bias Distortion	81
B. Rise/Fall Time Distortion	89
C. Approximations Used	97
D. Combination of Effects	98
VII. SPURIOUS PRODUCTS WITH SINUSOIDAL MODULATION	100
A. Voltage Error Products	103
B. Timing Error Products	109
VIII. SPURIOUS PRODUCTS FOR GENERAL CASE	116
IX. DISTORTION REDUCTION BY USE OF FEEDBACK	130
X. COMMENTS AND CONCLUSIONS	144
XI. REFERENCES	147
A. Additional References	149

	Page
XII. ACKNOWLEDGEMENT	149
XIII. APPENDIX I: OTHER AMPLIFIERS	151
A. Class B	151
B. Conventional Pulse Width Modulation	159
C. Other Amplifiers	173
XIV. APPENDIX II: PROTOTYPE	175
XV. APPENDIX III: SIMULATION	186
XVI. APPENDIX IV: COMMONLY-USED SYMBOLS	211

## LIST OF ILLUSTRATIONS

		Page
Figure 1.1	Light Dimmer	2
Figure 1.2	Types of Pulse Width Modulation	4
Figure 2.1	Class A Amplifier	9
Figure 2.2	Class B Amplifier	12
Figure 2.3	Class C Amplifier	14
Figure 2.4	Class CD Amplifier	14
Figure 2.5	Efficiencies of Class A, B, and C Amplifiers	16
Figure 2.6	Switching Amplifier	18
Figure 2.7	Class AD Amplifier	20
Figure 2.8	Rise/Fall Times in a Class AD Amplifier	22
Figure 2.9	Saturation Voltages in a Class AD Amplifier	24
Figure 2.10	Efficiency of Class AD and BD Amplifier	25
Figure 2.11	Class BD Amplifier	27
Figure 2.12	Class D RF Amplifier	28
Figure 2.13	Efficiency of a Class D RF Amplifier	32
Figure 3.1	Comparator Pulse Generation for Class AD	35
Figure 3.2	Relationships Between Modulating Signal and Pulse Width	35
Figure 3.3	Waveforms in Class D AM System	36
Figure 3.4	Class D AM Transmitter	38
Figure 3.5	Generation of AM and DSB/SC	39
Figure 3.6	Class D SSB Techniques	41
Figure 3.7	SSB Generation	42
Figure 3.8	Class D SSB Generation Using Kahn's Method	43



	Page	
Figure 4.1	Monopolar Pulse $f_+(\theta)$	49
Figure 4.2	Decomposition of Bipolar Pulse	50
Figure 4.3	Ramp Waveform	52
Figure 4.4	Triangular Wave $\Lambda(\theta)$	53
Figure 5.1	Modulating Function for DSB/SC	58
Figure 5.2	Spectrum of a Class D RF Amplifier	61
Figure 5.3	Spectrum of a Class D RF Amplifier	62
Figure 5.4	Locus of $E(\theta)$ and $\varphi(\theta)$	67
Figure 5.5	Spectrum of a Class D RF Amplifier	68
Figure 5.6	Spectrum of a Class D RF Amplifier	69
Figure 5.7	Waveform with Voltage Error	71
Figure 5.8	Modulation of Even Harmonics for DSB/SC	72
Figure 5.9	Spectrum of a Class D RF Amplifier	74
Figure 5.10	Spectrum of a Class D RF Amplifier	75
Figure 5.11	Saturation Voltage Effects	76
Figure 5.12	Saturation Effect Approximations	77
Figure 5.13	Spurious Products due to non-zero Saturation Voltage	78
Figure 5.14	Circuit Changes to Reduce Saturation Voltage Spurious Products	78
Figure 6.1	Cause of Pulse Bias	81
Figure 6.2	Bias Distortion Waveform	82
Figure 6.3	Modulation Functions for Timing Distortion	86
Figure 6.4	Types of Spurious Products due to Pulse Bias Distortion	88
Figure 6.5	Spectrum of a Class D RF Amplifier	90

	Page
Figure 6.6	Spectrum of a Class D RF Amplifier 91
Figure 6.7	Rise/Fall Time Distortion Waveform 92
Figure 6.8	Spectrum of a Class D RF Amplifier 95
Figure 6.9	Spectrum of a Class D RF Amplifier 96
Figure 6.10	Distortion Curves 98
Figure 6.11	Pulse Deterioration 99
Figure 7.1	Waveforms Used to Find Upper Limits on Spurious Products 102
Figure 7.2	Spurious Products at a Given Frequency 106
Figure 7.3	Maximum Spurious Products for Monopolar DSB/SC 108
Figure 7.4	Maximum Spurious Products for Bipolar DSB/SC with Various Timing Errors 112
Figure 7.5	Maximum Spurious Products for Bipolar AM-Like Signal with Various Timing Errors 114
Figure 8.1	Variation of Spurious Products with Depth of Modulation 120
Figure 8.2	Spectrum of a Class D RF Amplifier 121
Figure 8.3	Spectrum of a Class D RF Amplifier 122
Figure 8.4	Spectrum of a Class D RF Amplifier 123
Figure 8.5	Spectrum of a Class D RF Amplifier 124
Figure 8.6	Spectrum of a Class D RF Amplifier 127
Figure 8.7	Spectrum of a Class D RF Amplifier 128
Figure 9.1	Feedback System 131
Figure 9.2	Feedback System with $\sigma/2\pi = 0$ 138
Figure 9.3	Feedback System with $\sigma/2\pi = 0.001$ 139
Figure 9.4	Feedback System with $\sigma/2\pi = 0.01$ 140

	Page
Figure 9.5	Feedback System with $\sigma/2\pi = 0.1$ 141
Figure 9.6	Envelope and Phase Feedback System 143
Figure 13.1	Transfer Characteristic for Class B Amplifier 152
Figure 13.2	Waveform in a Class B Amplifier 153
Figure 13.3	Spectrum of a Class B Amplifier 154
Figure 13.4	Spectrum of a Class B Amplifier 156
Figure 13.5	Spectrum of a Class B Amplifier 157
Figure 13.6	Spectrum of a Class B Amplifier 158
Figure 13.7	Spectrum of Conventional PWM 161
Figure 13.8	Spectrum of a Class AD Amplifier 163
Figure 13.9	Spectrum of a Class AD Amplifier 164
Figure 13.10	Spectrum of a Class AD Amplifier 165
Figure 13.11	Spectrum of a Class BD Amplifier 166
Figure 13.12	Spectrum of a Class AD Amplifier 167
Figure 13.13	Spectrum of a Class AD Amplifier 170
Figure 13.14	Pulse Bias in Class BD Amplifier 171
Figure 13.15	Spectrum of a Class AD Amplifier 172
Figure 14.1	Power Supply 177
Figure 14.2	Audio Amplifier and RF Oscillator 178
Figure 14.3	Reference Generator and Detector 179
Figure 14.4	Clipper and Comparator 180
Figure 14.5	Logic 181
Figure 14.6	Power Amplifier 182
Figure 14.7	Pulse Train and Output Waveform 184

	Page
Figure 14.8 Envelope	184
Figure 14.9 Spectrum of Bipolar PWM	185
Figure 14.10 Spectrum of Monopolar PWM	185.
Figure 15.1 Arrays Used in Simulation	188
Figure 15.2 Exponential Mode	189
Figure 15.3 Methods of Iteration	191
Figure 15.4 Computer Errors in Square-Wave Spectrum	192

## I. INTRODUCTION

Since the demise of the spark-gap and the advent of the vacuum tube, RF amplifiers have been plagued by inefficiency. Recently, pulse width modulation (also called class D, class S, switched-mode, pulse duration modulation, PWM, or PDM) has offered a means of making an efficient audio amplifier by extracting the DC component and its modulation from a train of pulses of varying width. By extracting the fundamental component of a pulse train, this technique can be extended to make efficient RF amplifiers.

In conventional class A, B, and C amplifiers, a non-zero voltage and non-zero current are present simultaneously on the output device, causing it to dissipate power, resulting in inefficiency. In a class D amplifier, however, the current is zero whenever the voltage is non-zero, and the voltage is zero whenever the current is non-zero. Thus no power is dissipated (ideally) in the device, and it is (ideally) completely efficient.

To visualize this, consider two types of light dimmer circuits (Figure 1.1). The first type (class A) uses a series resistor to reduce the power in the light. However, the resistor has both non-zero voltage and non-zero current, so it consumes power, and the efficiency of the dimmer is low. The second type (class D) uses a switch in series with the light. When the switch is open, no current flows, and no

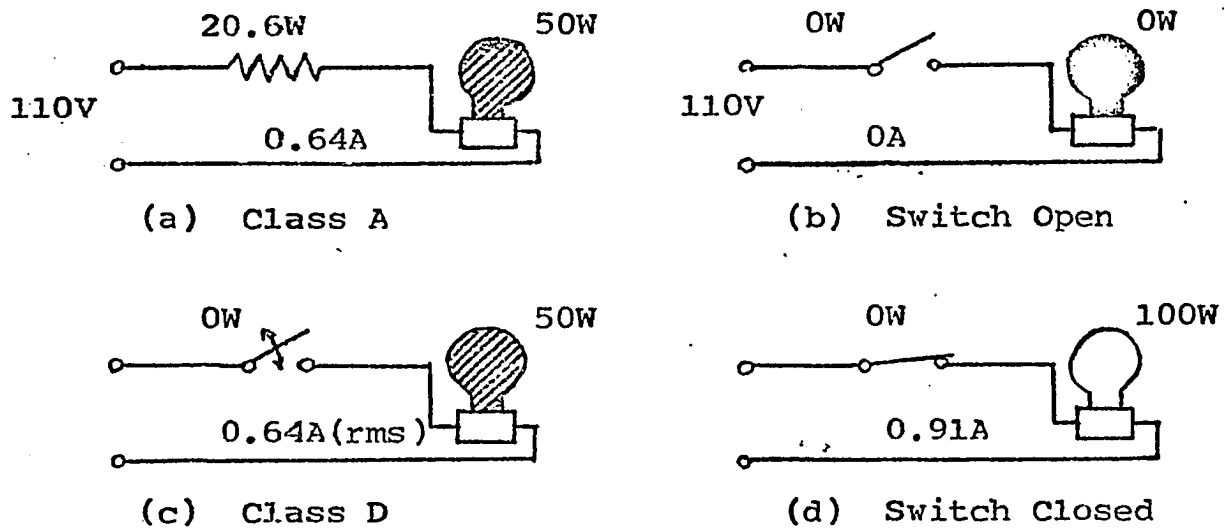


Figure 1.1. Light Dimmer.

power is dissipated in either the light or the switch. When the switch is closed, the light glows at full power, but there is no voltage across the switch, hence it dissipates no power. If the switch position is changed so that it is closed a certain fraction of the time, any average brightness less than the full brightness can be obtained. The switch, however, does not dissipate power, hence the dimmer is completely efficient. If switching is fast enough, the residual heat of the light's filament will make the switching effect unnoticeable.

Class D amplification of audio signals works in essentially the same way as does the light dimmer just described. The switching rate is several times higher than the highest audio frequency to be amplified. The switching frequency and higher harmonics are removed by the low pass action of the

loudspeaker and/or an additional low pass filter between the switch and the load. Several references on audio type PWM are given in Chapter XI.

The audio technique can be applied to the generation of a radio frequency signal. Experimental prototypes operating at 2MHz have been built by Brian Attwood of Mullard (1). However, the conventional PWM technique has two disadvantages when used for generation of radio-frequency signals. First, the switching frequency must be several times the carrier frequency, which can make it very high for most RF signals. Secondly, spurious products generated by inherent modulation of the switching frequency and its harmonics occur throughout the RF spectrum, including frequencies near the desired signal.

By switching at the carrier frequency and extracting the fundamental component, the switching rate can be reduced (Figure 1.2). In actual amplifiers, pulse rise times are not instantaneous, and some power is dissipated with every transition. Thus the lower the switching rate, the higher the efficiency. Amplifiers based on this principle have been built by Rose (2); Page, Hindson, and Chudobiak (3); and Osborne (4). However, these amplifiers produce a carrier of constant amplitude, and modulation is introduced only by varying the collector voltage by external modulator. This type of Class D amplification is also under investigation as a means of reducing intermodulation distortion arising from two transmitters using the same antenna (5).

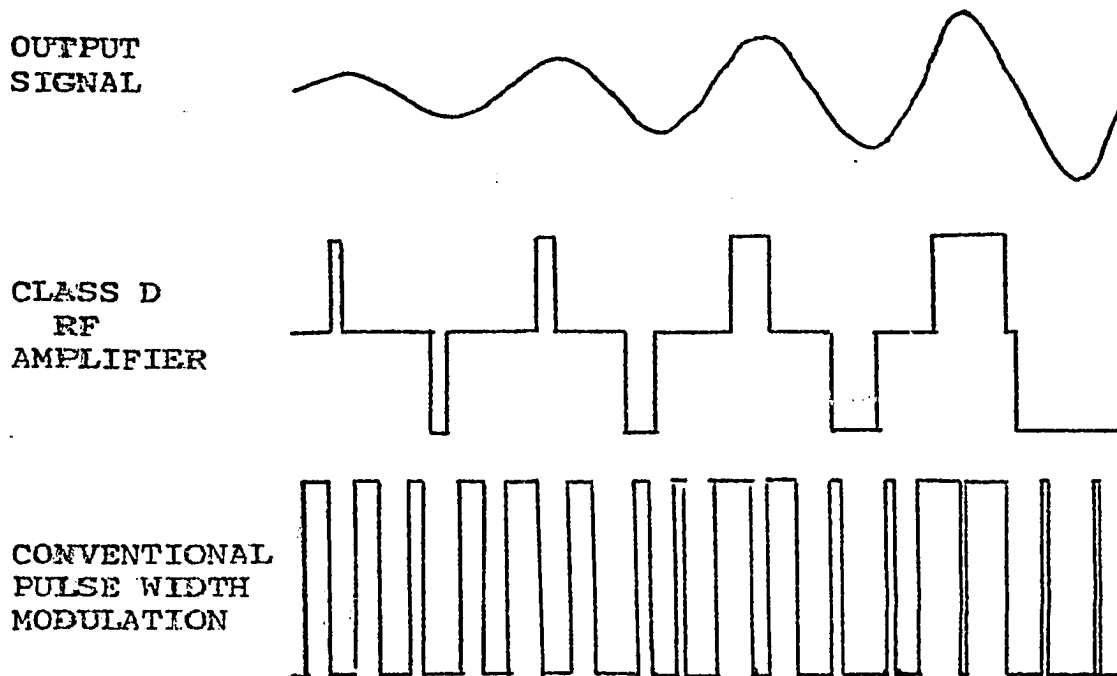


Figure 1.2. Types of Pulse Width Modulation.

If the widths of the pulses in such an amplifier are varied, the magnitude of the fundamental component (carrier) is also varied. Since the magnitude of the fundamental component varies as the sine of the pulse width, it is necessary to predistort the pulse width according to the inverse sine ( $\arcsin$ ) of the modulating signal. An amplifier based on this principle was apparently first invented by Phillip Besslich (6).

In addition to the advantages of a slower switching rate, spurious products inherent in this type of amplifier are limited (ideally) to finite bands around the odd harmon-



ics of the carrier frequency. Thus the spurious products are far removed from the carrier frequency, and are easily removed by a simple tuned circuit.

The terminology used to describe this amplifier is somewhat confusing. The first question is whether it should be called an amplifier or a modulator. When generating an amplitude modulated signal, the actual modulated carrier need not appear until after the output filter, in which case the circuit is a modulator. However, when generating single sideband signals, it appears easier to produce a low level SSB signal, detect the envelope and phase, and vary the pulse width and position accordingly; in this case, the circuit is an amplifier. Thus it appears that it can be either, depending on use. Because of the connotation of amplifier as a device to produce the signal output, rather than to impress information upon a signal, it will be called an amplifier in this dissertation. There is also a temptation to call it class E, to distinguish it from the version of a switching amplifier used to generate audio signals. Unfortunately, the term class D has already been applied to the constant carrier circuits.

There are two major advantages to the use of PWM. The first is the increase in output power, and the associated decrease in input power and dissipated power. The use of the increased output power is obvious. Probably more significant is the decrease in power dissipated by the amplifying device;

the heat sink problem is greatly reduced, and much smaller transistors can be used. For example, consider a 100 Watt class B transmitter. A typical efficiency might be 50%, in which case 50 Watts would be dissipated in the final amplifying transistors. If class D were used, a typical efficiency might be 90%, in which case only 10 Watts would be dissipated.

The second advantage is that of stability. Linear transistors need to be compensated for changes of gain with temperature. In the case of the 75 Watt linear RF transistor (2N6093), a typical circuit to regulate the Q-point (7), (8) involves four additional transistors and the circuitry associated with them. Pulse amplifiers need only be biased off well enough to stay off at the highest temperature, and driven hard enough to saturate at the lowest temperature.

The disadvantage of PWM is, of course, that transistors with higher cut-off frequencies are required. However, because much smaller power levels are required, the disadvantage may be offset. It is doubtful that class D will have much application to vacuum tube amplifiers, since the power consumed in the filament of a vacuum tube makes it an inherently inefficient device. Class D may be the most feasible way to extend solid state circuits to high power and high frequency operation.

An actual PWM amplifier will not have perfect timing of the pulse transitions, nor will the rise and fall times be

instantaneous; both of these cause an intermodulation distortion effect. Differences in the positive and negative supply voltages can introduce even harmonics of the carrier, and infinite bandwidth spurious products associated with them. Non-zero saturation voltages also contribute unwanted signals. However, a feedback system can be used to eliminate some of the distortion.

The usefulness of this type of amplifier will depend on knowledge of both its potential and limitations. The determination of some of the capabilities and limitations, and comparison with those of other RF amplifiers is then the purpose of this dissertation.

## II. TYPES AND EFFICIENCIES OF AMPLIFIERS

Before analyzing the operation and efficiency of a class D amplifier, it will be useful to review some of the characteristics of conventional class A, B, and C amplifiers.

There are many forms that each of these amplifiers can take. In particular, there generally exist both voltage and current switching (controlling) forms of each amplifier, as well as a variety of output coupling networks. Amplifiers may employ vacuum tubes, transistors, or any other appropriate devices. For convenience, transistors will usually be used; the analysis for tubes is little different.

For convenience, normalized supply voltages of 1V are assumed. Also, the load resistances are normalized to  $1\Omega$ , and transformers provide 1:1 matching and 1:1 impedance conversion.

### A. Conventional Amplifiers

#### 1. Class A

Class A is the only type of amplification which is completely linear in its operation. In the class A amplifier (Figure 2.1), the transistor acts as a variable resistor. As the transistor begins to conduct current, the collector voltage drops from the supply voltage toward zero. As the transistor begins to conduct less current, the collector voltage swings upward toward twice the supply voltage.

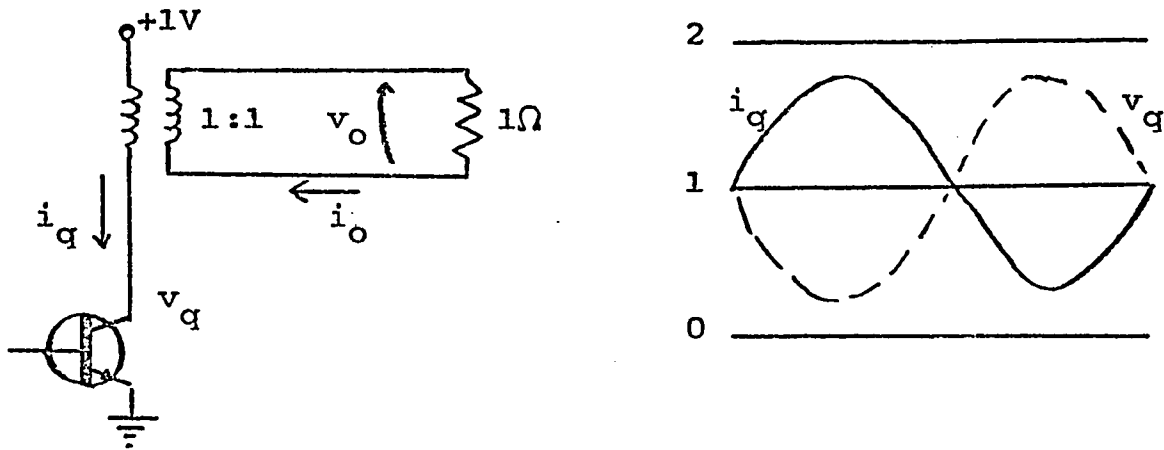


Figure 2.1. Class A Amplifier.

For such an amplifier, the collector voltage is

$$v_q(\theta) = 1 - b \sin \theta \quad (2.1)$$

Since the transformer matches 1:1, and the load resistance is  $1\Omega$ ,

$$i_q(\theta) = v_q(\theta) = 1 - b \sin \theta \quad (2.2)$$

In the load,

$$v_o(\theta) = i_o(\theta) = b \sin \theta \quad (2.3)$$

Thus the output power is given by

$$P_o = \frac{1}{2\pi} \int_0^{2\pi} 1 v_o^2(\theta) d\theta \quad (2.4)$$

$$= \frac{1}{2\pi} \int_0^{2\pi} b^2 \sin^2 \theta d\theta \quad (2.5)$$

$$= \frac{b^2}{2\pi} \left[ \frac{\theta}{2} - \frac{\sin 2\theta}{4} \right]_0^{2\pi} \quad (2.6)$$

$$= \frac{b^2}{2\pi} [\pi - 0] = \frac{b^2}{2} \quad (2.7)$$

The voltage input is 1.0 volt, and the current input is the same as the transistor current, thus the input power is

$$P_i = \frac{1}{2\pi} \int_0^{2\pi} 1 (1 - b \sin\theta) d\theta \quad (2.8)$$

$$= \frac{1}{2\pi} [\theta + b \cos \theta]_0^{2\pi} = 1 \quad (2.9)$$

The efficiency is defined as the ratio of power output to power input, or

$$\eta = \frac{P_o}{P_i} = \frac{b^2}{2} \quad (2.10)$$

Since the supply voltage limits  $b$  such that

$$0 \leq |b| \leq 1 \quad (2.11)$$

the efficiency is also limited:

$$0 \leq \eta \leq 0.5 \quad (2.12)$$

## 2. Class AB

Class AB is used to describe an amplifier which conducts current more than half of the RF cycle, as in class B (below), but not all of the time, as in class A. Its efficiency is higher than that of class A, but distortion is also introduced.

### 3. Class B

A class B amplifier operates as a linear (class A) amplifier during the half of the cycle when the input is positive, but is cut-off when the input is negative, producing waveforms such as shown in Figure 2.2. Harmonics generated by the rectified type waveforms are suppressed by the tuned circuit.

Let the output voltage be

$$v_o(\theta) = -b \sin \theta \quad . \quad (2.13)$$

For a normalized load resistance of  $1\Omega$ ,

$$i_o(\theta) = v_o(\theta) \quad . \quad (2.14)$$

and

$$P_o = \frac{b^2}{2} \quad . \quad (2.15)$$

The current flowing in the RF choke is assumed to be constant, and no DC can flow through the blocking capacitor, so the input current is the average value of the transistor current, or

$$i_i = \bar{i}_q = \frac{1}{2\pi} \int_0^{2\pi} i_q(\theta) d\theta \quad . \quad (2.16)$$

$$= \frac{2b}{2\pi} [ -\cos \pi + \cos 0 ] \quad (2.17)$$

$$= \frac{2b}{\pi} \quad . \quad (2.18)$$

The input power is then simply

$$P = 1 i_i = 2b/\pi \quad . \quad (2.19)$$

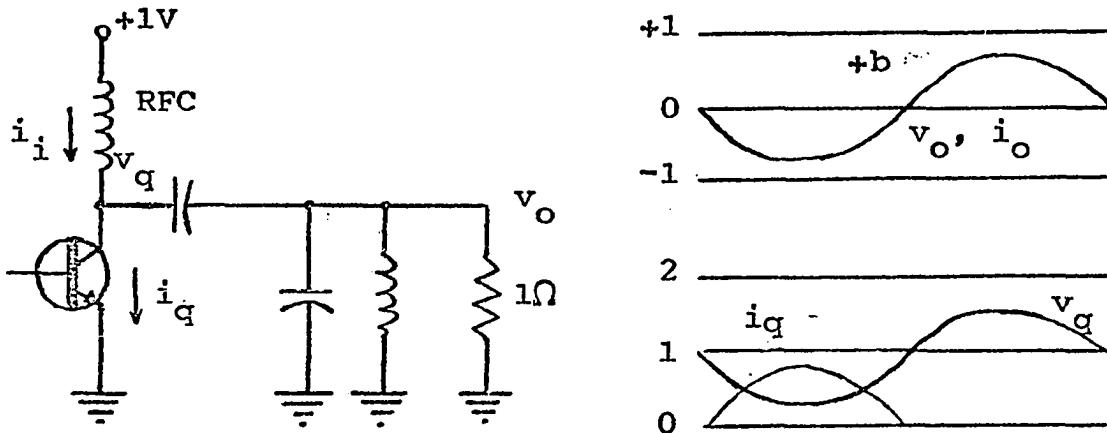


Figure 2.2. Class B Amplifier.

and the efficiency is

$$= \frac{b^2/2}{2b/\pi} = \frac{\pi}{4} b \quad (2.20)$$

The supply voltage requires that

$$0 \leq |b| \leq 1.0 \quad (2.21)$$

so

$$0 \leq \eta \leq 0.785 \quad (2.22)$$

The power dissipated can thus be reduced by approximately 57% (at maximum output) by the use of class B instead of class A. Two class B amplifiers can be operated "push-pull" to give fully linear operation as a system (thus cancelling harmonics and eliminating the need for a tuned output circuit), but allowing each transistor to operate class B and retain the higher efficiency.

#### 4. Class C

In class C operation, the transistor conducts current



during less than half of the RF cycle (Figure 2.3). Efficiency is improved, but the ability to amplify a signal linearly is lost, making class C suitable only for the generation of constant amplitude signals (unless the collector voltage is varied by an external modulator). Following the method of Terman (9), assume that the current in an ideal class C amplifier is a piece of a sinusoid:

$$i_q = \begin{cases} \sin \theta - q, & \frac{\pi}{2} - \delta < \theta < \frac{\pi}{2} + \delta \\ 0, & \text{otherwise.} \end{cases} \quad (2.23)$$

Where  $\delta$  represents the duty cycle, and  $q$  the quiescent point which gives a duty cycle of  $\delta$ . Thus,

$$q = \cos \frac{\delta}{2} \quad (2.24)$$

The input power is found by integrating the product of the supply voltage and the collector current:

$$P_i = \frac{1}{2\pi} \int_0^{2\pi} i_a(\theta) d\theta \quad (2.25)$$

$$= \frac{1}{2\pi} \int_{\frac{\pi}{2} - \delta}^{\frac{\pi}{2} + \delta} (\sin \theta - \cos \frac{\delta}{2}) d\theta \quad (2.26)$$

$$= \frac{1}{\pi} \left( \sin \frac{\delta}{2} - \frac{\delta}{2} \cos \frac{\delta}{2} \right) \quad (2.27)$$

The power output is then determined by

$$P_o = \frac{1}{2\pi} \int_0^{2\pi} i_q(\theta) v_o(\theta) d\theta \quad (2.28)$$

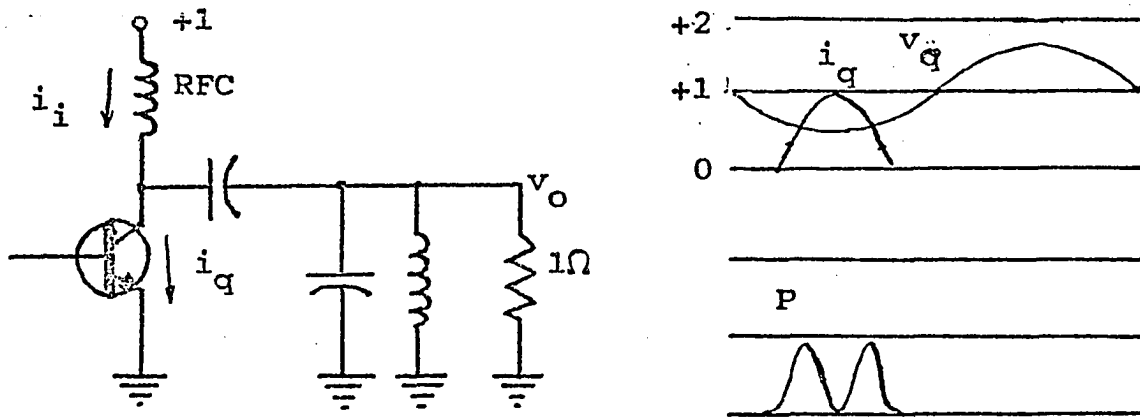


Figure 2.3. Class C Amplifier.

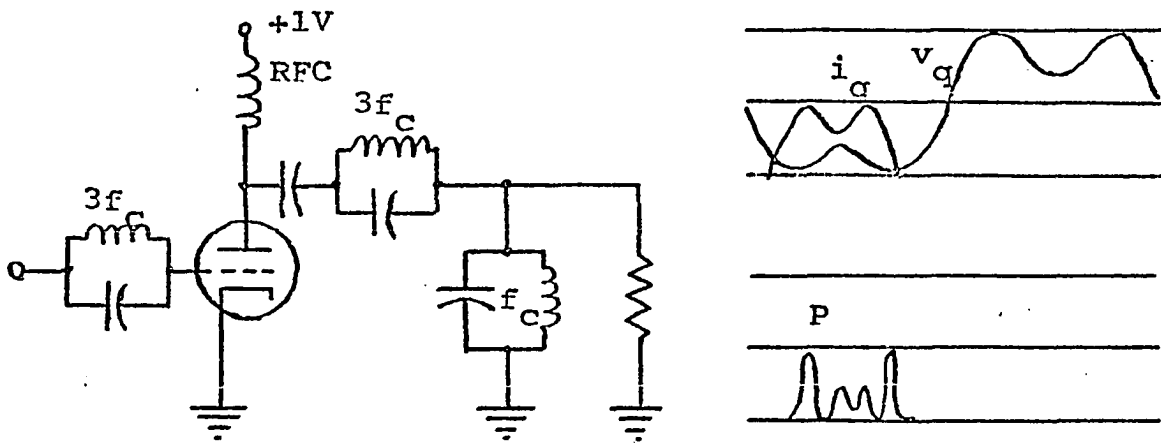


Figure 2.4. Class CD Amplifier.

$$= \frac{1}{2\pi} \int_{\frac{\pi-\delta}{2}}^{\frac{\pi+\delta}{2}} (\sin^2 \theta - \cos \frac{\delta}{2} \sin \theta) d\theta \quad (2.29)$$

$$= \frac{1}{4\pi} (\delta - \sin \delta) \quad (2.30)$$

Note that the integral above automatically ignores all but the energy at the fundamental frequency. The efficiency is then given by

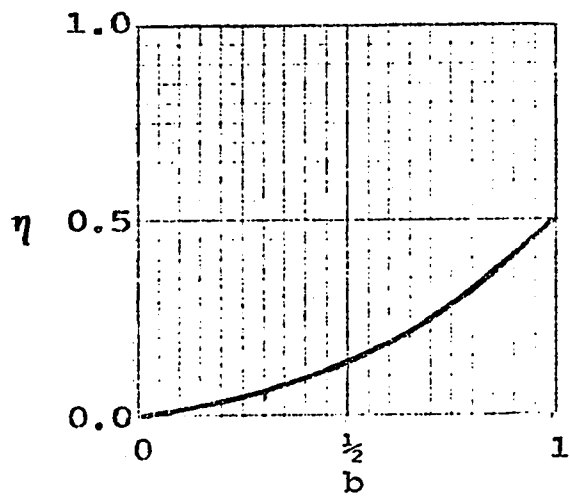
$$\eta = \frac{1}{4} \frac{(\delta - \sin \delta)}{(\sin \frac{\delta}{2} - \frac{\delta}{2} \cos \frac{\delta}{2})} \quad (2.31)$$

The graph of  $\eta$  versus output voltage  $b$  is presented in Figure 2.5. Efficiency approaching 100% is obtainable by making  $\delta$  small, but this also reduces the output to zero. A typical operating characteristic might have  $\delta \approx 0.4 \cdot 2\pi$  and  $\eta \approx 85\%$ . Note that by letting  $\delta$  be larger than  $\pi$ , the efficiency for classes A, AB, or B (at full output) is obtained. A more detailed analysis is given by Scott (10), including effects of waveforms differing slightly from the truncated sinusoid used herein.

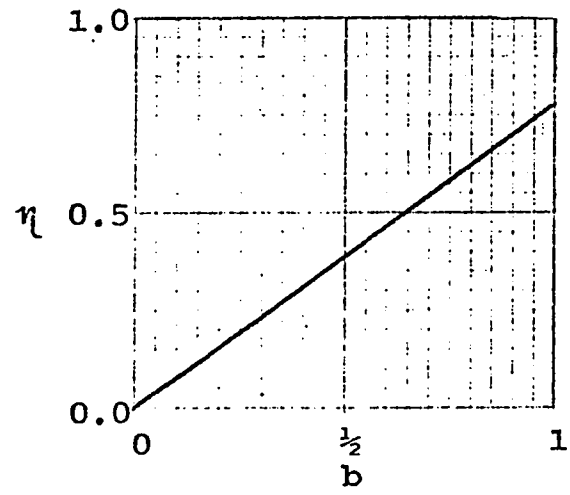
## 5. Class CD

Class CD is an appropriate name for what is more commonly called third-harmonic peaking. It is currently used in high-power medium-wave vacuum tube transmitters, such as the Gates VP-100 (11) to improve the efficiency.

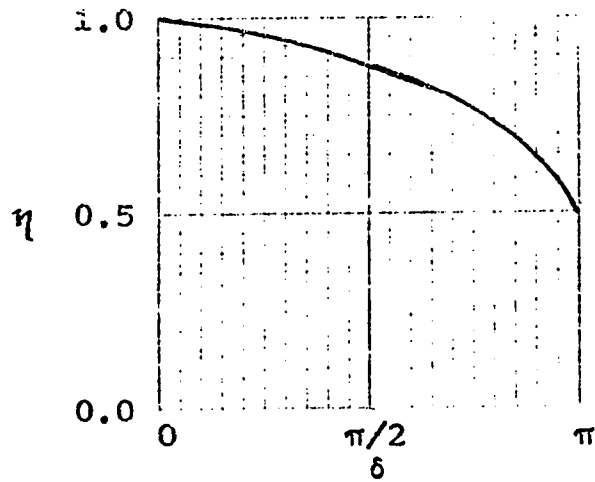
It is often difficult to generate a reasonable square



(a) Class A



(b) Class B



(c) Class C

Figure 2.5. Efficiencies of Class A, B, and C Amplifiers.

wave such as is required for true class D operation (described below). However, it is often possible to generate enough of the third harmonic to make the first approximation to a square wave. The third harmonic is controlled by means of additional tuned circuits which are added in the grid and plate circuits. As shown in Figure 2.4, the effect of the third harmonic is to flatten both the voltage and current waveforms. Power dissipated in the tube is reduced because the voltage is smaller while the tube is conducting current. In an example given by Stokes of a 125kW transmitter (12), class C operation produced an efficiency of 82%, while class CD produced an efficiency of 88%.

#### B. Switching Amplifiers

An ideal class D amplifier has either rectangular voltage waveforms, rectangular current waveforms, or both. The result of the rectangular waveforms is that power dissipated in the switching transistors is much less than the power dissipated in other kinds of amplifiers.

There are many different versions of switching, or class D, amplifiers. Consider first the simple case where both voltage and current waveforms are rectangular (Figure 2.6). When the transistor is saturated, it has zero resistance, and the voltage across it is zero. A current of 1A flows in the load, causing it to dissipate 1W of power. When the transistor is cut-off, no current flows and power is dissipated neither

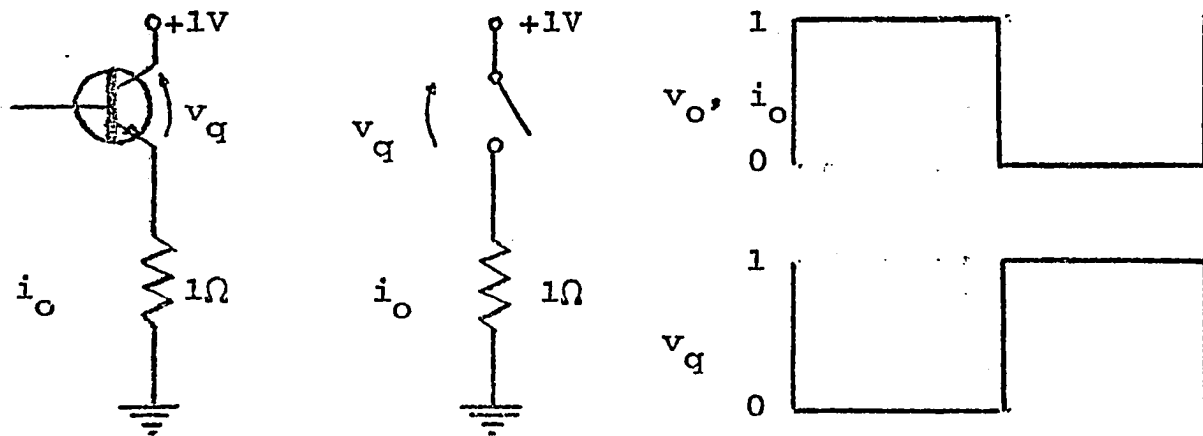


Figure 2.6. Switching Amplifier.

in the load nor in the transistor. Thus the average power delivered to the load is 0.5W (1/2 duty cycle), and the efficiency is 100%.

In a real amplifier, however, the pulse transitions are not instantaneous, and the saturation voltage is not zero, so some power is dissipated in the transistor. A detailed analysis of the efficiency of this type of amplifier is presented by Ramachandran (13). One significant advantage of such an amplifier is that efficiency improves with increasing output power.

### 1. Class AD amplifier

The terms class AD and class BD (which follows) were apparently originated by Martin (14), (15) to describe different types of conventional PWM amplifiers. These amplifiers will

be analyzed as they are used to generate an RF carrier (i. e., generation of a single sinusoid).

Consider the voltage switching version of the class AD amplifier shown in Figure 2.7. A set of four transistors operates as a two-position switch to generate a rectangular voltage waveform  $w(\theta)$ . A tuned circuit (or low pass circuit) passes the energy at the carrier frequency with no attenuation, and rejects energy at the switching frequency and its harmonics.

The instantaneous width  $y$  is made to vary as

$$y = \frac{2\pi}{\beta} [q + b \sin \theta] , \quad (2.32)$$

where

$$\theta = \omega_c t = 2\pi f_c t , \quad (2.33)$$

and

$$\beta = f_s / f_c , \quad (2.34)$$

where  $f_s$  is the switching frequency and  $f_c$  is the carrier frequency. For class AD operation,  $q$ , which determines the quiescent (no signal) pulse width, is restricted:

$$0 \leq q \leq 1 , \quad (2.35)$$

so  $b$  is also restricted

$$0 \leq q \pm b \leq 1 . \quad (2.36)$$

To achieve maximum output,

$$q = b = 0.5 , \quad (2.37)$$

although to reduce distortion, it is sometimes desirable to use smaller values of  $q$  and  $b$  (See Black (16) or Ramachandran

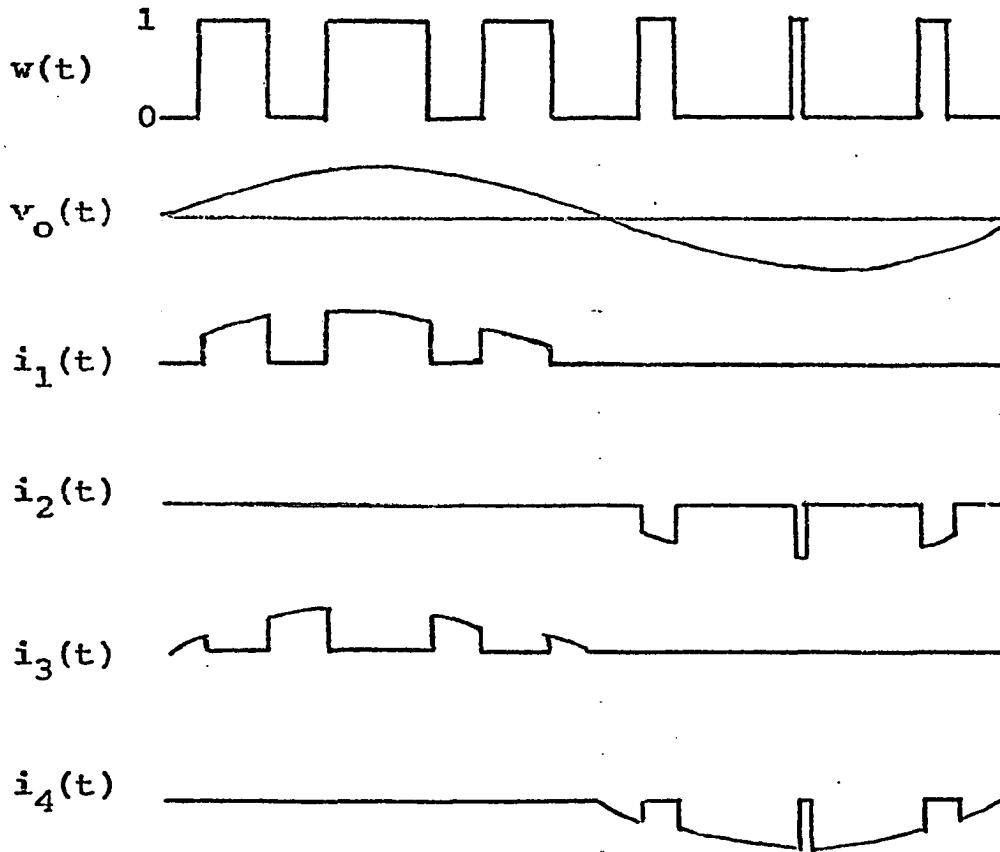
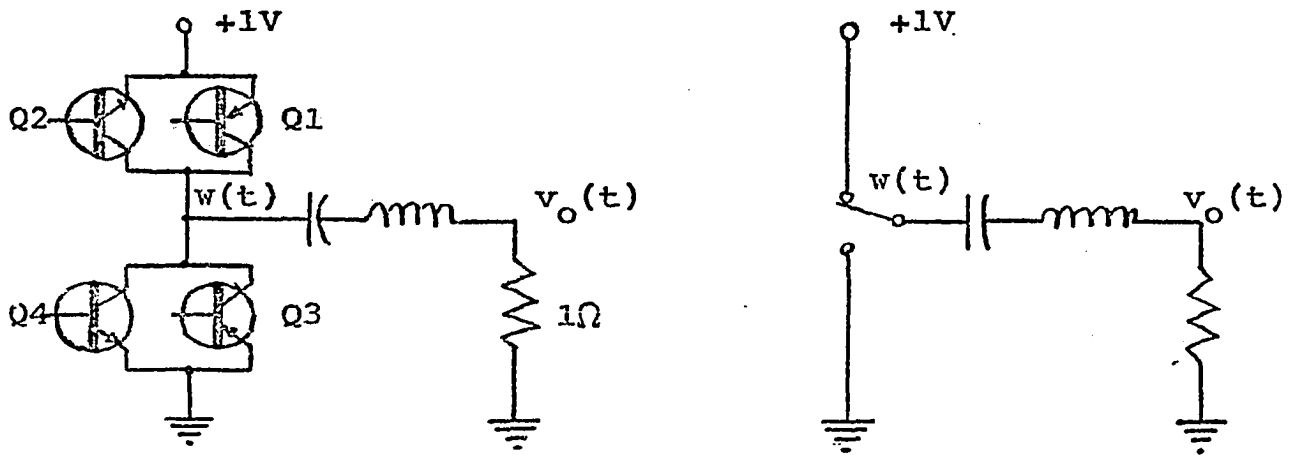


Figure 2.7. Class AD Amplifier.



(13).

Current can flow either direction through either side of the switch, as is required to maintain sinusoidal current through the series tuned circuit. In Figure 2.7, it can be seen that there is a net flow of current from the supply to ground.

The ideal efficiency is 100%, as in the switching amplifier previously described, but, as before, actual circuit parameters prevent this. Assume that the deviations of the actual circuit from ideal operation are small. The power output will undergo little change, and will be approximately

$$P_o = \frac{b^2}{2\pi} \quad (2.38)$$

Let the rise and fall times be represented by  $\tau_5$  and  $\tau_6$ , respectively, the values of which are given in terms of a cycle at  $f_s$  (i.e., if a rise time takes 10% of one cycle at  $f_s$ ,  $\tau_5 = 0.1 \cdot 2\pi/f_s$ ). For small  $\tau_i$ , the output current is approximately the same over the entire switching interval, or

$$i_q(\theta + \tau_i) \approx i_q(\theta) \quad (2.39)$$

This allows the assumption of a linear rise/fall of the current between 0 and  $i_q(\theta)$ , and a linear fall/rise of voltage between 1 and 0 (Figure 2.8). Thus

$$P_{DR \text{ TRANS}}(\theta) = \frac{1}{2\pi} \int_0^{\tau_i} v_q(\theta) i_q(\theta) d\theta \quad (2.40)$$

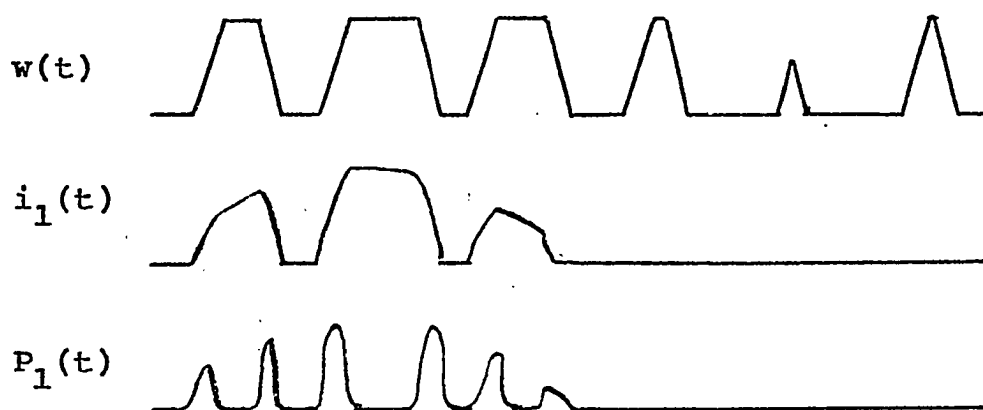


Figure 2.8. Rise/Fall Times in a Class AD Amplifier.

$$= \frac{i_q(\theta)}{2\pi} \int_0^{\tau_i} (1 - \frac{\theta}{\tau_i}) (\frac{\theta}{\tau_i}) d\theta \quad (2.41)$$

$$= \frac{i_q(\theta)}{2\pi} \left( \frac{1}{\tau} \int_0^{\tau_i} \theta d\theta - \frac{1}{\tau_i^2} \int_0^{\tau_i} \theta^2 d\theta \right) \quad (2.42)$$

$$= \frac{1}{2\pi} \frac{1}{6} \tau_i i_q(\theta) \quad (2.43)$$

The total power dissipated is then the sum of the power dissipated at each pulse transition, multiplied by two, since two transistors are switching at each transition. Assuming that there are  $\beta$  pulses per cycle,

$$P_{DR} = 2 \sum_{n=1}^{2\beta} i(\theta_n) \cdot \frac{1}{2} \frac{\tau_i}{6} \quad (2.44)$$

$$= \frac{1}{16\pi} \left[ \tau_5 \sum_{n=1}^{\beta} i(\theta_{2n-1}) + \tau_6 \sum_{n=1}^{\beta} i(\theta_{2n}) \right] \quad (2.45)$$

The effect of these summations is to average  $i_q(\theta)$ , thus

$$P_{DR} \approx \frac{1}{6\pi} \left( \frac{\beta\tau_5 qb}{2} + \frac{\beta\tau_6 qb}{2} \right) \quad (2.46)$$

$$= \frac{\beta qb}{12\pi} (\tau_5 + \tau_6) = \frac{\beta qb}{12\pi} \sigma \quad (2.47)$$

Consideration must also be given to the effects of non-zero saturation voltages. Osborne (4) has approached this problem by insertion of a saturation resistance in series with switch. It would seem that a constant saturation resistance would be accurate for square-wave current, but based on observations of the prototype class D RF amplifier (see Chapter XIV), a saturation voltage seems more appropriate.

Let  $v_s$  be the normalized saturation voltage (i.e., if the actual supply voltage is 10V, and the actual saturation voltage is 0.5V, then  $v_s = 0.05$ ). The power dissipated due to the saturation effects can then be determined by inserting sources of voltage  $v_s$  in series with the ideal transistors, with polarity such that power is consumed instead of generated (Figure 2.9).

The saturation voltage always acts to consume power, thus

$$P_{DS} = \frac{1}{2\pi} \int_0^{2\pi} v_s |i_o(\theta)| d\theta \quad (2.48)$$

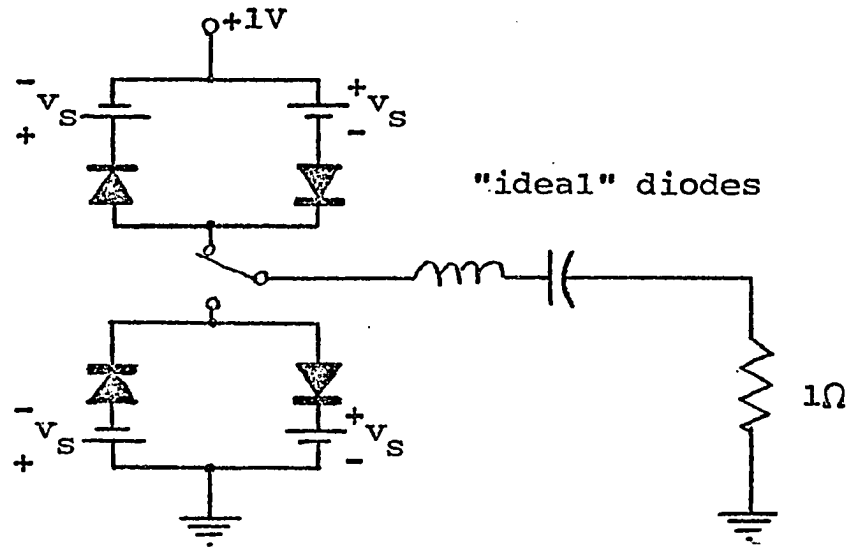


Figure 2.9. Saturation Voltages in a Class AD Amplifier.

$$= \frac{v_s}{2\pi} 2 \int_0^{\pi} b \sin \theta \, d\theta \quad (2.49)$$

$$= \frac{v_s b}{\pi} (-\cos \pi + \cos 0) = \frac{2v_s b}{\pi} \quad (2.50)$$

The input power is then

$$P_i = P_o + P_{DR} + P_{DS} \quad (2.51)$$

and the efficiency is

$$\eta = \frac{P_o}{P_o + P_i} \quad (2.52)$$

A plot of the efficiency for several values of  $\sigma$ ,  $v_s$ , and  $\beta$  is given in Figure 2.10 (Remember that for class AD,  $b \leq \frac{1}{2}$ ).

Note that  $\sigma$  is a ratio, and amplifiers with identical rise/fall times have  $\sigma$  proportional to  $f_s$ .

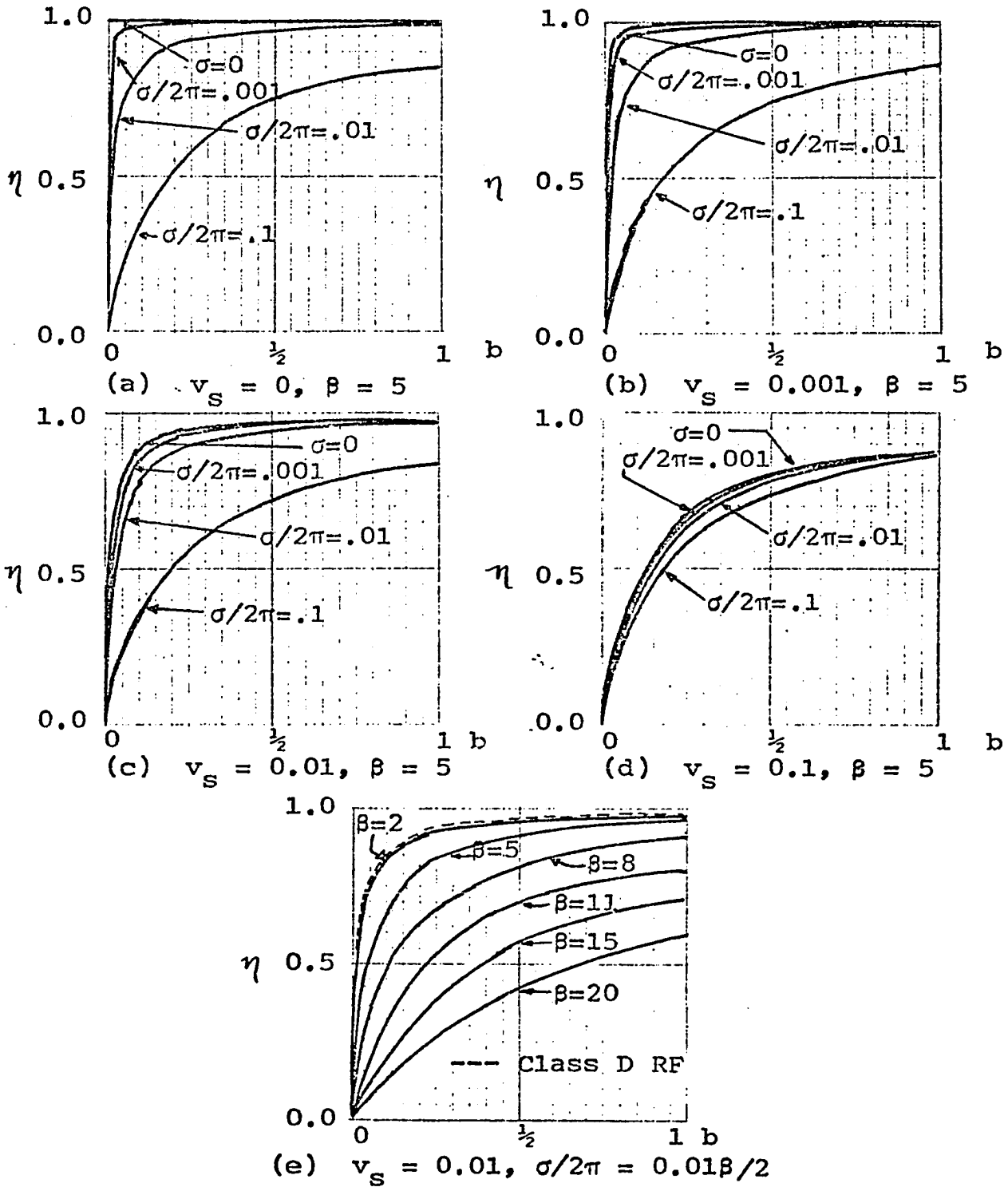


Figure 2.10. Efficiency of Class AD and BD Amplifiers.

## 2. Class BD amplifier

The class BD amplifier might be called a bipolar or push-pull version of the class AD amplifier just discussed. The quiescent pulse width is zero, so for no signal input, all transistors are idle. Positive pulses are generated when the input signal is positive, and negative pulses are generated when the input signal is negative. In either case, the linear relationship between input signal and pulse width remains. This amplifier has the advantage of eliminating drive when there is no signal input, but has the disadvantage of crossover distortion due to the difficulty of making very short pulses when the signal is small.

A circuit for the class BD amplifier is shown in Figure 2.11.

The efficiency is determined in the same manner as for the class AD amplifier, and the same equations apply. However, for class BD,

$$0 \leq |b| \leq 1 \quad , \quad (2.53)$$

as compared with a maximum value of 0.5 for the class AD amplifier. The significance of this is that in a class BD amplifier, the output power can become four times as large as that of the class AD amplifier, while the power dissipated is only doubled.

Also, note that in class BD, there are four possibly different rise/fall times, so

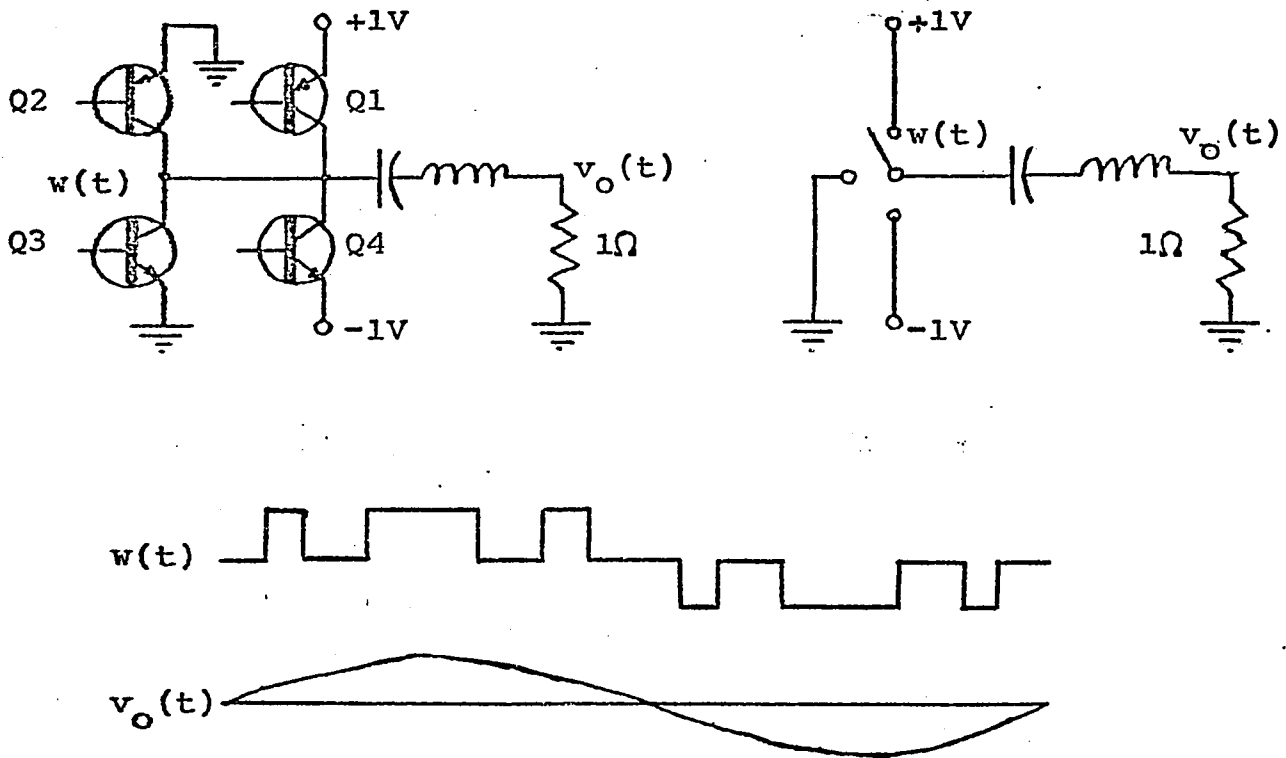


Figure 2.11. Class BD Amplifier.

$$\sigma = (\tau_5 + \tau_6 + \tau_7 + \tau_8) \quad (2.54)$$

### 3. Class D RF amplifier

The class D RF amplifier (Figure 2.12) has a circuit similar in form to the circuit of the class BD amplifier. However, the operation is markedly different, in that switching occurs at the carrier frequency, instead of a higher frequency.

A set of four transistors forms a bipolar pulse train with instantaneous width  $y$ . The fundamental component which

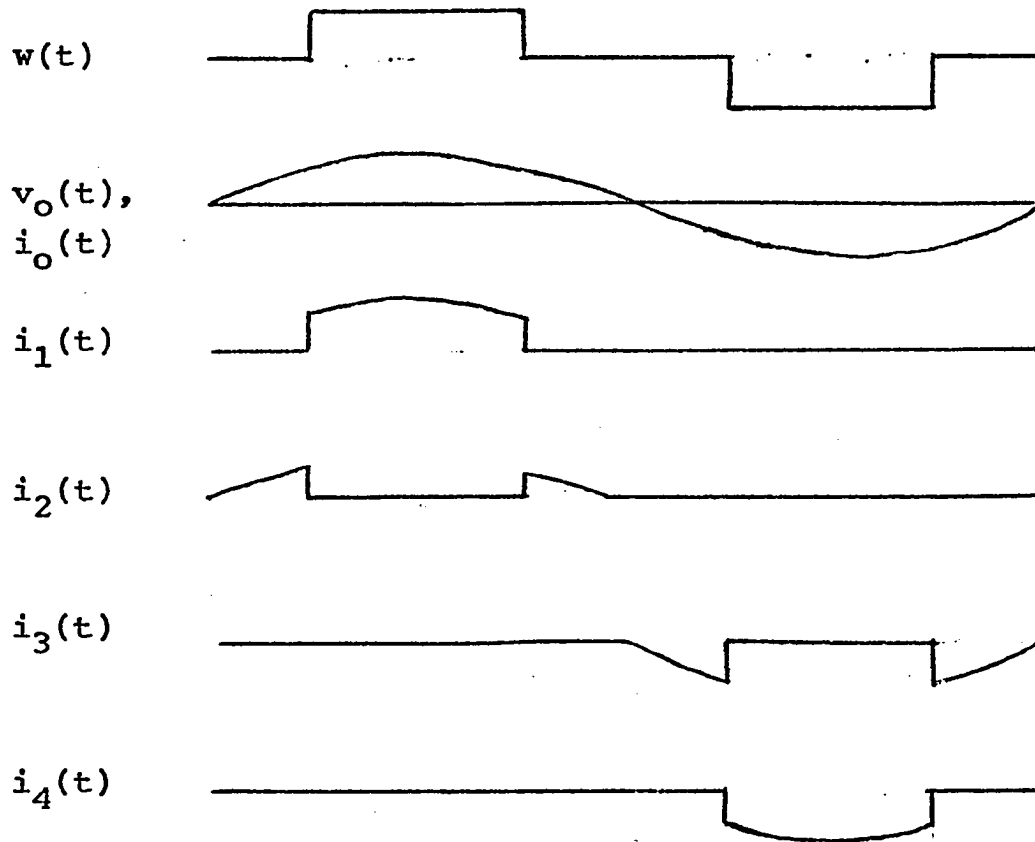
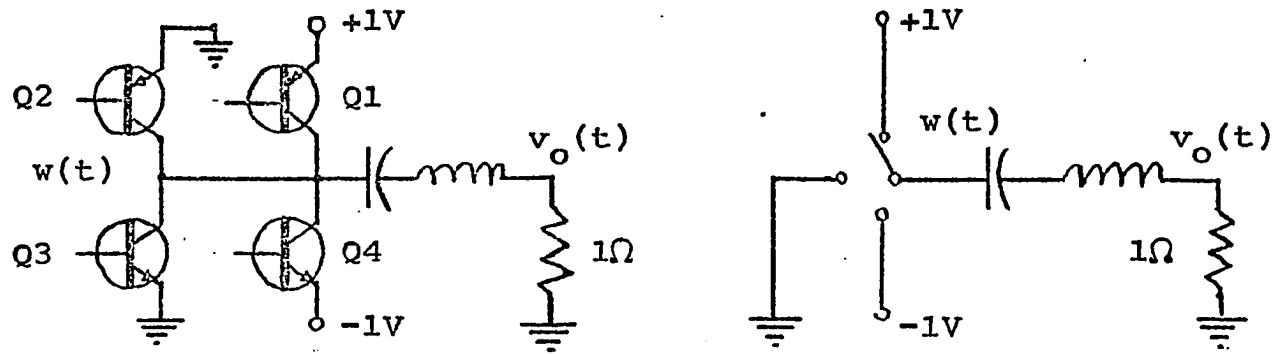


Figure 2.12. Class D RF Amplifier.



appears at the output is

$$v_o(\theta) = i_o(\theta) = b \sin \theta \quad , \quad (2.55)$$

and is proportional to the sine of the pulse width:

$$b = \frac{4}{\pi} \sin y \quad . \quad (2.56)$$

Thus

$$P_o = \frac{b^2}{2} = \frac{8}{\pi^2} \sin^2 y \quad . \quad (2.57)$$

Again, the ideal efficiency is 100%, but is reduced by actual circuit parameters. If the same assumptions are made about linear rise/fall shape as with the class AD amplifier, the power dissipated in any one transistor during one transition is given by

$$P_{DR \text{ TRANS}} = \frac{1}{2\pi} \frac{\tau_i}{6} |i_q(\theta)| \quad (2.58)$$

$$= \frac{\tau_i}{12\pi} \left( \frac{4}{\pi} \sin y \right) |\sin \theta| \quad (2.59)$$

$$= \frac{2\tau_i}{3\pi^2} \sin y |\cos y| \quad (2.60)$$

$$= \frac{2\tau_i}{3\pi^2} |\sin 2y| \quad . \quad (2.61)$$

There are four pulse transitions during each RF cycle, and two transistors switching at each transition, so

$$P_{DR} = \frac{4\sigma}{3\pi^2} |\sin 2y| \quad , \quad (2.62)$$

where

$$\sigma = \tau_5 + \tau_6 + \tau_7 + \tau_8 \quad . \quad (2.63)$$

The power dissipated due to non-zero saturation voltage

is again computed by insertion of sources of  $v_s$  in series with the switch. Since only one transistor conducts at a time,

$$P_{DS} = \frac{1}{2\pi} \int_0^{2\pi} v_s |i_q(\theta)| d\theta \quad (2.64)$$

$$= \frac{2}{\pi^2} v_s \sin \gamma \int_0^{\pi} \sin \theta d\theta \quad (2.65)$$

$$= \frac{8}{\pi^2} v_s \sin \gamma \quad (2.66)$$

The above equations [(2.57), (2.62), and (2.65)] are accurate when the grounding transistors are connected to small voltage sources rather than the ground, to eliminate changes in the signal output (Chapter V). However, if connections are made directly to the ground, the saturation voltage injects a signal at the carrier frequency which reduces the output power, and hence the efficiency.

Exact calculations of these effects are difficult, since the saturation effect does not reinject a signal which varies linearly with the carrier amplitude. However, for large amplitudes ( $\gg v_s$ ) of the carrier, the saturation effect is simply a square wave of frequency  $f_c$  and peak to peak height  $2v_s$ . In Chapter IV, it is shown that the fundamental component of such a wave has magnitude  $4v_s/\pi$ .

The previous equations can be modified accordingly.

First,

$$v_o(\theta) = i_o(\theta) = (b - \frac{4}{\pi} v_s) \sin \theta \quad (2.67)$$

$$= \frac{4}{\pi} (\sin y - v_s) \sin \theta \quad , \quad (2.68)$$

and

$$P_o = \frac{8}{\pi^2} (\sin y - v_s)^2 \quad \dots \quad (2.69)$$

Similarly,

$$P_{DR} = \frac{4\sigma}{3\pi^2} (\sin y - v_s) |\cos y| \quad (2.70)$$

$$= \frac{4\sigma}{3\pi^2} (|\sin 2y| - v_s \cos y) \quad , \quad (2.71)$$

and

$$P_{DS} = \frac{8}{\pi^2} v_s (\sin y - v_s) \quad . \quad (2.72)$$

Note that these hold only when  $\sin y$  is large enough that saturation occurs nearly instantaneously. These equations tend to be worse than the actual case for small  $y$ .

A monopolar version of this amplifier is also possible (Possibly, if the term class E were used, it could be called class AE, and the bipolar version class BE.). As in the case of class AD and BD amplifiers, the efficiency of the monopolar version is generally lower than that of the bipolar version, due to the decreased output voltage ( $b \leq 2/\pi$  for monopolar). However, the monopolar amplifier has half the number of pulse transitions, which can result in higher efficiency. If a power supply of +2V is used with monopolar PWM, (without damage to the transistors),  $P_o$  and  $P_{DS}$  remain the same as for

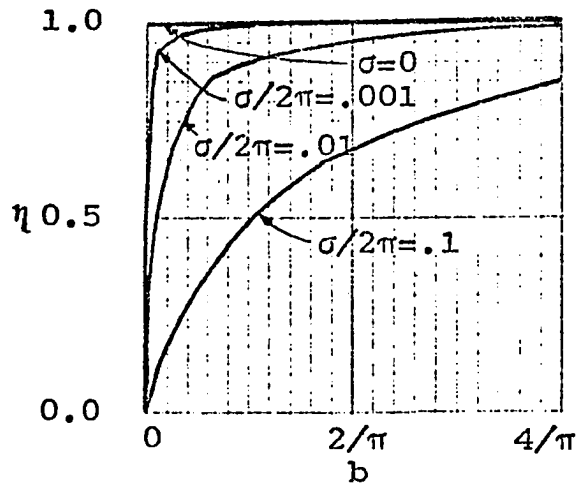
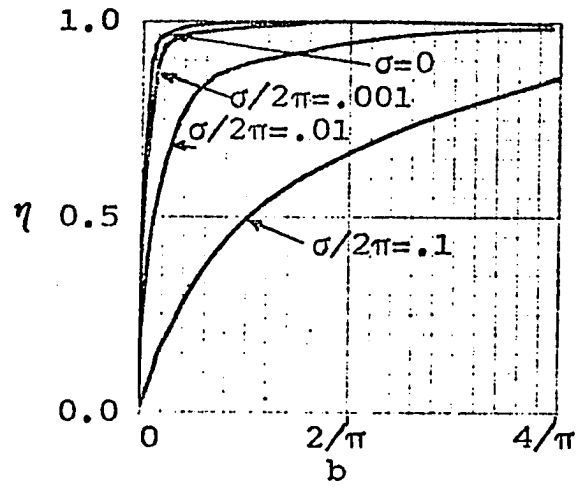
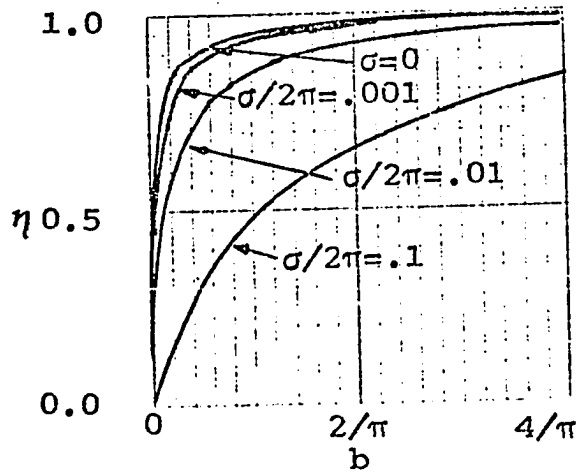
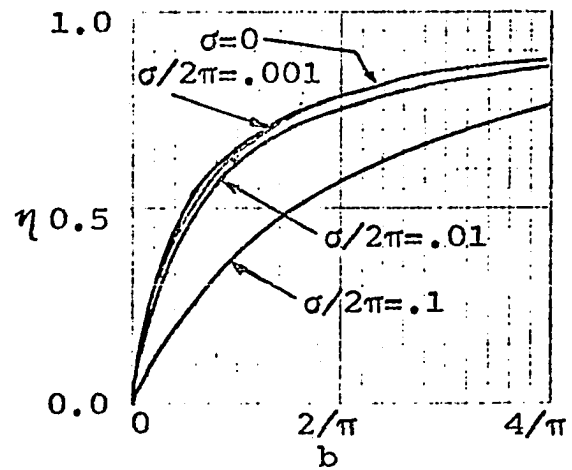
(a)  $v_s = 0$ (b)  $v_s = 0.001$ (c)  $v_s = 0.01$ (d)  $v_s = 0.1$ 

Figure 2.13. Efficiency of a Class D RF Amplifier.

bipolar PWM, ( $\pm 1V$ ) while  $P_{DR}$  is halved. This might have applications where  $\sigma$  is large and the dominant source of inefficiency, since its effect is to reduce  $\sigma$  to half of its value for bipolar PWM.

A graph of efficiency for the class D RF amplifier is given in Figure 2.13. A slight increase in efficiency over class AD or BD with the same parameters is due to two effects. First, the number of pulse transitions is reduced. Secondly, when a transition occurs in the RF amplifier, the current is small. When the output is large, the pulse is wide, and switching occurs near the minimum value. When the pulse is narrow, switching occurs near the peak current, but the current is small. Either way, the efficiency is increased.

## III. BASIC IMPLEMENTATION

The generation of pulses whose width varies as the inverse sine of a modulating signal seems, at first, to be a formidable task. However, it is actually somewhat easier to generate these pulses than pulses whose width is linearly related to the modulating signal, as are required by ordinary (class AD) PWM. Possibly, the problem of generating the pulses has discouraged previous researchers. The use of a feedback network as a means to generate the inverse sine pulses has been suggested (17), (18), but is not actually necessary.

First consider the method used by a typical conventional pulse width modulator (Figure 3.1). A triangular reference wave  $r(t)$ , periodic at switching frequency  $f_s$ , is generated and compared with input signal  $v(t)$ . Whenever  $v(t)$  is greater than  $r(t)$ , the output produces a pulse (+1). Otherwise, the output remains at 0. (In actual implementation, the difference  $v(t) - r(t)$  is compared with 0).

Figure 3.2(a) illustrates the action of comparison of the modulating signal  $x(t)$  to  $r(t)$  to obtain a linear pulse width. To obtain an inverse sine relationship, it is only necessary to predistort the ramp shape to get a sinusoidal shape (Figure 3.2(b)).

The application of a predistorted reference wave to the generation of pulses in an AM transmitter ( $x(t) \geq 0$ ) is shown in Figure 3.3. A block diagram of this transmitter is shown

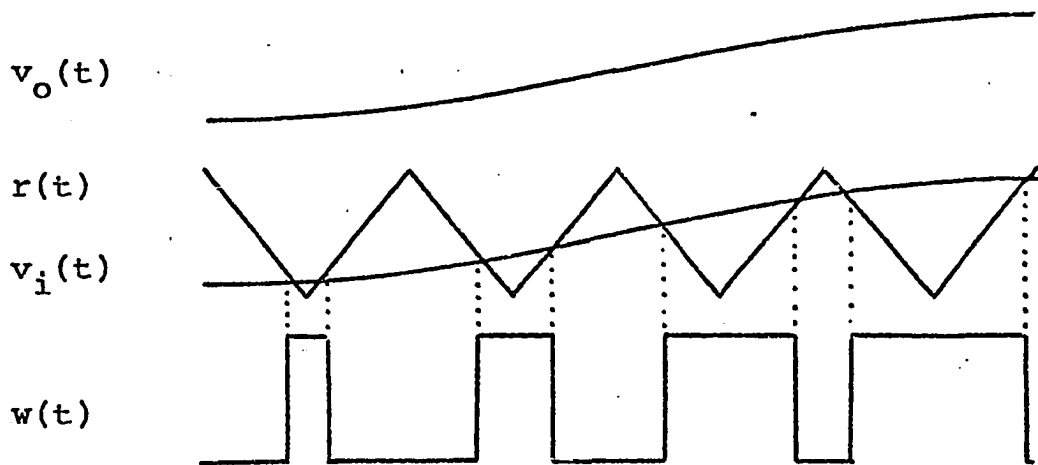


Figure 3.1. Comparator Pulse Generation for Class AD.

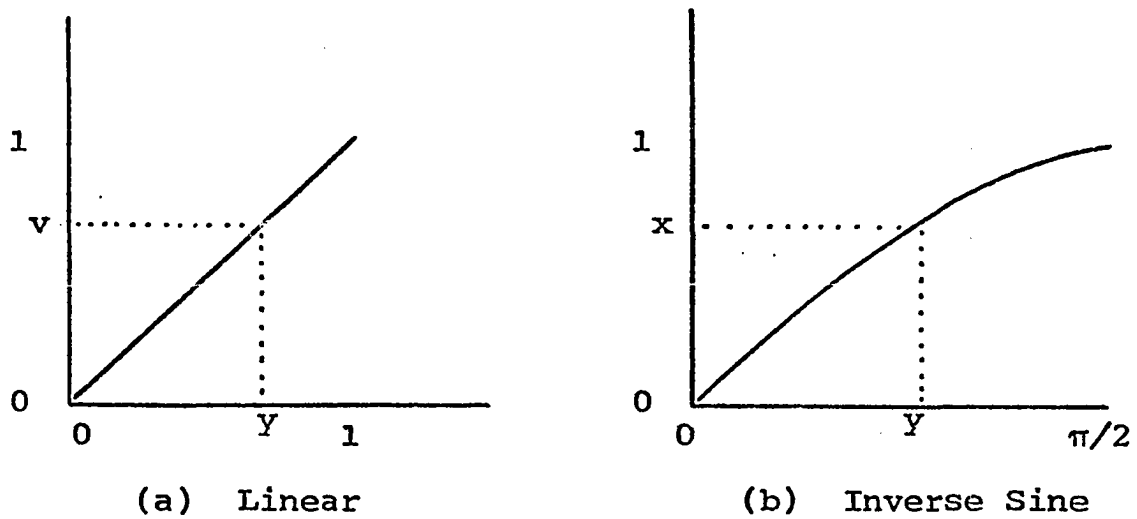


Figure 3.2. Relationships Between Modulating Signal and Pulse Width.

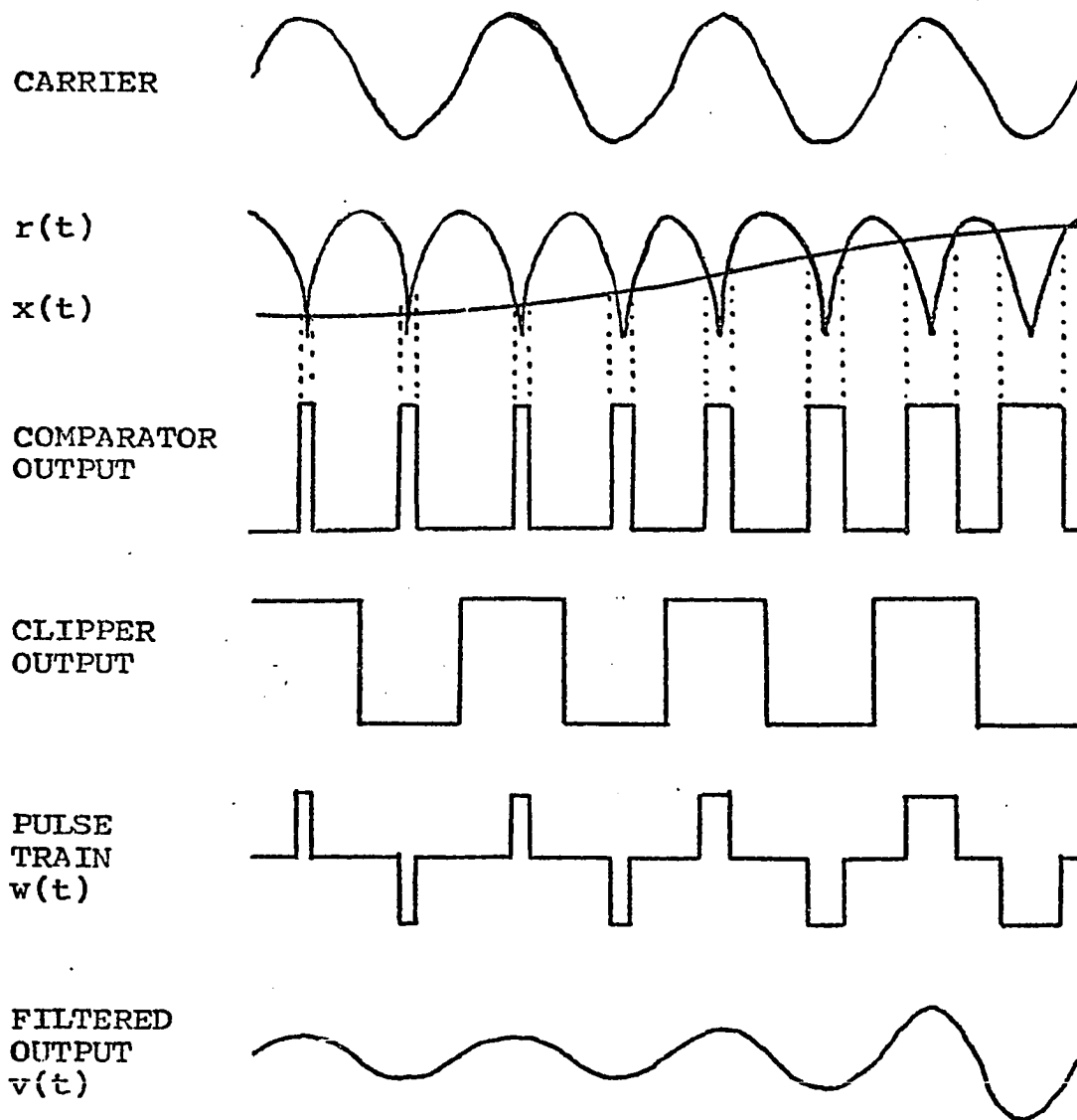


Figure 3.3. Waveforms in Class D AM System.



in Figure 3.4.

The transmitter has inputs from a sinusoidal oscillator at the desired carrier frequency, and from the audio frequency (AF) modulating signal. The carrier frequency sinusoid is clipped to produce square wave  $s(\omega_c t)$ . It is also phase shifted by  $\pi/2$ , and then inverted. The inverted and uninverted cosine waves thus produced are then rectified, and the outputs combined to produce the reference wave  $r(t)$ . The reference wave is then compared to the AF input  $x(t)$ , and pulses are generated whenever the latter is greater.

An AND gate generates a pulse whenever both the comparator output and the clipped wave  $s(\omega_c t)$  are positive. Similarly, a second AND acts on the comparator output and the inverted  $s(\omega_c t)$ , and generates a pulse when both are positive. These two pulses are amplified to drive Q1 and Q4, which are the positive and negative positions of the three position switch, respectively. The output of the comparator is inverted and amplified to drive transistors Q2 and Q3, which form the grounding position of the switch.

A balanced (two polarity) modulator for the generation of double sideband suppressed-carrier signals (DSB/SC) can be made by some simple additions to the AM transmitter. Referring to Figure 3.5, note that in a DSB/SC signal, a phase shift of the carrier occurs when the modulating signal changes sign. This effect can be accomplished in the class D transmitter by reversing the pulse polarities. A circuit to do

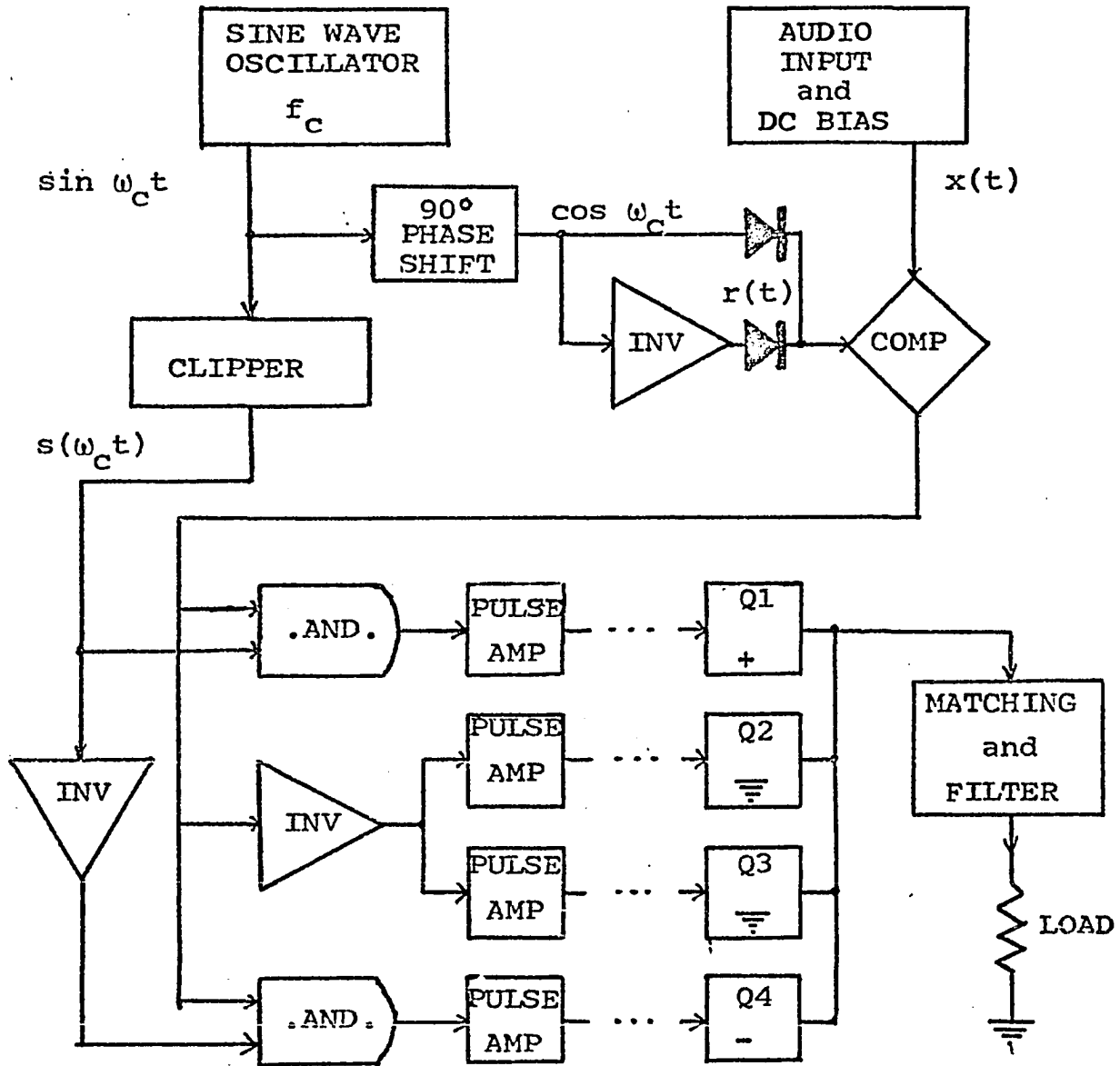


Figure 3.4. Class D AM Transmitter.

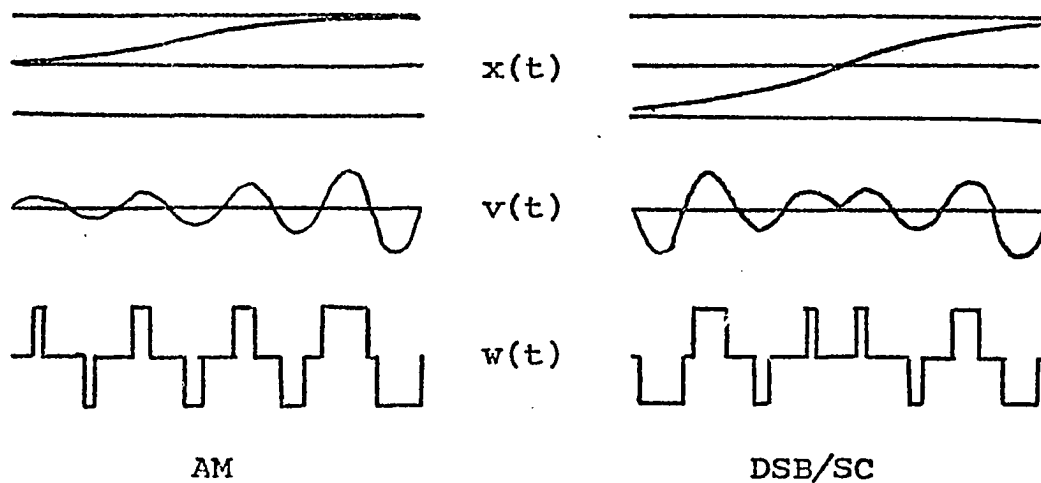


Figure 3.5. Generation of AM and DSB/SC.

this compares the absolute value of the modulating signal to the reference wave, and uses a clipped audio wave and additional logic to determine pulse polarity.

Generation of single-sideband signals (SSB) is also possible, but is slightly more complicated. Note that any signal can be regarded as a single sideband signal; generation of independent sideband, vestigial sideband, etc., is also possible.

There are two commonly used methods of producing a single sideband signal: the filter method and the phasing method; the same signal is produced either way. Although the filter method is somewhat easier to implement, the phasing more clearly illustrates the operation of class D SSB amplification. In the phasing method, the audio signal and the carrier are both phase shifted by  $90^\circ$  (the direction of the shifts deter-

mines whether upper sideband or lower sideband is produced). The phase-shifted audio signal then modulates the unshifted carrier, and the unshifted audio modulates the shifted carrier. The sum of these two modulated signals, properly balanced, cancels one sideband.

There are three possible means of using class D to amplify a single sideband signal (Figure 3.6). The first two, interlacing and overlapping, are similar in that they both require use of the phasing type method to produce two separate signals. A DSB/SC modulating system is required for each signal. In the interlacing method, the magnitudes of both  $x_p(t)$  and  $x_q(t)$  are reduced so that the pulses generated by either modulation do not exceed  $\pi/2$ . The outputs from the logic circuits of both modulators drive the same final switching transistors, producing two interlaced pulse trains. In the overlapping method, the magnitudes of  $x_p(t)$  and  $x_q(t)$  have the usual restriction of less than 1 (to produce pulses whose total widths are less than  $\pi$ ). When pulses from the two modulators overlap, either a 0 (ground) or double-value pulse is generated, depending on whether the pulses are of different or similar polarities.

The third method is an application of Kahn's method of envelope elimination and restoration (19), (20). Referring to Figure 3.7, one can see that it is possible to represent the sum of the outputs of the two balanced modulators used in the phasing method as a signal with envelope  $E(t)$  and

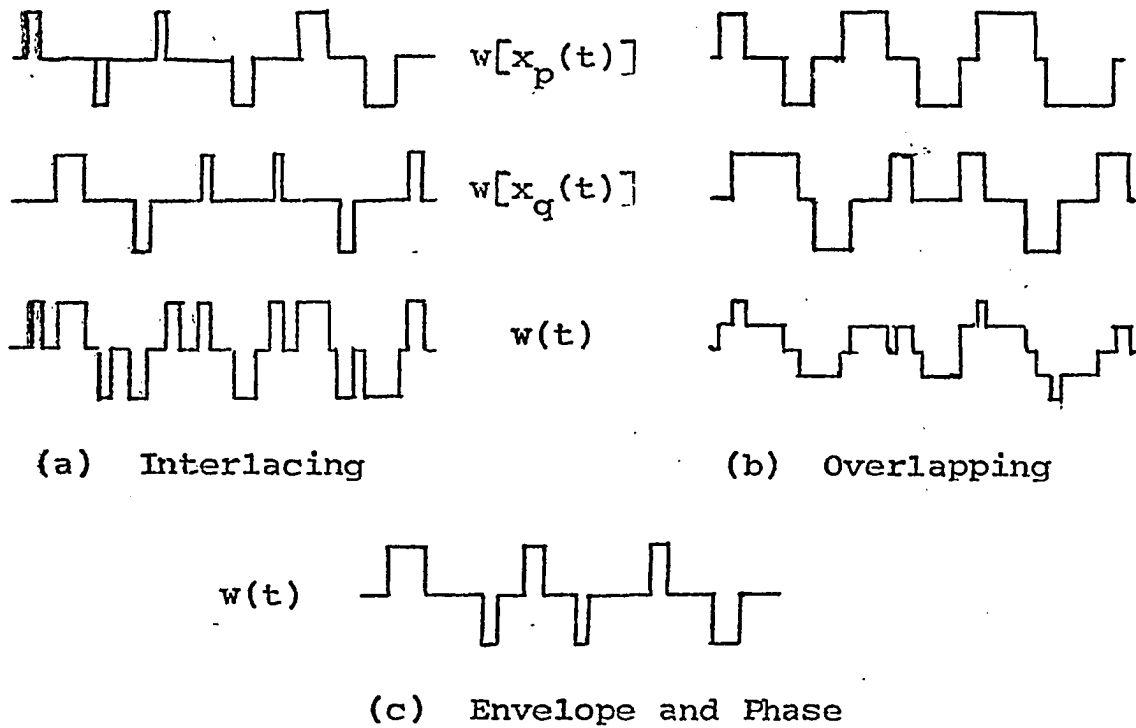


Figure 3.6. Class D SSB Techniques.

phase  $\varphi(t)$ :

$$\begin{aligned} x_p(t) \sin \omega_c t + x_q(t) \cos \omega_c t \\ = E(t) [\sin \omega_c t + \varphi(t)] \end{aligned} \quad (3.1)$$

where

$$E(t) = \sqrt{x_p^2(t) + x_q^2(t)} \quad (3.2)$$

and

$$\varphi(t) = \arctan \frac{x_q(t)}{x_p(t)} \quad (3.3)$$

(The function  $\arctan x_q/x_p$  as used herein should really be written  $\arctan(x_q, x_p)$ , since it is to determine the quadrant

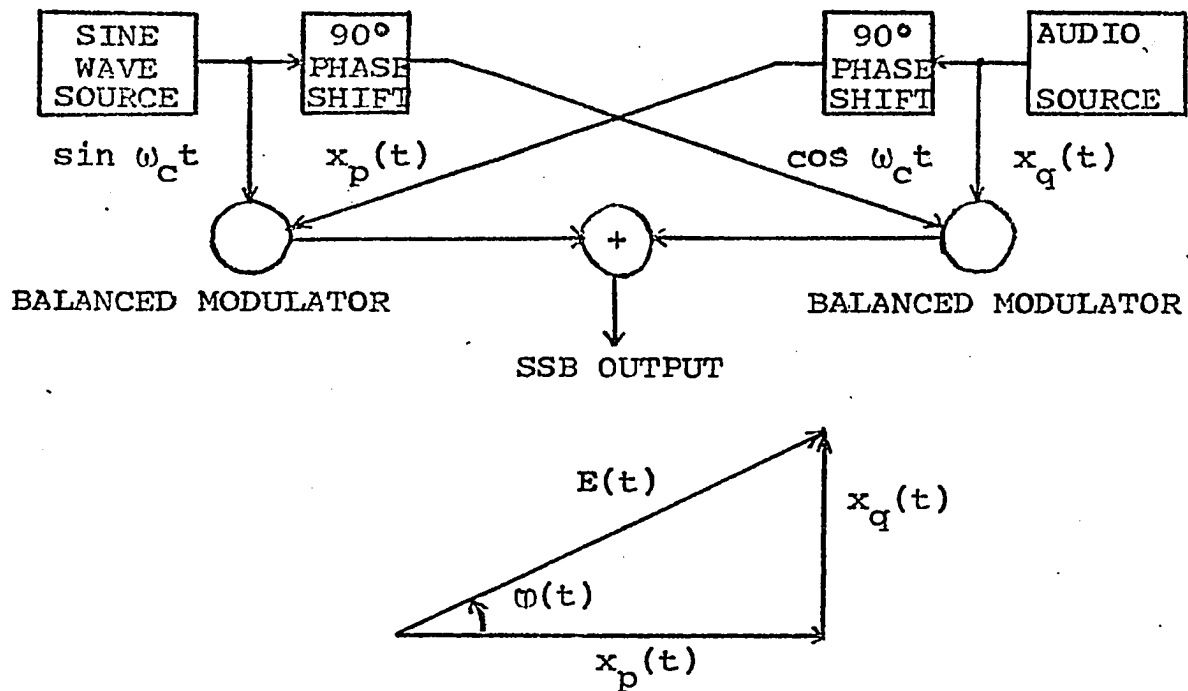


Figure 3.7. SSB Generation.

of the point  $(x_q, x_p)$ .)

A system for implementing this method is shown in Figure 3.8. with waveforms for a two tone signal. A low-level SSB signal is generated by any convenient method. An envelope detector produces  $E(t)$ , which is the audio input to the AM transmitter previously described. The input signal is also fed to a clipping circuit to produce square wave  $s[\omega_c t + \varphi(t)]$ . Note that the phase information is retained, but the amplitude information is eliminated. If this square wave is expanded in a Fourier series,

$$s[\omega_c t + \varphi(t)] = \frac{4}{\pi} \sin[\omega_c t + \varphi(t)]$$

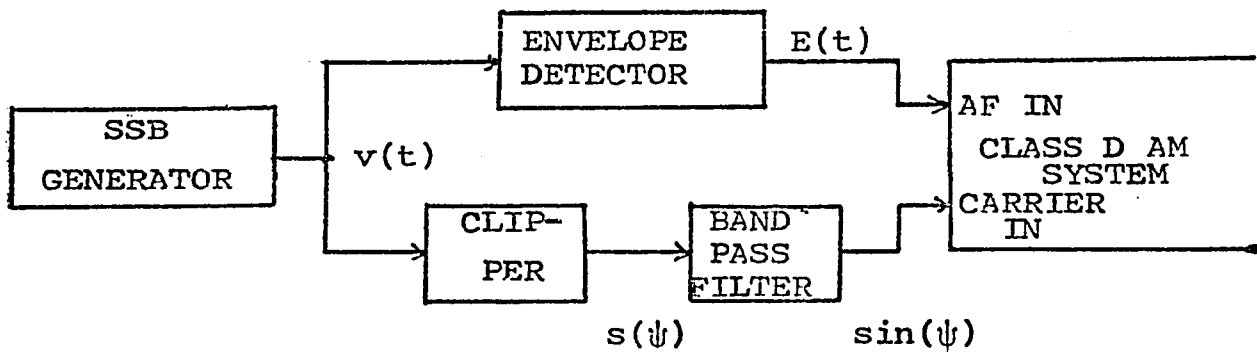
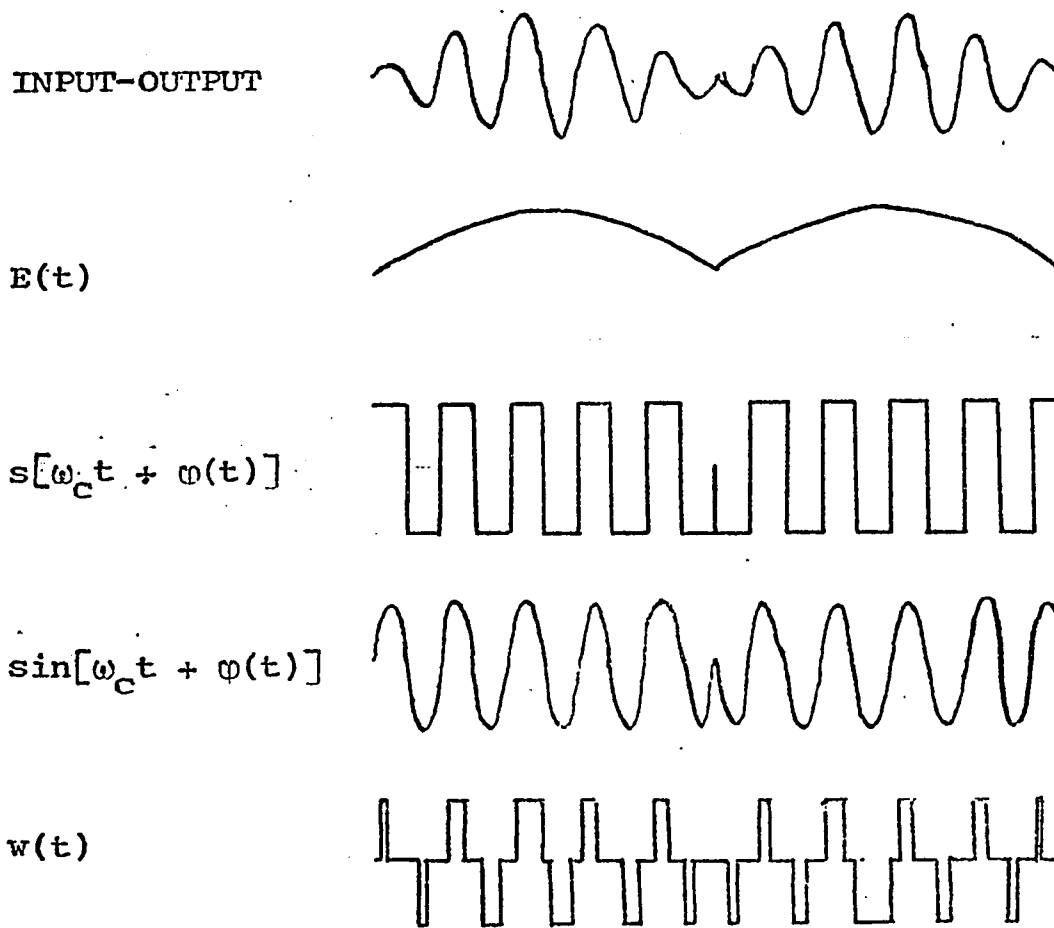


Figure 3.8. Class D SSB Generation Using Kahn's Method.

$$\begin{aligned}
 &+ \frac{4}{3\pi} \sin[3\omega_c t + 3\phi(t)] \\
 &+ \dots \qquad \qquad \qquad (3.4)
 \end{aligned}$$

When this is applied to a bandpass filter, only the fundamental frequency and its modulation (  $\sin[\omega_c t + \phi(t)]$  ) remain (assuming negligible splatter from modulation of the harmonics of the carrier). The output of this bandpass filter replaces the sinusoidal oscillator input to the AM transmitter.

Of the three methods, the third is probably the most advantageous. First, it requires no additional high speed logic (the SSB signal can be generated at a low frequency, envelope and phase detected at that frequency, and the phase signal heterodyned to the desired carrier frequency). Secondly, it requires fewer pulse transitions, which should make it more efficient. The overlapping method also requires the addition of switches for +2 and -2 volts.

There is a drawback to Kahn's method applied to class D RF generation: Spurious products may result from inherent modulation of the odd harmonics of the carrier. If these products are serious enough (Chapter V), one of the other methods might be used. Interlacing might be preferred due to its simplicity compared to overlapping.

It should be noted that Kahn's method can be used with transmitters other than class D. At very high frequencies, it may be difficult to control the pulse width accurately, but it may be possible to make a constant-carrier class D amplifier



with high efficiency. At even higher frequencies, square wave generation (class D) may be impossible altogether, but class C may be used. In these cases, the class D or C RF amplifiers can amplify the phase-modulated carrier, and a class AD audio type amplifier can be used for the envelope. These two signals are then combined by collector modulation. The resultant system would be more efficient than class B, but somewhat more complicated than a class D RF version.

## IV. BASIC SPECTRAL ANALYSIS

The distortion in any amplifier is one of the factors which limit its usefulness. In an RF amplifier, spurious products, which are distortion products which fall outside of the allocated frequency band, can be a serious problem. An unwanted product 30dB below the desired signal level is nearly unnoticeable if it is inside the desired bandwidth. However, this same product falling outside of the channel allocated can be much stronger than a distant (weak) station occupying the adjacent channel. Thus knowledge of the spurious products is crucial to application of the class D RF amplifier.

The method used in this dissertation to analyze the spectrum of a non-linear amplifier is to analyze the modulation of the harmonics of the carrier or switching frequency. A waveform basic to the particular amplifier is decomposed into its Fourier components, whose amplitudes are functions of some parameter of the waveform (e.g., pulse width). A relationship between the modulating waveform and the parameter is obtained, and each of the Fourier coefficients of the basic waveform is then expanded into a Fourier series whose period is that of the modulating function.

This technique was called "quasi-static" by Ramachandran (13), and was used by Black (16) to analyze the spectrum of ordinary pulse width modulation. It is similar to the method of Volterra (21), in which the time variable for the modula-

tion and the time variable for the carrier are regarded as two completely independent variables.

The reliability of this method is best understood conceptually by considering it in reverse. Choose a time  $t$ . At this time  $t$ , a pulse width  $y$  can be determined, based on the modulating voltage at that time. Substitution of the values of  $y$  into the formula for the Fourier coefficients of a pulse train yields a series of constants. Now for this series of constants, the waveform which is the sum of the specified components must have the value  $+1$ ,  $0$ , or  $-1$ , since for any value of  $y$  some pulse train is generated. This will hold for any  $y$ , hence the pulse train is produced for all values of  $t$  from the time-varying Fourier coefficients obtained in this method of analysis.

Once the time varying Fourier coefficients have been decomposed into their own series of Fourier components, these can be thought of as modulation around the Fourier components of the basic waveforms, and the total spectrum determined from this. A continuous spectrum could be used in the analysis which follows, but it adds little and complicates much. Therefore, all spectra herein will be discrete; *i.e.*, composed of bias, sinusoids, and cosinusoids periodic in a known interval.

Possibly the best argument in favor of this method of analysis is that results obtained with it have been verified by computer simulation.

Begin by considering a monopolar pulse train  $f_+(\theta)$  (Figure 4.1). The Fourier series for  $f_+(\theta)$  is

$$f_+(\theta) = a_0 + \sum_{n=1}^{\infty} (a_n \cos n\theta + b_n \sin n\theta) \quad , \quad (4.1)$$

where  $a_0$ ,  $a_n$ , and  $b_n$  are determined as follows:

$$a_0 = \frac{1}{2\pi} \int_0^{2\pi} f_+(\theta) d\theta = \frac{y}{\pi} \quad . \quad (4.2)$$

$$a_n = \frac{1}{\pi} \int_0^{2\pi} f_+(\theta) \cos n\theta d\theta \quad (4.3)$$

$$= \frac{1}{\pi} \int_{\varphi-y}^{\varphi+y} \cos n\theta d\theta \quad (4.4)$$

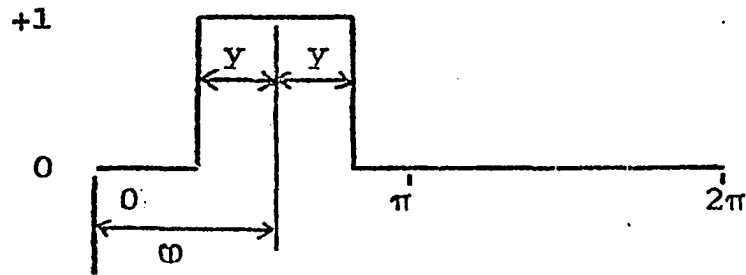
$$= \frac{1}{n\pi} [\sin n(\varphi + y) - \sin n(\varphi - y)] \quad (4.5)$$

$$= \frac{2}{n\pi} (\cos n\varphi) (\sin ny) \quad . \quad (4.6)$$

$$b_n = \frac{1}{\pi} \int_0^{2\pi} f_+(\theta) \sin n\theta d\theta \quad (4.7)$$

$$= \frac{1}{\pi} \int_{\varphi-y}^{\varphi+y} \sin n\theta d\theta \quad (4.8)$$

$$= \frac{-1}{n\pi} [\cos n(\varphi + y) - \cos n(\varphi - y)] \quad (4.9)$$

Figure 4.1. Monopolar Pulse  $f_+(\theta)$ .

$$= \frac{2}{n\pi} (\sin n\varphi) (\sin ny) \quad (4.10)$$

Combining these,

$$f_+(\theta) = \frac{Y}{\pi} + \frac{2}{\pi} \sum_{n=1}^{\infty} (\sin ny) [(\cos n\varphi) (\sin n\theta) + (\sin n\varphi) (\sin n\theta)\theta] \quad (4.11)$$

$$= \frac{Y}{\pi} + \frac{2}{\pi} \sum_{n=1}^{\infty} \frac{(\sin ny)}{n} [\cos(n\theta - n\varphi)] \quad (4.12)$$

The spectrum of a bipolar pulse train can now be determined by decomposing it into two monopolar pulse trains, one negative, and one positive (Figure 4.2).

$$f_-(\theta) = -\frac{Y}{\pi} - \frac{2}{\pi} \sum_{n=1}^{\infty} \frac{\sin ny}{n} \cos[n\theta - n(\varphi + \pi)] \quad (4.13)$$

$$= -\frac{Y}{\pi} - \frac{2}{\pi} \sum_{n=1}^{\infty} \frac{\sin ny}{n} \cos[(n\theta - n\varphi) - n\pi] \quad (4.14)$$

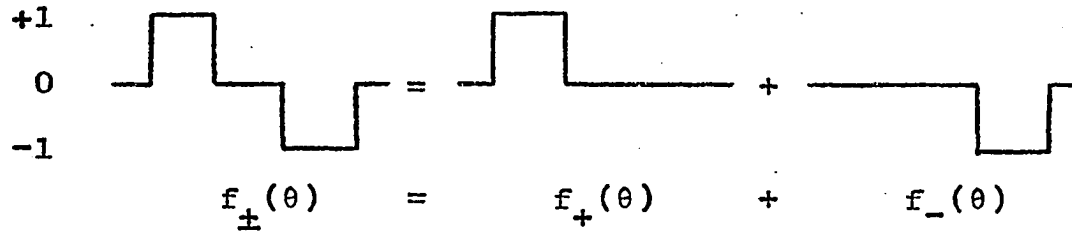


Figure 4.2. Decomposition of Bipolar Pulse.

$$= -\frac{y}{\pi} - \frac{2}{\pi} \sum_{n=1}^{\infty} (-1)^n \frac{\sin ny}{n} \cos(n\theta - n\varphi) \quad (4.15)$$

Thus,

$$f_{\pm}(\theta) = f_{+}(\theta) + f_{-}(\theta) \quad (4.16)$$

$$= \frac{4}{\pi} \sum_{n=1,3,5,\dots} \frac{\sin ny}{n} \cos(n\theta - n\varphi) \quad (4.17)$$

$$= \frac{4}{\pi} \sum_{m=1}^{\infty} \frac{\sin(2m-1)y}{2m-1} \cos(2m-1)(\theta - \varphi) \quad (4.18)$$

The special case of  $\varphi = \pi/2$  (sine wave carrier) will be used frequently. In this case,

$$f_{+}(\theta) = \frac{y}{\pi} + \frac{2}{\pi} \sum_{m=1}^{\infty} \left[ \frac{(-1)^m}{2m} \sin 2my \cos 2m\theta + \frac{(-1)^{m+1}}{2m-1} \sin(2m-1)y \sin(2m-1)\theta \right] \quad (4.19)$$

and

$$f_{\pm}(\theta) = \frac{4}{\pi} \sum_{m=1}^{\infty} \frac{(-1)^{m+1}}{2m-1} \sin(2m-1)y \sin(2m-1)\theta \quad (4.20)$$

There are two special cases of square waves which will be used later. These are the infinitely-clipped sinusoid  $s(\theta)$  and the infinitely-clipped cosinusoid  $c(\theta)$ :

$$s(\theta) = f_{\pm}(\theta; \varphi = \frac{\pi}{2}, y = \frac{\pi}{2}) \quad (4.21)$$

$$= \frac{4}{\pi} \sum_{m=0}^{\infty} \frac{1}{2m+1} \sin(2m+1)\theta \quad (4.22)$$

$$c(\theta) = f_{\pm}(\theta; \varphi = 0, y = \frac{\pi}{2}) \quad (4.23)$$

$$= \frac{4}{\pi} \sum_{m=0}^{\infty} \frac{(-1)^m}{2m+1} \cos(2m+1)\theta \quad (4.24)$$

Another waveform to be used is the truncated ramp  $r(\theta; \lambda, \tau)$  (Figure 4.3). A piecewise description of this waveform is

$$r(\theta) = \begin{cases} 0 & , 0 \leq \theta \leq \lambda \\ \frac{1}{\tau} (\theta + \lambda - \tau), & \lambda \leq \theta \leq \lambda + \tau \\ 0 & , \lambda + \tau \leq \theta \end{cases} \quad (4.25)$$

The Fourier coefficients are then evaluated, as for  $f_{+}(\theta)$ :

$$a_0 = \frac{1}{2\pi} \cdot \frac{1\tau}{2} = \frac{\tau}{4\pi} \quad (4.26)$$

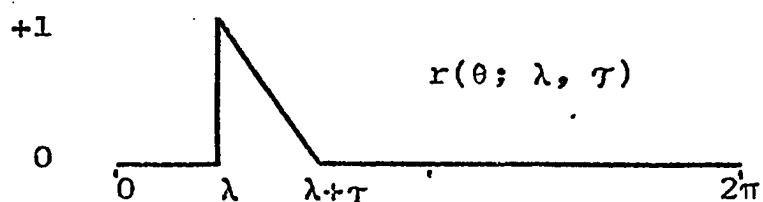


Figure 4.3. Ramp Waveform.

$$a_n = \frac{1}{\pi} \int_0^{2\pi} r(\theta) \cos n\theta \, d\theta \quad (4.27)$$

$$= \frac{1}{\pi} \int_{\lambda}^{\lambda+\tau} \frac{1}{\tau} (\lambda + \theta - \tau) \cos n\theta \, d\theta \quad (4.28)$$

$$= \frac{1}{\pi\tau n^2} \int_{\lambda}^{\lambda+\tau} [n(\lambda+\tau) \cos n\theta - n \cos n\theta] \, d\theta \quad (4.29)$$

$$= \frac{1}{\pi\tau n^2} [(\sin n\tau - n\tau)\sin n\theta + (1 - \cos n\tau)\cos n\theta] \quad (4.30)$$

$$b_n = \frac{1}{\pi} \int_0^{2\pi} r(\theta) \sin n\theta \, d\theta \quad (4.31)$$

$$= \frac{1}{\pi} \int_{\lambda}^{\lambda+\tau} \frac{1}{\tau} (\lambda + \theta - \tau) \sin n\theta \, d\theta \quad (4.32)$$

$$= \frac{1}{\pi\tau n^2} \int_{\lambda}^{\lambda+\tau} [n(\lambda+\tau) \sin n\theta - n\theta \sin n\theta] \, d\theta \quad (4.33)$$



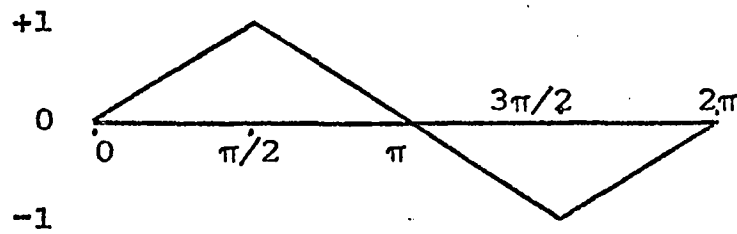


Figure 4.4. Triangular Wave  $\Lambda(\theta)$ .

$$= \frac{1}{\pi n^2} [(1 - \cos n\lambda)\sin n\lambda + (n\tau - \sin n\tau)\cos n\lambda] \quad (4.34)$$

The decomposition of a triangular wave  $\Lambda(\theta)$  (Figure 4.4) can be obtained by use of four ramp-type waveforms:

$$\begin{aligned} \Lambda(\theta) = & r[-\theta; \frac{\pi}{2}, -\frac{\pi}{2}] + r[\theta; \frac{\pi}{2}, \frac{\pi}{2}] \\ & -r[-\theta; \frac{3\pi}{2}, -\frac{\pi}{2}] - r[\theta; \frac{3\pi}{2}, \frac{\pi}{2}] \end{aligned} \quad (4.35)$$

$$= \frac{8}{\pi^2} \sum_{m=1}^{\infty} \frac{(-1)^{m+1}}{(2m-1)^2} \sin(2m-1)\theta \quad (4.36)$$

The composition of other special waveforms will be derived as required.

## V. BASIC SPECTRUM OF A CLASS D RF AMPLIFIER

The techniques developed in Chapter IV will now be used to determine the nature of the spurious products generated by width modulation of a class D RF amplifier.

The modulating signal will be denoted  $x(t)$  or  $x(\theta)$ . The spectrum of the modulating signal is assumed to be bandlimited, i.e.,

$$X(\omega) = 0, \quad |\omega| \geq \omega_x \quad (5.1)$$

When the notation  $x(\theta)$  is used, it will be understood that

$$\theta = \omega_x t = 2\pi f_x t \quad (5.2)$$

unless specified otherwise. (The equivalents for the carrier are denoted  $\theta_c$ ,  $\omega_c$ , and  $f_c$ .)

For single-tone amplitude modulation,

$$x(\theta) = a_{x0} + b_{x1} \sin \theta \quad (5.3)$$

For double-sideband suppressed-carrier modulation,  $a_{x0} = 0$ , and for maximum output,

$$x(\theta) = \sin \theta \quad (5.4)$$

This is regarded as a severe or extreme test signal, since all of the energy in the modulating signal is concentrated at the bandedges (It is equivalent to the commonly-used two-tone test for SSB.).

The inverse-sine predistorted signal for  $x(\theta)$  is denoted by  $y(\theta)$  and is given by

$$y(\theta) = \arcsin x(\theta) \quad (5.5)$$

Note that  $y(\theta)$  may never actually appear in an actual ampli-

fier. However, it is a convenience in the analysis of the amplifier.

#### A. Bipolar PWM

The modulation of the  $k^{\text{th}}$  harmonic of the carrier is denoted by  $z_k(\theta)$ . A bipolar train for AM and DSB/SC signals can then be written

$$w(\theta) = \frac{4}{\pi} \sum_{m=0}^{\infty} \frac{\sin(2m+1)y(\theta)}{2m+1} \sin[\theta_c + \varphi(\theta)] \quad (5.6)$$

$$= \frac{4}{\pi} \sum_{m=0}^{\infty} \frac{z_{2m+1}(\theta)}{2m+1} \sin(2m+1)\theta_c \quad (5.7)$$

(Note that  $\varphi(\theta)$  used above indicates phase shift from a sinusoidal carrier and is not the same  $\varphi$  used in Chapter IV.)

It is important to remember that negative modulation ( $x < 0$ ) is not accomplished by an actual negative pulse width, but by phase shifting the pulse train ( $\varphi(\theta) = \pi$ ). Thus

$$0 \leq y(\theta) \leq \frac{\pi}{2} \quad (5.8)$$

and

$$y(\theta) = |\arcsin x(\theta)| = \arcsin |x(\theta)| \quad (5.9)$$

The phase shift depends on the polarity or sign of  $x$ , thus

$$\varphi(\theta) = \begin{cases} 0, & x(\theta) \geq 0 \\ \pi, & x(\theta) < 0 \end{cases} \quad (5.10)$$

$$(5.11)$$

$$= \pi \left[ \frac{-\operatorname{sgn} x(\theta) + 1}{2} \right] , \quad (5.12)$$

where

$$\operatorname{sgn} x = \begin{cases} +1, & x > 0 \\ 0, & x = 0 \\ -1, & x < 0 \end{cases} \quad (5.13)$$

For sinusoidal modulation,

$$\operatorname{sgn}(\sin \theta) = s(\theta) , \quad (5.14)$$

and

$$\varphi(\theta) = \pi \left[ \frac{-s(\theta) + 1}{2} \right] \quad (5.15)$$

Now

$$\sin(2m+1)[\theta_c + \varphi(\theta)] = \sin[(2m+1)\theta_c + (2m+1)\varphi(\theta)] \quad (5.16)$$

$$= \sin \left[ (2m+1)\theta_c + (2m+1)\pi \left[ \frac{-\operatorname{sgn}(\theta)+1}{2} \right] \right] . \quad (5.17)$$

Subtracting  $m$  multiples of  $2\pi$ ,

$$= \sin \left[ (2m+1)\theta_c + \pi \left[ \frac{-s(\theta)+1}{2} \right] \right] . \quad (5.18)$$

$$= s(\theta) \sin(2m+1)\theta_c . \quad (5.19)$$

The predistorted wave  $y(\theta)$  then has a triangular shape:

$$y(\theta) = \arcsin \sin \theta \quad (5.20)$$

$$\left\{ \begin{array}{l} \theta , \quad 0 \leq \theta \leq \pi/2 \\ \pi - \theta , \quad \pi/2 \leq \theta \leq \pi \\ \theta - \pi , \quad \pi \leq \theta \leq 3\pi/2 \\ 2\pi - \theta , \quad 3\pi/2 \leq \theta \leq 2\pi \\ \theta - 2\pi , \quad 2\pi \leq \theta \leq 5\pi/2 \\ \dots \end{array} \right. \quad (5.21)$$

$$= \frac{\pi}{2} \cdot \frac{1}{2}(1 + \Lambda(\theta)) = \frac{\pi}{2}\Lambda(\theta)s(\theta) \quad (5.22)$$

Now

$$\sin(2m+1)y(\theta) = \begin{cases} \sin(2m+1)\theta \\ \sin[-(2m+1)\theta + (2m+1)\pi] \\ \sin[(2m+1)\theta - (2m+1)\pi] \\ \sin[-(2m+1)\theta + (2m+1)2\pi] \\ \sin[(2m+1)\theta - (2m+1)2\pi] \\ \dots \end{cases} \quad (5.23)$$

Subtracting multiples of  $2\pi$ ,

$$= \begin{cases} \sin(2m+1)\theta \\ \sin[-(2m+1)\theta + \pi] \\ \sin[(2m+1)\theta - \pi] \\ \sin[-(2m+1)\theta] \\ \sin[(2m+1)\theta] \\ \dots \end{cases} \quad (5.24)$$

$$= \sin(2m+1)\theta s(\theta) \quad (5.25)$$

Combining (5.25) and (5.19),

$$\begin{aligned} \sin(2m+1)\theta s(\theta) s(\theta) \sin(2m+1)\theta_c \\ = \sin(2m+1)\theta \sin(2m+1)\theta_c \end{aligned} \quad (5.26)$$

or

$$z_{2m+1}(\theta) = \sin(2m+1)\theta \quad (5.27)$$

The modulation of the  $k^{\text{th}}$  odd harmonic of the carrier is then simply a sinusoid of  $k$  times the frequency of the sinusoid modulating the carrier itself (Figure 5.1). The only spurious products generated are bandlimited and near the har-

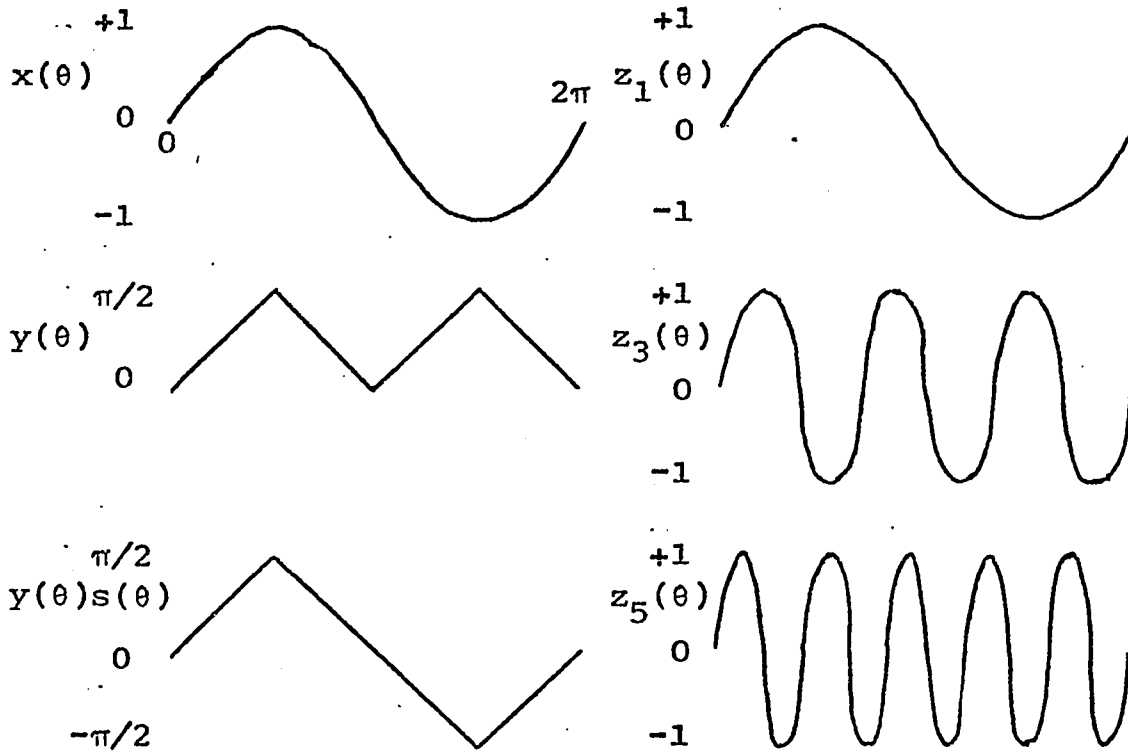


Figure 5.1. Modulating Functions for DSB/SC.

monics of the carrier.

This important result can be generalized for AM and DSB signals other than DSB/SC at maximum modulation. To do this, consider the power series given by Jolley (22):

$$\sin k \arcsin x = kx - \frac{k(k^2-1^2)}{3!}x^3 + \frac{k(k^2-3^2)}{5!}x^5 \dots \quad (5.28)$$

Since  $k$  is odd, the term containing  $x^{k+2}$  and all higher terms will contain the factor  $(k^2 - k^2) = 0$ . Thus the series terminates with  $x^k$ . For example,

$$\sin 3 \arcsin x = 3x - 4x^3, \quad (5.29)$$

and 
$$\sin 5 \arcsin x = 5x - 20x^3 + 16x^5. \quad (5.30)$$

When  $x(\theta)$  is composed of sinusoids and cosinusoids whose maximum frequency is  $\omega_x$ , it is apparent that the highest product of any combination of them will be of  $k^{\text{th}}$  order. Since the decomposition of  $\sin^k \theta$  or  $\cos^k \theta$  contains sinusoids and cosinusoids with arguments up to  $k\theta$ , it is also apparent that the spectrum of  $\sin k \arcsin x$  will be limited to  $k\omega_x$ .

To show that this is true for any bandlimited signal, consider the convolution process which is used to determine the spectrum of a product of two time functions. Here  $X_k(\omega)$  will denote the spectrum of  $x^k(\theta)$  and  $*$  will be used to denote convolution.

$$X_2(\omega) = X(\omega) * X(\omega) \quad (5.31)$$

$$= \frac{1}{2\pi} \int_{-\infty}^{+\infty} X(u) X(\omega-u) du \quad (5.32)$$

Since  $X(\omega)$  is bandlimited according to (5.1),

$$X_2(\omega) = \frac{1}{2\pi} \int_{-\omega_x}^{+\omega_x} X(u) X(\omega-u) du, \quad (5.33)$$

Now

$$X(\omega-u) = 0, \quad |\omega-u| > \omega_x, \quad (5.34)$$

thus

$$X(\omega-u) = 0, \quad |\omega| > 2\omega_x, \quad (5.35)$$

and

$$X_2(\omega) = 0, \quad |\omega| > 2\omega_x. \quad (5.36)$$

Extension of this yields

$$X_n(\omega) = 0, \quad |\omega| > n\omega_x. \quad (5.37)$$

The spectrum of  $x^n(\theta)$  is thus bandlimited to  $n$  times the bandwidth of  $x(\theta)$ . Since  $\sin k \arcsin x$  contains powers of  $x$  no higher than  $x^k$ , it is bandlimited to  $k$  times the original bandwidth.

One technicality remains:

$$\begin{aligned} z_k(\theta) &= \sin k \arcsin |x(\theta)| \cdot \operatorname{sgn} x(\theta) \\ &= \left[ k|x| - \frac{k(k^2-1^2)}{3!} |x|^3 + \dots \right] \operatorname{sgn} x(\theta) \end{aligned} \quad (5.38)$$

noting that

$$x = |x| \operatorname{sgn} x, \quad (5.39)$$

and

$$|x|^3 = x^3, \quad (5.40)$$

$$z_k(\theta) = \sin k \arcsin x(\theta), \quad (5.41)$$

and is therefore bandlimited. Computer simulations of the spectra of DSB/SC and AM signals are shown in Figures 5.2 and 5.3.

The bandlimited characteristic of the inherent modulation of the harmonics of the carrier makes bipolar class D highly advantageous for RF amplification. For an ideal amplifier, no overlap between the desired carrier and its sidebands and the spurious products occurs unless the highest modulation frequency is greater than half the carrier frequency. Thus for AM, DSB, or SSB generated by interlacing or overlapping, it is possible to remove the spurious products as completely



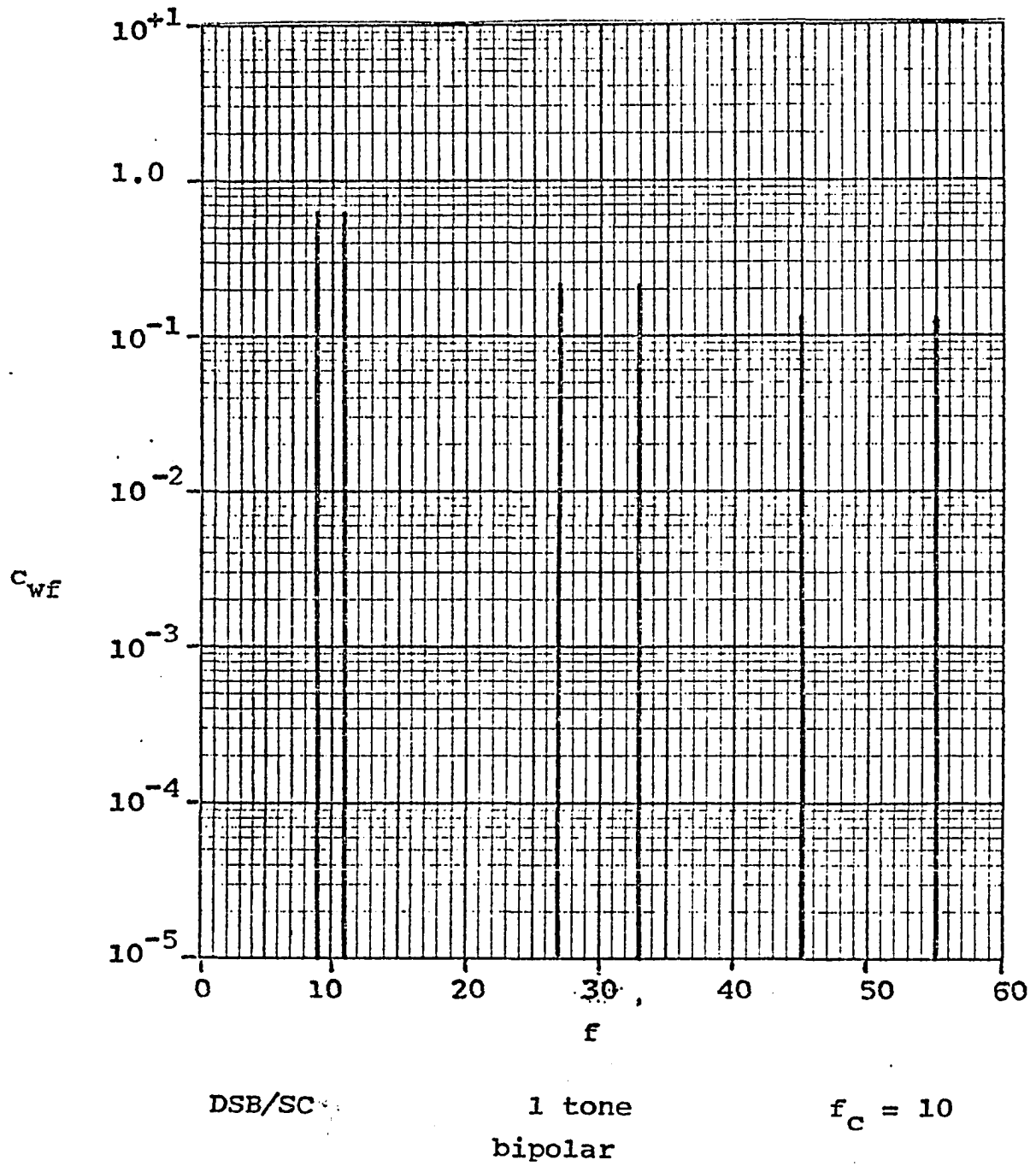


Figure 5.2. Spectrum of a Class D RF Amplifier.

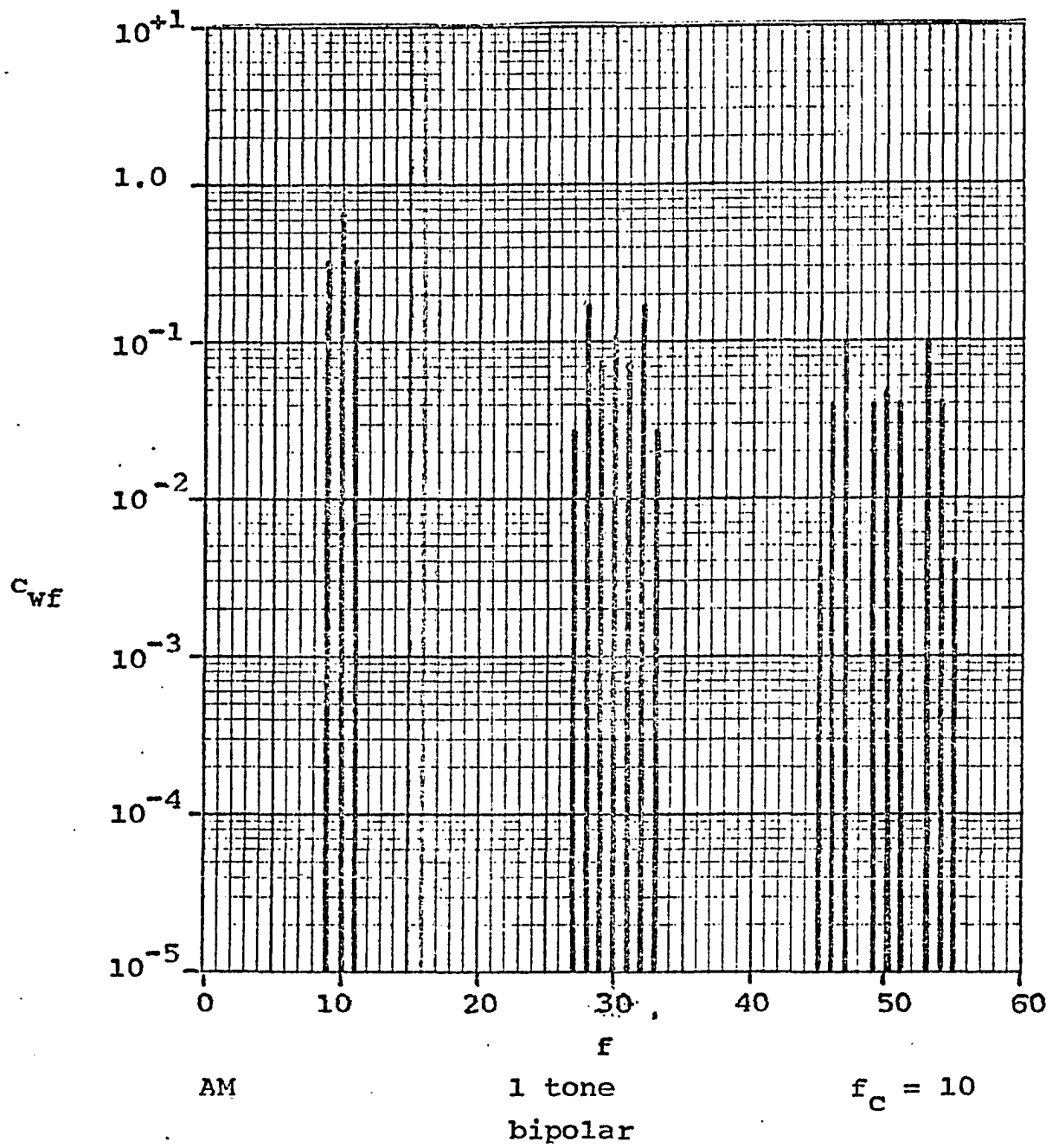


Figure 5.3. Spectrum of a Class D RF Amplifier.

as desired. This is not the case with audio PWM, where spurious products fall in the signal bandwidth and cannot, therefore, be removed.

Unfortunately, class D SSB generation using envelope and phase modulation does not have this property. Since  $\varphi(\theta)$  is no longer limited to only 0 or  $\pi$ , the form of  $w(\theta)$  cannot be limited simply to a series of sine waves, as in (5.7). Now

$$w(\theta) = \frac{4}{\pi} \sum_{m=1}^{\infty} \frac{\sin(2m+1)y(\theta)}{2m+1} \sin(2m+1)[\theta_c + \varphi(\theta)] \quad (5.42)$$

$$= \frac{4}{\pi} \sum_{m=0}^{\infty} \frac{\sin(2m+1)y(\theta)}{2m+1} \cos(2m+1)\varphi(\theta) \sin(2m+1)\theta_c + \sin(2m+1)\varphi(\theta) \cos(2m+1)\theta_c \quad (5.43)$$

$$= \frac{4}{\pi} \sum_{m=0}^{\infty} \frac{1}{2m+1} [z_{p\ 2m+1}(\theta) \sin(2m+1)\theta_c + z_{q\ 2m+1}(\theta) \cos(2m+1)\theta_c] \quad (5.44)$$

where

$$z_{pk}(\theta) = \sin ky(\theta) \cos k\varphi(\theta) \quad , \quad (5.45)$$

$$z_{qk}(\theta) = \sin ky(\theta) \sin k\varphi(\theta) \quad , \quad (5.46)$$

$$y(\theta) = \arcsin E(\theta) \quad , \quad (5.47)$$

$$\varphi(\theta) = \arctan \frac{x_q(\theta)}{x_p(\theta)} \quad . \quad (5.48)$$

Consider the third harmonic of the carrier:

$$\cos 3\varphi(\theta) = 4 \cos^3 \varphi(\theta) - 3 \cos \varphi(\theta) \quad , \quad (5.49)$$

$$\sin 3\varphi(\theta) = 3 \sin \varphi(\theta) - 4 \sin^3 \varphi(\theta) \quad , \quad (5.50)$$

$$\sin 3\gamma(\theta) = 3E(\theta) - 4E^3(\theta) \quad , \quad (5.51)$$

$$\begin{aligned} z_p^3(\theta) = & -9E(\theta)\cos\varphi(\theta) + 12E(\theta)\cos^3\varphi(\theta) \\ & + 12E^3(\theta)\cos\varphi(\theta) - 16E^3(\theta)\cos^3\varphi(\theta) \quad , \quad (5.52) \end{aligned}$$

$$\begin{aligned} z_q^3(\theta) = & 9E(\theta)\sin\varphi(\theta) - 12E(\theta)\sin^3\varphi(\theta) \\ & - 12E^3(\theta)\sin\varphi(\theta) + 16E^3(\theta)\sin^3\varphi(\theta) \quad . \quad (5.53) \end{aligned}$$

(Terms such as  $E^{2n+1}(\theta)\cos^{2m+1}(\theta)$  are generated for any odd harmonic.)

In the triangle of Figure 3.7, it is apparent that

$$E(\theta)\cos \varphi(\theta) = x_p(\theta) \quad (5.54)$$

$$E(\theta)\sin \varphi(\theta) = x_q(\theta) \quad , \quad (5.55)$$

so both terms containing these factors are bandlimited.

Since

$$E^3(\theta)\cos^3\varphi(\theta) = x_p^3(\theta) \quad , \quad (5.56)$$

it is bandlimited by (5.37), as is  $E^3(\theta)\sin^3\varphi(\theta)$ .

Now

$$E^2(\theta) = x_p^2(\theta) + x_q^2(\theta) \quad , \quad (5.57)$$

and since both  $x_p^2(\theta)$  and  $x_q^2(\theta)$  are bandlimited by (5.37),

$E^2(\theta)$  must also be bandlimited. Now

$$E^3(\theta)\cos\varphi(\theta) = E^2(\theta)x_p(\theta) \quad (5.58)$$

and

$$E^3(\theta)\sin\varphi(\theta) = E^2(\theta)x_q(\theta) \quad . \quad (5.59)$$

Since both factors on the right are bandlimited, the term on the left must also be bandlimited by generalizing (5.57).

The terms remaining are

$$E(\theta)\cos^3\varphi(\theta) = x_p(\theta)\cos^2\varphi(\theta) \quad (5.60)$$

and

$$E(\theta)\sin^3\varphi(\theta) = x_q(\theta)\sin^2\varphi(\theta) \quad (5.61)$$

The terms  $\cos^2\varphi(\theta)$  and  $\sin^2\varphi(\theta)$  are not bandlimited. It is difficult to say much about the nature of these terms for anything other than a two-tone signal, which is equivalent to DSB/SC, and therefore yields no information.

However, it is possible to determine the nature of the discontinuities, which yields information on the asymptotic behavior of the spectra.

Since  $x_p(\theta)$  and  $x_q(\theta)$  are continuous,  $x_q(\theta)/x_p(\theta)$  and hence  $\varphi(\theta)$  are continuous, except when  $E(\theta)$  is near zero (a change from 0 to  $2\pi$  is not a discontinuity). When  $x_p(\theta)$  is zero, the arctangent function suppresses the abrupt change in  $\varphi$ . Thus the slope is continuous and cannot change instantaneously as either  $x_p$  or  $x_q$  goes through 0.

For  $x_p(\theta)$  and  $x_q(\theta)$  near zero,

$$x_p(\theta) \approx 0 + x'_p(\theta) d\theta \quad (5.62)$$

$$x_q(\theta) \approx 0 + x'_q(\theta) d\theta \quad (5.63)$$

Thus

$$\frac{x'_q(\theta)(-d\theta)}{x'_p(\theta)(-d\theta)} = \frac{x'_q(\theta)(d\theta)}{x'_p(\theta)(d\theta)} = \frac{x'_q(\theta)}{x'_p(\theta)} \quad (5.64)$$

The arctangent function, however, changes by  $\pi$  when the change in quadrant occurs (Figure 5.4).

A change of  $\pi$  in  $\varphi$  produces a sign reversal in  $\cos \varphi$  and  $\sin \varphi$ , but no change in  $\cos^2 \varphi$  or  $\sin^2 \varphi$ ,

$$\cos^2[\varphi(\theta) \pm \pi] = [-\cos \varphi(\theta)]^2 = \cos^2 \varphi(\theta) \quad (5.65)$$

$$\sin^2[\varphi(\theta) \pm \pi] = [-\sin \varphi(\theta)]^2 = \sin^2 \varphi(\theta) \quad (5.66)$$

Thus there are no abrupt jumps in  $\sin^2 \varphi(\theta)$  or  $\cos^2 \varphi(\theta)$ . The derivatives of these are

$$\frac{d}{d\theta} \cos^2[\varphi(\theta)] = -2\cos \varphi(\theta) \sin \varphi(\theta) \frac{d\varphi(\theta)}{d\theta} \quad (5.67)$$

$$\frac{d}{d\theta} \sin^2[\varphi(\theta)] = 2\sin \varphi(\theta) \cos \varphi(\theta) \frac{d\varphi(\theta)}{d\theta} \quad (5.68)$$

These equations indicate the possibility of an impulsive first derivative. Hence the spectrum must decrease asymptotically at least as fast as  $1/f$  (see Bracewell (23)). One might expect these spurious products to behave somewhat similarly to the timing error spurious products for DSB/SC (discussed later).

Simulations of the spectra of signals composed of three unsymmetrical tones and two unequal tones are shown in Figure 5.5 and 5.6. Note that neither of these signals can be construed as a DSB/SC signal. A simulation with the tones interchanged produced sideband reversals around the harmonics of the carrier (not shown). (The spurious products at approxi-

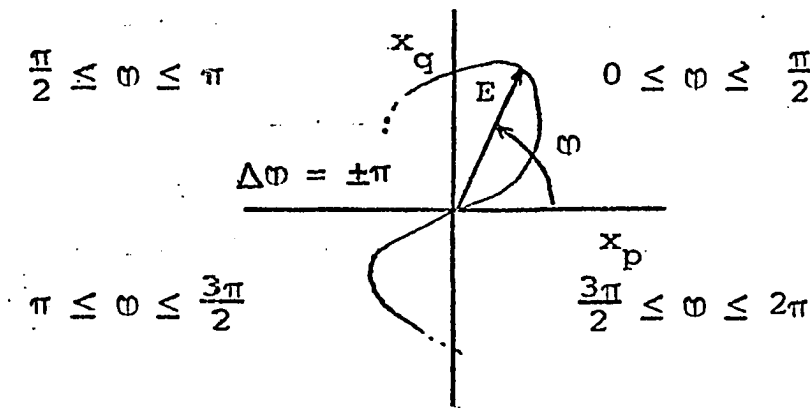


Figure 5.4. Locus of  $E(\theta)$  and  $\phi(\theta)$ .

mately  $5 \cdot 10^{-5}$  may be computer errors; see Appendix III.) In the three tone case, the ratio of the carrier frequency to modulation frequency ( $\alpha$ ) is approximately 6.7, and spurious products are approximately 50 dB below the signal at  $f_c$ . For the two tone signal,  $\alpha \approx 20$ , and the spurious products are 80 dB below the signal. It therefore appears that for practical values of  $\alpha$ , splatter from the odd harmonics of  $f_c$  will not be serious.

#### B. Monopolar PWM

The spectrum of monopolar class D is of interest for two reasons: First, monopolar PWM can be implemented by simpler circuitry than bipolar PWM, since neither a negative power supply nor a negative switch position is required. Secondly, a difference in the positive and negative supply voltages can

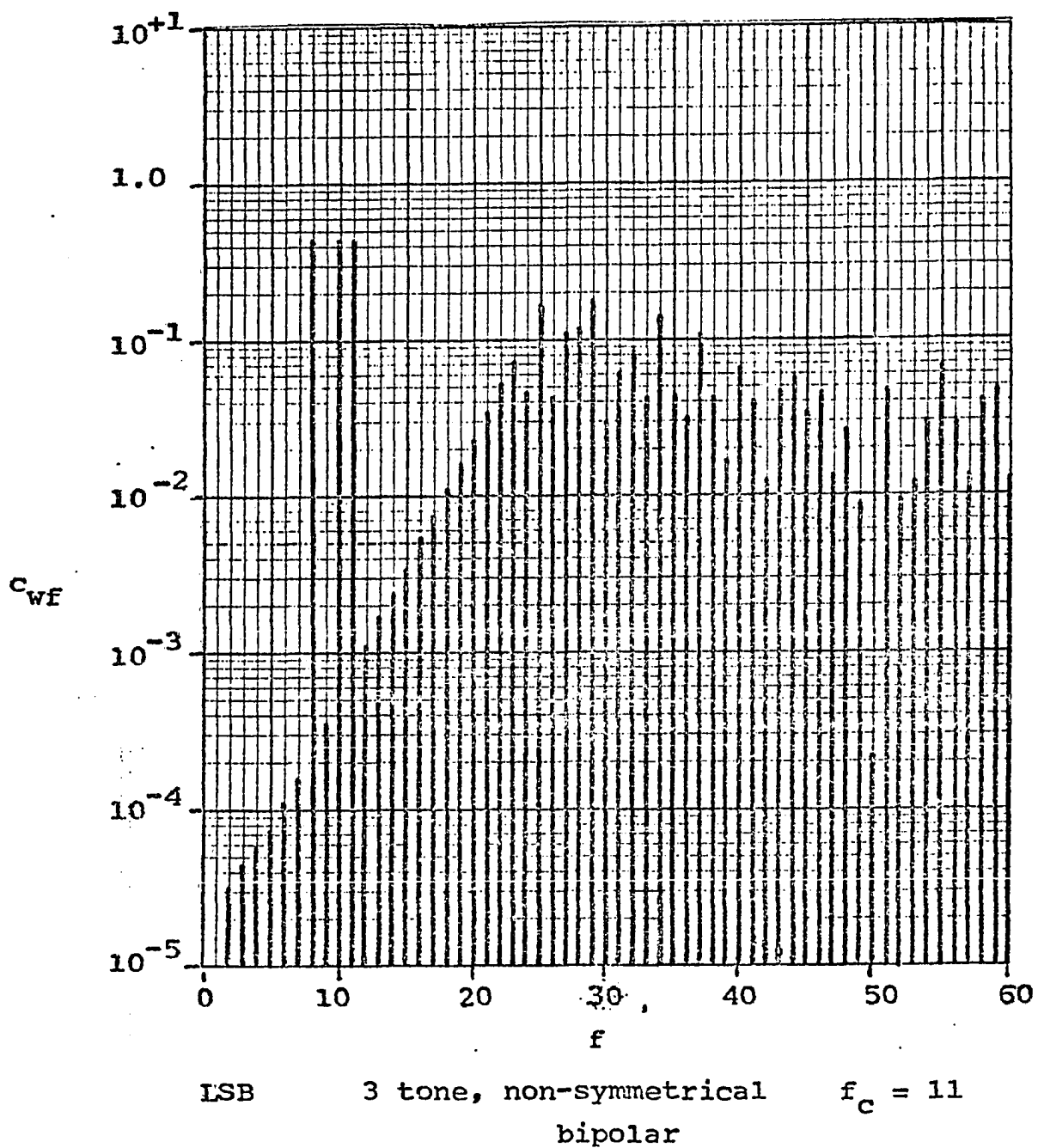


Figure 5.5. Spectrum of a Class D RF Amplifier.





inject a small monopolar pulse train in addition to the desired bipolar pulse train (Figure 5.7). In the following analysis, a 1V monopolar pulse train will be used; by multiplying its terms by the per cent voltage error, the spectra for a given voltage error can be found.

From (4.19), the monopolar pulse train is

$$w(\theta) = \frac{y(\theta)}{\pi} + \frac{2}{\pi} \sum_{m=1}^{\infty} \left[ \frac{(-1)^m}{2m} \sin 2m\gamma \cos 2m\theta + \frac{(-1)^{m+1}}{2m-1} \sin(2m-1)\gamma \sin(2m-1)\theta \right] \quad (5.69)$$

which for AM or DSB/SC can be resolved to

$$w(\theta) = \frac{y(\theta)}{\pi} + \frac{2}{\pi} \sum_{m=1}^{\infty} \left[ \frac{z_{2m}(\theta)}{2m} \cos 2m\omega_c t + \frac{z_{2m-1}(\theta)}{2m-1} \sin(2m-1)\omega_c t \right]. \quad (5.70)$$

Consider first the example of DSB/SC used for the bipolar case. As before,

$$\phi(\theta) = \pi \frac{-\text{sgn } x(\theta) + 1}{2} = \pi \frac{-s(\theta) + 1}{2} \quad (5.71)$$

and

$$y(\theta) = \arcsin|x(\theta)| = \frac{\pi}{2} |\Lambda(\theta)| \quad (5.72)$$

The odd harmonics are modulated by the same functions as in the bipolar case. However, for the even harmonics

$$\sin 2m\gamma(\theta) = \begin{cases} \sin 2m\gamma(\theta) & , 0 \leq \theta < \frac{\pi}{2} \\ \sin [-2m\theta + 2m\pi] & , \frac{\pi}{2} \leq \theta \leq \pi \\ \sin [2m\theta - 2m\pi] & , \pi \leq \theta \leq \frac{3\pi}{2} \end{cases}$$

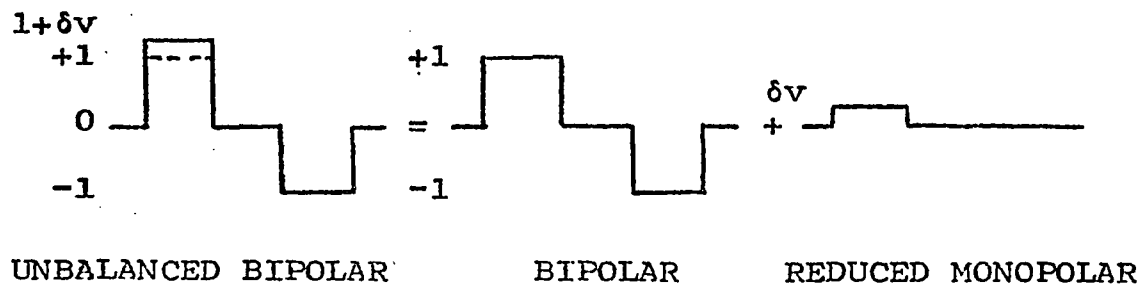


Figure 5.7. Waveform with Voltage Error.

$$\left\{ \begin{array}{l} \sin [-2m\theta + (2m-2)\pi] , \frac{3\pi}{2} \leq \theta \leq 2\pi \\ \sin [2m\theta - (2m-2)\pi] , 2\pi \leq \theta \leq \frac{5\pi}{2} \\ \dots \end{array} \right. \quad (5.73)$$

Removing multiples of  $2\pi$ ,

$$\sin 2m\varphi(\theta) = \begin{cases} \sin 2m\theta \\ -\sin 2m\theta \\ \sin 2m\theta \\ -\sin 2m\theta \\ \dots \end{cases} \quad (5.74)$$

$$= \sin 2m\theta s(2\theta) \quad (5.75)$$

Now

$$\cos 2m[\theta_c + \varphi(\theta)] = \cos[2m\theta_c + 2m\varphi(\theta)] \quad (5.76)$$

$$= \cos 2m\theta_c \quad (5.77)$$

because  $2m\varphi(\theta)$  produces only multiples of  $2\pi$ . Thus as in Figure 5.8,

$$z_{2m}(\theta) = \sin 2m\theta s(2\theta) \quad (5.78)$$

The modulation functions for  $k$  even and  $y(\theta)$  have sharp

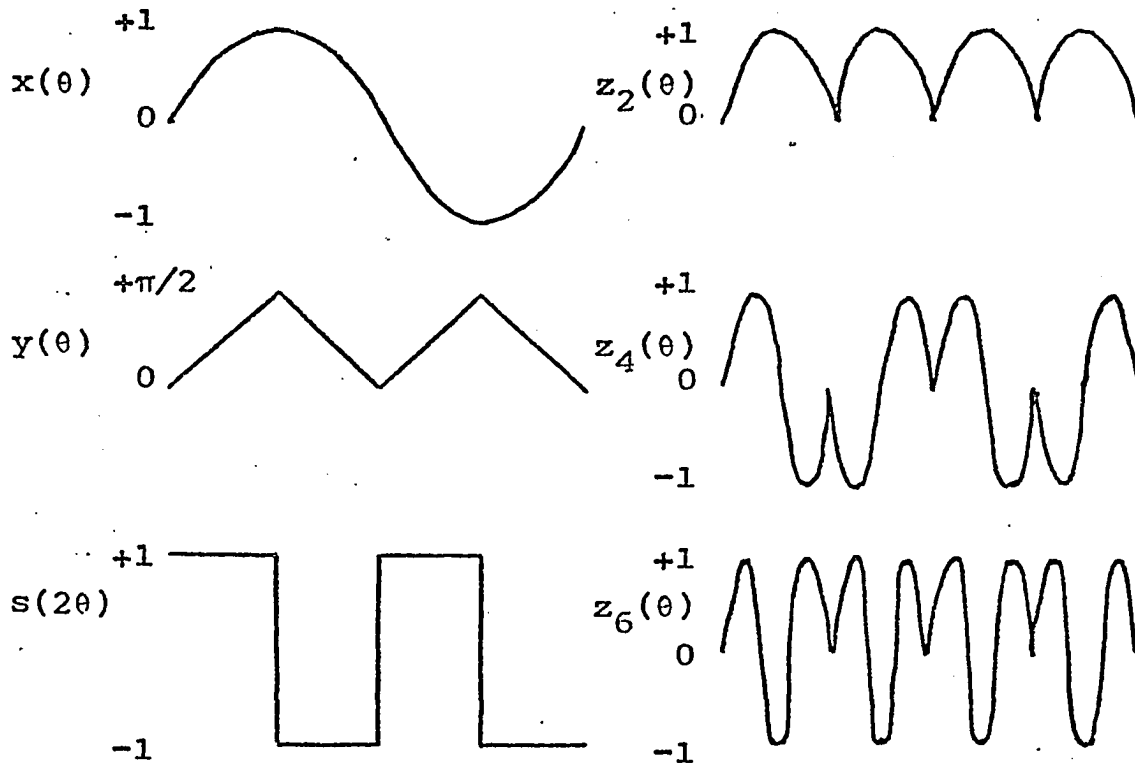


Figure 5.8. Modulation of Even Harmonics for DSB/SC.

corners, thus are not bandlimited. Inclusion of the even harmonics of the carrier can thus generate non-removable splatter. Some limits on this are determined in Chapter VII.

The characteristics just determined for sinusoidal modulation can be generalized for other AM and DSB/SC signals. First note that phase shifts to reverse the polarity of the fundamental always shift the even harmonics by multiples of  $2\pi$ , thus producing no effect on them.

As before,  $\sin k \arcsin x$  can be expanded in a series:

$$z_k(\theta) = \sin k \arcsin |x(\theta)| \quad (5.79)$$

$$= k|x| - \frac{k(k^2-1^2)}{3!} |x|^3 + \frac{k(k^2-1^2)(k^2-3^2)}{5!} |x|^5 \dots \quad (5.80)$$

$$= \left[ kx - \frac{k(k^2-1^2)}{3!} x^3 + \frac{k^2(k^2-1)(k^2-3^2)}{5!} x^5 \dots \right] \operatorname{sgn} x \quad (5.81)$$

$$= \sin k \arcsin x(\theta) \operatorname{sgn} x(\theta) \quad (5.82)$$

The infinite series will not be bandlimited in general, because it never terminates ( $k$  is even). When an AM signal is used,  $\operatorname{sgn} x(\theta)$  will be bandlimited, but not for DSB/SC where negative modulation is involved. Simulations of the spectra of DSB/SC and AM generated by monopolar PWM are shown in Figures 5.9 and 5.10.

### C. Saturation Voltage

Non-zero saturation voltages can also introduce spurious signals. The dominant effect, based upon observations of the prototype, is that of a saturation voltage, introducing a square waveform, but there is also some resistive voltage drop, which adds a slight curvature (Figure 5.11).

Any exact analysis would be very complicated. However, by the use of several simplifying assumptions, some reasonable results can be obtained. Consider the saturated transistor characteristics shown in Figure 5.12. First, assume that the current flowing in the output is approximately the same as with no saturation voltages. The actual effect shown in (a) is difficult to handle. However, a piecewise linearization (b) simplifies the problem. Unfortunately, the transition

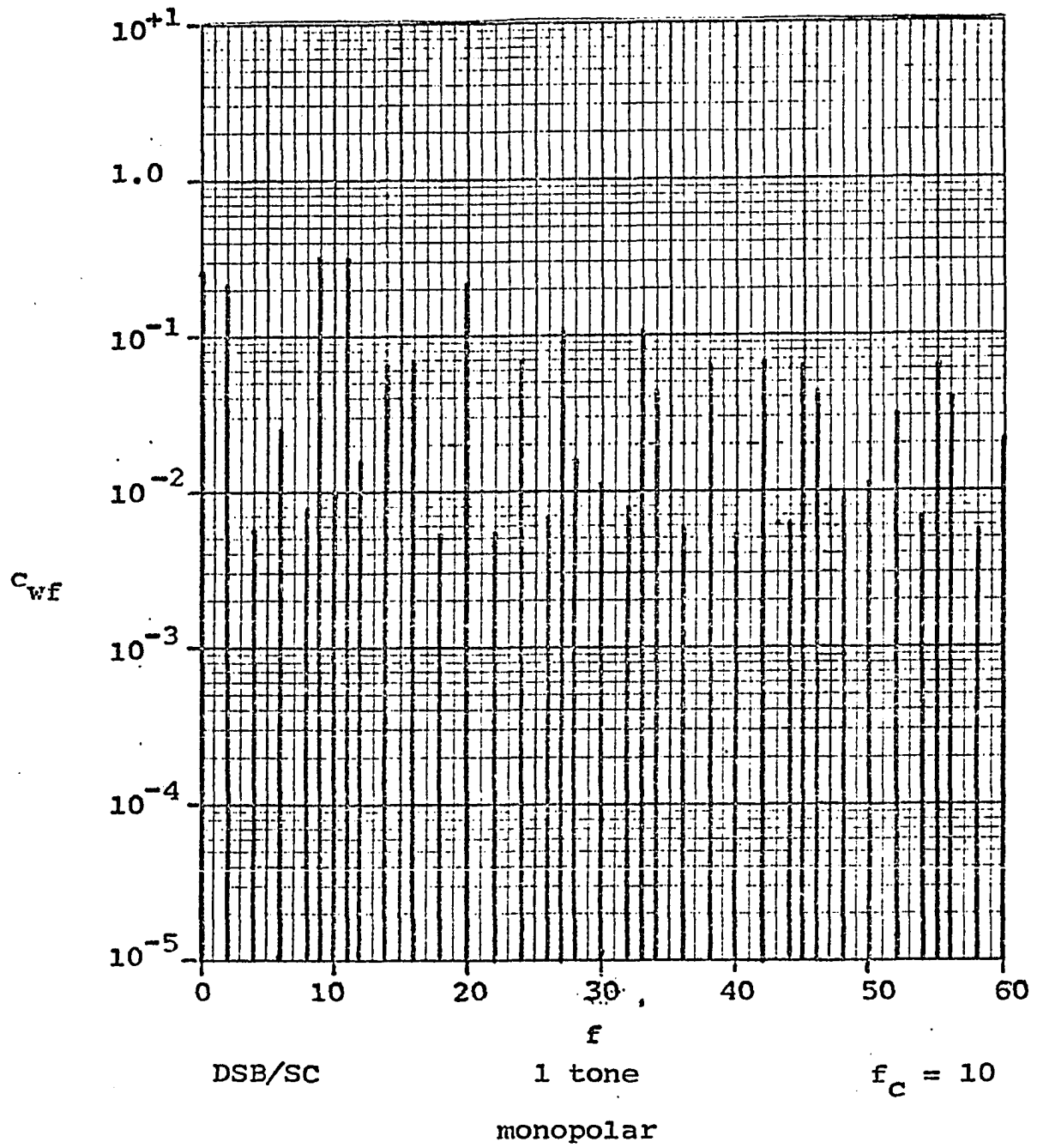


Figure 5.9. Spectrum of a Class D RF Amplifier.



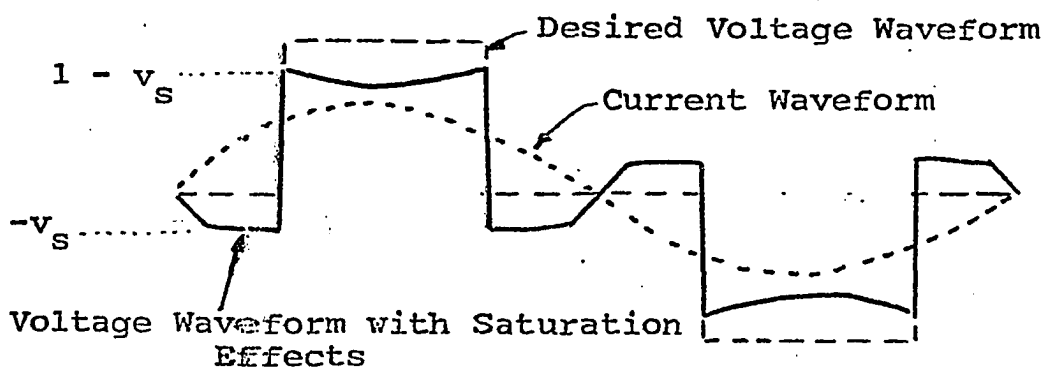


Figure 5.11. Saturation Voltage Effects.

from one slope to another is a complicated function of the modulation function.

This problem is eliminated by the use of (c). When current flows, voltage  $v_s$  is obtained instantly, followed by a small increase with increasing current. The effect of the changing current flow is to produce a small voltage, proportional to the output voltage, but of opposite polarity. The only consequence of this is a slight reduction in the output, and will therefore be neglected, and the more simple model (d) used.

Under the assumptions made above, the only serious effect of saturation voltage is to generate a square wave whose magnitude is  $v_s$ , with polarity opposite that of the current flowing:

$$u_s(\theta) = -v_s \operatorname{sgn} i_o(\theta) \quad (5.83)$$

$$= -v_s \operatorname{sgn} [x(\theta) \sin \theta_c] \quad (5.84)$$



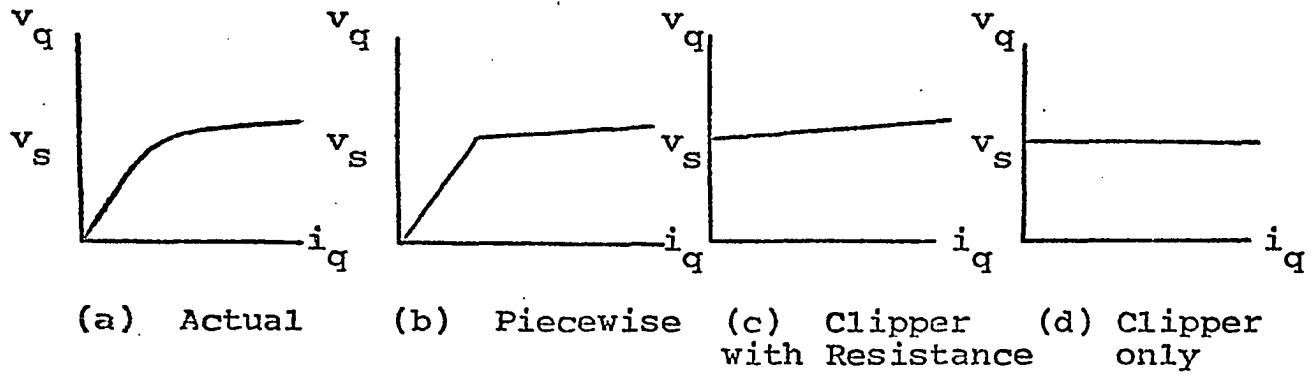


Figure 5.12. Saturation Effect Approximations.

$$= -v_s \operatorname{sgn} x(\theta) s(\theta_c) \quad (5.85)$$

For an AM signals,  $x(\theta) \geq 0$ , so

$$\operatorname{sgn} x(\theta) = 1 \quad (5.86)$$

and

$$u_s(\theta) = -v_s s(\omega_c t) \quad (5.87)$$

$$= \frac{-4v_s}{\pi} \sum_{m=1}^{\infty} \frac{1}{2m-1} \sin(2m-1)\omega_c t \quad (5.88)$$

In this case, the only effect is a change in the carrier level, proportional to  $v_s$ , which probably will not be harmful.

However, for a DSB/SC signal,  $\operatorname{sgn} x(\theta)$  changes, and intermodulation distortion results. In the case of sinusoidal modulation,

$$\operatorname{sgn} x(\theta) = \operatorname{sgn} \sin \theta = s(\theta) \quad (5.89)$$

and

$$u_s(\theta) = -v_s s(\theta) s(\omega_c t) \quad (5.90)$$

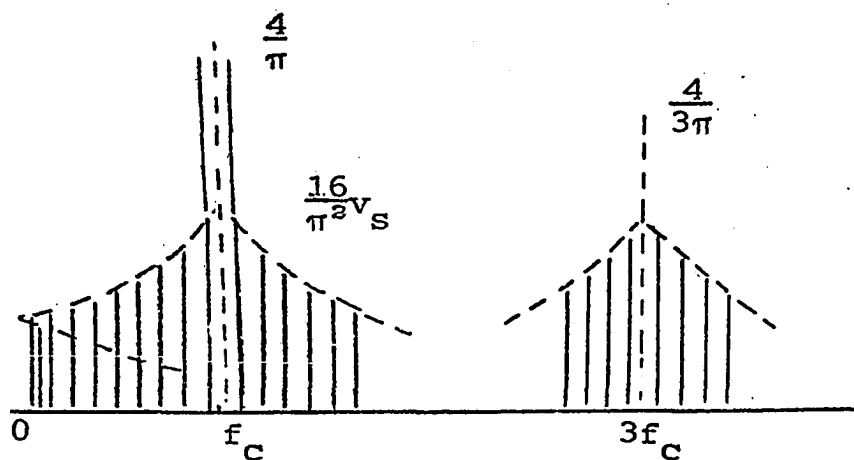


Figure 5.13. Spurious Products due to non-zero Saturation Voltage.

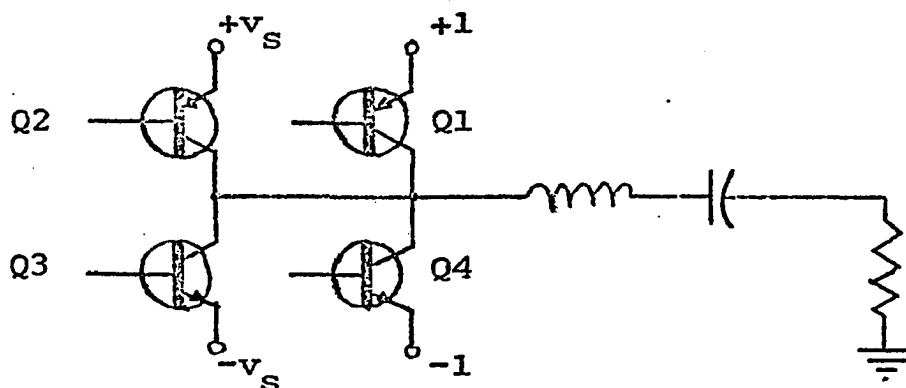


Figure 5.14. Circuit Changes to Reduce Saturation Voltage Spurious Products.

The products generated fall off as  $1/f$  and occur at odd multiples of  $f_x$  from odd harmonics of the carrier frequency, as shown in Figure 5.13. The severity of this IMD is not reduced by reducing the modulation depth.

Depending on the severity of these products, it might

be desirable to replace the ground connection of output transistors Q2 and Q3 with voltages equal to  $v_s$ . This not only improves the efficiency slightly, but can remove most of the spurious product generated (Figure 5.14).

## VI. PULSE TIMING DISTORTION

Two distortion problems peculiar to the class D RF amplifier are errors in pulse length (bias) and non-zero transition times. The primary effects of both of these problems are shown to produce intermodulation distortion.

Several assumptions will be necessary to arrive at a meaningful characterization of the spurious products. The basic method will be to add a distortion waveform  $u(\theta)$ , which changes the ideal waveform  $w(\theta)$  to the distorted waveform  $w_D(\theta)$ . One critical assumption is that the effects of  $u(\theta)$  overlapping itself for large pulse widths, and the effects of pulse deterioration for small pulse widths can be neglected. A small value of bias or rise time will also be assumed, when needed, since a class D amplifier with large errors would either have too much distortion or be inefficient.

When products generated by the distortion wave  $u(\theta)$  have the same form as the desired signal or the distortion products already present, they will be neglected. There is very little practical difference between a spurious product 20dB below the desired signal and one which is 20.1dB below the signal. What is important is new spurious products appearing in places where there were no spurious products without the timing distortion.

### A. Pulse Bias Distortion

Pulse bias distortion occurs when a pulse is transferred from one amplifier to another. In Figure 6.1, the input pulse suffers from unequal rise and fall times, and the second (output) amplifier does not cut in half way between the on and off levels of the input. As a result, the turn off transition is delayed more than the turn on transition, and the pulse is elongated.

To analyze the spurious products produced by such a process, let the desired pulse train be distorted by lengths  $\tau_1$ ,  $\tau_2$ ,  $\tau_3$ , and  $\tau_4$ , as shown in Figure 6.2. Note that the  $\tau_i$  are in terms of one cycle at the carrier frequency, *i.e.*, if  $t_i$  is the actual length of time involved,

$$\tau_i = t_i \frac{2\pi}{f_c} \quad (6.1)$$

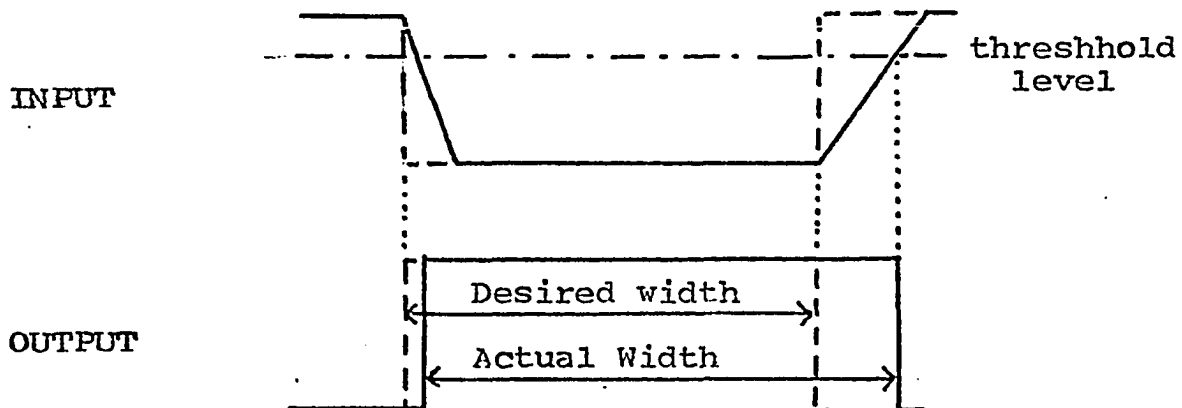


Figure 6.1. Cause of Pulse Bias.

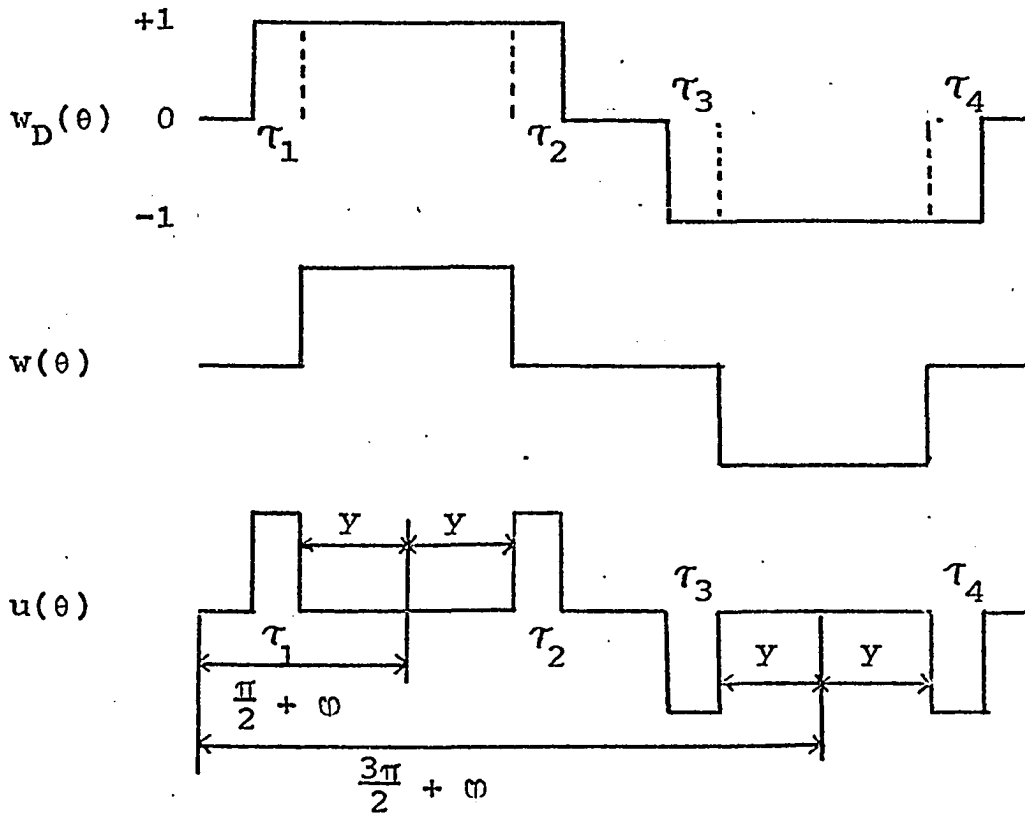


Figure 6.2. Bias Distortion Waveform.

The distorted wave is decomposed into the ideal wave and the distorted wave:

$$w_D = w(\theta) + u(\theta) \quad (6.2)$$

The distortion waveform can in turn be decomposed into four waveforms:

$$u_B(\theta) = u_{B1}(\theta) + u_{B2}(\theta) + u_{B3}(\theta) + u_{B4}(\theta) \quad (6.3)$$

Each of these four waveforms represents a monopolar pulse of constant width with position depending on  $y(\theta)$  and  $\varphi(\theta)$ . Attention will first be focused on  $u_{B1}(\theta)$ , and the results then extended to the other waveforms and combined. By

use of (4.12).

$$u_{B1}(\theta) = f_+ \left\{ \omega_c t, \tau_1, \frac{\pi}{2} - \left[ y(\theta) - \frac{\tau_i}{2} + \varphi(\theta) \right] \right\} \quad (6.4)$$

$$= \frac{1}{2\pi} + \frac{2}{\pi} \sum_{n=1}^{\infty} \frac{\sin \frac{n\tau_1}{2}}{n} \cos \left\{ n\omega_c t - n \left[ \frac{\pi}{2} - \left( y + \frac{\tau_i}{2} \right) + \varphi \right] \right\} \quad (6.5)$$

First approximate

$$\frac{\sin \frac{n\tau_1}{2}}{n} \approx \frac{\tau_1}{2} = \frac{\tau_1}{2} ; \quad (6.6)$$

this will be valid for low frequencies, but will make higher frequencies stronger than they really are. In the argument of the cosine in (6.5), approximate

$$y + \frac{\tau_i}{2} \approx y . \quad (6.7)$$

The cosine then takes the form

$$\cos \psi = \cos \left[ n\omega_c t - \frac{n\pi}{2} + n(y-\varphi) \right] \quad (6.8)$$

$$= \begin{cases} (-1)^{\frac{n}{2}} \cos[n\omega_c t + n(y-\varphi)] & , n \text{ even} \\ (-1)^{\frac{n-1}{2}} \sin[n\omega_c t + n(y-\varphi)] & , n \text{ odd} \end{cases} \quad (6.9)$$

$$= \begin{cases} (-1)^{\frac{n}{2}} [\cos n(y-\varphi) \cos \omega_c t - \sin n(y-\varphi) \sin \omega_c t] & \\ (-1)^{\frac{n-1}{2}} [\cos n(y-\varphi) \sin \omega_c t + \sin n(y-\varphi) \cos \omega_c t] & \end{cases} \quad (6.10)$$

Thus the Fourier coefficients of  $u_{B2}(\theta)$  are

$$a_{u_{B1}0}(\theta) = \frac{\tau_1}{2\pi} \quad (6.11)$$

$$a_{u_{B1}n}(\theta) \cong \frac{\tau_1}{\pi} \begin{cases} (-1)^{\frac{n}{2}} \cos n(y-\varphi) & , n \text{ even} \\ (-1)^{\frac{n-1}{2}} \sin n(y-\varphi) & , n \text{ odd} \end{cases} \quad (6.12)$$

$$b_{u_{B1}n}(\theta) \cong \frac{\tau_1}{\pi} \begin{cases} -(-1) \sin n(y-\varphi) & , n \text{ even} \\ (-1) \cos n(y-\varphi) & , n \text{ odd} \end{cases} \quad (6.13)$$

In the case of DSB signals,  $\varphi = 0$  or  $\pi$ , and

$$\cos n(y-\varphi) = \begin{cases} \cos ny \operatorname{sgn} x, & n \text{ odd} \\ \cos ny & , n \text{ even} \end{cases} \quad (6.14)$$

and

$$\sin n(y-\varphi) = \begin{cases} \sin ny \operatorname{sgn} x, & n \text{ odd} \\ \sin ny & , n \text{ even} \end{cases} \quad (6.15)$$

Thus

$$a_{u_{B1}n}(\theta) = \frac{\tau_1}{\pi} \begin{cases} (-1)^{\frac{n}{2}} \cos ny & , n \text{ even} \\ (-1)^{\frac{n-1}{2}} \sin ny \operatorname{sgn} x, & n \text{ odd} \end{cases} \quad (6.16)$$

$$b_{u_{B1}n}(\theta) = \frac{\tau_1}{\pi} \begin{cases} -(-1)^{\frac{n}{2}} \sin ny & , n \text{ even} \\ (-1)^{\frac{n-1}{2}} \cos ny \operatorname{sgn} x, & n \text{ odd} \end{cases} \quad (6.17)$$

By performing similar operations on the other three bias pulses,

$$a_{u_B0}(\theta) = \frac{\tau_1 + \tau_2 - \tau_3 - \tau_4}{2\pi} \quad (6.18)$$

The changes required for (6.16) and (6.17) are as follows:

For  $\tau_2$  and  $\tau_4$ ; replace  $y$  by  $-y$ .

$\tau_3$  and  $\tau_4$ ; multiply whole term by  $-1$ .



$$\tau_3 \text{ and } \tau_4; \quad \frac{n\pi}{2} \rightarrow \frac{3n\pi}{2} = \frac{n\pi}{2} + n\pi \quad (6.19)$$

This multiplies terms with odd  $n$  by  $-1$  and leaves even terms unchanged. Thus

$$a_{u_B^n}(\theta) = \begin{cases} \frac{\tau_1 + \tau_2 - \tau_3 - \tau_4}{\pi} (-1)^{\frac{n}{2}} \cos ny & , n \text{ even} \\ \frac{\tau_1 + \tau_2 + \tau_3 + \tau_4}{\pi} (-1)^{\frac{n-1}{2}} \sin ny \operatorname{sgn} x, & n \text{ odd} \end{cases} \quad (6.20)$$

$$b_{u_B^n}(\theta) = \begin{cases} \frac{-\tau_1 + \tau_2 + \tau_3 - \tau_4}{\pi} (-1)^{\frac{n}{2}} \sin ny & \\ \frac{\tau_1 + \tau_2 + \tau_3 + \tau_4}{\pi} (-1)^{\frac{n-1}{2}} \cos ny \operatorname{sgn} x, & n \text{ odd} \end{cases} \quad (6.21)$$

Now

$$\sin(2m-1)y \operatorname{sgn} x = z_{2m-1}(\theta) \quad , \quad (6.22)$$

so this term represents only the introduction of a low-level bandlimited signal of the same spectral shape of signals produced by the ideal signal.

$$\sin 2my = z_{2m}(\theta) \quad , \quad (6.23)$$

and is of the same form as modulation introduced by a voltage error or monopolar PWM.

To illustrate the significance of (6.20) and (6.21), consider DSB/SC sinusoidal modulation. From Figure 6.3, it is apparent that for odd  $n$ ,

$$\cos ny = \cos n\theta c(\theta) \quad , \quad (6.24)$$

so

$$\cos ny s(\theta) = \cos n\theta s(2\theta) \quad . \quad (6.25)$$

For even  $n$ ,

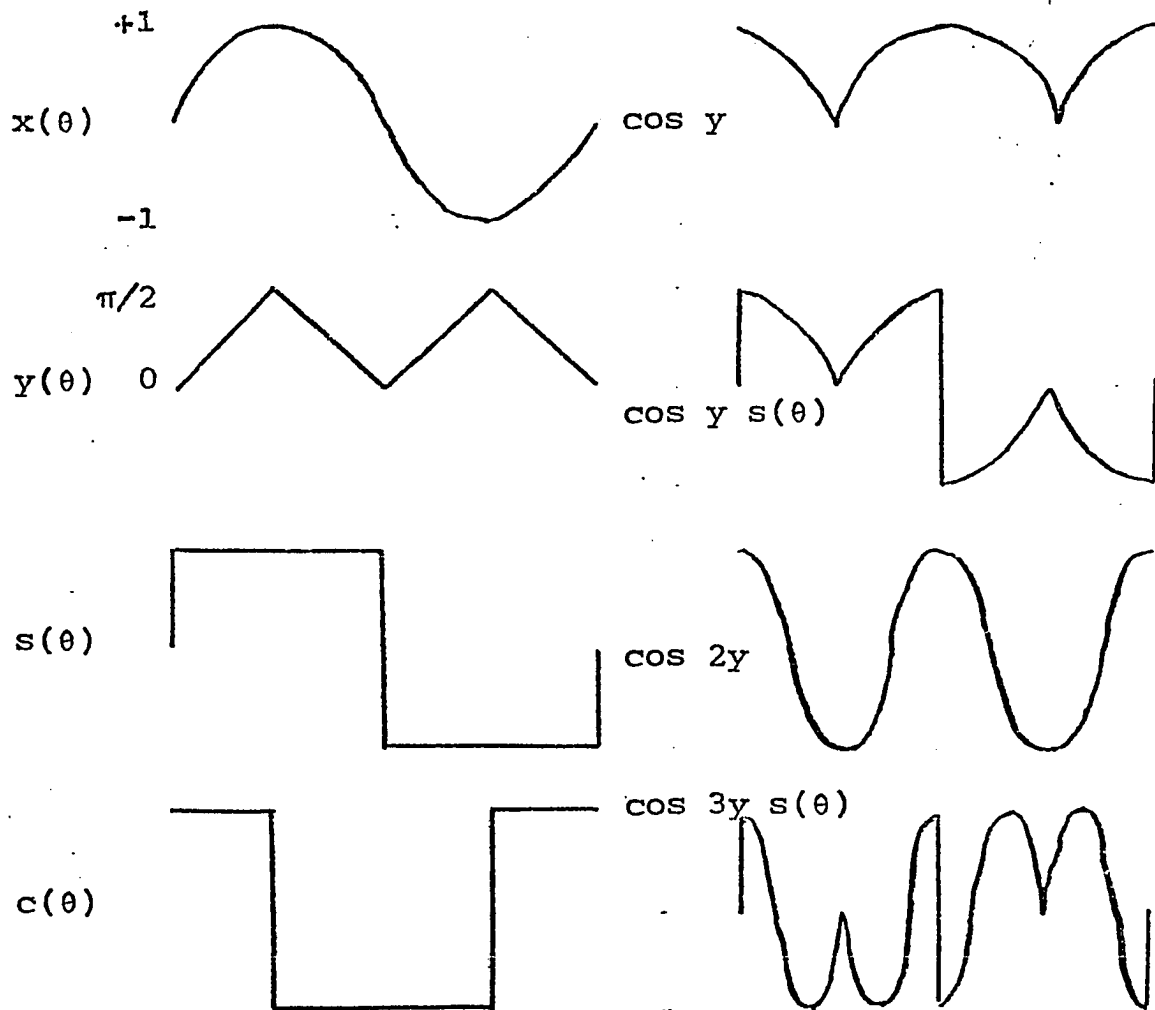


Figure 6.3. Modulation Functions for Timing Distortion.

$$\cos ny = \cos n\theta. \quad (6.26)$$

These results can be generalized for other than DSB/SC. The power series for  $\cos k \arcsin x$  is (see Jolley (22))

$$\cos k \arcsin x = 1 - \frac{k^2}{2!} x^2 + \frac{k^2(k^2-2^2)}{4!} x^4 - \dots \quad (6.27)$$

When  $k$  is even, this series terminates in the term containing  $x^k$ , since all higher order terms contain a factor of zero.

When  $k$  is odd, the series never terminates. Thus  $\cos 2m\gamma$  is bandlimited to  $2m$  the basic modulating frequency, and  $\cos (2m-1)\gamma \operatorname{sgn} x$  is not generally bandlimited.

As discussed earlier, the slight change in the desired signal level can be neglected. Also, the introduction of a bandlimited signal at the second harmonic is, although undesirable, not likely to be very harmful, since it can be removed by a filter. This leaves only the terms in (6.21) to cause harmful interference. Different types of spurious products which can be generated are shown in Figure 6.4. Equation (6.21) can then be used to write

$$u_B(\theta) \cong \frac{u_{0B}(\theta)}{2\pi} + \frac{\sigma_B}{\pi} \sum_{m=1}^{\infty} (-1)^m u_{2m-1}(\theta) \sin(2m-1)\omega_c t$$

$$+ \frac{\delta_B}{\pi} \sum_{m=1}^{\infty} (-1)^m u_{2m}(\theta) \sin 2m\omega_c t, \quad (6.28)$$

where

$$u_{0B}(\theta) = \tau_1 + \tau_2 - \tau_3 - \tau_4, \quad (6.29)$$

$$u_{2m}(\theta) = \sin 2m\gamma(\theta), \quad (6.30)$$

and

$$u_{2m-1}(\theta) = \cos(2m-1)\gamma(\theta) \operatorname{sgn} x(\theta) \quad (6.31)$$

$$= \operatorname{sgn} x - \frac{k^2}{2!} x^2 \operatorname{sgn} x + \frac{k^2}{4!} x^4 \operatorname{sgn} x - \dots \quad (6.32)$$

$$\sigma_B = \tau_1 + \tau_2 + \tau_3 + \tau_4 \quad (6.33)$$

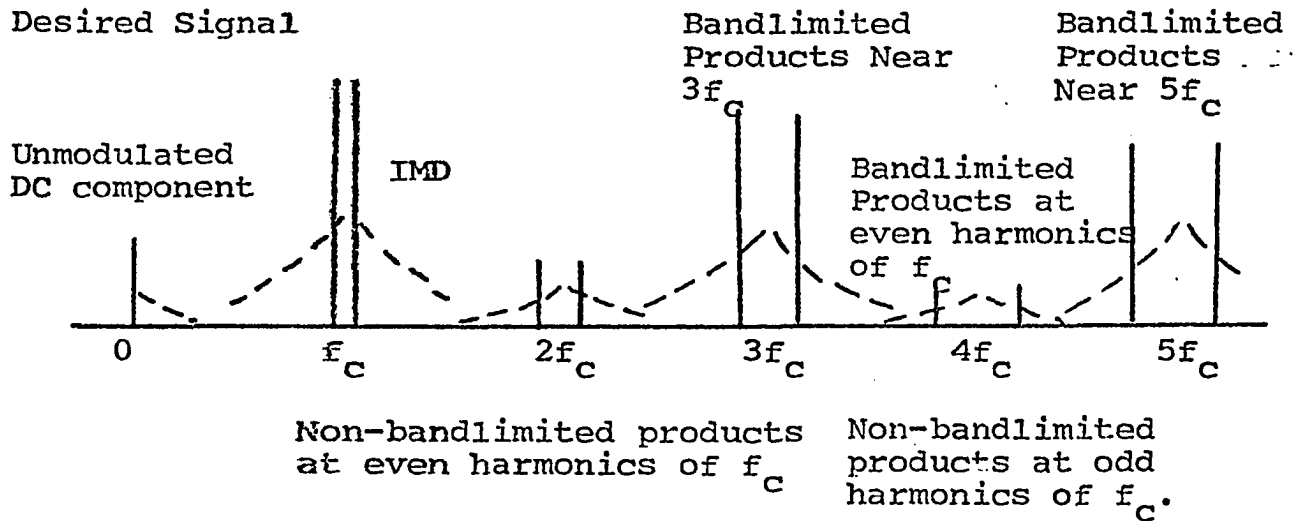


Figure 6.4. Types of Spurious Products due to Pulse Bias Distortion.

$$\delta_B = -\tau_1 + \tau_2 + \tau_3 - \tau_4 \quad (6.34)$$

For monopolar PWM, all the equations remain the same, with

$$\tau_3 = \tau_4 = 0 \quad (6.35)$$

The nature of these spurious products is discussed more fully in Chapters VII and VIII. However, there are some readily made observations. First, the most harmful interference should be due to the IMD ( $u(\theta)$ ), since the other spurious products will have decayed to small values near  $f_c$ . Secondly, the magnitude of the IMD for a given  $x(\theta)$  varies linearly with the bias error,  $\sigma_B$ . Thirdly, for AM signals,  $\text{sgn } x(\theta) = 1$ , which should reduce the IMD somewhat. The exact nature of the

IMD for SSB signals is difficult to determine without more involved study, but it should not be too different from that of DSB/SC, since both involve abrupt phase shifts. Simulations of AM and DSB generation with several levels of bias distortion are shown in Figures 6.5 and 6.6. Note that the maximum value of  $x$  was restricted so that overmodulation does not occur. Lowering the maximum value of  $x$  (modulation depth) tends to cause more rapid decay of the IMD, causing that generated by a 10% error to be smaller than that for a 1% error at a few frequencies.

#### B. Rise/Fall Time Distortion

An added correction waveform will again be used to determine the effects of non-zero rise and fall times on the spurious products of a class D amplifier (Figure 6.7). A truncated ramp rise and fall characteristic will be used for convenience. Again, the effects of overlapping and deterioration are ignored, so that

$$w_D(\theta) = w(\theta) + u_R(\theta) \quad (6.36)$$

and

$$u_R(\theta) = u_{R5}(\theta) + u_{R6}(\theta) + u_{R7}(\theta) + u_{R8}(\theta) \quad (6.37)$$

From (4.26), (4.30), and (4.34), which give the basic Fourier coefficients for a truncated ramp waveform,

$$a_{u_{R5}0} = \frac{-T_5}{4\pi} \quad (6.38)$$

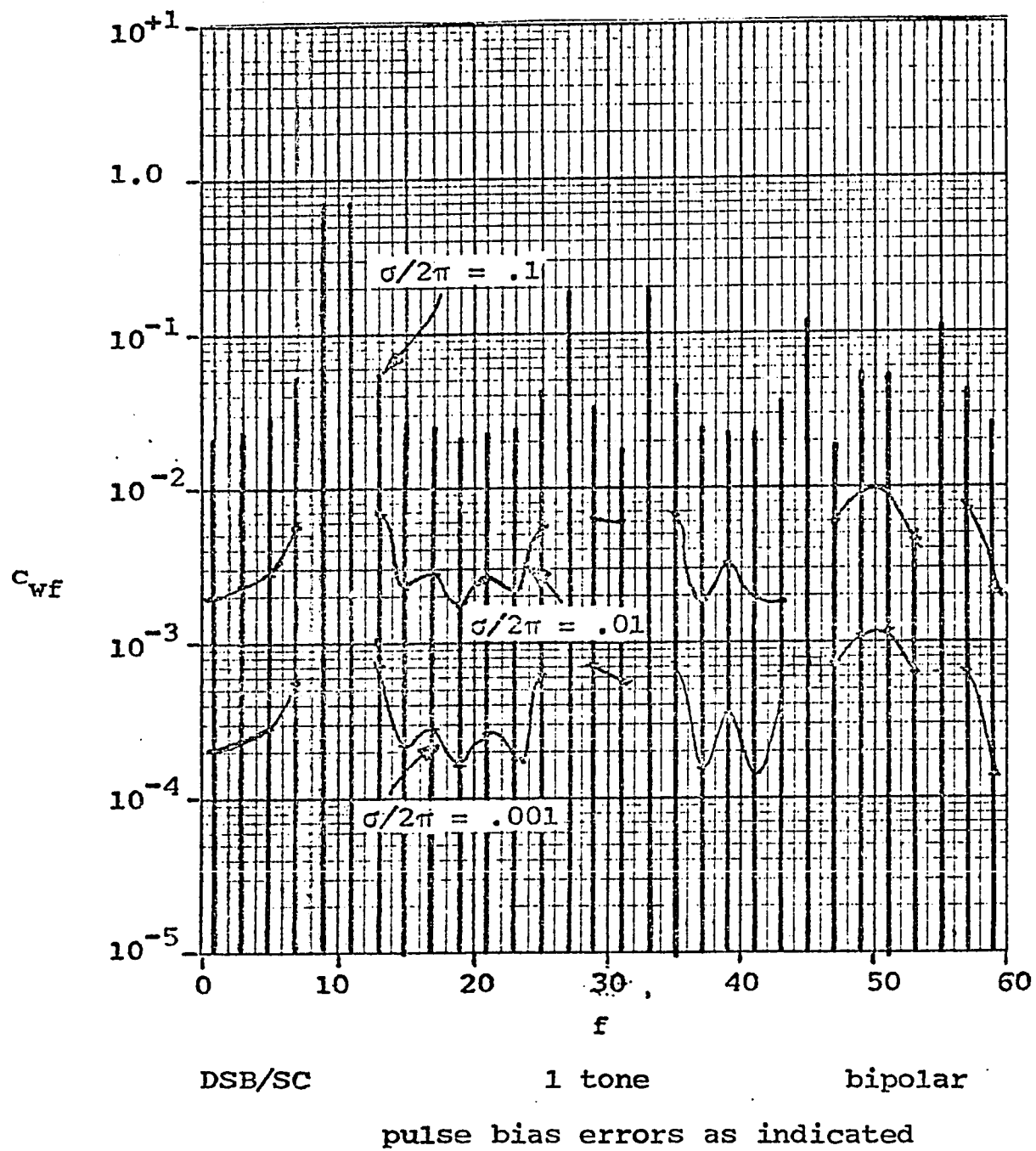
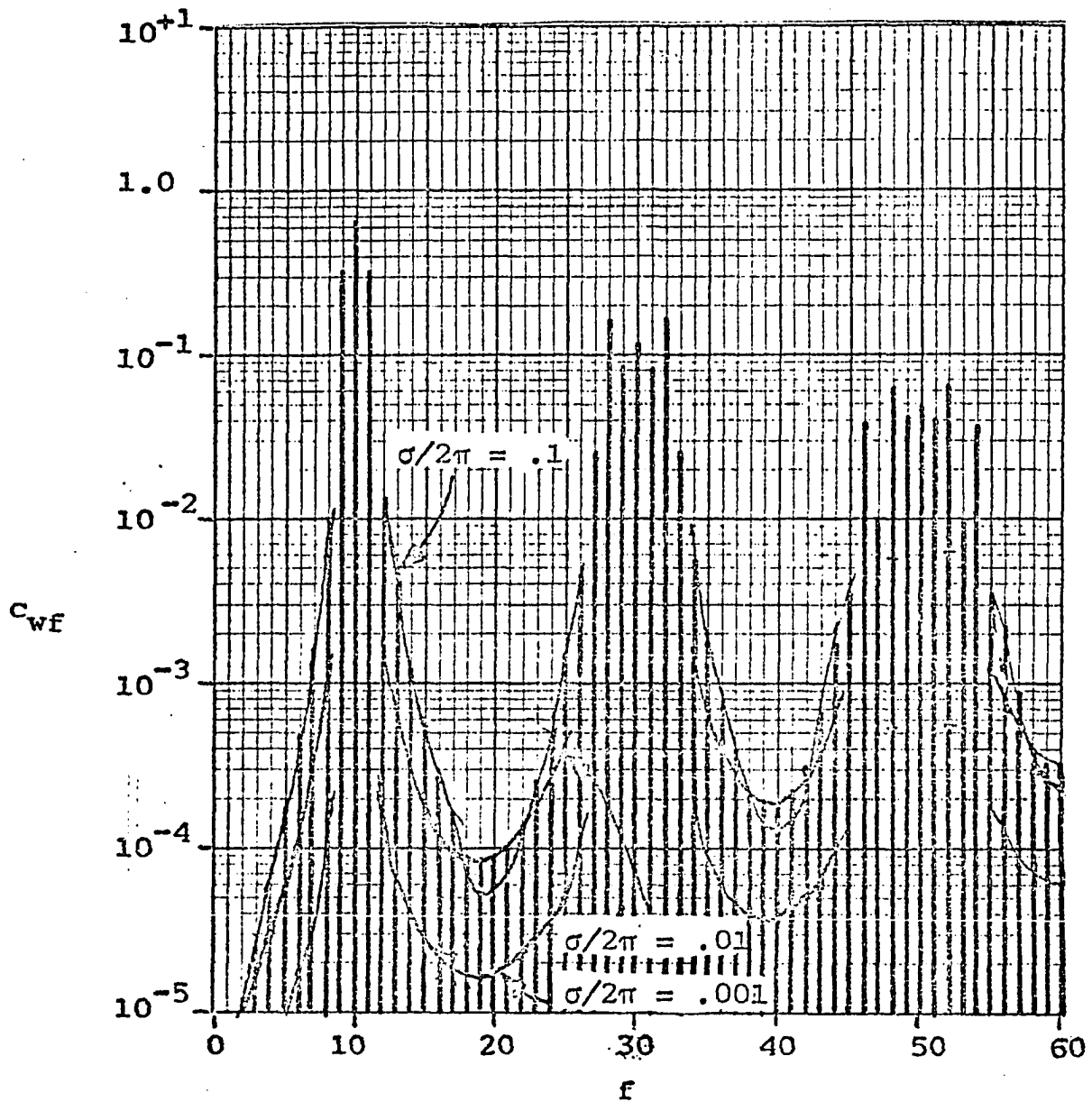


Figure 6.5. Spectrum of a Class D RF Amplifier.



AM

1 tone

bipolar

pulse bias errors as indicated

Figure 6.6. Spectrum of a Class D RF Amplifier.

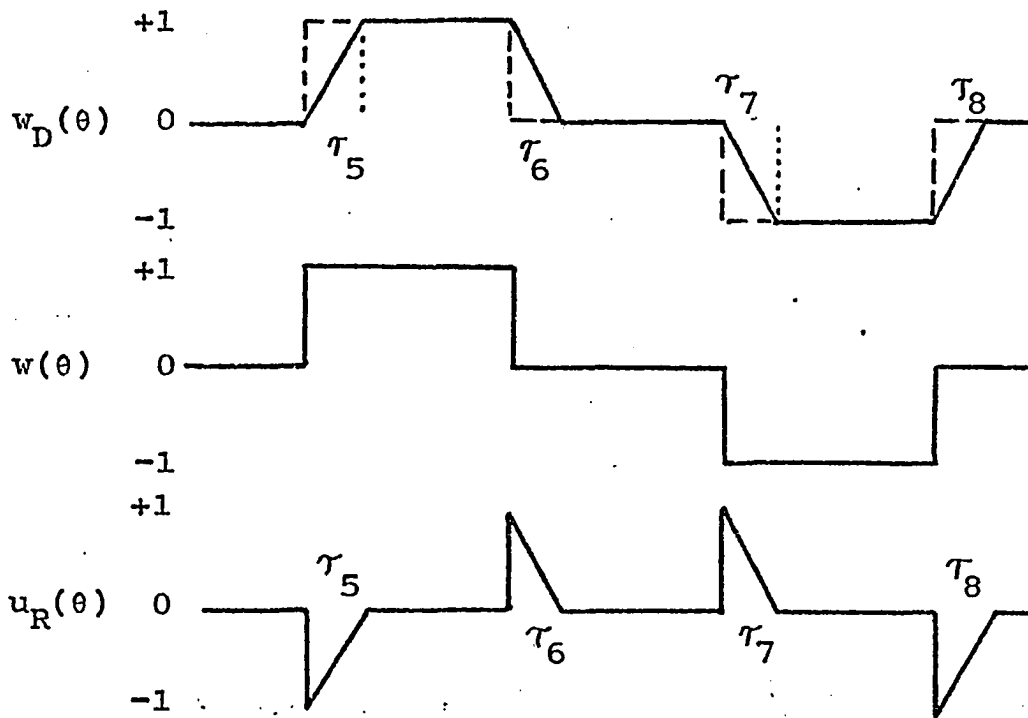


Figure 6.7. Rise/Fall Time Distortion Waveforms.

$$a_{u_{R5}n} = \frac{-1}{\pi n^2 \tau_5} [(\sin n\tau_5 - n\tau_5) \sin n\lambda + (\cos n\tau_5) \cos n\lambda] \quad (6.39)$$

$$b_{u_{R5}n} = \frac{-1}{\pi n^2 \tau_5} [(1 - \cos n\tau_5) \sin n\lambda + (n\tau_5 - \sin n\tau_5) \cos n\lambda] \quad (6.40)$$

For small values of  $n$ ,

$$\sin n\tau - n\tau = n\tau - \frac{1}{3!}n^3\tau^3 + \frac{1}{5!}n^5\tau^5 - \dots - n\tau \quad (6.41)$$

$$\approx -\frac{1}{3!}n^3\tau^3 \quad (6.42)$$

$$1 - \cos n\tau = 1 - 1 + \frac{1}{2!}n^2\tau^2 - \frac{1}{4!}n^4\tau^4 + \dots \quad (6.43)$$



$$\approx \frac{1}{2!} n^2 \tau^2 \quad (6.44)$$

These reduce (6.37) and (6.38) to

$$a_{u_{R5}n} \approx \frac{-1}{\pi} \left[ \left( -\frac{n\tau_5^2}{3!} \right) \sin n\lambda + \left( \frac{\tau_5}{2} \right) \cos n\lambda \right] \quad (6.45)$$

$$\approx -\frac{\tau_5}{2\pi} \cos n\lambda \quad (6.46)$$

$$b_{u_{R5}n} \approx \frac{-1}{\pi} \left[ \left( \frac{\tau_5}{2} \right) \sin n\lambda - \left( \frac{n\tau_5^2}{3!} \right) \cos n\lambda \right] \quad (6.47)$$

$$\approx -\frac{\tau_5}{2\pi} \sin n\lambda \quad (6.48)$$

Now for  $\tau_5$ ,

$$\lambda_5 = \frac{\pi}{2} - (y - \varphi), \quad (6.49)$$

so

$$a_{u_{R5}n} = -\frac{\tau_5}{2\pi} \begin{cases} (-1)^{\frac{n}{2}} \cos ny & , n \text{ even} \\ (-1)^{\frac{n-1}{2}} \sin ny \operatorname{sgn} x, & n \text{ odd} \end{cases} \quad (6.50)$$

$$b_{u_{R5}n} = -\frac{\tau_5}{2\pi} \begin{cases} -(-1)^{\frac{n}{2}} \sin ny & , n \text{ even} \\ (-1)^{\frac{n-1}{2}} \cos ny \operatorname{sgn} x, & n \text{ odd} \end{cases} \quad (6.51)$$

The above equations have exactly the same form (except for a  $-\frac{1}{2}$  factor) as (6.20) and (6.21), so the types of spurious products are the same. Noting that rise/fall correction pulses 5 and 7 have polarity opposite to bias pulses 1 and 3, (6.28) can be modified to produce

$$\begin{aligned}
u_R(\theta) \approx & \frac{\sigma_R}{4\pi} + \frac{\sigma_R}{2\pi} \sum_{m=1}^{\infty} (-1)^m u_{2m-1}(\theta) \sin(2m-1)\omega_c t \\
& + \frac{\delta_R}{2\pi} \sum_{m=1}^{\infty} (-1)^m u_{2m}(\theta) \sin 2m\omega_c t, \quad (6.52)
\end{aligned}$$

where  $u_k(\theta)$  is the same as before, but

$$\sigma_R = -\tau_5 + \tau_6 + \tau_7 - \tau_8 \quad (6.53)$$

$$\delta_R = \tau_5 + \tau_6 - \tau_7 - \tau_8 \quad (6.54)$$

It is interesting to note that under certain conditions, both  $\sigma_R$  and  $\delta_R$  can be reduced to zero, hence the distortion is reduced almost to zero (until the approximations used break down). If the rise and fall times of each pulse are equal,  $\sigma_R = 0$ , and the IMD as well as the modulation around the odd harmonics disappear. If the rise and fall times of the positive pulse are equal to the rise and fall times of the negative pulse,  $\delta_R = 0$  also, and the even harmonics disappear. In a bipolar amplifier, the positive and negative switching should be symmetrical, so  $\delta_R$  should be small and even harmonic products should be negligible.

However, when such balances do not exist, IMD and/or splatter appear. Simulations of DSB/SC with net timing errors of  $2\pi \cdot 0.01$  are shown in Figures 6.8 and 6.9. In the former, the rise and fall times are all equal, and spurious products are slight. However, in the latter, rise times are zero

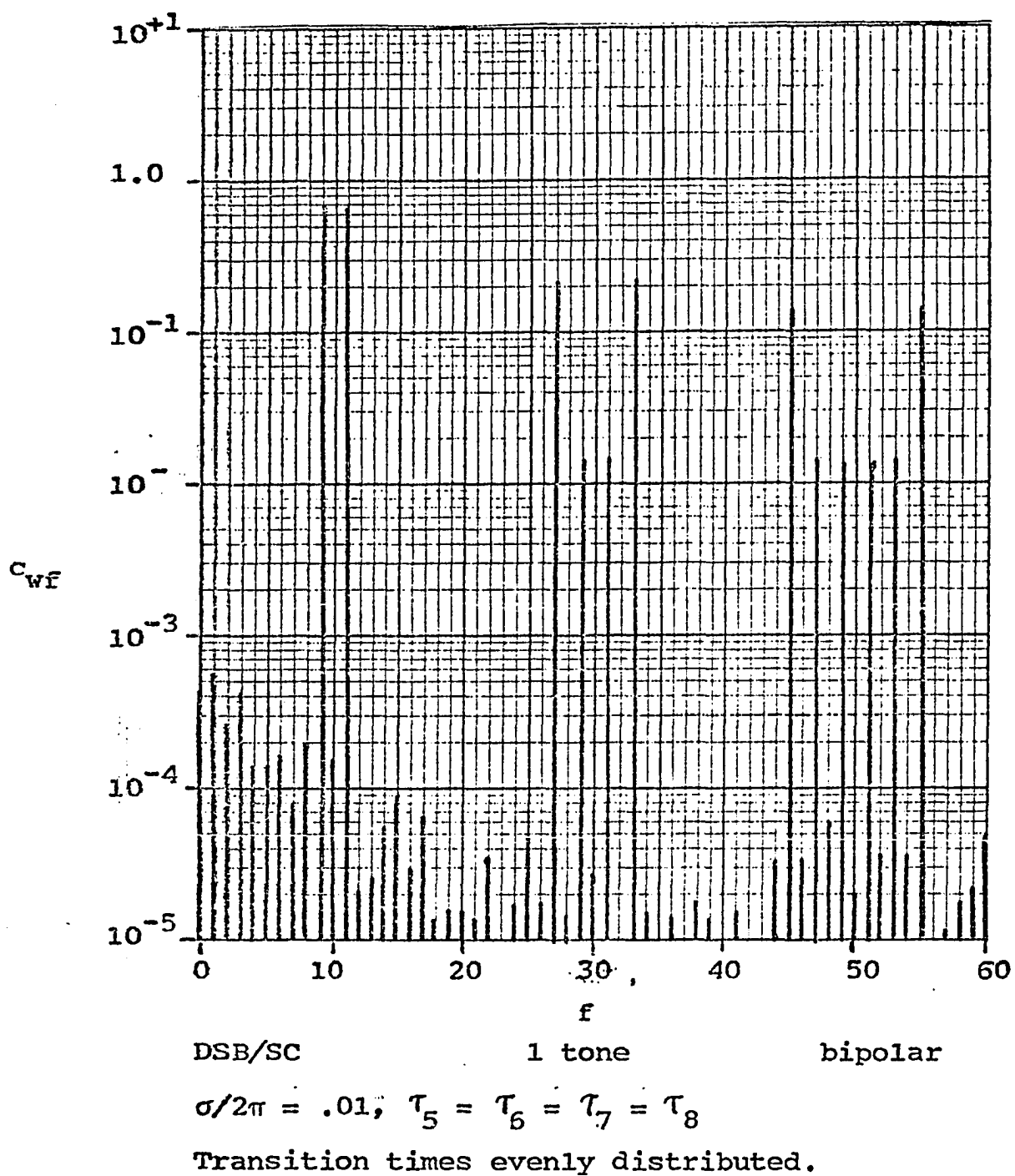


Figure 6.8. Spectrum of a Class D RF Amplifier.

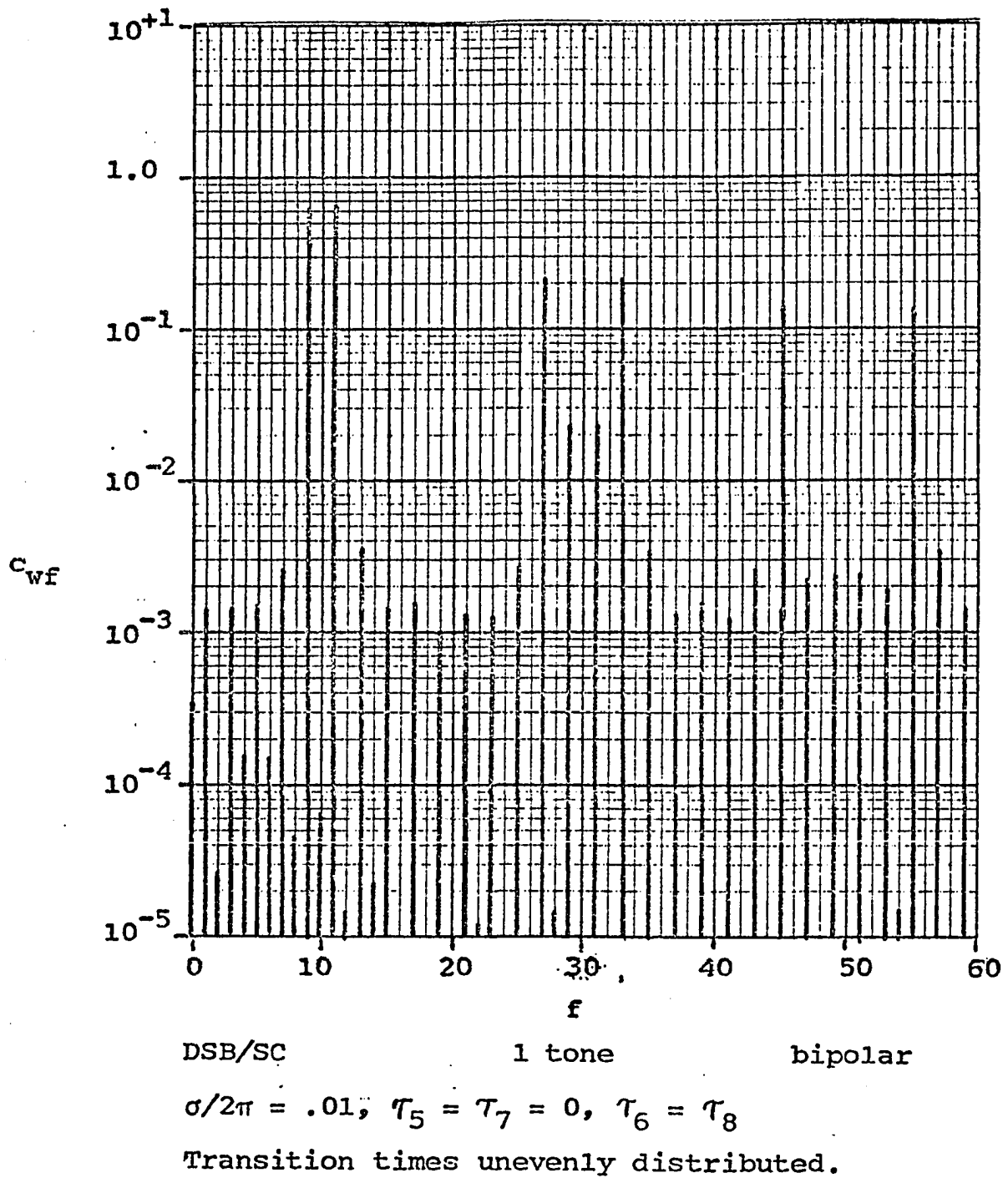


Figure 6.9. Spectrum of a Class D RF Amplifier.

and all the error is in the fall time, and spurious products are worse.

It was not chance that the approximate spurious products for rise/fall distortion are exactly one-half those of bias distortion. The phase modulation is the same, regardless of the shape of the correction pulse. Thus as long as there is neither overlapping nor deterioration, the only difference for other rise/fall shapes will be a constant multiplying the same basic distortion products. The value of the constant depends upon the area of the correction pulses.

### C. Approximations Used

As stated previously, it has been assumed that the correction pulses neither overlap nor deteriorate. This produces a distortion curve as shown in Figure 6.10.

The addition of bias or fall time necessitates a slight reduction in the maximum allowable value of  $y$ . If this is not done, the output signal will suffer an additional distortion due to clipping, and both the positive and negative output transistors may be on simultaneously, causing inefficiency and possibly resulting in damage to the transistors.

The abrupt transition from positive to negative used here is probably more severe than the actual case. As illustrated in Figure 6.11, an actual amplifier will have gradual transitions due to pulse rise and fall times. The effect of this is to round the distortion curve in Figure 6.10, which

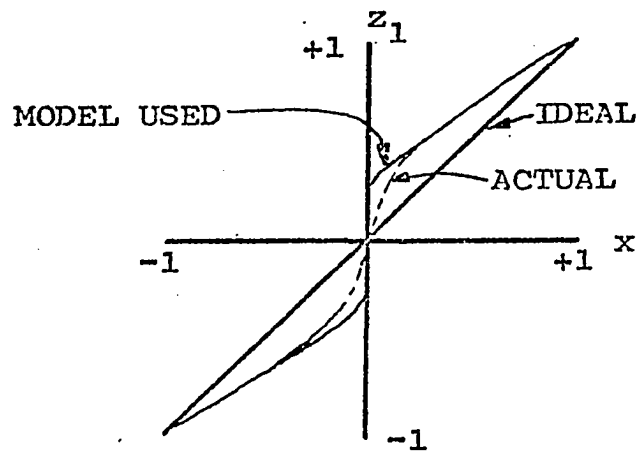


Figure 6.10. Distortion Curves.

should result in decreased distortion products.

#### D. Combination of Effects

A real amplifier may suffer from all of the distortion problems discussed in Chapters V and VI, so it is important to know how these may be combined.

The two forms of timing distortion can be combined directly, superpositioning the correction pulses of both, which results in superimposing the distortions of both. One important aspect of this is that a bias error may be introduced deliberately to compensate for IMD due to rise/fall time errors. Although this may be difficult to do in an open loop system, a feedback system can be used to reduce significantly the IMD (Chapter VIII).

Voltage-error and timing-error distortions might easily be mixed by considering any cross products to be the square of



Figure 6.11. Pulse Deterioration.

two already-small parameters, and therefore negligible. If additional accuracy is needed, voltage errors may be included by replacing  $\tau$  for the correction pulses involved with  $(1 + v_s)\tau$ . However, several approximations were used to obtain the equations contained herein, so it is doubtful that additional accuracy could be obtained by more exact analysis of those equations.

## VII. SPURIOUS PRODUCTS WITH SINUSOIDAL MODULATION

In Chapters V and VI, the distortion and/or spurious products caused by voltage or timing errors was characterized by functional equations. It was further shown that in the special case of DSB/SC with sinusoidal modulation, these functional equations could be reduced to relatively simple phase-shifting or chopped sinusoids or cosinusoids. This simplification allows the calculation of some upper limits on the spurious products generated.

The forms of the distortion functions are

$$y(\theta) = \arcsin |x(\theta)| \quad , \quad (7.1)$$

which modulates the DC bias, and

$$z_k(\theta) = \sin k \arcsin |x(\theta)| \quad , \quad (7.2)$$

which modulates even harmonics of the carrier, and arises from voltage or timing errors, and

$$u_k(\theta) = \cos k \arcsin |x(\theta)| \operatorname{sgn} x(\theta) \quad , \quad (7.3)$$

which modulates odd harmonics of the carrier, and arises only from timing errors.

For DSB/SC modulation,

$$x(\theta) = \sin \theta \quad , \quad (7.4)$$

and as shown in (5.74) and (6.25),

$$y(\theta) = \frac{\pi}{4} + \frac{\pi}{4} \Lambda(2\theta) \quad (7.5)$$

$$z_k(\theta) = \sin k\theta \operatorname{s}(2\theta) \quad (7.6)$$

and



$$u_k(\theta) = \cos k\theta \, s(2\theta) \quad (7.7)$$

The spectra of these can be determined and used to compute the maximum amount of spurious products falling on a given frequency.

Amplitude modulation has smaller spurious products in general than DSB/SC, in part due to the lack of one phase shift (sgn  $x = 1$  for AM). For AM at 100% modulation,

$$x(\theta) = \frac{1}{2} + \frac{1}{2} \sin \theta \quad (7.8)$$

However, an exact form for  $z_k(\theta)$  or  $u_k(\theta)$  is difficult (see Chapter VIII). To get a (very) crude idea of what upper limits would be for AM, the sgn  $x$  or  $|x|$  phase shifting will be ignored, although (7.3) will be used to generate manageable equations. This results in

$$\dot{y}(\theta) = \frac{\pi}{2} \Lambda(\theta) \quad (7.9)$$

$$z_k(\theta) = \sin k \arcsin x(\theta) \quad (7.10)$$

$$= \sin k\theta \, c(\theta) \quad (7.11)$$

and 
$$u_k(\theta) = \cos k \arcsin x(\theta) \quad (7.12)$$

$$= \cos k\theta \, c(\theta), \quad (7.13)$$

each of which has half as many phase shifts as its DSB counterpart (Figure 7.1). The actual forms of  $y$ ,  $z_k$ , and  $u_k$  for AM are shown, along with the ones used for computation. It appears that the actual waveforms are more rounded, hence the limits found should exceed the actual limits.

Begin by recalling (4.24) and (4.22),

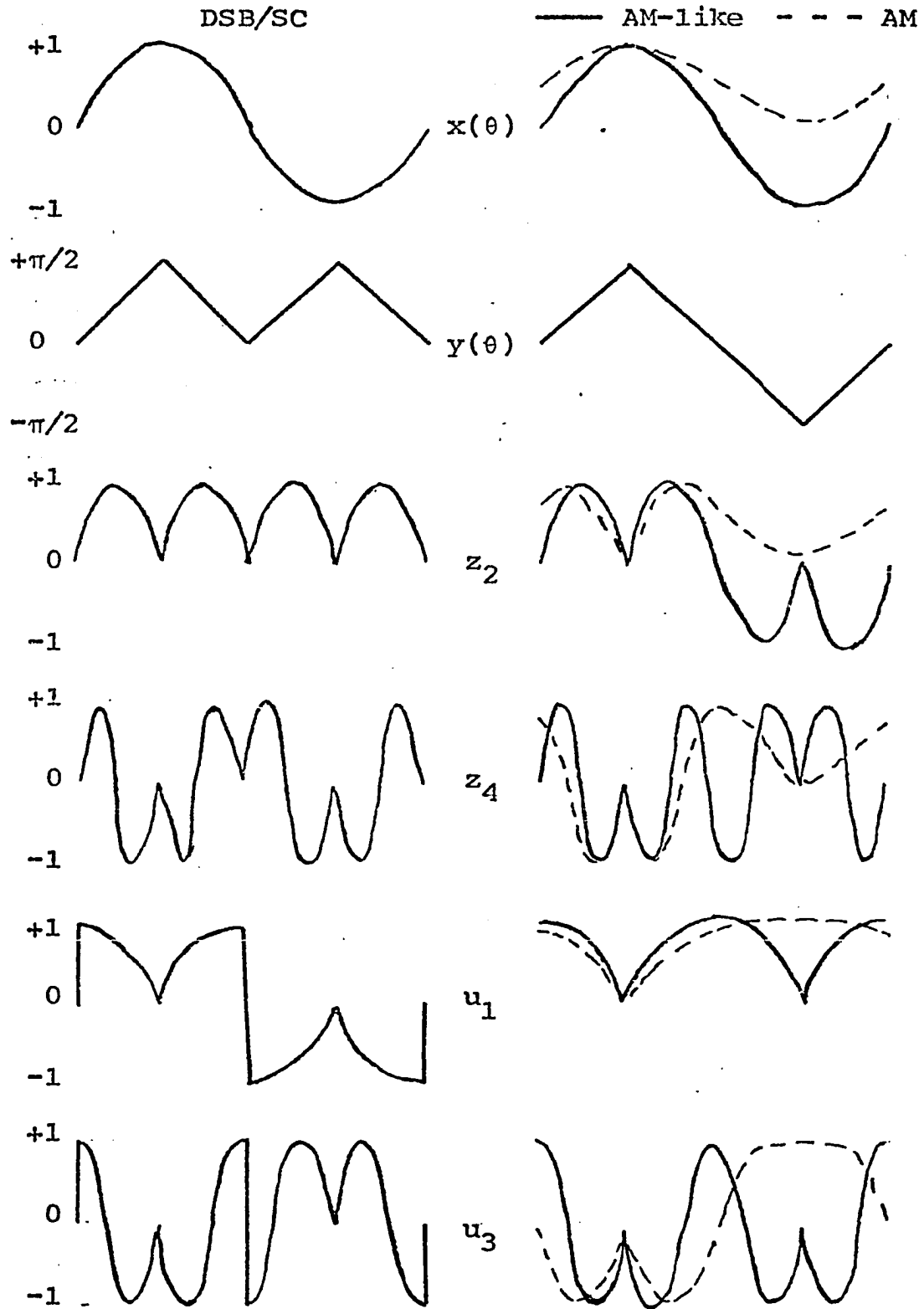


Figure 7.1. Waveforms Used to Find Upper Limits on Spurious Products.

$$c(\theta) = \frac{4}{\pi} \left[ \cos \theta - \frac{1}{3} \cos 3\theta + \frac{1}{5} \sin 5\theta \dots \right] \quad (7.14)$$

$$= \frac{4}{\pi} \sum_{m=0}^{\infty} \frac{(-1)^m}{2m+1} \cos(2m+1)\theta \quad (7.15)$$

and

$$s(2\theta) = \frac{4}{\pi} \left[ \sin 2\theta + \frac{1}{3} \sin 6\theta + \frac{1}{5} \sin 10\theta + \dots \right] \quad (7.16)$$

$$= \frac{4}{\pi} \sum_{m=0}^{\infty} \frac{1}{2m+1} \sin(4m+2)\theta \quad (7.17)$$

#### A. Voltage Error Products

DSB/SC generated by monopolar PWM will be considered first. To apply these results to voltage errors, the spectra derived are multiplied by a normalized  $\Delta V$ .

Modulation of the DC component also occurs, and has the form

$$y(\theta) = \left| \frac{\pi}{2} \Lambda(\theta) \right| = \frac{\pi}{4} + \frac{\pi}{4} \Lambda(2\theta) \quad (7.18)$$

$$= \frac{\pi}{4} + \frac{2}{\pi} \sum_{i=0}^{\infty} \frac{(-1)^i}{(2i+1)^2} \sin(4i+2)\theta \quad (7.19)$$

Letting  $f$  be a frequency where a spurious product may occur,

$$2i + 1 = \frac{f}{2} \quad (7.20)$$

A factor of  $1/\pi$  occurs in (5.69), thus the magnitude of a distortion product at frequency  $f$  is approximately

$$D_0(f) = \frac{1}{\pi} \cdot \frac{2}{\pi} \cdot \frac{1}{(f/2)^2} = \frac{8}{\pi^2} \cdot \frac{1}{f^2} \quad (7.21)$$

If the ratio of carrier frequency to modulation frequency is

$$\alpha = \frac{f_c}{f_x}, \quad (7.22)$$

then the spurious products falling near the desired signal are approximately

$$D_0(f_c) \approx \frac{8}{\pi^2 \alpha^2} \quad (7.23)$$

From (7.17),

$$\sin k\theta \sin(2\theta) = \frac{4}{\pi} \left[ \sin k\theta \sin 2\theta + \frac{1}{3} \sin k\theta \sin 6\theta + \dots \right] \quad (7.24)$$

$$\begin{aligned} &= \frac{2}{\pi} \left\{ [\cos(k-2)\theta - \cos(k+2)\theta] + \frac{1}{3} [\cos(k-6)\theta - \right. \\ &\quad \left. \cos(k+6)\theta] + \frac{1}{5} [\cos(k-10)\theta - \cos(k+10)\theta] \right. \\ &\quad \left. + \dots \right\} \quad (7.25) \end{aligned}$$

When  $k = 2$ ,

$$z_2(\theta) = \frac{2}{\pi} \left\{ 1 - \cos 4\theta + \frac{1}{3} \cos 4\theta - \frac{1}{3} \cos 8\theta + \dots \right\} \quad (7.26)$$

$$= \frac{2}{\pi} \left\{ 1 - \left(1 - \frac{1}{3}\right) \cos 4\theta - \left(\frac{1}{3} - \frac{1}{5}\right) \cos 8\theta - \dots \right\} \quad (7.27)$$

$$= \frac{2}{\pi} \left\{ 1 - \frac{2}{1 \cdot 3} \cos 4\theta - \frac{2}{3 \cdot 5} \cos 8\theta - \dots \right\} \quad (7.28)$$

The terms for  $k = 2$  show an asymptotic  $1/f^2$  decay, a similar result holds for other values of  $k$ . Consider the coefficient of  $\cos m\theta$  where  $m$  is large; contributions come from the  $i^{\text{th}}$  and  $j^{\text{th}}$  terms such that

$$m = 4j + 2 - k = 4i + 2 + k \quad (7.29)$$

Then

$$2j + 1 = \frac{m+k}{2} \quad (7.30)$$

and

$$2i + 1 = \frac{m-k}{2} \quad (7.31)$$

Now

$$c_{km} = \left| -\frac{1}{2j+1} + \frac{1}{2i+1} \right| \frac{2}{\pi} \quad (7.32)$$

$$= \frac{2}{\pi} \left| -\frac{2}{m+k} + \frac{2}{m-k} \right| \quad (7.33)$$

$$= \frac{4}{\pi} \left| \frac{-m+k+m+k}{(m+k)(m-k)} \right| \quad (7.34)$$

$$= \frac{8}{\pi} \left| \frac{k}{m^2-k^2} \right| \quad (7.35)$$

Modulation of the  $k^{\text{th}}$  harmonic causes two sidebands to appear, halving the magnitude of the product ( $D_k$ ) at any given frequency. However, foldover contributes an additional product ( $D_k^*$ ). There is also a constant of  $2/\pi k$  for the  $k^{\text{th}}$  harmonic (Figure 7.2). Thus

$$D_k = \frac{2}{\pi k} \cdot \frac{8k}{\pi |m^2-k^2|} \cdot \frac{1}{2} \quad (7.36)$$

$$= \frac{8}{\pi^2} \cdot \left| \frac{1}{m^2-k^2} \right| \quad (7.37)$$

Frequency differences of  $kf_c - f$  and  $kf_c + f$  apply to the direct and foldover products, respectively, so

$$D_k(f) = \frac{8}{\pi^2} \frac{1}{\left| \left[ (kf_c - f) \frac{a}{f_c} \right]^2 - k^2 \right|} \quad (7.38)$$

and

$$D_k^*(f) = \frac{8}{\pi^2} \frac{1}{\left| \left[ (kf_c + f) \frac{a}{f_c} \right]^2 - k^2 \right|} \quad (7.39)$$

When  $f = f_c$ ,

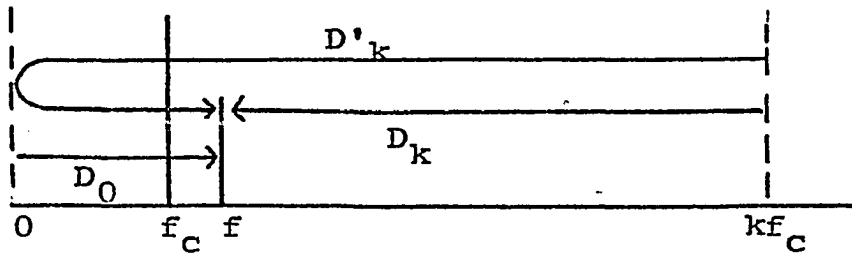


Figure 7.2. Spurious Products at a Given Frequency.

$$kf_c \pm f = (k \pm 1)f_c, \quad (7.40)$$

and

$$D_k(f_c) = \frac{8}{\pi^2} \left| \frac{1}{(k-1)^2 \alpha^2 - k^2} \right| \quad (7.41)$$

and

$$D'_k(f_c) = \frac{8}{\pi^2} \left| \frac{1}{(k+1)^2 \alpha^2 - k^2} \right| \quad (7.42)$$

By assuming that all products add, the worst case spurious product at a given frequency can be determined:

$$D(f) = D_0(f) + \sum [D_k(f) + D'_k(f)] \quad (7.43)$$

$$k=2, 4, \dots$$

When  $f = f_c$ , a numerical answer can be obtained easily by dropping the  $-k^2$  in the denominators of (7.41) and (7.42):

$$D(f_c) = \frac{8}{\pi^2 \alpha^2} \left\{ 1 + \sum_{k=2, 4, \dots} \frac{1}{(k-1)^2} + \frac{1}{(k+1)^2} \right\} \quad (7.44)$$

$$= \frac{8}{\pi^2 \alpha^2} \left\{ 1 + \sum_{m=1, 3, \dots} \frac{1}{m^2} + \sum_{m=3, 5, \dots} \frac{1}{m^2} \right\} \quad (7.45)$$

$$= \frac{16}{\pi^2 \alpha^2} \sum_{m=1, 3, 5, \dots} \frac{1}{m^2} = \frac{16}{\pi^2 \alpha^2} \cdot \frac{\pi^2}{8} = \frac{2}{\alpha^2}, \quad (7.46)$$

(by use of #339 from (22)). To reduce the maximum spurious level to -80 dB below one of the desired sidebands of a monopolar generated signal,

$$\alpha^2 \geq 2 \cdot \pi \cdot 10^{+4} \quad , \text{ or} \quad (7.47)$$

$$\alpha \geq 250 \quad . \quad (7.48)$$

For other frequencies, a summation can be carried out as above, but numerical evaluation is easier. Since the terms decrease as  $1/k^2$ , 32 terms will result in an error of approximately  $.001 \approx 1/32^2$ . Plots of D vs f for  $\alpha = 10, 100,$  and 1000 are shown in Figure 7.3. For reasonable values of  $\alpha$ , the limit on the spurious products is nearly constant near  $f_c$ .

The procedure for an AM-like signal is the same.

$$y(\theta) = \frac{\pi}{2} \Lambda(\theta) \quad (7.49)$$

$$= \frac{4}{\pi} \sum_{i=0}^{\infty} \frac{(-1)^i}{(2i+1)^2} \sin(2i+1)\theta \quad (7.50)$$

$$D_0(f) = \frac{4}{\pi} \cdot \frac{1}{f^2} \quad (7.51)$$

$$z_k(\theta) = \sin k\theta \ c(\theta) \quad (7.52)$$

$$= \frac{4}{\pi} \left\{ \sin k\theta \cos \theta - \frac{1}{3} \sin k\theta \cos 3\theta + \dots \right\} \quad (7.53)$$

$$= \frac{2}{\pi} \left\{ [\sin(k+1)\theta + \sin(k-1)\theta] - \frac{1}{3} [\sin(k+3)\theta + \sin(k-3)\theta] \dots \right\} \quad (7.54)$$

$$z_i(\theta) = \frac{2}{\pi} \left\{ [\sin 3\theta + \sin \theta] - \frac{1}{3} [\sin 5\theta - \sin \theta] \dots \right\} \quad (7.55)$$

$$= \frac{2}{\pi} \left\{ \left(1 + \frac{1}{3}\right) \sin \theta + \left(1 - \frac{1}{3}\right) \sin 3\theta + \left(-\frac{1}{3} + \frac{1}{7}\right) \sin 5\theta \right.$$

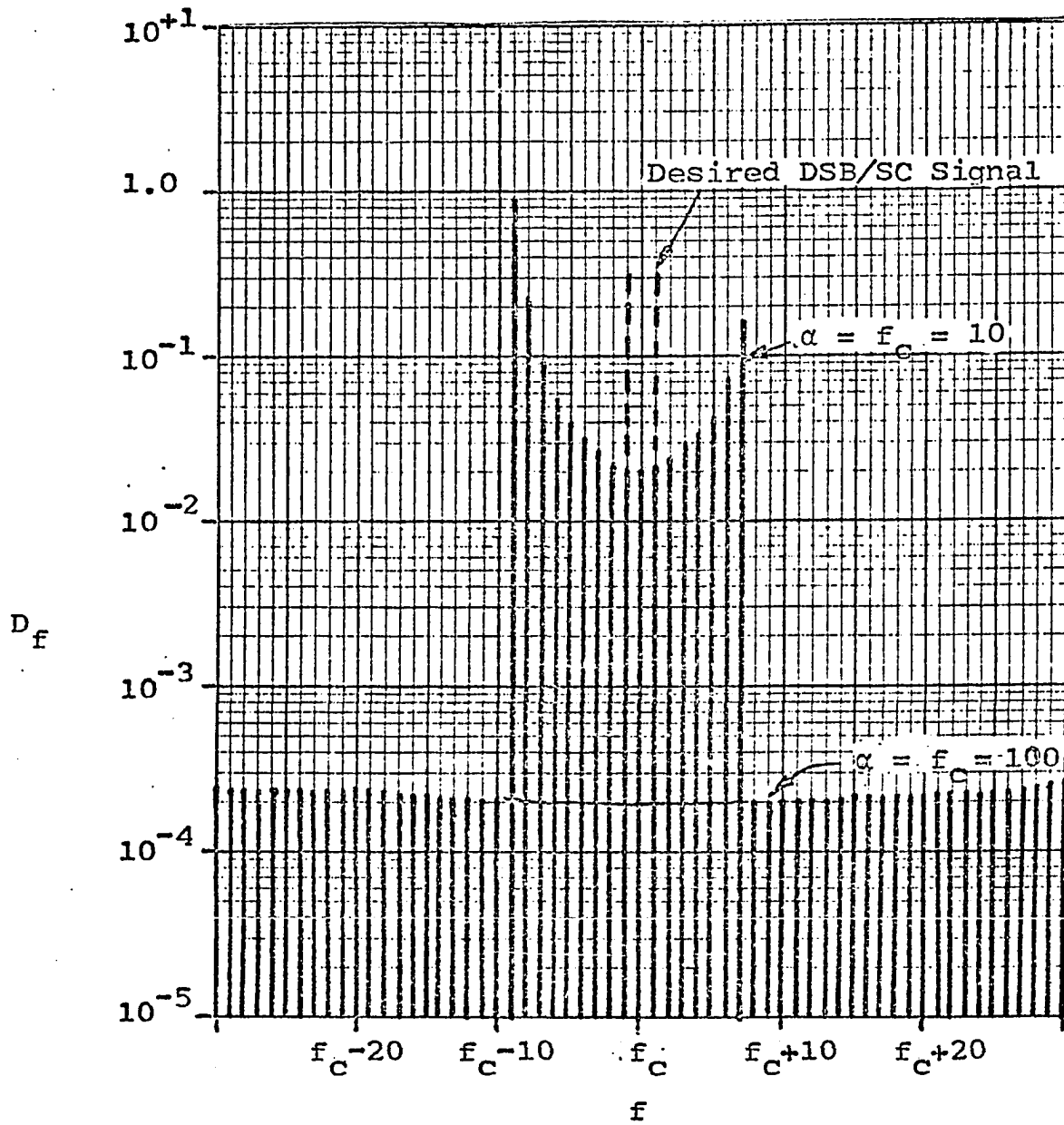


Figure 7.3. Maximum Spurious Products for Monopolar DSB/SC.



$$+ \left( \frac{1}{5} - \frac{1}{9} \right) \sin 7\theta + \dots \} \quad (7.56)$$

$$= \frac{8}{\pi} \left\{ \frac{1}{3} \sin \theta + \frac{1}{1.5} \sin 3\theta - \frac{1}{3.7} \sin 5\theta + \dots \right. \\ \left. + \frac{1}{5.9} \sin 7\theta - \dots \right\} \quad (7.57)$$

$$c_{km} = \frac{2}{\pi} \left| \frac{1}{m-k} - \frac{1}{m+k} \right| \quad (7.58)$$

$$= \frac{2}{\pi} \left| \frac{m+k-m+k}{m^2-k^2} \right| = \frac{4}{\pi} \left| \frac{k}{m^2-k^2} \right| \quad (7.59)$$

At this point it becomes apparent that since  $D_0$  and  $c_{km}$  are half of their equivalents for DSB/SC, the maximum spurious limits will be half those for DSB/SC. Thus for AM,  $\alpha \geq 177$  should keep the spurious products -80 dB from the carrier.

#### B. Timing Error Products

As discussed in Chapter VI, timing error spurious products can be divided into two types: IMD and background. The determination of upper limits for timing error products is, however, complicated somewhat by their non-linear dependence on the timing error parameter  $\sigma$ .

The simplifying assumption used in (6.6) that

$$\frac{\sin \frac{n\tau_i}{2}}{n} \approx \frac{\tau_i}{2} \quad (7.60)$$

must be dropped. It eliminates one factor of  $1/n$  in the summation to determine background products, and the remaining terms contain only a factor of  $1/n$ , and are therefore not summable. Using  $\sin \frac{n\tau_i}{2}$  produces summable terms, but the magni-

tude may vary both up and down with changes in  $\tau$ , making upper limits difficult to find. Replacement of  $\sin \frac{n\tau_i}{2}$  by 1 produces an upper limit, but eliminates all dependence on  $\tau$ .

The use of the piecewise clipping function

$$g(x) = \begin{cases} x, & x < 1 \\ 1, & x \geq 1 \end{cases} \quad (7.61)$$

can eliminate this problem by allowing the lower frequency terms to depend on  $\tau$ , while preventing decreases in the higher frequency terms.

For a DSB/SC signal,

$$u_k(\theta) = \cos k\theta \sin(2\theta) \quad (7.62)$$

$$= \frac{4}{\pi} \left\{ \cos k\theta \sin 2\theta + \frac{1}{3} \cos k\theta \sin 6\theta + \dots \right\} \quad (7.63)$$

$$= \frac{2}{\pi} \left\{ [\sin(k+2)\theta - \sin(k-2)\theta] + \frac{1}{3} [\sin(k+6)\theta - \sin(k-6)\theta] + \frac{1}{5} [\sin(k+10)\theta - \sin(k-10)\theta] + \dots \right\} \quad (7.64)$$

For the IMD,

$$u_1(\theta) = \frac{2}{\pi} \left\{ [\sin 3\theta + \sin \theta] + \frac{1}{3} [\sin 7\theta + \sin 5\theta] + \frac{1}{5} [\sin 11\theta + \sin 9\theta] + \dots \right\} \quad (7.65)$$

None of the terms above is the same frequency, so no cancellation can occur, and decay is slow ( $1/f$ ). For large  $m$ ,

$$c_{kf} \approx \frac{2}{\pi} / \frac{f}{2} = \frac{4}{m\pi} \quad (7.66)$$

This gives IM products of the form

$$I(f) \approx \frac{\sigma}{\pi} \cdot \frac{4}{m\pi} \cdot \frac{1}{2} \quad (7.67)$$

$$= \frac{2\sigma}{\pi^2} \frac{1}{|f_c - f| \cdot \frac{\alpha}{f_c}} \quad (7.68)$$

Assume that the errors are evenly distributed, i.e.,

$$\tau_i = \frac{\sigma}{4} \quad (7.69)$$

Thus

$$B_k(f) = \frac{4g(\frac{\sigma}{4})}{k\pi} \cdot \frac{4}{\pi} \frac{1}{|kf_c - f|} \cdot \frac{1}{2} \quad (7.70)$$

$$= \frac{8g(\frac{\sigma}{4})}{\pi} \frac{1}{k|kf_c - f|} \quad (7.71)$$

and

$$B'_k(f) = \frac{8g(\frac{\sigma}{4})}{\pi} \frac{1}{k|kf_c + f|} \quad (7.72)$$

The maximum product is then

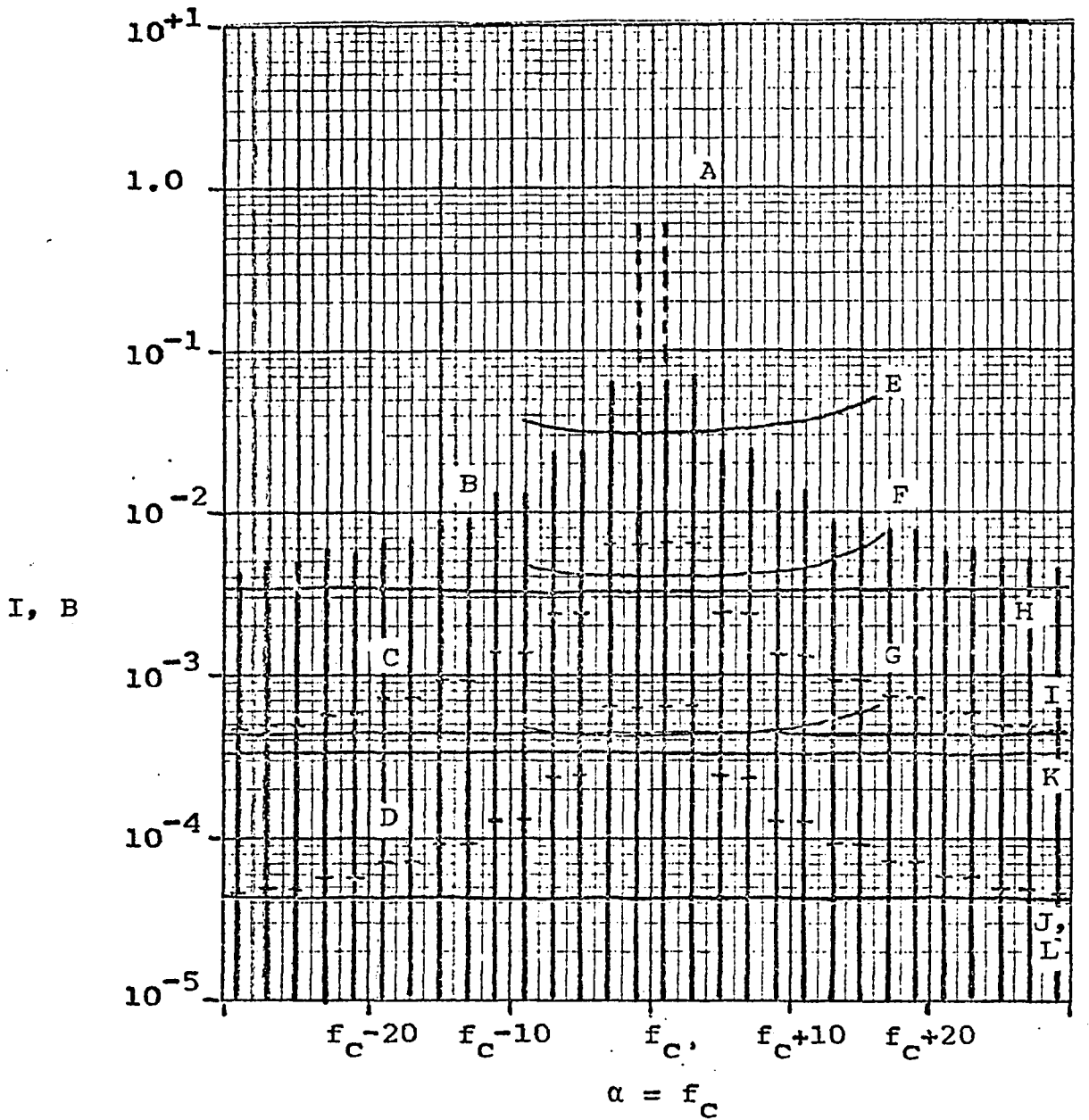
$$B(f) = B'_1(f) + \sum_{k=3,5,\dots} [B_k(f) + B'_k(f)] \quad (7.73)$$

Numerical evaluation of (7.68) and (7.73) was performed, for various values of  $\sigma$  and  $\alpha$ , and the results are displayed in Figure 7.4. Note the approximately linear relationships between  $B(f)$  and  $\sigma$  and  $1/\alpha$ . It can be seen that near the carrier frequency,  $I(f)$  dominates  $B(f)$ .

For an AM-like signal,

$$u_k(\theta) = \cos k\theta \quad (7.74)$$

$$= \frac{4}{\pi} \cos k\theta \left[ \cos \theta - \frac{1}{3} \cos 3\theta + \frac{1}{3} \cos 5\theta - \dots \right] \quad (7.75)$$



- |  |  |
|--|--|
| A: DSB/SC SIGNAL                       | G: B, $\alpha=10$ , $\sigma/2\pi=0.001$  |
| B: I, $\sigma/2\pi=0.1$                | H: B, $\alpha=100$ , $\sigma/2\pi=0.1$   |
| C: I, $\sigma/2\pi=0.01$               | I: B, $\alpha=100$ , $\sigma/2\pi=0.01$  |
| D: I, $\sigma/2\pi=0.001$              | J: B, $\alpha=100$ , $\sigma/2\pi=0.001$ |
| E: B, $\alpha=10$ , $\sigma/2\pi=0.1$  | K: B, $\alpha=1000$ , $\sigma/2\pi=0.1$  |
| F: B, $\alpha=10$ , $\sigma/2\pi=0.01$ | L: B, $\alpha=1000$ , $\sigma/2\pi=0.01$ |

Figure 7.4. Maximum Spurious Products for Bipolar DSB/SC with Various Timing Errors.

$$= \frac{2}{\pi} \left\{ [\cos(k+1)\theta + \cos(k-1)\theta] - \frac{1}{3}[\cos(k+3)\theta + \cos(k-3)\theta] + \dots \right\} \quad (7.76)$$

$$u_i(\theta) = \frac{2}{\pi} \left\{ [\cos 2\theta + 1] - \frac{1}{3}[\cos 4\theta + \cos 2\theta] + \dots \right\} \quad (7.77)$$

$$= \frac{2}{\pi} \left\{ 1 + (1-\frac{1}{3}) \cos 2\theta - (\frac{1}{3}-\frac{1}{5}) \cos 4\theta + \dots \right\} \quad (7.78)$$

$$= \frac{2}{\pi} + \frac{4}{\pi} \left\{ \frac{1}{1 \cdot 3} \cos 2\theta - \frac{1}{3 \cdot 5} \cos 4\theta + \dots \right\} \quad (7.79)$$

The AM-like signal has a  $1/f^2$  decay, thus

$$c_{km} = \frac{2}{\pi} \left| \frac{1}{m-k} - \frac{1}{m+k} \right| \quad (7.80)$$

$$= \frac{2}{\pi} \left| \frac{m+k-m+k}{(m-k)(m+k)} \right| = \frac{4}{\pi} \left| \frac{k}{m^2-k^2} \right| \quad (7.81)$$

The IMD then has the form

$$I(f) = \frac{\sigma}{\pi} \cdot \frac{4}{\pi} \cdot \left| \frac{1}{m^2-1} \right| \cdot \frac{1}{2} \quad (7.82)$$

$$= \frac{2\sigma}{\pi^2} \cdot \left| \frac{1}{m^2-1} \right| \quad (7.83)$$

$$= \frac{2\sigma}{\pi^2} \frac{1}{\left| \left[ (f_c - f) \frac{\alpha}{f_c} \right]^2 - 1 \right|} \quad (7.84)$$

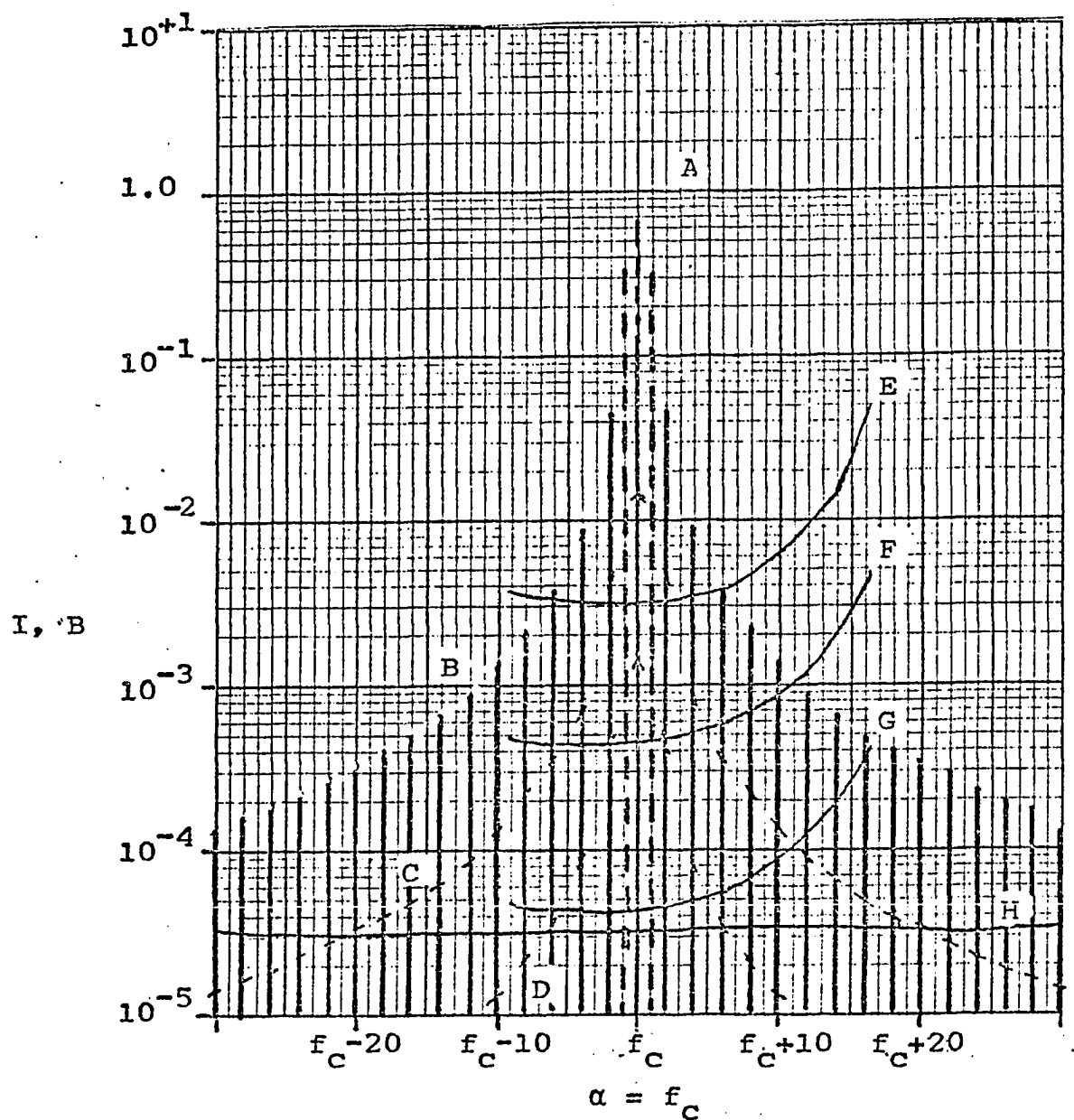
As before,

$$B_k(f) = \frac{4g(\frac{\sigma}{4})}{k\pi} \cdot \frac{4}{\pi} \left| \frac{k}{m^2-k^2} \right| \cdot \frac{1}{2} \quad (7.85)$$

$$= \frac{8g(\frac{\sigma}{4})}{\pi^2} \frac{1}{\left| (kf_c + f)^2 \left( \frac{\alpha}{f_c} \right)^2 - k^2 \right|} \quad (7.86)$$

and

$$B_k^*(f) = \frac{8g(\frac{\sigma}{4})}{\pi^2} \frac{1}{\left| (kf_c + f)^2 \left( \frac{\alpha}{f_c} \right)^2 - k^2 \right|} \quad (7.87)$$



- |                           |   |
|---------------------------|---|
| A: AM-Like Signal         | E: B, $\alpha=10$ , $\sigma/2\pi=0.1$   |
| B: I, $\sigma/2\pi=0.1$   | F: B, $\alpha=10$ , $\sigma/2\pi=0.01$  |
| C: I, $\sigma/2\pi=0.01$  | G: B, $\alpha=10$ , $\sigma/2\pi=0.001$ |
| D: I, $\sigma/2\pi=0.001$ | H: B, $\alpha=100$ , $\sigma/2\pi=0.1$  |

Figure 7.5. Maximum Spurious Products for Bipolar AM-Like Signal with Various Timing Errors.

Numerical evaluation of (7.86) and (7.87) was performed as for DSB/SC, and the results are shown in Figure 7.5. Note that the  $B(f)$  are still approximately linearly related to  $\sigma$ , but now decrease according to  $\alpha^2$ . Again,  $I(f)$  dominates near  $f_c$ .

## VIII. SPURIOUS PRODUCTS FOR GENERAL CASE

It would be useful to have general expressions such as

$$u_k(\theta) = a_{u_k 0} + \sum_{n=1}^{\infty} [a_{u_k n} \cos n\theta + b_{u_k n} \sin n\theta] \quad (8.1)$$

for a general modulating function

$$x(\theta) = a_{x 0} + \sum_{n=1}^N [a_{x n} \cos n\theta + b_{x n} \sin n\theta] \quad (8.2)$$

Unfortunately, such formulae are not easily obtainable .

There are several basic relationships which may be used to attack this problem: (1) Power series for the distortion functions ((22), #845 and #844):

$$\cos k \arcsin x = 1 - \frac{k^2}{2!} x^2 + \frac{k^2(k^2-2^2)}{4!} x^4 - \dots \quad (8.3)$$

$$\sin k \arcsin x = kx - \frac{k(k^2-1^2)}{3!} x^3 + \frac{k(k^2-1^2)(k^2-3^2)}{5!} x^5 - \dots \quad (8.4)$$

(2) Binomial and multinomial theorems:

$$(x_1 + x_2)^n = x_1^n + nx_1^{n-1}x_2 + \dots + \binom{n}{k}x_1^{n-k}x_2^k + \dots + x_2^n \quad (8.5)$$

$$(x_1 + \dots + x_m)^n = \sum_{n_1, n_2, \dots, n_m} n! \prod_{j=0}^{m-1} \frac{x_j^{n_j}}{n_j!} \quad (8.6)$$

where

$$\sum_{i=1}^m n_i = n \quad (8.7)$$



and  $\Sigma$  indicates the sum of all possible unique combinations.  
 $n_1, \dots, n_m$

(3) Trigonometric expansions of powers of sine and cosine ((22), #654, 655, 652, and 653):

$$\sin^{2n}\theta = \frac{(-1)^n}{2^{2n-1}} [\cos 2n\theta - \binom{2n}{1} \cos(2n-2)\theta + \binom{2n}{2} \cos(2n-4)\theta + \dots + (-1)^{\frac{n-1}{2}} \binom{2n}{\frac{2n-1}{2}}] \quad (8.8)$$

$$\sin^{2n+1}\theta = \frac{(-1)^n}{2^{2n}} [\sin(2n+1)\theta - \binom{2n+1}{1} \sin(2n-1)\theta + \binom{2n+1}{2} \sin(2n-3)\theta + \dots + (-1)^n \binom{2n+1}{n} \sin\theta] \quad (8.9)$$

$$\cos^{2n}\theta = \frac{1}{2^{2n-1}} [\cos 2n\theta + \binom{2n}{1} \cos(2n-2)\theta + \binom{2n}{2} \cos(2n-4)\theta + \dots + \frac{1}{2} \binom{2n}{n} \cos\theta] \quad (8.10)$$

$$\cos^{2n+1}\theta = \frac{1}{2^{2n}} [\cos(2n+1)\theta + \binom{2n+1}{1} \cos(2n-1)\theta + \dots + \binom{2n+1}{n} \cos\theta] \quad (8.11)$$

Combinations of the above result in very awkward expressions, as will be shown. The clipping effects of  $\text{sgn } x(\theta)$  add further complications. However, some basic relationships can be derived.

A recursive relationship can be used to convert  $\cos \arcsin x = u_1(\theta)$  to other distortion functions: For example

$$\sin 2 \arcsin x = 2 \sin \arcsin x \cos \arcsin x \quad (8.12)$$

$$= 2x \cos \arcsin x \quad , \quad (8.13)$$

and

$$\begin{aligned} \cos 3 \arcsin x &= \cos 2 \arcsin x \cos \arcsin x \\ &+ \sin 2 \arcsin x \sin \arcsin x \quad (8.14) \end{aligned}$$

$$\begin{aligned} &= \left(1 - \frac{(1-2^2)}{2} x^2\right) \cos \arcsin x \\ &+ 2x(\cos \arcsin x) x \quad (8.15) \end{aligned}$$

$$= \left(1 + \frac{7}{2} x^2\right) \cos \arcsin x \quad (8.16)$$

This process can be continued to as high an order as desired.

The power series expansions can be used to show the effects of varying modulation depths. Let

$$x(\theta) = b \sin n\theta, \quad (8.17)$$

where

$$0 \leq b \leq 1 \quad (8.18)$$

Then

$$\cos k \arcsin x = 1 - \frac{k^2 b^2 \sin^2 n\theta}{2!} + \frac{k^2 (k^2 - 2^2) b^4 \sin^4 n\theta}{4!} - \dots \quad (8.19)$$

$$= 1$$

$$\begin{aligned} &- \frac{k^2 b^2}{2!2} \left[ \frac{2!}{2(1!)^2} - \cos 2n\theta \right] \\ &+ \frac{k^2 (k^2 - 2^2) b^4}{4! 2^3} \left[ \frac{4!}{2(2!)^2} - 4 \cos 2n\theta + \cos 4n\theta \right] \\ &+ \dots \quad (8.20) \end{aligned}$$

$$= \left[ 1 - \left( \frac{k^2}{2!2} \frac{2!}{2(1!)^2} \right) + \left( \frac{k^2 (k^2 - 2^2) 4!}{4! 2^3 2(2!)^2} \right) b^4 - \dots \right]$$

$$+ b^2 \left[ \frac{k^2}{2!2} - \frac{k^2 (k^2 - 2^2) 4b^2}{4! 2^3} + \dots \right] \cos 2n\theta$$

$$+ b^4 \left[ \frac{k^2 (k^2 - 2^2)}{4! 2^3} - \dots \right] \cos 4n\theta$$

$$+ \dots \quad (8.21)$$

It is apparent that  $\cos mn\theta$  is multiplied by  $b^n$ ,  $n \geq m$ , and hence must decrease at least as fast as  $b^m$  as  $b$  is decreased. This effect is shown in Figure 8.1. If  $x(\theta)$  also contains lower frequencies, the results are the same, since the highest frequency term produced contains  $b^m$  or a higher power.

Simulations of the spectrum generated by monopolar PWM for AM and DSB/SC signals are shown in Figures 8.2 and 8.3, with the modulation reduced to half of its maximum depth. For DSB/SC, spurious products drop 19.2 dB near the carrier; for AM, 87 dB.

Simulations of a 1% bias error are shown in Figures 8.4 and 8.5. An IMD reduction of 9.4 dB (compared to the desired sidebands) can be observed for the AM signal. However, for the DSB/SC signal, the IMD to sideband ratio increases 2.4 dB (although the actual IMD magnitude decreases). The cause of this is that the bias correction pulses ( $u_B(\theta)$ ) still suffer abrupt phase shifts according to  $\text{sgn } x(\theta)$ . Thus decrease of signal magnitude does not help IMD much for DSB/SC (or SSB).

The method of finding the spectrum of a distortion function will be illustrated for  $u_1(\theta)$  of an AM modulating signal:

$$x(\theta) = \frac{1}{2}(1 + \sin \theta) \quad , \quad (8.22)$$

$$x^2(\theta) = \frac{1}{2^2}(1 + 2\sin \theta + \sin^2\theta), \quad (8.23)$$

etc. Then substitution into (8.3) produces

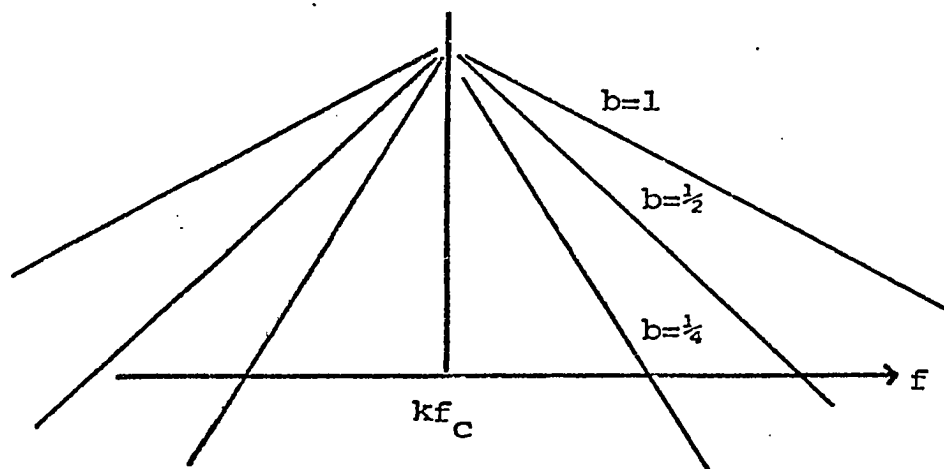


Figure 8.1. Variation of Spurious Products with Depth of Modulation.

$$\begin{aligned}
 u_1(\theta) &= 1 - \frac{1}{2} \frac{1}{2^2} (1 + 2\sin\theta + \sin^2\theta) \\
 &+ \frac{(1-2)}{4!} \frac{1}{2^4} (1 + 4\sin\theta + 6\sin^2\theta + 4\sin^3\theta + \sin^4\theta) \\
 &- \frac{(1-2^2)(1-4^2)}{6!} \frac{1}{2^6} (1 + 6\sin\theta + \frac{6 \cdot 5}{1 \cdot 2} \sin^2\theta) \\
 &+ \frac{6 \cdot 5 \cdot 4}{1 \cdot 2 \cdot 3} \sin^3\theta + \frac{6 \cdot 5}{1 \cdot 2} \sin^4\theta + \frac{6 \cdot 5}{1 \cdot 2} \sin^5\theta + \sin^6\theta) \\
 &+ \dots \tag{8.24} \\
 &= \left[ 1 - \frac{1}{2!2^2} + \frac{(1-2^2)}{2^4} \frac{1}{4!} - \frac{(1-2^2)(1-4^2)}{2^6} \frac{1}{6!} + \frac{(1-2^2)(1-4^2)(1-6^2)}{2^8} \frac{1}{8!} \right. \\
 &\quad \left. - \dots \right] \\
 &+ \left[ 0 - \frac{1}{2!2^2} \binom{2}{1} + \frac{(1-2^2)}{4!} \frac{1}{2^4} \binom{4}{1} - \frac{(1-2^2)(1-4^2)}{6!} \frac{1}{2^6} \binom{6}{1} + \dots \right] \sin\theta \\
 &+ \left[ 0 - \frac{1}{2!2^2} \binom{2}{2} + \frac{(1-2^2)}{4!} \frac{1}{2^4} \binom{4}{2} - \frac{(1-2^2)(1-4^2)}{6!} \frac{1}{2^6} \binom{6}{2} + \dots \right] \sin^2\theta \\
 &+ \left[ 0 + 0 + \frac{(1-2^2)}{4!} \frac{1}{2^4} \binom{4}{3} - \frac{(1-2^2)(1-4^2)}{6!} \frac{1}{2^6} \binom{6}{3} + \dots \right] \sin^3\theta
 \end{aligned}$$

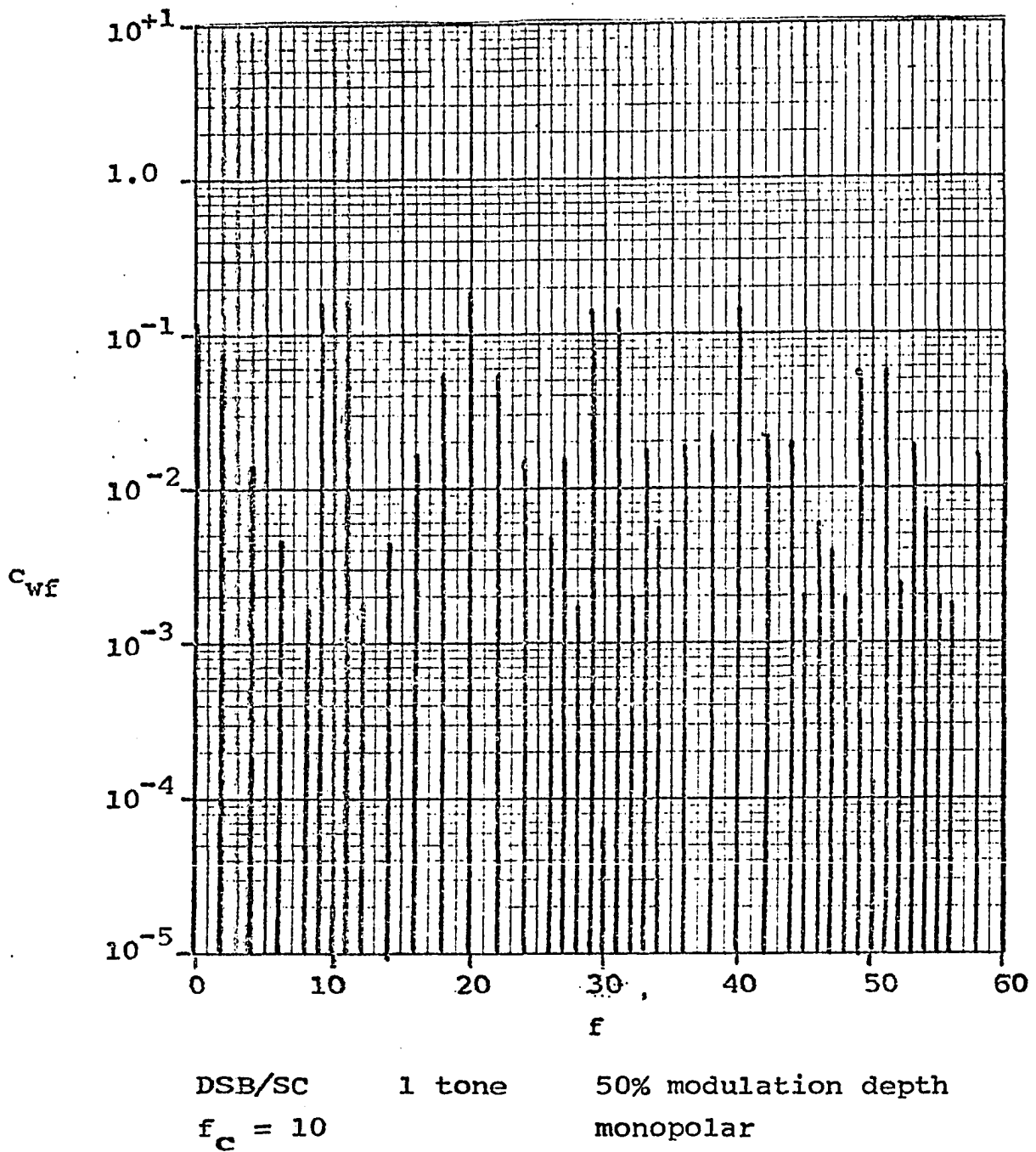


Figure 8.2. Spectrum of a Class D RF Amplifier.

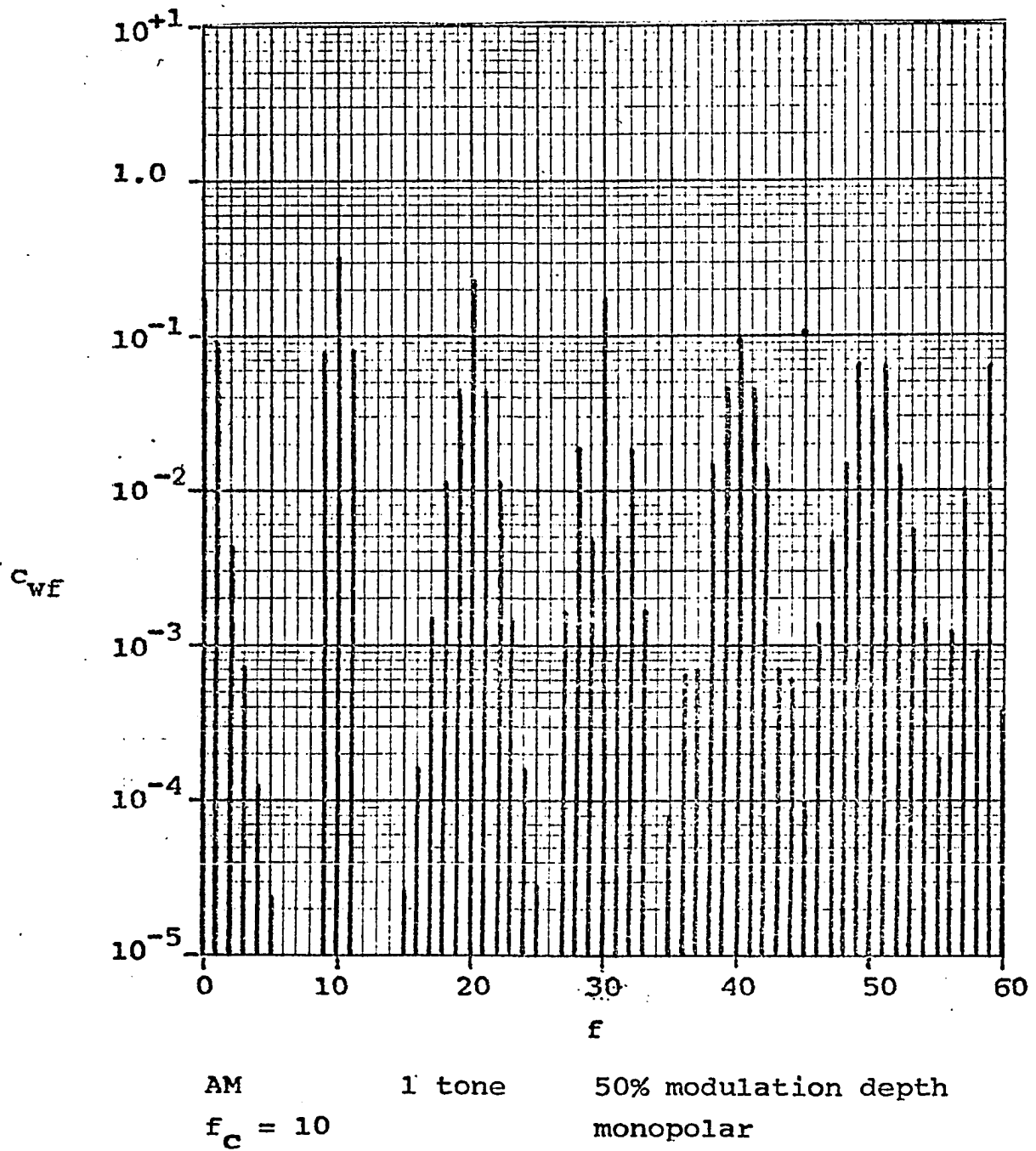


Figure 8.3. Spectrum of a Class D RF Amplifier.

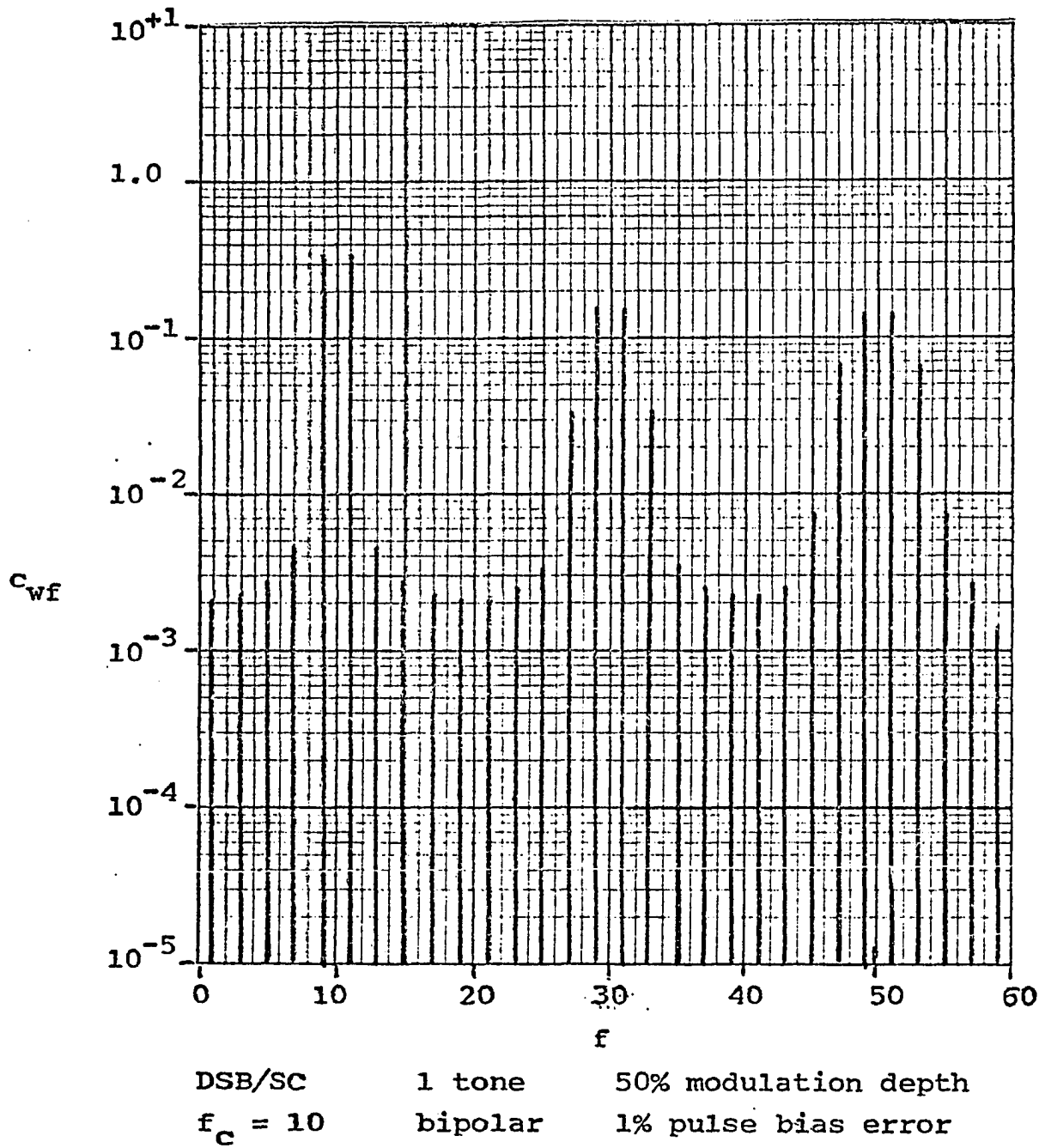
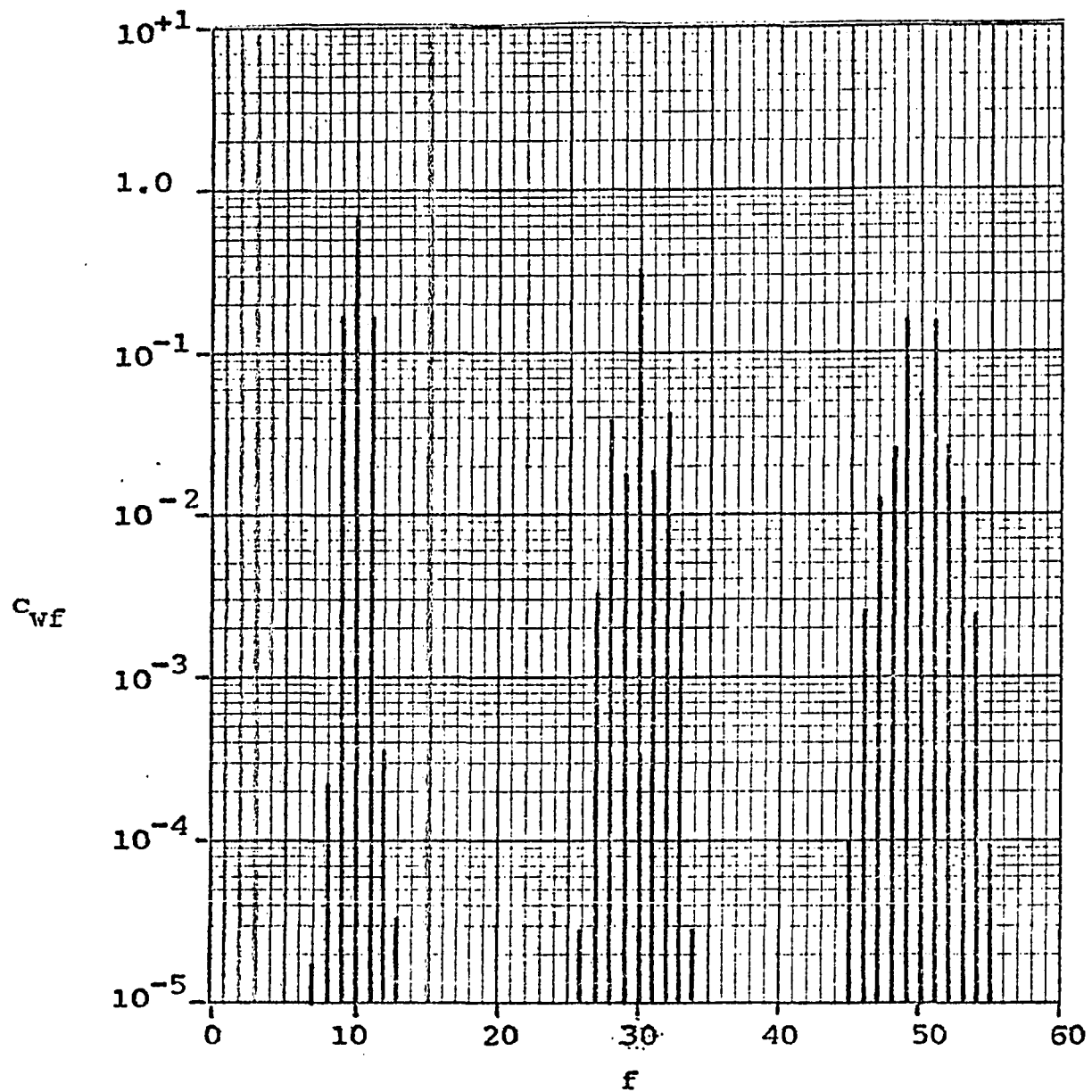


Figure 8.4. Spectrum of a Class D RF Amplifier.



AM                    1 tone                    50% modulation depth  
 $f_c = 10$             bipolar                    1% pulse bias error

Figure 8.5. Spectrum of a Class D RF Amplifier.



$$+ [0 + 0 + \frac{(1-2^2)}{4!} \binom{4}{2^4} - \frac{(1-2^2)(1-4^2)}{6!} \binom{6}{2^6} + \dots] \sin^4 \theta$$

$$+ \dots \quad (8.25)$$

$$= \eta_0 + \eta_1 \sin \theta + \eta_2 \sin^2 \theta + \dots \quad (8.26)$$

(The above also could have been obtained by a Taylor series expansion.)

The decompositions of powers of sine and cosine are then used to produce

$$\begin{aligned} u_1(\theta) &= \eta_0 [1] \\ &+ \eta_1 [\sin \theta] \\ &+ \eta_2 \frac{(-1)}{2} \left[ \frac{-1}{2} \binom{2}{1} + \cos 2\theta \right] \\ &+ \eta_3 \frac{1}{2^2} \left[ -\binom{3}{1} \sin \theta + \sin 3\theta \right] \\ &+ \eta_4 \frac{1}{2^3} \left[ \frac{1}{2} \binom{4}{2} - \binom{4}{1} \cos 2\theta + \cos 4\theta \right] \\ &+ \dots \quad (8.27) \end{aligned}$$

Thus

$$\begin{aligned} a_{u0} &= \eta_0 + \frac{1}{2^2} \binom{2}{1} \eta_2 + \frac{1}{2^4} \binom{4}{2} \eta_4 + \dots \\ b_{u1} &= \eta_1 - \frac{1}{2^2} \binom{3}{1} \eta_3 + \frac{1}{2^4} \binom{5}{2} \eta_5 + \dots \\ a_{u2} &= -\frac{1}{2} \eta_2 - \frac{1}{2^3} \binom{4}{1} \eta_4 - \frac{1}{2^5} \binom{6}{2} \eta_6 + \dots \quad (8.28) \end{aligned}$$

etc.

The equations above work, but due to the infinite sums involving other infinite sums, are very difficult to evaluate. Introduction of variable carrier level and modulation depth

can further complicate the situation.

It seems that expressions for the spurious product spectrum for a general modulating signal are too general to be useful (without more work). Some work on the spectrum of an FM signal with a general modulating signal has been done (24), but results are still general.

The above results apply only to AM signals. For DSB signals,  $\text{sgn } x(\theta)$  has to be decomposed, and then multiplied with power series results. Possibly the most practical way to attack this problem would be to use a polynomial approximation for  $\cos y \text{sgn } x$ . Such an approximation might actually come closer to the actual situation, since it would, in a sense, introduce pulse deterioration rather than abrupt polarity reversals.

Finally, for single sideband signals, substitutions replacing

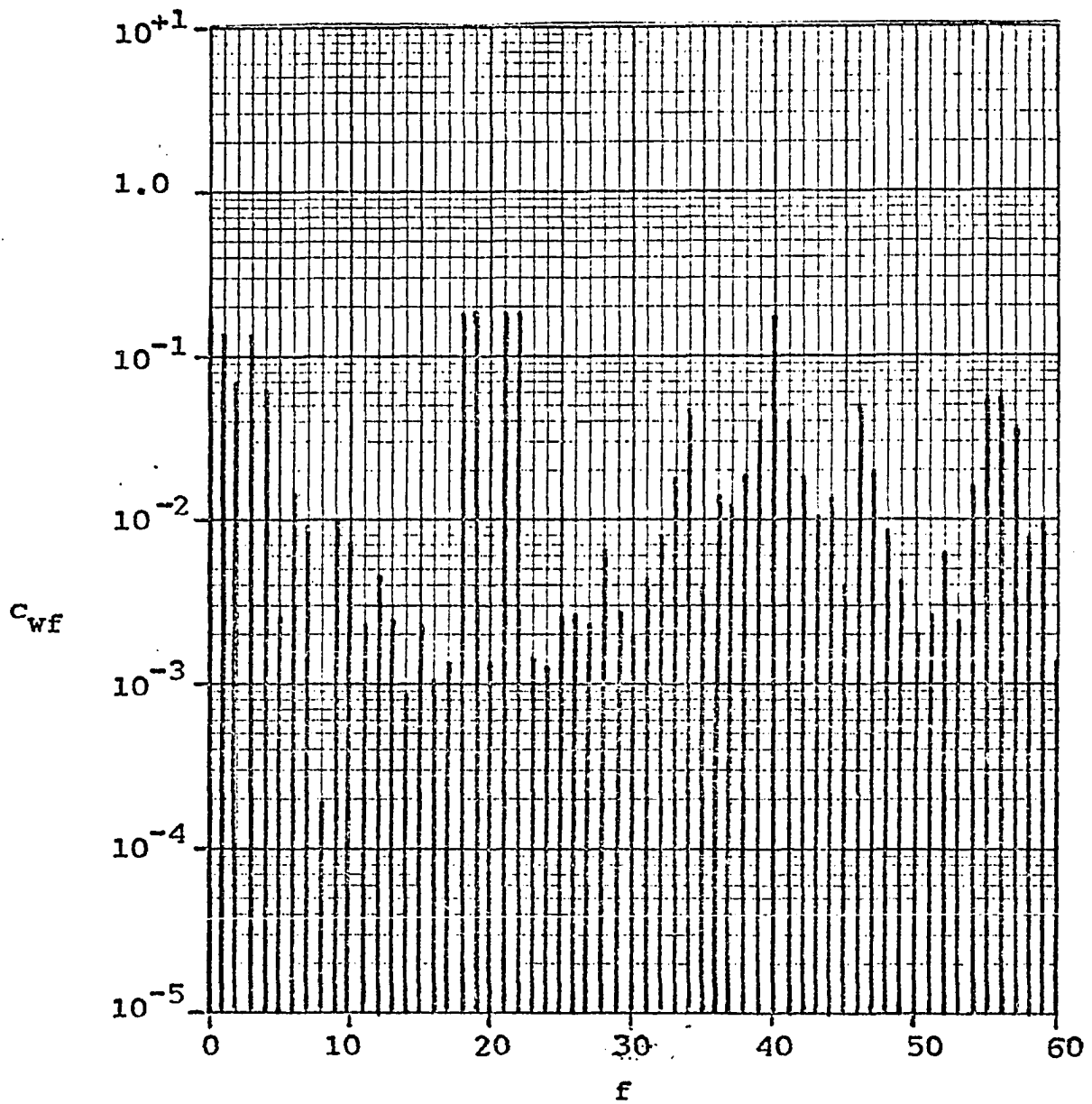
$$g(\theta) \text{sgn } x(\theta) \sin \omega_c t \quad (8.29)$$

with

$$g(\theta) [\cos \varpi(\theta) \sin \omega_c t + \sin \varpi(\theta) \cos \omega_c t] \quad (8.30)$$

must be used. Again, without further work, (8.30) has little meaning.

In Chapter V it was suggested that a single tone at the highest frequency used (two tones for SSB) produced a severe test of the system, since all the energy is packed at the edge of the band. While qualitatively this seems correct, it must



DSB/SC 2 tone ( $\alpha = .10$ ) 50% modulation depth  
 $f_c = 20$  monopolar

Figure 8.6. Spectrum of a Class D RF Amplifier.

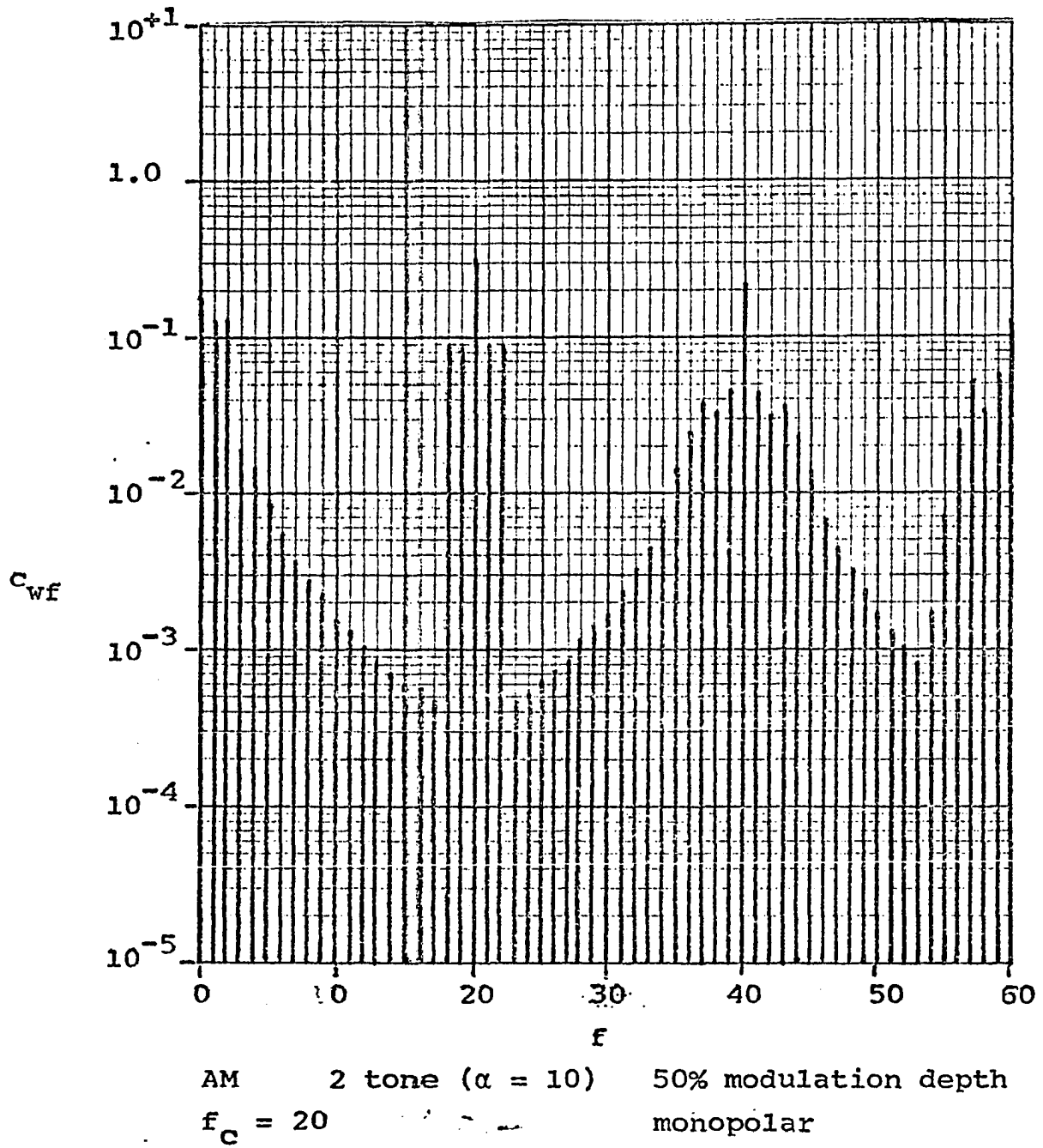


Figure 8.7. Spectrum of a Class D RF Amplifier.

be applied with caution. For example, a two-tone (equal magnitude) test of an SSB class D transmitter might produce small spurious products. Introduction of a third tone (with corresponding decreases in the other two to prevent overmodulation), can result in spurious products if its frequency is not halfway between the frequencies of the other two tones.

Simulations of DSB/SC and AM with two equal tones (whose peak is 1) are shown in Figures 8.6 and 8.7. The carrier frequencies are 20 instead of 10, so  $\alpha$  is the same as in previous simulations. The spurious products near the carrier decrease by 16.5 dB and 13.6 dB, respectively, from the single tone case. While this certainly does not prove absolute validity of the single-tone test, it does illustrate some usefulness.

## IX. DISTORTION REDUCTION BY USE OF FEEDBACK

Feedback systems offer a means of reducing spurious products due to timing errors. Efficiency may still be high for rise/fall times of 10%, but distortion may be too great to make the amplifier useful unless feedback is used.

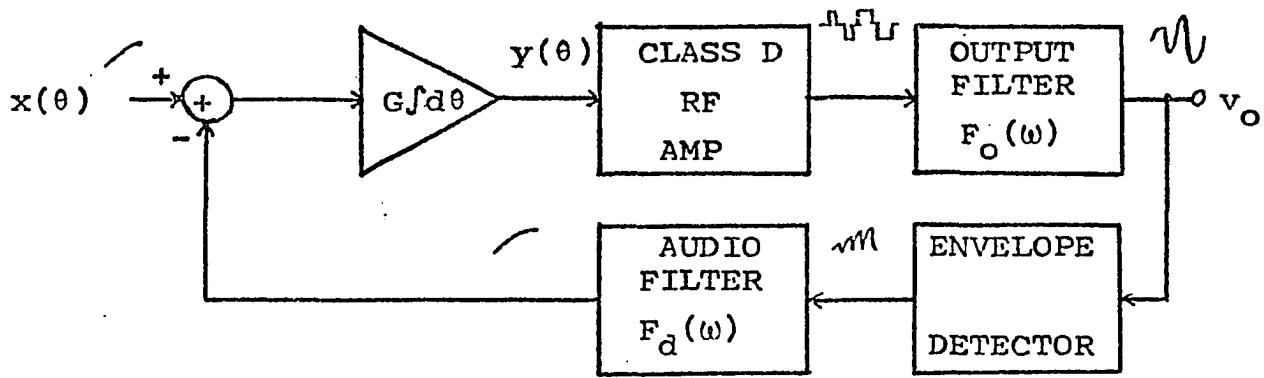
The basic principle of a feedback system is that it examines both output and input, and adjusts the output to equal the input. Determination of the behavior of a feedback system containing a non-linearity is difficult, but by making some approximations, approximate characteristics can be determined.

Figure 9.1(a) shows the basic form of an actual system. The pulse train output from the class D amplifier can be decomposed into harmonics of  $f_c$ . By assuming negligible splatter from modulation of these harmonics, they can be neglected, and the characteristics of the output filter  $F_0(\omega)$  and detector filter  $F_D(\omega)$  lumped into one audio filter  $F(\omega)$  (Figure 9.1(b)). The system can then be reduced to an audio system, where the distortion effects are performed by a function  $p(y;\sigma)$  (Figure 9.1(c)).

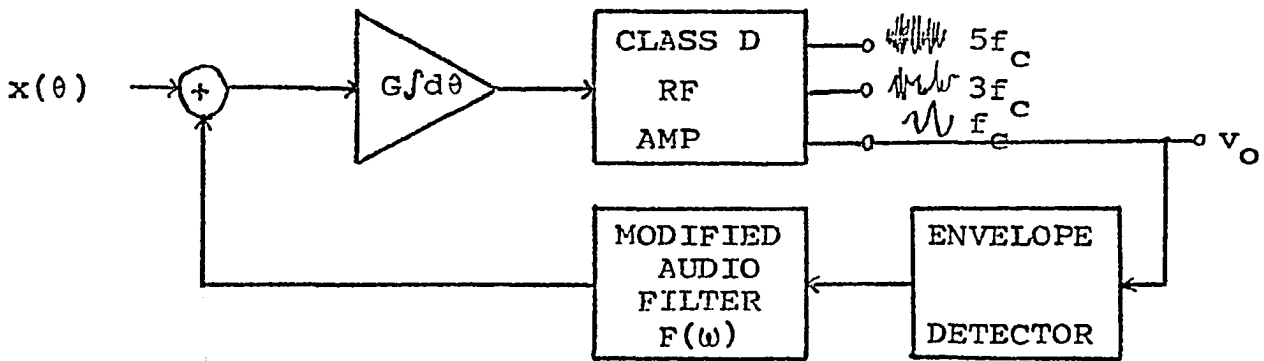
By specifying the Fourier coefficients of  $x(\theta)$ , it should be possible to set up and solve equations for the Fourier coefficients of  $u(\theta)$  which give a steady state solution. However, the function  $p(y;\sigma)$  has the form (for bipolar AM)

$$p(y;\sigma) = y + \frac{\sigma}{4} [\cos \arcsin x] , \quad (9.1)$$

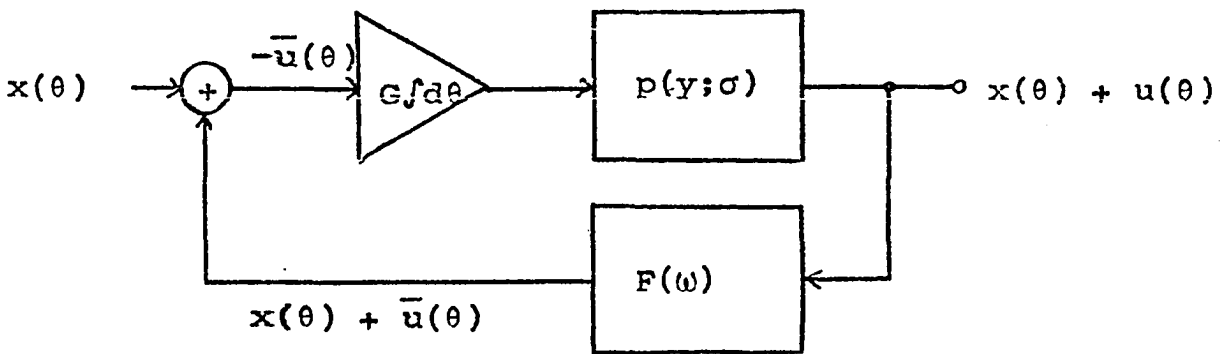
since



(a) Actual System



(b) Decomposition by Harmonics of the Carrier



(c) Reduction to Audio System

Figure 9.1. Feedback System.

$$\begin{aligned} & \frac{4}{\pi} x(\theta) \sin \omega_c t + \frac{\sigma}{\pi} \cos \arcsin x \sin \omega_c t \\ & = \frac{4}{\pi} \left[ x(\theta) + \frac{\sigma}{4} \cos \arcsin x(\theta) \right] , \end{aligned} \quad (9.2)$$

and generates an infinite number of frequencies for any input other than DC. It is not hard to see that this complicates the problem tremendously.

A means of avoiding this is to approximate  $p(y; \sigma)$  by a finite number of terms. For example, if

$$p(y; \sigma) \approx y + \frac{\sigma}{4} \left[ 1 - \frac{1}{2} y^2 \right] , \quad (9.3)$$

the frequencies generated will be no greater than twice the highest frequency in  $x(\theta)$ .

Even with this simplification, the feedback loop can cause an infinite number of frequencies to be generated. As the second harmonic generated by  $p(y; \sigma)$  is fed back, it generates a fourth harmonic, etc. This can be eliminated by assuming that  $F(\omega)$  cuts off completely at a certain frequency, eliminating completely all higher frequency products.

The resultant equations are still complicated but can be solved by the use of numerical iteration. The technique will be illustrated for an AM signal.

$$x(\theta) = a_{x0} + b_{x1} \sin \theta , \quad (9.4)$$

with the approximation (9.3) for  $p(y; \sigma)$  and an  $F(\omega)$  which passes frequencies up to  $2\frac{1}{2}\omega_x$  with no attenuation, while rejecting completely all higher frequencies.

The resultant form of  $\bar{u}(\theta)$  is



$$\begin{aligned} \bar{u}(\theta) = & a_{u0} + a_{u1} \cos \theta + b_{u1} \sin \theta \\ & + a_{u2} \cos 2\theta + b_{u2} \sin 2\theta \end{aligned} \quad (9.5)$$

Then the integrated error signal has the form

$$\begin{aligned} y(\theta) = & a_{y0} + a_{y1} \cos \theta + b_{y1} \sin \theta \\ & + a_{y2} \cos 2\theta + b_{y2} \sin 2\theta - Ga_{u0}\theta \end{aligned} \quad (9.6)$$

$$= G \int u(\theta) d\theta, \quad (9.7)$$

Unless  $y(\theta)$  is to become larger without limit,  $Ga_{u0}\theta$  must be zero, so

$$a_{u0} = 0. \quad (9.8)$$

This causes

$$a_{y1} = -Gb_{u1} \quad (9.9)$$

$$b_{y1} = +Ga_{u1} \quad (9.10)$$

$$a_{y2} = -\frac{G}{2}b_{u2} \quad (9.11)$$

$$b_{y2} = +\frac{G}{2}a_{u2} \quad (9.12)$$

The DC term,  $a_{y0}$ , is a constant which is determined by the rest of the equations.

The term  $y^2$  in (9.3) can be expanded:

$$\begin{aligned} y^2(\theta) = & [a_{y0}^2 + \frac{1}{2}a_{y1}^2 + \frac{1}{2}b_{y1}^2 + \frac{1}{2}a_{y2}^2 + \frac{1}{2}b_{y2}^2] \\ & + [2a_{y0}a_{y1} + a_{y1}a_{y2} + b_{y1}b_{y2}] \cos \theta \\ & + [2a_{y0}b_{y1} + a_{y1}b_{y2} - b_{y1}a_{y2}] \sin \theta \\ & + [2a_{y0}a_{y2} + \frac{1}{2}a_{y1}^2 - \frac{1}{2}b_{y1}^2] \cos 2\theta \end{aligned}$$

$$\begin{aligned}
& + [2a_{y0}b_{y2} + a_{y1}b_{y1}] \sin 2\theta \\
& + [a_{y1}a_{y2} - b_{y1}b_{y2}] \cos 3\theta \\
& + [a_{y1}b_{y2} + b_{y1}a_{y2}] \sin 3\theta \\
& + \left[\frac{1}{2}a_{y2}^2 - \frac{1}{2}b_{y2}^2\right] \cos 4\theta \\
& + [a_{y2}b_{y2}] \sin 4\theta \quad . \quad (9.13)
\end{aligned}$$

The resulting distorted output then has the form

$$p(y;\sigma) = a_{p0} + a_{p1} \cos \theta + \dots + b_{p4} \sin 4\theta \quad , \quad (9.14)$$

where

$$\begin{aligned}
a_{p0} = & a_{y0} + \frac{\sigma}{4} - \frac{\sigma}{8}a_{y0}^2 - \frac{\sigma}{16}G^2b_{u1}^2 - \frac{\sigma}{16}G^2a_{u1}^2 \\
& - \frac{\sigma}{4 \cdot 16}G^2b_{u2}^2 - \frac{\sigma}{4 \cdot 16}G^2a_{u2}^2 \quad (9.15)
\end{aligned}$$

$$a_{p1} = -Gb_{u1} + \frac{\sigma}{4}Ga_{y0}b_{u1} - \frac{\sigma}{16}G^2b_{u1}b_{u2} - \frac{\sigma}{16}G^2a_{u1}a_{u2} \quad (9.16)$$

$$b_{p1} = Ga_{u1} - \frac{\sigma}{16}Ga_{y0}a_{u1} + \frac{\sigma}{16}G^2b_{u1}a_{u2} - \frac{\sigma}{16}G^2a_{u1}b_{u2} \quad (9.17)$$

$$a_{p2} = -\frac{G}{2}b_{u2} + \frac{\sigma}{8}Ga_{y0}b_{u2} - \frac{\sigma}{16}G^2b_{u1}^2 + \frac{\sigma}{16}G^2a_{u1}^2 \quad (9.18)$$

$$b_{p2} = \frac{G}{2}a_{u2} - \frac{\sigma}{8}Ga_{y0}a_{u2} + \frac{\sigma}{8}G^2b_{u1}a_{u1} \quad (9.19)$$

$$a_{p3} = -\frac{\sigma}{16}G^2b_{u1}b_{u2} + \frac{\sigma}{16}G^2a_{u1}a_{u2} \quad (9.20)$$

$$b_{p3} = \frac{\sigma}{16}G^2b_{u1}a_{u2} + \frac{\sigma}{16}G^2a_{u1}b_{u2} \quad (9.21)$$

$$a_{p4} = -\frac{\sigma}{64}G^2b_{u2}^2 + \frac{\sigma}{64}G^2a_{u2}^2 \quad (9.22)$$

$$b_{p4} = \frac{\sigma}{32}b_{u2}a_{u2} \quad . \quad (9.23)$$

The balance of these against the Fourier coefficients of

$x + u$  requires

$$a_{p0} = a_{x0} + 0 \quad , \quad (9.24)$$

$$a_{p1} = 0 + a_{u1} \quad , \quad (9.25)$$

$$b_{p1} = b_{x1} + b_{u1} \quad , \quad (9.26)$$

$$a_{p2} = 0 + a_{u2} \quad , \quad (9.27)$$

and

$$b_{p2} = 0 + b_{u2} \quad . \quad (9.28)$$

Five non-linear equations in five unknowns result. For notational simplicity, let

$$c_1 = a_{y0} \quad , \quad (9.29)$$

$$c_2 = a_{u1} \quad , \quad (9.30)$$

$$c_3 = b_{u1} \quad , \quad (9.31)$$

$$c_4 = a_{u2} \quad , \quad (9.32)$$

$$c_5 = b_{u2} \quad . \quad (9.33)$$

The five non-linear equations are then

$$c_1 + \frac{\sigma}{4} - \frac{\sigma}{8}c_1^2 - \frac{\sigma}{16}G^2c_3^2 - \frac{\sigma}{16}c_2^2 - \frac{\sigma}{64}c_5^2 - \frac{\sigma}{64\pi}c_4^2 = a_{x0} \quad (9.34)$$

$$-Gc_3 + \frac{\sigma}{4}Gc_1c_3 - \frac{\sigma}{16}G^2c_3c_5 - \frac{\sigma}{16}G^2c_2c_4 = c_2 \quad (9.35)$$

$$Gc_2 - \frac{\sigma}{4}Gc_1c_2 + \frac{\sigma}{16}G^2c_3c_4 - \frac{\sigma}{16}G^2c_2c_5 = b_{x1} + c_3 \quad (9.36)$$

$$-\frac{G}{2}c_4 + \frac{\sigma}{8}Gc_1c_4 - \frac{\sigma}{16}G^2c_3^2 + \frac{\sigma}{16}G^2c_2^2 = c_4 \quad (9.37)$$

$$\frac{G}{2}c_5 - \frac{\sigma}{8}Gc_1c_4 + \frac{\sigma}{8}G^2c_3c_2 = c_5 \quad . \quad (9.38)$$

Any sort of direct solution appears difficult. However, when  $\sigma = 0$ , the non-linearities are removed, and a solution

can be obtained. The equations can then be linearized, and solutions found for  $\sigma \neq 0$  by iteration. The linearization process uses

$$c_1 c_2 \rightarrow (c_1 + dc_1)(c_2 + dc_2) \quad (9.39)$$

$$\approx c_1 c_2 + c_1 dc_2 + c_2 dc_1 \quad (9.40)$$

( $dc_1 dc_2$  is dropped). The resultant linearized equations are

$$\begin{aligned} (1 - \frac{\sigma}{4}c_1)dc_1 + (-\frac{\sigma}{8}G^2c_2)dc_2 + (-\frac{\sigma}{8}G^2c_3)dc_3 + (-\frac{\sigma}{8}G^2c_4)dc_4 \\ + (-\frac{\sigma}{8}G^2c_5)dc_5 = a_{x0} - \frac{\sigma}{4} - c_1 + \frac{\sigma}{8}c_1^2 \\ + \frac{\sigma}{16}G^2(c_2^2 + c_3^2 + c_4^2 + c_5^2) \end{aligned} \quad (9.41)$$

$$\begin{aligned} (\frac{\sigma}{4}Gc_3)dc_3 + (-\frac{\sigma}{16}G^2c_4 - 1)dc_2 + (\frac{\sigma}{4}Gc_1 - \frac{\sigma}{16}G^2c_5 - G)dc_3 \\ + (-\frac{\sigma}{16}G^2c_2)dc_4 + (-\frac{\sigma}{16}G^2c_3)dc_5 = c_2 + Gc_3 - \frac{\sigma}{4}Gc_1c_3 \\ + \frac{\sigma}{16}G^2c_3c_5 + \frac{\sigma}{16}G^2c_2c_4 \end{aligned} \quad (9.42)$$

$$\begin{aligned} (-\frac{\sigma}{4}Gc_2)dc_1 + (-\frac{\sigma}{4}Gc_1 - \frac{\sigma}{16}G^2c_5 + G)dc_2 + (\frac{\sigma}{16}G^2c_4 - 1)dc_3 \\ + (\frac{\sigma}{16}G^2c_3)dc_4 + (-\frac{\sigma}{16}G^2c_2)dc_5 = b_{x1} + c_3 - Gc_2 \\ + \frac{\sigma}{4}Gc_1c_2 - \frac{\sigma}{16}G^2c_3c_4 + \frac{\sigma}{16}G^2c_2c_5 \end{aligned} \quad (9.43)$$

$$\begin{aligned} (\frac{\sigma}{8}Gc_4)dc_1 + (\frac{\sigma}{8}G^2c_2)dc_2 + (-\frac{\sigma}{8}G^2c_3)dc_3 + (\frac{\sigma}{8}Gc_1 - \frac{G}{2} - 1)dc_4 \\ + (0)dc_5 = c_4 + \frac{G}{2}c_4 - \frac{\sigma}{8}Gc_1c_4 + \frac{\sigma}{16}G^2c_3^2 - \frac{\sigma}{16}G^2c_2^2 \end{aligned} \quad (9.44)$$

$$\begin{aligned} (-\frac{\sigma}{8}Gc_4)dc_1 + (\frac{\sigma}{8}G^2c_3)dc_2 + (\frac{\sigma}{8}G^2c_2)dc_3 + (-\frac{\sigma}{8}Gc_1)dc_4 \\ + (\frac{G}{2} - 1)dc_5 = c_5 - \frac{G}{2}c_5 + \frac{\sigma}{8}Gc_1c_4 + \frac{\sigma}{8}G^2c_2c_3 \end{aligned} \quad (9.45)$$

These can be arranged in matrix form

$$\overline{\mathbf{D}}(c_1, c_2, c_3, c_4, c_5) \cdot \overline{dC} = \overline{D}(c_1, c_2, c_3, c_4, c_5) \quad (9.46)$$

Given starting values, (9.46) is solved, and then the  $c_i$  are revised according to

$$c_i \leftarrow c_i + dc_i \quad (9.47)$$

and the process is repeated until the  $dc_i$  are insignificant. A convenient starting point is provided by  $G = 0$  and  $\sigma = 0$ . The values with  $\sigma = 0$  can then be computed, and from these, the values with  $\sigma > 0$  can be computed.

With no feedback,

$$x^2(\theta) = (a_{x0} + b_{x1} \sin \theta)^2 \quad (9.48)$$

$$= a_{x0}^2 + 2a_{x0}b_{x1} \sin \theta + b_{x1}^2 \sin^2 \theta \quad (9.49)$$

$$= (a_{x0}^2 + \frac{1}{2}b_{x1}^2) + (2a_{x0}b_{x1}) \sin \theta + (-\frac{1}{2}b_{x1}^2) \cos 2\theta \quad (9.50)$$

The Fourier coefficients of the distortion are then

$$|a_{u1}| = \frac{\sigma}{4} a_{x0}^2 + \frac{1}{2}b_{x1}^2 \quad (9.51)$$

$$|b_{u1}| = \frac{\sigma}{2} a_{x0}b_{x1} \quad (9.52)$$

$$|a_{u2}| = \frac{\sigma}{8}b_{x1}^2 \quad (9.53)$$

For the signal used,

$$|a_{u0}| = \frac{\sigma}{4} \left( \frac{1}{4} + \frac{1}{8} \right) = (.09375)\sigma \quad (9.54)$$

$$|b_{u1}| = \frac{\sigma}{2} \left( \frac{1}{2} \cdot \frac{1}{2} \right) = (.125)\sigma \quad (9.55)$$

$$|a_{u2}| = \frac{\sigma}{8} \left( \frac{1}{2} \right)^2 = (.03125)\sigma \quad (9.56)$$

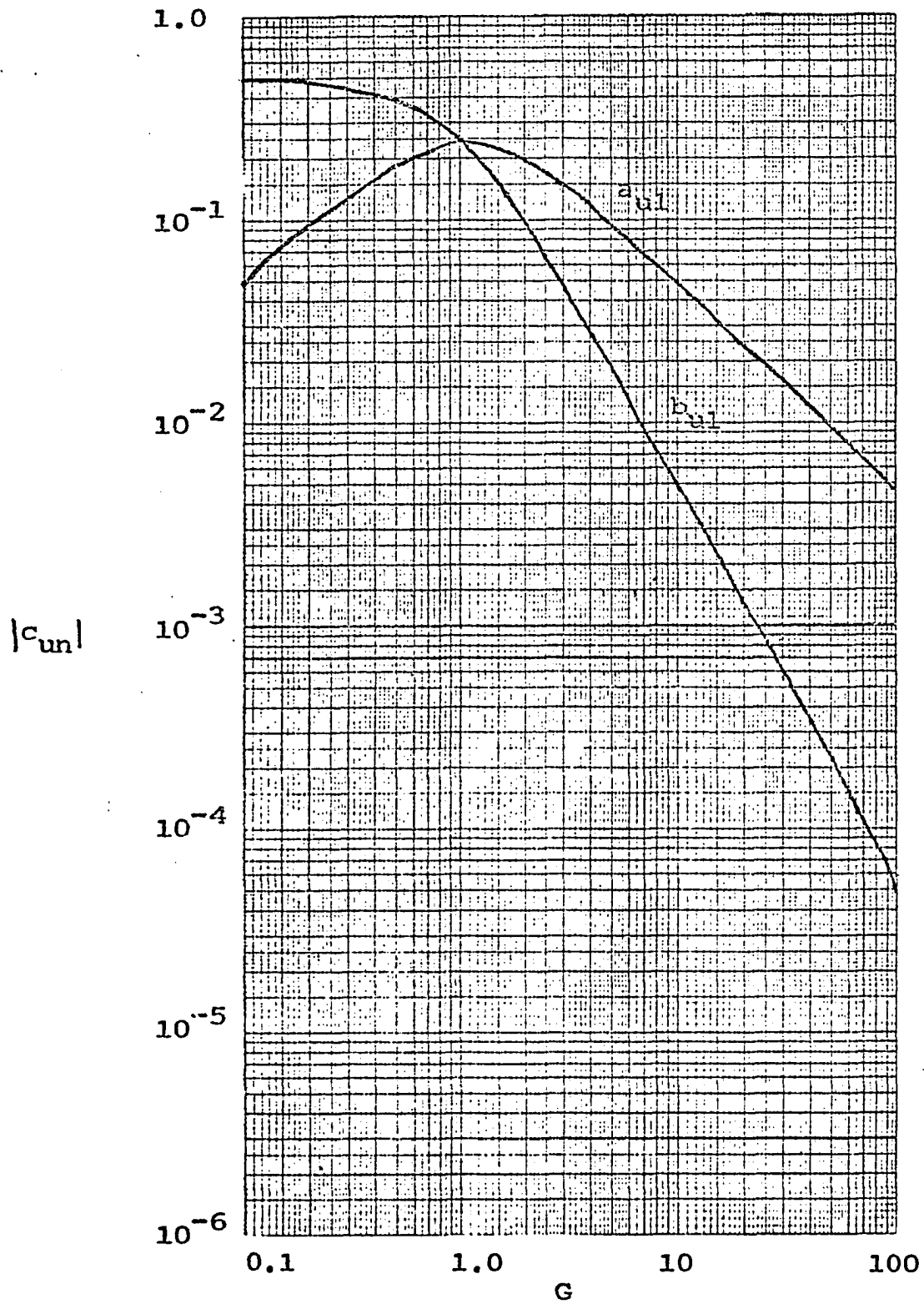


Figure 9.2. Feedback System with  $\sigma/2\pi = 0$ .

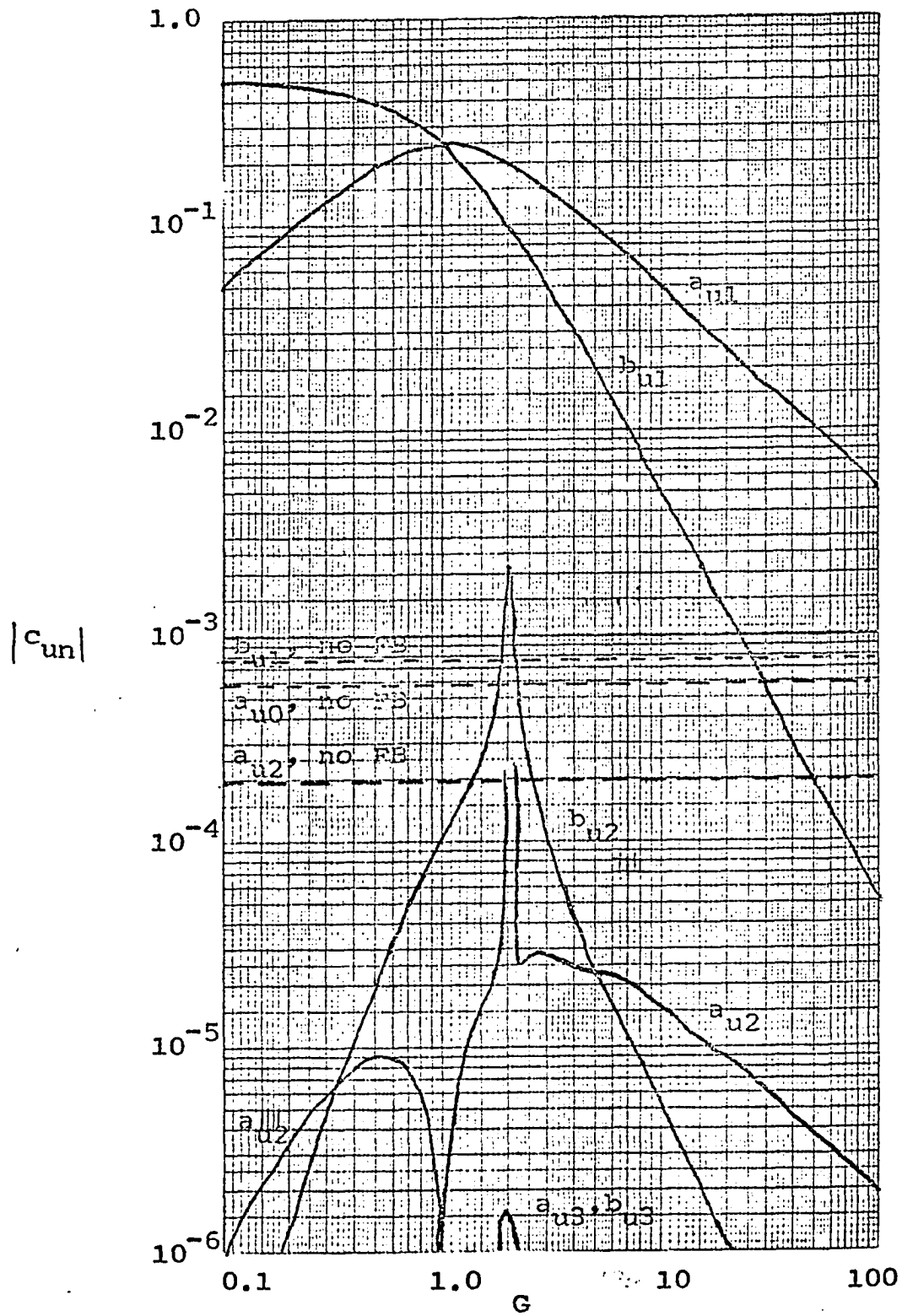


Figure 9.3. Feedback System with  $\sigma/2\pi = 0.001$ .

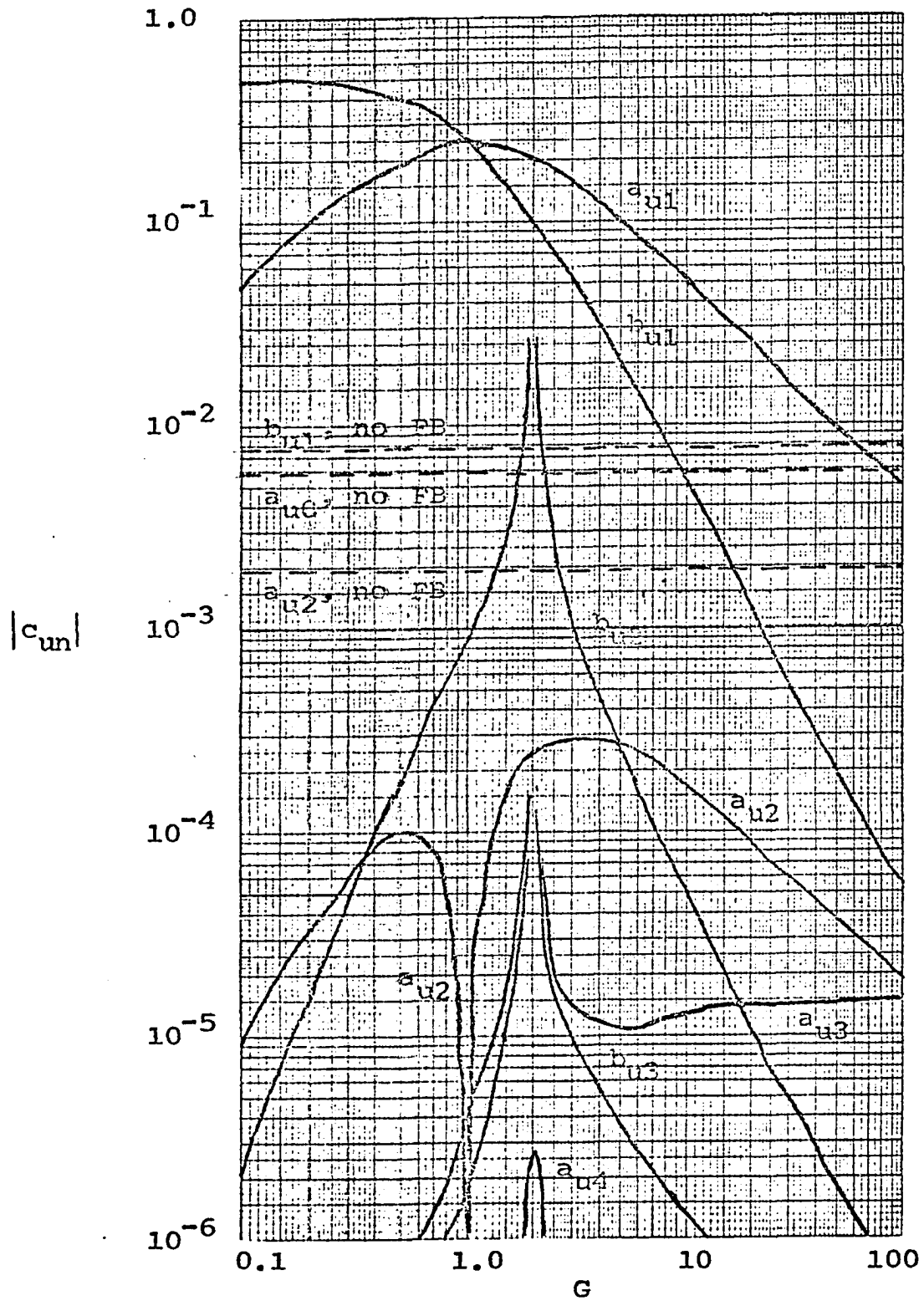


Figure 9.4. Feedback System with  $\sigma/2\pi = 0.01$ .



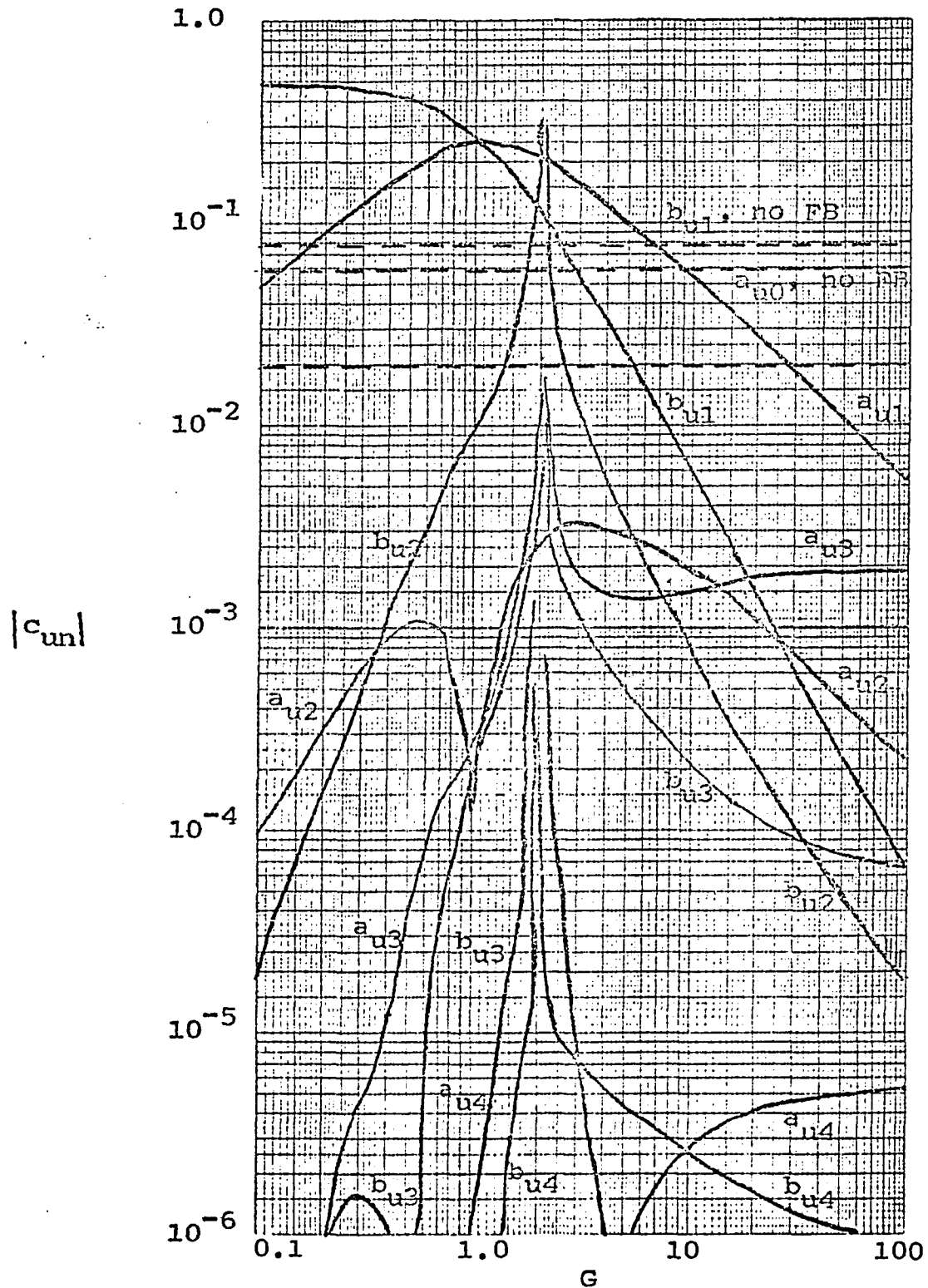


Figure 9.5. Feedback System with  $\sigma/2\pi = 0.1$ .

Solutions for values of  $G$  from 0.1 to 100 and timing errors of 0, 0.1%, 1%, and 10% were found by computer, and are shown in Figures 9.2 through 9.5. Figure 9.2 shows the ability of such a feedback system to "track" the input signal when there is no distortion. In the other figures, variations of the spurious products with gain are shown. There appears to be a sort of resonance at  $G = 2$ , as the filter begins to track, but for higher gains, the magnitudes of the spurious products decrease. A decrease of 20 to 40 dB, depending on  $\sigma$ , is possible with a gain of 100.

This is a long way from a good solution to the feedback system effectiveness. However, the incorporation of additional terms generates an enormous amount of additional work. Possibly computer aided sorting could be used to eliminate the manual differentiation and sorting involved with deriving (9.40) through (9.44).

Some consideration should also be given to application of a feedback system to DSB and SSB generation. The same technique should apply to DSB/SC signals, but the function  $p(y;\sigma)$  will have to be modified. It would probably be best to incorporate pulse deterioration into the model, rather than to use  $\cos \arcsin x \operatorname{sgn}(x)$ , due to discontinuities of the derivatives at  $x = 0$ . For SSB, both envelope and phase feedback might be employed, as in Figure 9.6, and the analysis is likely to be fairly complicated.

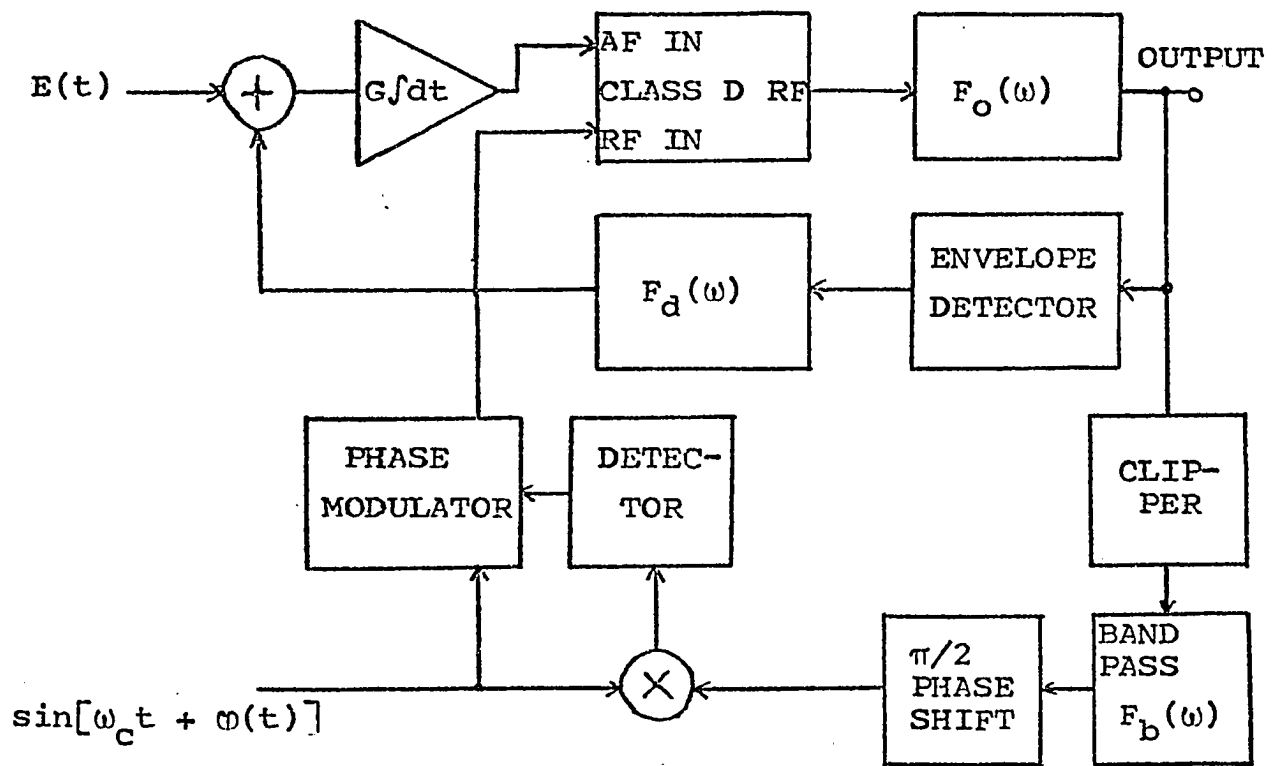


Figure 9.6. Envelope and Phase Feedback System.

## X. COMMENTS AND CONCLUSIONS

The use of pulse-width modulation or class D amplification to generate a modulated radio-frequency signal has been investigated with regard to efficiency and spurious products.

Two significant advantages of PWM switching at the carrier frequency were found: First, its efficiency is higher than that of other types of amplification. Secondly, for double-sideband signals, spurious products for the ideal amplifier are bandlimited around the harmonics of the carrier, and can easily be removed.

Distortions particular to this type of amplifier were analyzed. There are three important types: Voltage error, saturation voltage, and timing error. Voltage-error distortion occurs when positive and negative voltages are unequal, and generates infinite bandwidth spurious products around the even harmonics of the carrier. Non-zero saturation voltage does not generate harmful spurious products for AM, but for DSB/SC or SSB, it generates IMD around the carrier and its odd harmonics. Timing error arises from elongated or shortened pulses, or from unequal transition times. It generates infinite bandwidth products around odd harmonics of the carrier. Generally, the only significant effect is IMD around the carrier. The largest IMD product generated is reduced below the desired signal by approximately the ratio of the net timing error to the period of the carrier.

Further work needs to be done on the spurious products of a general SSB signal. The inherent modulation of odd harmonics of the carrier is not bandlimited. Although simulations show it to decay rapidly, no theoretical assessment was made. Knowledge of the characteristics of this modulation would be very useful in determining whether the interlacing/overlapping methods or Kahn's method would be best for SSB generation.

Knowledge of the spectrum of the spurious products (8.1) for a general modulating signal would be useful, particularly if it can be used to determine absolute upper limits for the spurious products. It may suggest the definition of a new set of special functions to do this.

The applicability of feedback systems, both amplitude and envelope-phase types, should be examined more fully, since reduction of the distortion by feedback will allow the class D amplifier to operate as much as a decade higher in frequency.

Comparisons with other types of high-efficiency amplifiers should be made, including classes AD and BD (see appendix), quantization, and multi-level hybrid methods. The Avco report (18) should be interesting in this respect.

Also interesting would be the combination of a digital single-sideband generator (25) with the class D RF amplifier to make a completely digital transmitter. Spurious products may make this combination unworkable, however.

Because of its high efficiency and desirable spectral

characteristics, the class D RF amplifier may be the best means of extending solid state circuitry to high-power, high-frequency transmitters.

## XI. REFERENCES

1. New Mullard technique amplifies R. F. linearly with efficiency of 90%. Mullard Press Information, London, England. January 1971.
2. Rose, B. E. Notes on class D transistor amplifiers. IEEE Transactions on Solid State Circuits SC-4, No. 3: 178-179. June 1969.
3. Page, D. F., W. D. Hindson, and W. J. Chudobiak. On solid state class D systems. IEEE Proceedings 53: 423-424. 1965.
4. Osborne, M. R. Design of tuned transistor power amplifiers. Electronic Engineering (Australia) 40: 436-443. August 1968.
5. Lohrmann, Dieter R. and James P. Hubert. If back intermodulation is a problem... Electronic Design 19, No. 23: 48-49. 11 November 1971.
6. Besslich, Phillip. Device for amplitude-modulating a high frequency carrier wave. U. S. Patent 3,363,199. 9 January 1968.
7. RCA Power Circuits: DC to Microwave. RCA Electronic Components, Harrison, New Jersey. 1969.
8. RF Power Transistor 2N6093 (Data Sheet). File Number 484. RCA Solid State Division, Somerville, New Jersey. March 1971.
9. Alley, Charles L., and Kenneth W. Attwood. Electronic Engineering. John Wiley and Sons, New York. 1966.
10. Scott, Thomas M. Tuned power amplifiers. IEEE Transactions of Circuit Theory CT-11: 206-211. June 1965.
11. Gates 100,000 Watt Medium Wave AM Broadcast Transmitter (Advertising brochure for VP-100). Gates Radio Company, Quincy, Illinois. 1970.
12. Stokes, V. O. Radio Transmitters: R. F. Power Amplification. Van Nostrand Reinhold Company, London. 1970.
13. Ramachandran, Gopal. A Survey of Pulse Width Modulation. Unpublished M. S. thesis. Library, Iowa State University, Ames, Iowa. 1970.

14. Martin, J. D. Theoretical efficiencies of class-D power amplifiers. IEE Proceedings (London) 117: 1089-1090. 1970.
15. Martin, J. D. Class-BD amplifier circuit. Electronic Letters 6, No. 26: 839-841. December 1970.
16. Black, H. S. Modulation Theory. D. Van Nostrand Company, New York. 1953.
17. Swanson, Hilmer. Private conversation. 1 September 1971.
18. Proposal for High Efficiency Linear SSB Power Amplifier. RFQ DAAB07-71-Q-0179, File Number 17,4183N-1270-USAECOM, Ft. Manmouth, New Jersey. Avco Corporation Electronics Division, Cincinnati, Ohio. 27 January 1971.
19. Kahn, L. R. Single sideband transmission by envelope elimination and restoration. IRE Proceedings, 40, No. 7: 803-806. July 1952.
20. Kahn, L. R. Comparison of linear single-sideband transmitters with envelope elimination and restoration single-sideband transmitters. IRE Proceedings. Vol. 44, No. 6: 1706-1712. December 1956.
21. George, D. A. Continuous Non-Linear Systems. Technical Report Number 355. MIT Research Laboratory of Electronics, Cambridge, Massachusetts. 24 July 1959.
22. Jolley, L. B. W. Summation of Series. Dover Publications, New York. 1961.
23. Bracewell, Ron. The Fourier Transform and its Applications. McGraw-Hill, New York. 1965.
24. Slepian, David. An expansion for FM spectra. IEEE Transactions on Communication Technology COM-19, No. 2: 223. April 1971.
25. Darlington, S. On digital single sideband modulators. IEEE Transactions on Circuit Theory CT-17, No. 3: 409-414. August 1970.
26. Wylie, C. R., Jr. Advanced Engineering Mathematics. McGraw-Hill, New York. 1960.



## A. Additional References

- Baxandall, P. J. Transistor sine-wave LC oscillators. IEE Proceedings (London). Pt. B, Supplement 16 (International convention on Transistors and Associated Semiconductor Devices). May 1959.
- Bell, W. W. Special Functions for Scientists and Engineers. D. Van Nostrand Company, Ltd., London. 1968.
- Johnson, K. C. 1: Class D principles analysed. Wireless World 73, No. 12: 576-580. December 1967.
- Johnson, K. C. 2: The design of a circuit. Wireless World 73, No. 13: 645-649. January 1968.
- Johnson, K. C. 3: Distortion inherent in PWM. Wireless World 73, No. 14: 672-676. February 1968.
- Kretzmer, E. R. Distortion in pulse-duration modulation. IRE Proceedings 35: 1230-1235. 1947.
- Schaefer, R. A. New pulse modulation method varies both frequency and width. Electronics 35: 50-53. 12 October 1962.

## XII. ACKNOWLEDGEMENT

The author wishes to thank his major professors Dr. Grover Brown and Dr. Paul Bond for their advice and assistance during his graduate program. The author is especially grateful for the consultation with Paul Bond during the research for and preparation of the dissertation.

The author wishes to thank the Electrical Engineering Department for providing computer time which was used to obtain many of the results contained herein. The interesting and informative discussions with Hilmer Swanson of Gates Radio Company and Eugene Janning of Avco Electronics were also appreciated. Thanks are in order for Clayton Clifford, who provided valuable assistance in preparing a printed circuit board for the prototype and in taking data. Finally, the author wishes to thank his wife for many long hours spent typing this dissertation, and Avco Electronics Division for the use of their photo-reproduction facilities.

## XIII. APPENDIX I: OTHER AMPLIFIERS

The attention given spurious products generated by a class D RF amplifier might give the impression that it has more severe problems with spurious products than classes B, AD, or BD. It appears, however, that the spurious product problem is no more severe, or even slightly less severe, than those of the other amplifiers. A detailed analysis of the spurious products generated by these amplifiers is beyond the scope of this dissertation, but several quick observations are possible.

## A. Class B

The operation of a single-ended (non push-pull) amplifier may be approximated by a piece-wise linear model shown in Figure 13.1, for unity gain. With no signal input, the amplifier output  $w$  (before the tuned circuit) is the quiescent voltage  $q$ . The amplifier operates linearly, saturating at  $w = 1$  and cutting off at  $w = 0$ .

The waveforms generated by such an amplifier are shown in Figure 13.2. For purposes of analysis, it is convenient to decompose the output waveform  $w(t)$  into a rectified wave  $r(t)$ , quiescent voltage  $q$ , and clipped wave  $u(t)$ :

$$w(t) = r(t) + q + u(t) \quad . \quad (13.1)$$

Ideally,  $q = 0$ , so  $u(t) = 0$ , and the only waveform to contend with is  $r(t)$ . The spectrum of  $r(t)$  can be determined by multiplying the input wave  $r(t)$  by a switching function:

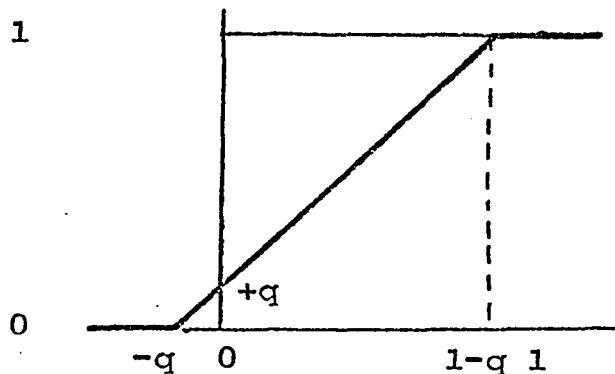


Figure 13.1. Transfer Characteristic for Class B Amplifier.

$$r(t) = v(t) \left[ \frac{\text{sgn } v(t) + 1}{2} \right] \quad (13.2)$$

$$= E(t) \sin[\omega_c t + \varphi(t)] \left\{ \frac{\text{sgn}[\omega_c t + \varphi(t)] + 1}{2} \right\} \quad (13.3)$$

$$= E(t) \sin \psi \left[ \frac{s(\psi) + 1}{2} \right] \quad (13.4)$$

$$= E(t) (\sin \psi) \cdot \frac{2}{\pi} \left( \frac{\pi}{4} + \sin \psi + \frac{1}{3} \sin 3\psi + \dots \right) \quad (13.5)$$

$$= E(t) \frac{2}{\pi} \left[ \frac{\pi}{4} \sin \psi + \frac{1}{2} (\cos 0 - \cos 2\psi) \right. \\ \left. + \frac{1}{3} - \frac{1}{2} (\cos 2\psi - \cos 4\psi) + \dots \right] \quad (13.6)$$

$$= E(t) \left[ \frac{1}{\pi} \frac{1}{2} \sin \psi + \frac{-3+1}{2 \cdot 1 \cdot 3} \sin 2\psi \right. \\ \left. + \frac{-5+3}{2 \cdot 3 \cdot 5} \sin 4\psi + \dots \right] \quad (13.7)$$

$$= \frac{1}{2} E(t) \sin[\omega_c t + \varphi(t)] \\ + \frac{2}{\pi} E(t) \left\{ \frac{1}{2} - \sum_{k=0}^{\infty} \frac{1}{(4k^2-1)} \cos[2k\omega_c t + 2k\varphi(t)] \right\} \quad (13.8)$$

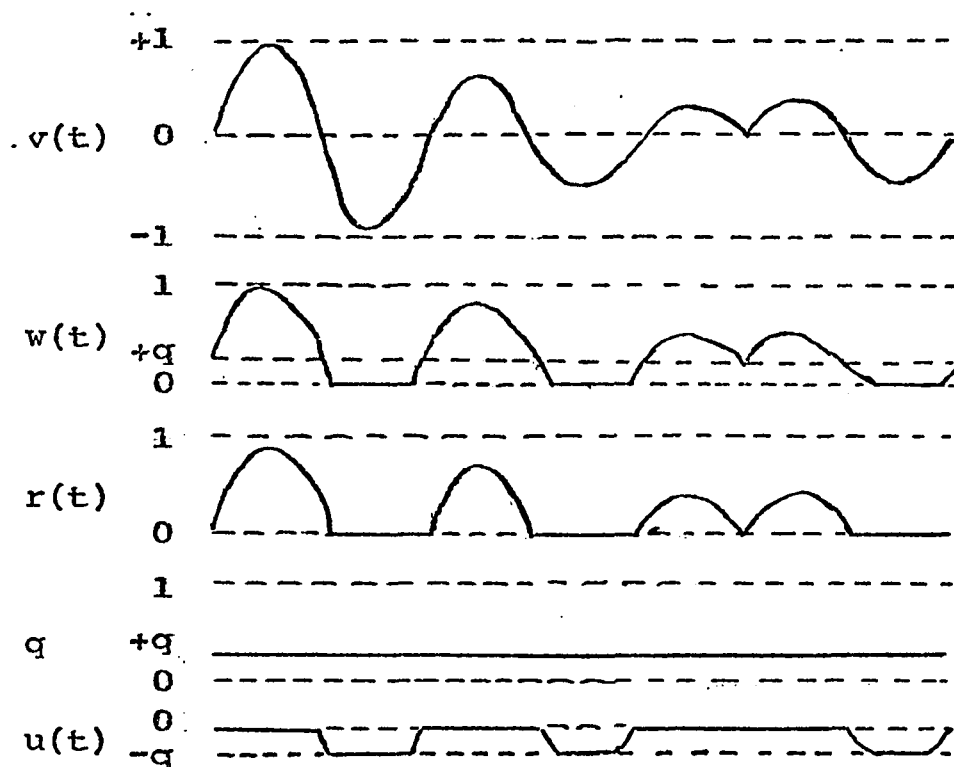


Figure 13.2. Waveforms in a Class B Amplifier.

When unmodulated ( $E = \text{constant}$ ,  $\varphi = 0$ ),  $r(t)$  consists of the carrier frequency, DC, and even harmonics. When  $r(t)$  is an amplitude-modulated signal,

$$E(t) = x(t) \quad (13.9)$$

and 
$$\varphi(t) = 0 \quad , \quad (13.10)$$

so  $r(t)$  becomes simply a series of amplitude-modulated harmonics. A simulation of this is shown in Figure 13.3.

However, for DSB/SC signals (or SSB 2-tone),

$$\varphi(t) = 0 \text{ or } \pi \quad . \quad (13.11)$$

For the even harmonics, a phase shift of  $2k\pi$  produces no polarity reversal. Hence the harmonic and DC component are mod-

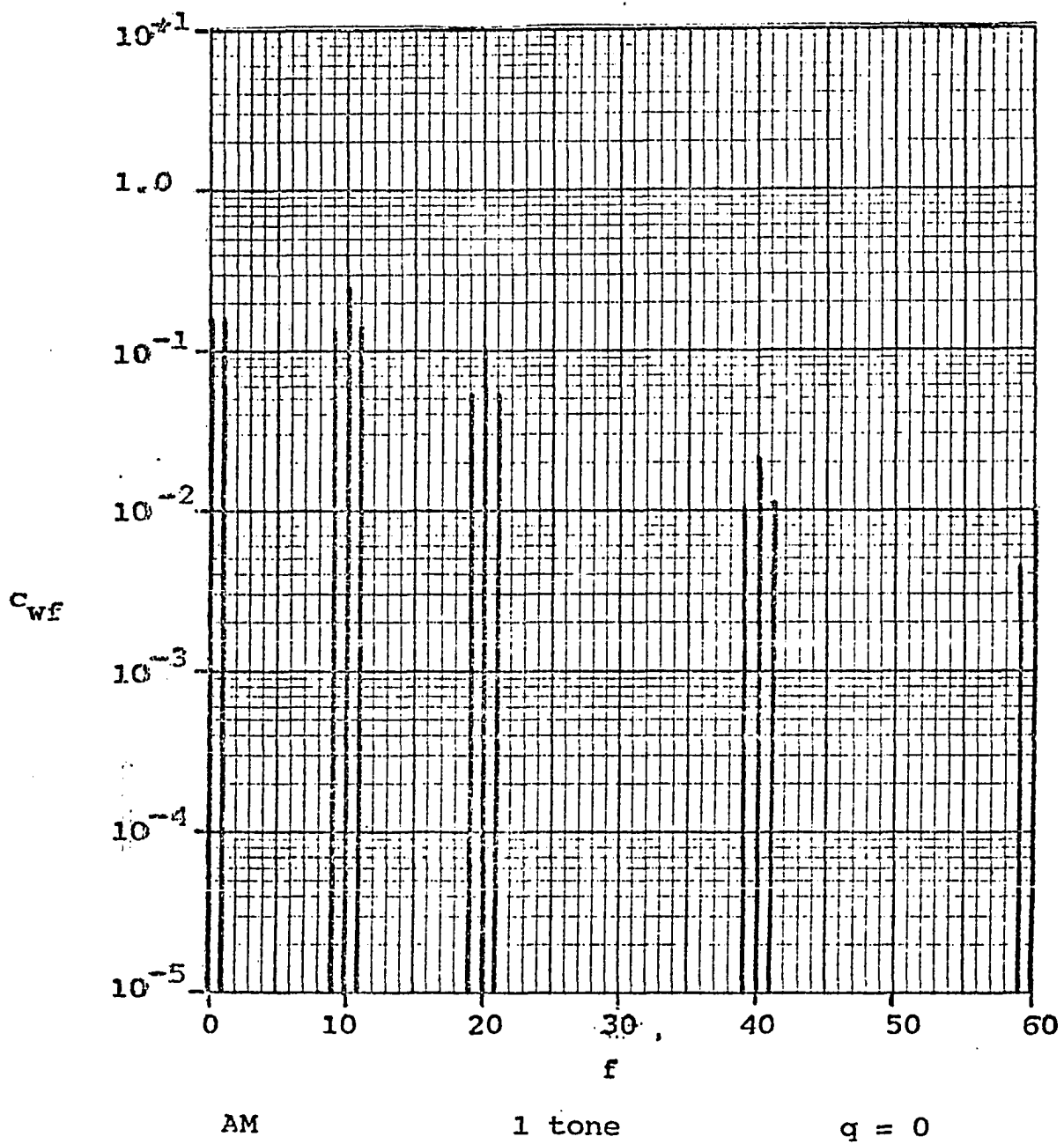


Figure 13.3. Spectrum of a Class B Amplifier.

ulated by  $E(t)$ , which is not bandlimited. A simulation is shown in Figure 13.4. For SSB, the situation is more complicated, but non-bandlimited modulation of the DC component and harmonics occurs as with DSB/SC.

Actual class B amplifiers have a small but non-zero quiescent voltage or current. Any exact analysis of the spectrum of  $u(t)$  is very difficult, and doubtfully warranted, since operation is not exactly linear in this region. However, for small values of  $q$ , cutoff occurs almost instantaneously, producing a square wave

$$u(t) = -q \frac{1 - \operatorname{sgn} v(t)}{2} \quad (13.12)$$

$$\approx -q \frac{1 - s[\omega_c t + \varphi(t)]}{2} \quad (13.13)$$

This is analagous to the effects of non-zero saturation voltage in a class D RF amplifier (Chapter V), and produces phase-modulated odd harmonics of the carrier. (In the case of AM, there is no phase modulation, so the only effects are variation of the carrier level and introduction of odd harmonics of the carrier. A simulation with  $q = 0.01$  (Figure 13.5) shows this to be valid. For  $q = 0.1$  (Figure 13.6), the square wave assumption is no longer valid, although IMD around the carrier and odd harmonics are still apparent.

It is interesting to note that the class B amplifier has spurious products analogous to both voltage error (monopolar) and saturation voltage products in the class D RF amplifier.

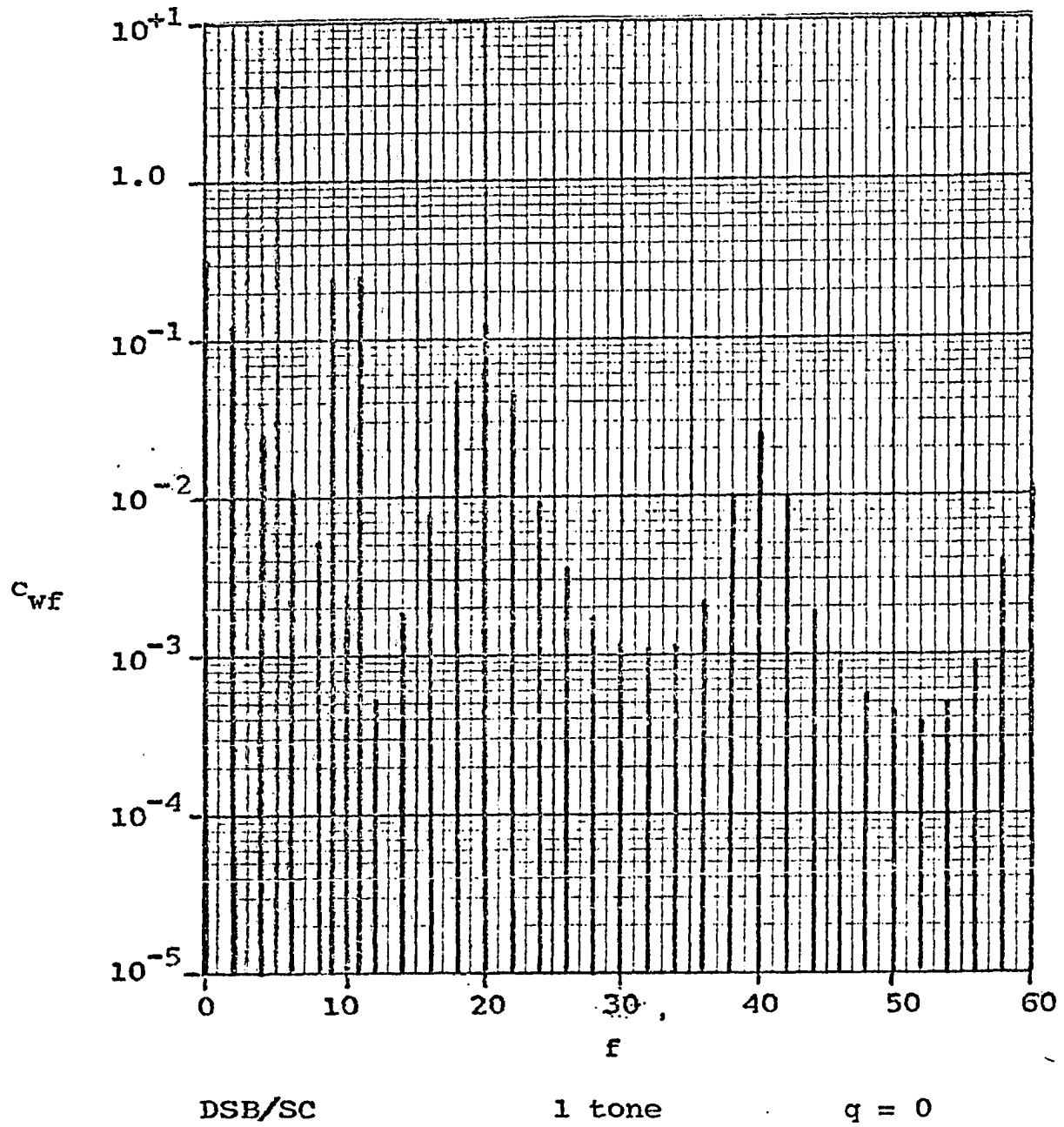


Figure 13.4. Spectrum of a Class B Amplifier.



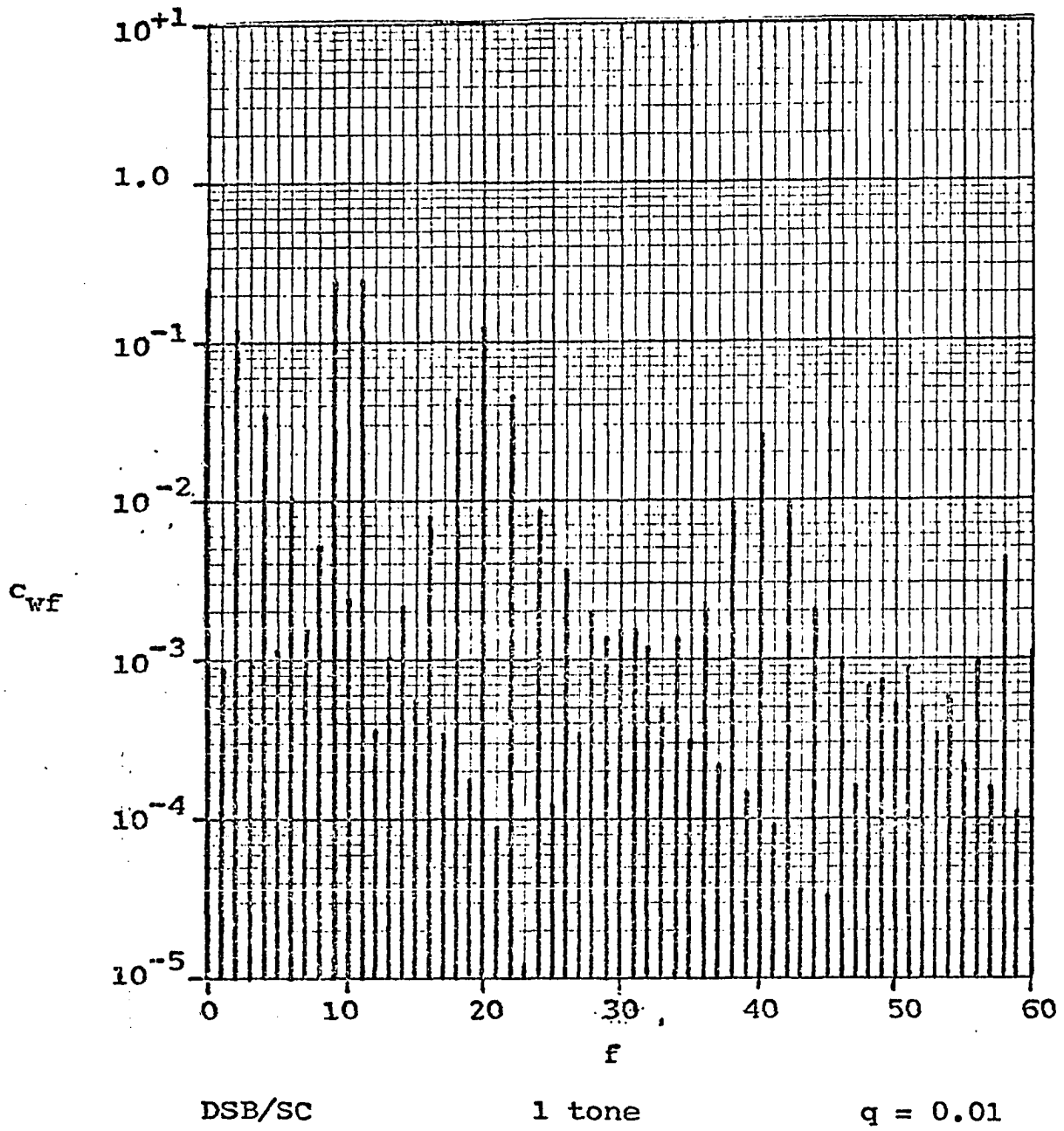


Figure 13.5. Spectrum of a Class B Amplifier.

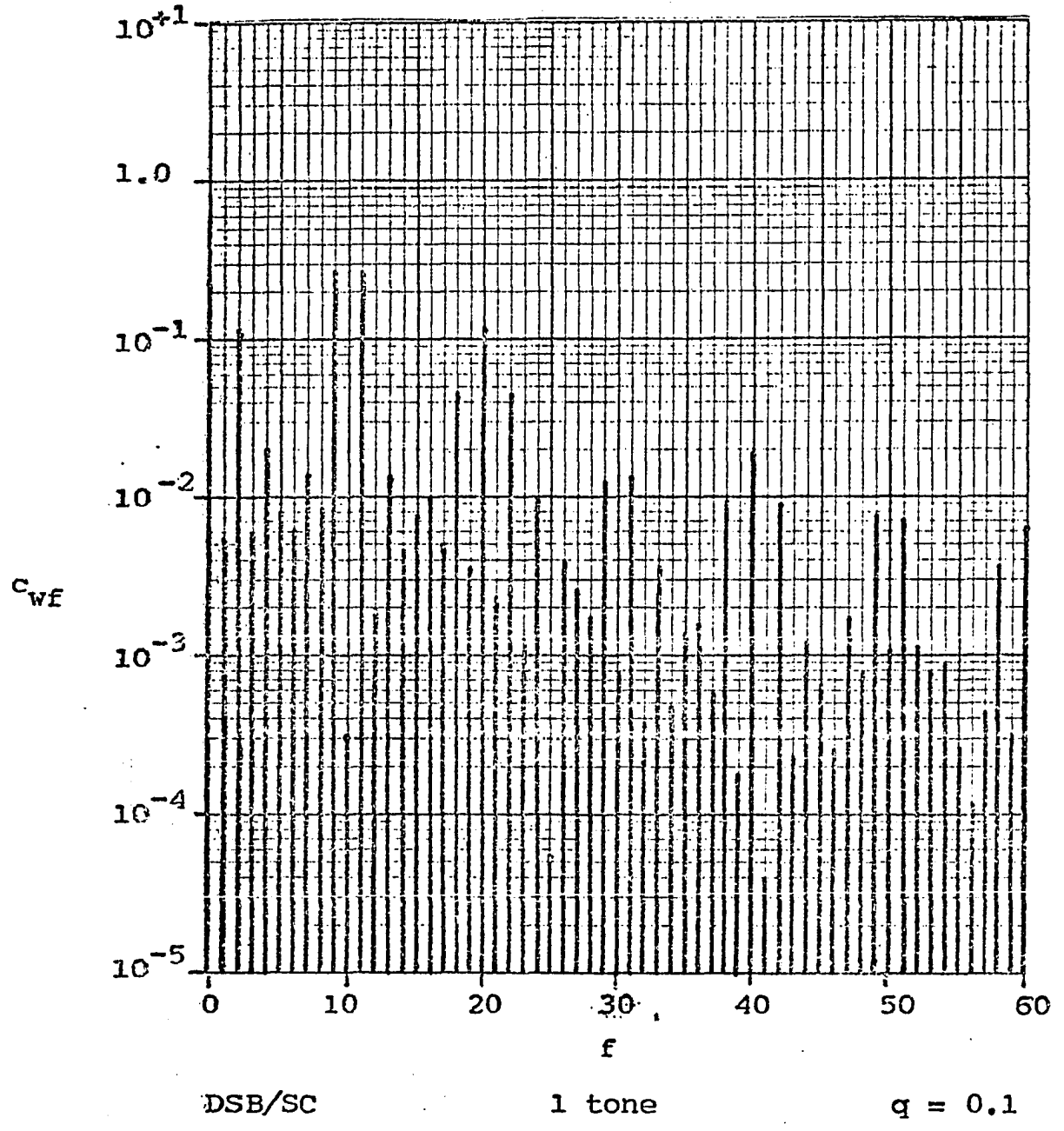


Figure 13.6. Spectrum of a Class B Amplifier.

However, class B is the most commonly used linear RF amplifier. Large values of  $q$  are not uncommon; in the popular 6146 tetrode, a quiescent current of 25 mA is recommended, with a peak current of 150 mA, which is a normalized  $q = 0.167$ .

### B. Conventional Pulse Width Modulation

The spectra (before filtering) of a class AD or BD amplifier (see Chapter II) is determined in essentially the same way as for the class D RF amplifier. The pulse width varies such that

$$|y| = \pi [q + v(\theta)] \quad , \quad (13.14)$$

where  $q$  determines the quiescent width. The pulse train generated can be characterized as a monopolar pulse train of frequency  $f_s$ , with constant phase, whose width varies as the magnitude of  $y$ , and whose polarity depends on the polarity of  $y$ :

$$w(t) = f_+ (w_s t, |y|, \phi_s) \operatorname{sgn}(y) \quad (13.15)$$

Note that in the class AD amplifier,  $q$  and  $x$  are restricted so that  $y$  is never negative.

The value of  $\phi_s$  is relatively unimportant, since it merely phase shifts the whole pulse train and otherwise has no effect on the spectrum generated. Expanding (13.15),

$$w(\theta) = \left[ \frac{|y|}{\pi} + \frac{2}{\pi} \sum_{n=1}^{\infty} \frac{\sin n|y|}{n} \cos(nw_s t - n\phi_s) \right] \operatorname{sgn} y \quad (13.16)$$

$$= \frac{1}{\pi} |y| \operatorname{sgn} y + \frac{2}{\pi} \sum_{n=1}^{\infty} \frac{z_n}{n} \cos(n\omega_s t - n\theta) \quad (13.17)$$

In any case,

$$|y| \operatorname{sgn} y = y = \pi[q + v(\theta)] \quad , \quad (13.18)$$

which includes the desired output  $v(\theta)$  and possibly a DC component, which may be removed by the output filter.

Spurious products arise from inherent modulation of the switching frequency and its harmonics:

$$z_k = \sin k|y| \operatorname{sgn} y = \sin ky \quad (13.19)$$

$$= \sin k\pi q \cos k\pi v(t) + \cos k\pi q \sin k\pi v(t); \quad (13.20)$$

$z_k$  is not generally bandlimited. The spectrum of  $z_k$  can be described in terms of Bessel functions (26). Let

$$v(t) = b \sin \theta_c \quad (13.21)$$

Then

$$\cos(k\pi b \sin \theta_c) = J_0(k\pi b) + 2 \sum_{n=1}^{\infty} J_{2n}(k\pi b) \cos 2n\theta_c \quad (13.22)$$

and

$$\sin(k\pi b \sin \theta_c) = 2 \sum_{n=1}^{\infty} J_{2n-1}(k\pi b) \sin(2n-1)\theta_c \quad . \quad (13.23)$$

Thus

$$z_k(t) = \sin k\pi q \left[ J_0(k\pi b) + 2 \sum_{n=1}^{\infty} J_{2n}(k\pi b) \cos 2n\theta_c \right]$$

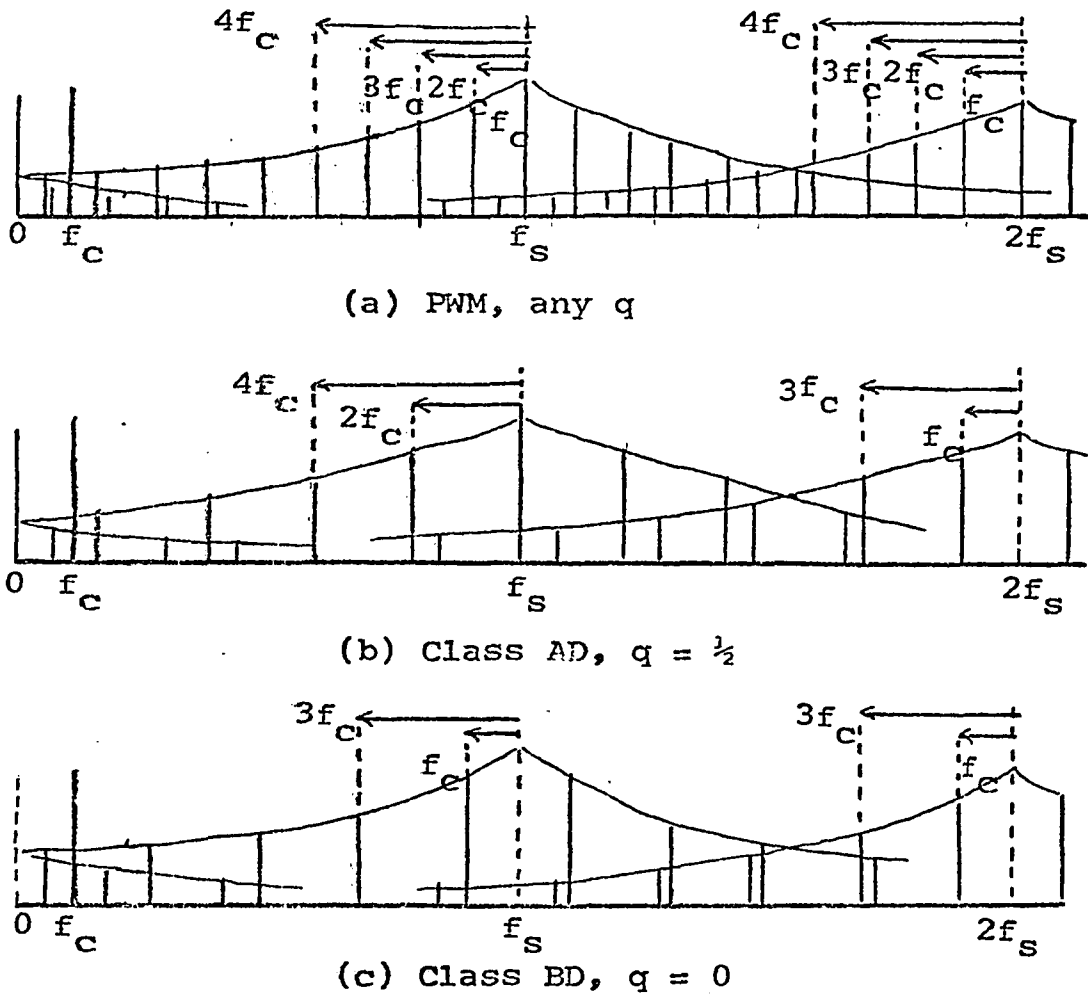


Figure 13.7. Spectrum of Conventional PWM.

$$\pm \cos k\pi q \left[ 2 \sum_{n=1}^{\infty} J_{2n-1}(k\pi b) \sin(2n-1)\theta_c \right] \quad (13.24)$$

Figure 13.7 illustrates the type of spectrum generated.

For a class AD amplifier, to get maximum output,

$$b = q = \frac{1}{2} \quad , \quad (13.25)$$

This particular value of  $q$  eliminates some of the distortion

products while maximizing others:

$$\sin k\pi q = \begin{cases} (-1)^{k+1}, & k \text{ odd} \\ 0 & , k \text{ even} \end{cases} \quad (13.26)$$

$$\cos k\pi q = \begin{cases} 0 & , k \text{ odd} \\ (-1)^{k+1}, & k \text{ even} \end{cases} \quad (13.27)$$

Similarly, for class BD,

$$q = 0 \quad (13.28)$$

and  $b = 1$  . (13.29)

In this case,

$$\sin k\pi q = 0 \quad (13.30)$$

and  $\cos k\pi q = 1$  . (13.31)

A simulation of the class AD amplifier is shown in Figure 13.8.

When modulation is introduced,

$$v(t) = x(t) \sin \omega_c t \quad , \quad (13.32)$$

and  $b$  is replaced with  $x(t)$  in (13.24). This secondary modulation is characterized by  $J_m[x(t)]$ . It should be possible, with some difficulty, to develop a Fourier series for  $J_m(\sin \theta)$ ; however, it is beyond the scope of this dissertation.

Simulations (Figures 13.9, 13.10, and 13.11) show that this secondary modulation dies away fairly rapidly (note that in actual amplifiers, an  $\alpha$  larger than used in the simulation is probable, so decay would be faster than in the simulation).

Careful choice of  $\beta = f_s/f_c$  can prevent stronger spurious products from falling on or near the desired output frequency. Note that in Figure 13.12 spurious products near  $f_c$  are actu-

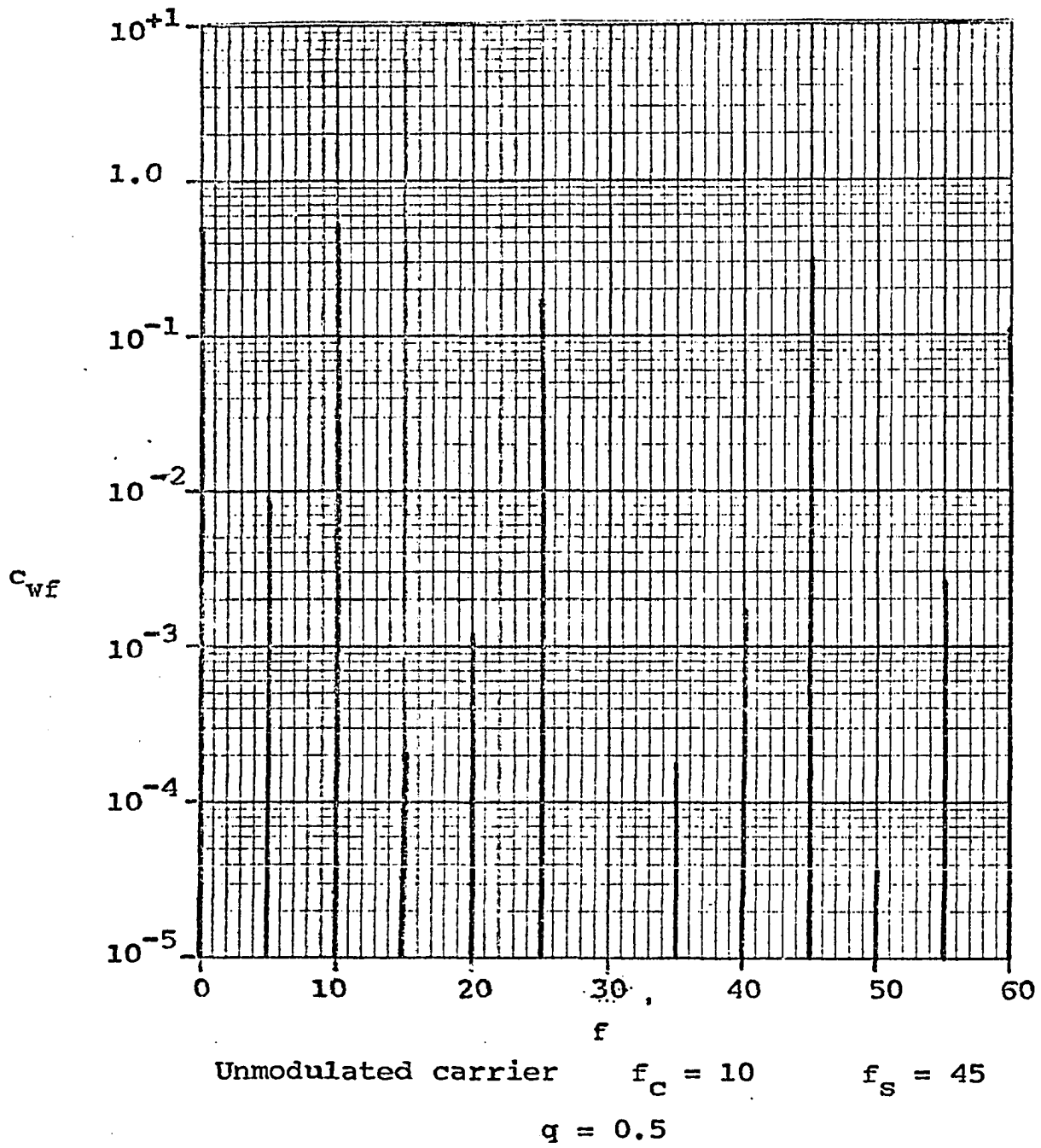


Figure 13.8. Spectrum of a Class AD Amplifier.

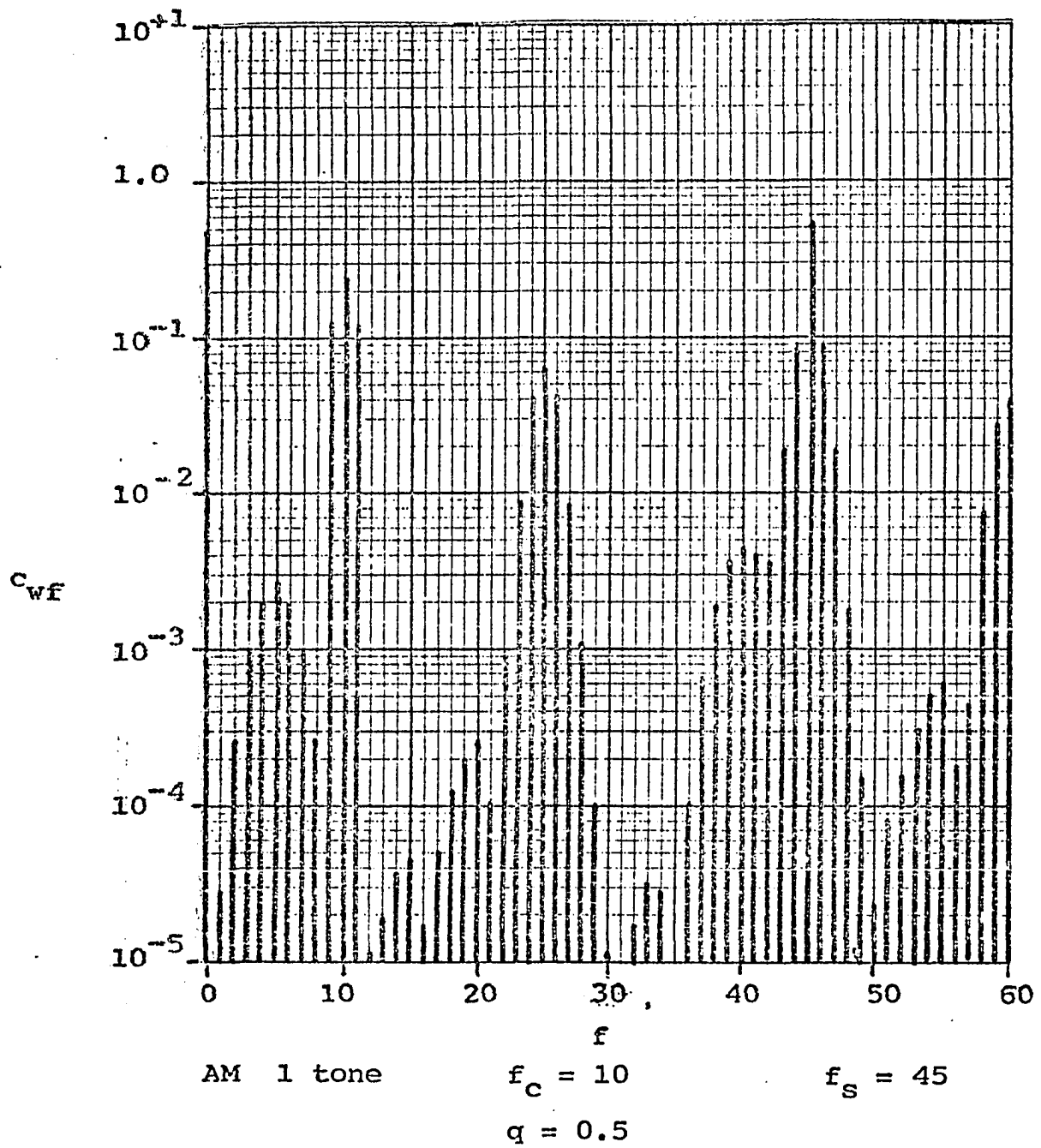


Figure 13.9. Spectrum of a Class AD Amplifier.



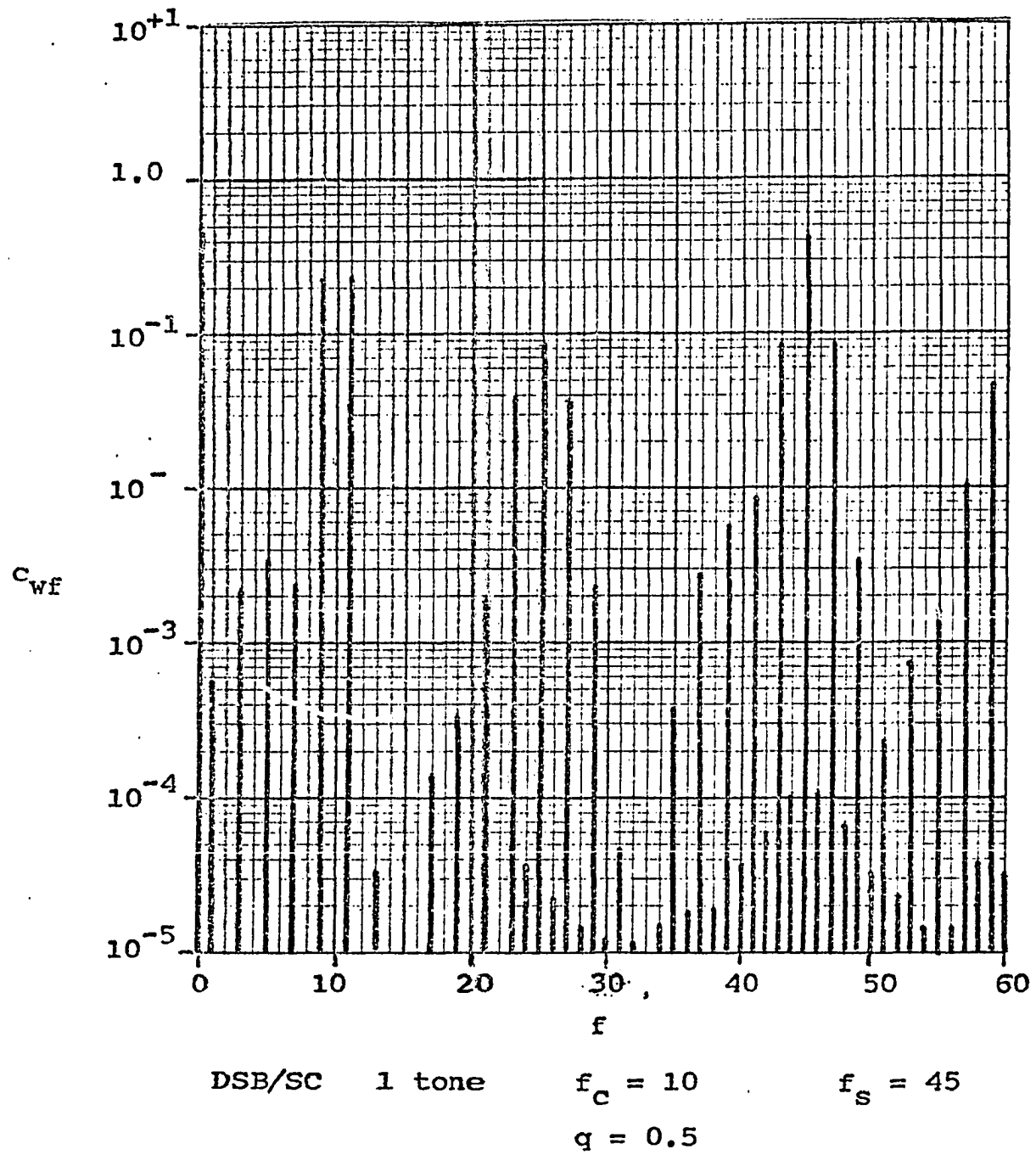


Figure 13.10. Spectrum of a Class AD Amplifier.

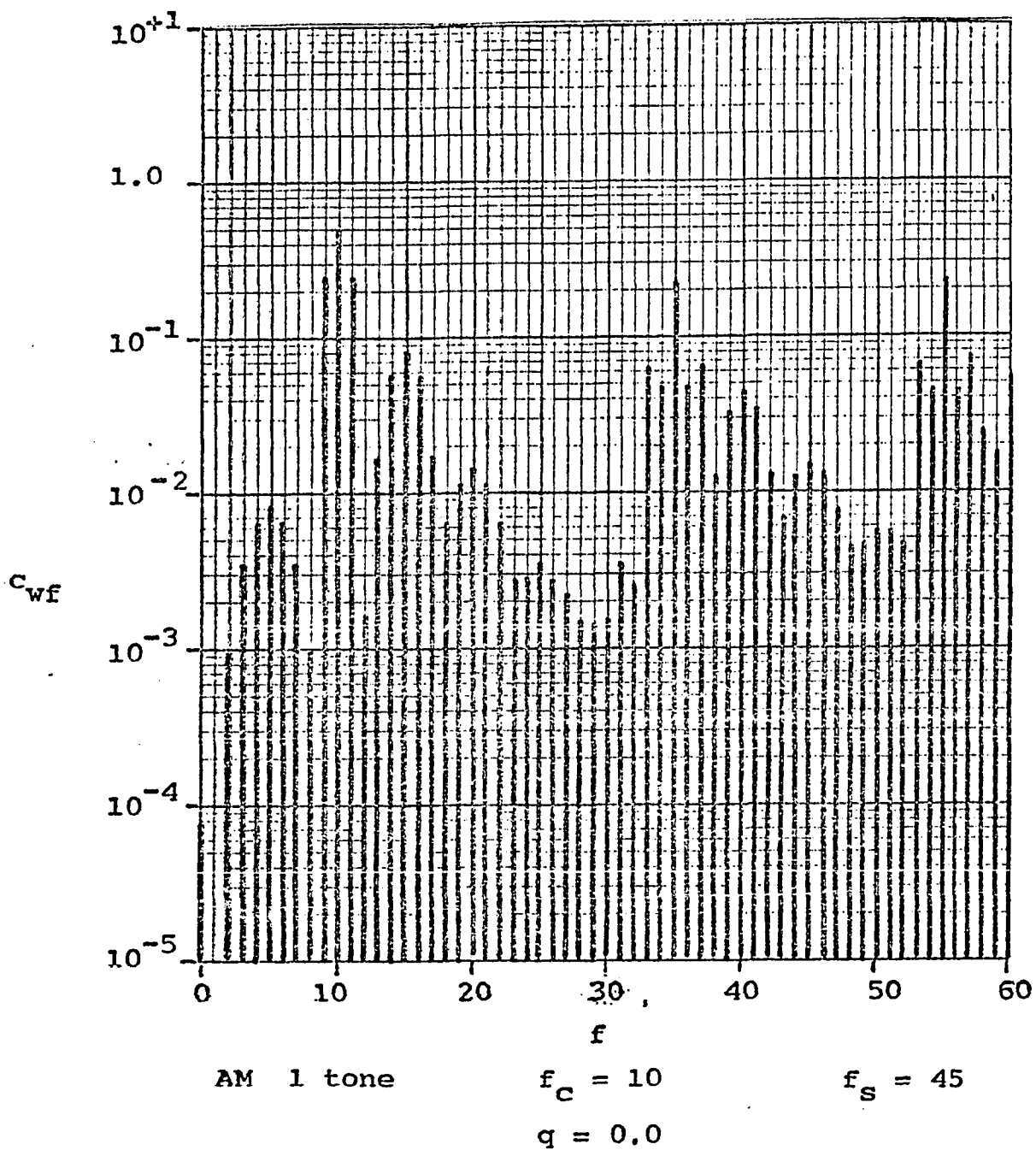


Figure 13.11. Spectrum of a Class BD Amplifier.

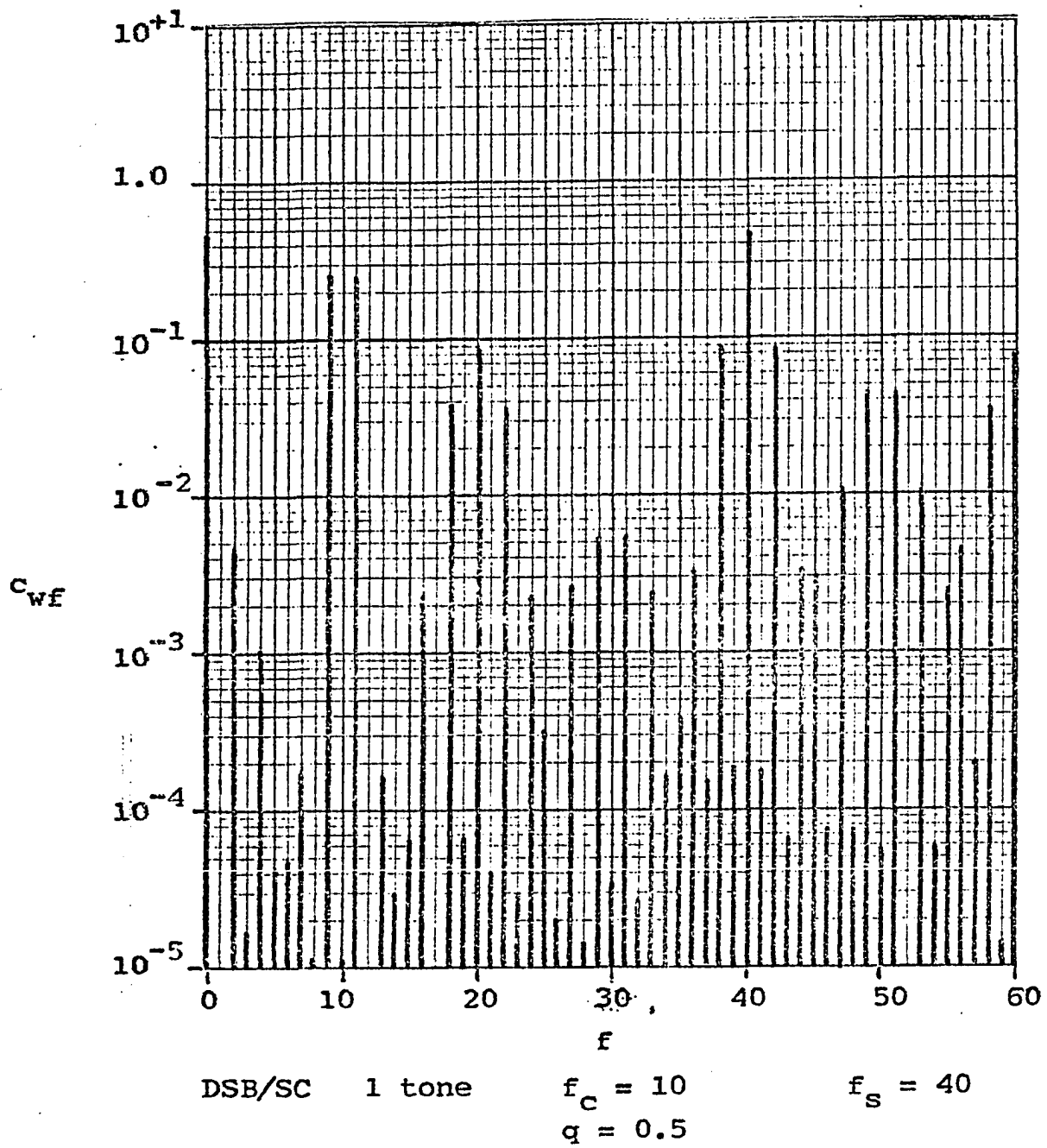


Figure 13.12. Spectrum of a Class AD Amplifier.

ally reduced, even though  $f_s$  is lower. It is not possible, however, to prevent all spurious products from being near  $f_c$ . If this were attempted (for either class AD or BD), it would be necessary to prevent modulation of even harmonics of  $f_s$  from falling at  $f_c$ :

$$2k\beta f_c - (2i - 1)f_c \neq f_c \quad (13.33)$$

$$2k\beta \neq 2i \quad (13.34)$$

$$\beta \neq \frac{i}{k} \quad (13.35)$$

Whereas it is certainly possible to choose  $\beta$  not equal to any particular ratio of integers, it is not possible to avoid all such ratios. It should be possible, however to choose  $\beta$  to reduce the spurious products near  $f_c$ .

Further distortions can arise from quiescent voltage error, non-zero saturation voltage, (BD only) and pulse-timing errors. Some general ideas about the nature of these may be obtained, but due to the complexity and number of combinations of parameters, these ideas are fairly non-specific.

Suppose that  $q$  differs from its exact value by  $\delta q$ . Then

$$\sin k\pi(q + \delta q) = \cos \delta q \sin k\pi q + \sin \delta q \cos k\pi q \quad (13.36)$$

$$\approx \sin k\pi q + k\pi\delta q \cos k\pi q \quad (13.37)$$

Similarly

$$\cos k\pi(q + \delta q) \approx \cos k\pi q - k\pi\delta q \sin k\pi q \quad (13.38)$$

If  $\beta$  has been chosen to minimize spurious products near  $f_c$ ,  $\delta q$  can introduce products which were zero with the correct value of  $q$ . A simulation with  $\delta q = 0.1$  ( $q = 0.4$ ) is shown in Figure

13.13; note the introduction of a signal at  $f = 15$ .

Non-zero saturation voltage has approximately the same effect as in the class D RF amplifier; it produces a square wave at  $f_c$ . When a DSB/SC or SSB signal is generated, phase modulation of the square wave occurs, generating the same kind of IMD as before.

There are two philosophies which might be used. One would spread the spurious products, keeping those near the carrier small. The other would fix  $\beta$  as some ratio of small integers (5, 9/4, etc.), so that spurious products would occur only on multiples of a specified frequency (e. g.  $\frac{1}{2}f_c$ ,  $f_c$ ,  $\frac{3}{2}f_c$ , etc.). With this method, secondary modulation products of spurious products not at  $f_c$  should die away rapidly, leaving only an IMD effect. Finding means of choosing  $\beta$  for either philosophy would make an interesting study.

To analyze the effects of pulse bias (or rise/fall), a distortion waveform  $u(t)$  is added, as for class D RF amplifier (Figure 13.14).

Consider first only the pulse associated with  $\tau_1$  in a class AD amplifier:

$$u_{B1}(t) = \frac{\tau_1}{2\pi} + \frac{2}{\pi} \sum_{n=1}^{\infty} \frac{\sin \frac{n\tau_1}{2}}{n} \cos \left\{ n\omega_s t - n \left[ \pi - \left( \gamma + \frac{\tau_1}{2} \right) \right] \right\} \quad (13.39)$$

As before, for small  $\tau_1$ ,

$$\frac{\sin \frac{n\tau_1}{2}}{n} \approx \frac{\tau_1}{2} \quad (13.40)$$

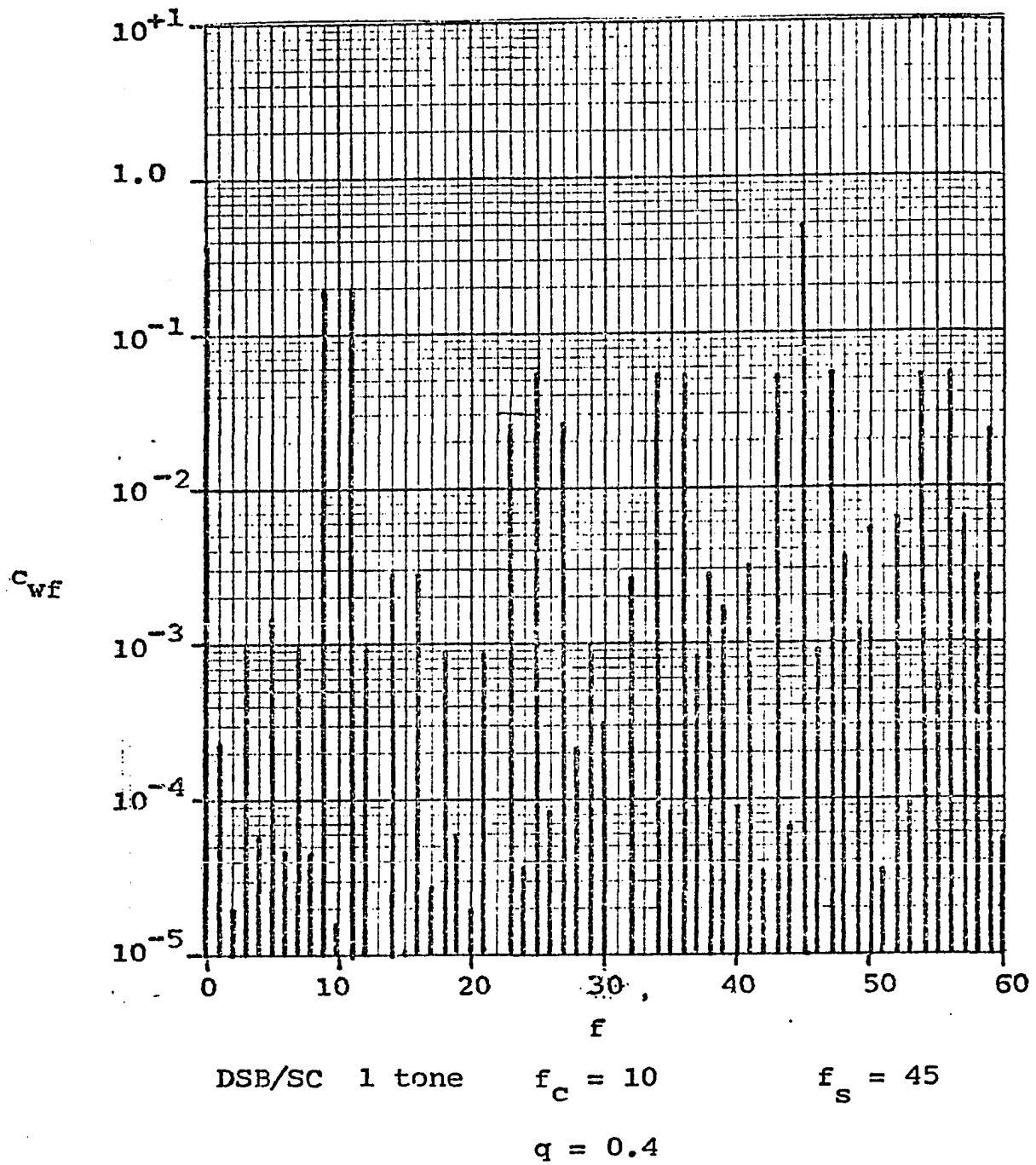


Figure 13.13. Spectrum of a Class AD Amplifier.

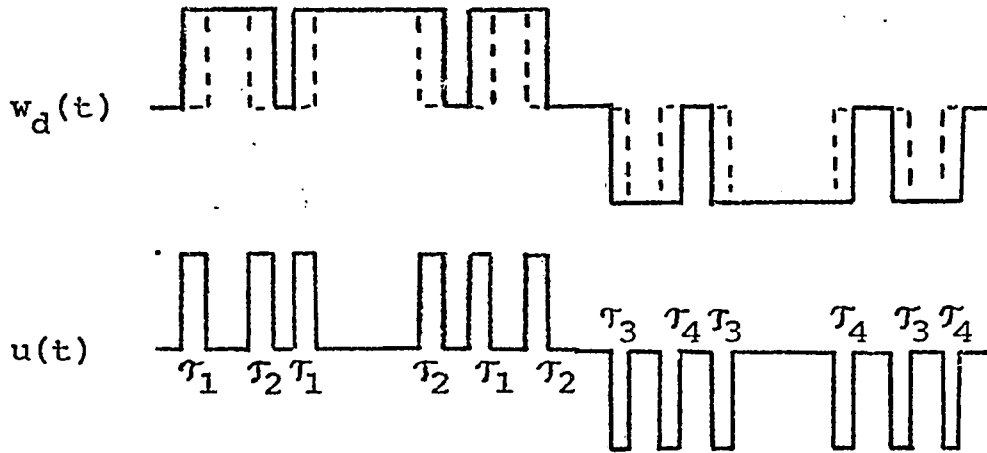


Figure 13.14. Pulse Bias in Class BD Amplifier.

$$\cos \left\{ n\omega_s t - n \left[ \pi - \left( y + \frac{\tau_1}{2} \right) \right] \right\} \approx \cos [n\omega_s t - n\pi + ny] \quad (13.41)$$

$$= \frac{(-1)^n}{2} [\cos ny \cos n\omega_s t - \sin ny \sin n\omega_s t] \quad (13.42)$$

The process for  $u_{B2}(t)$  is similar, and the combined result is

$$u_{B+}(t) \cong \frac{\tau_1 + \tau_2}{2\pi} + \frac{1}{\pi} \sum_{n=1}^{\infty} (-1)^n [(\tau_1 + \tau_2) \cos n|y| \cos n\omega_s t + (-\tau_1 + \tau_2) \sin n|y| \sin \omega_s t] \quad (13.43)$$

Although there is no IMD generated at  $f_c$ , both  $\cos ny$  and  $\sin ny$  are reducible to a set of Bessel functions, and may cause spurious products to appear where the choice of  $q$  should have suppressed them. A simulation of a class AD amplifier with a pulse bias error of 10% is shown in Figure 13.15.

For class BD, the situation is more complicated. An expression similar to (13.43) can be developed for the negative

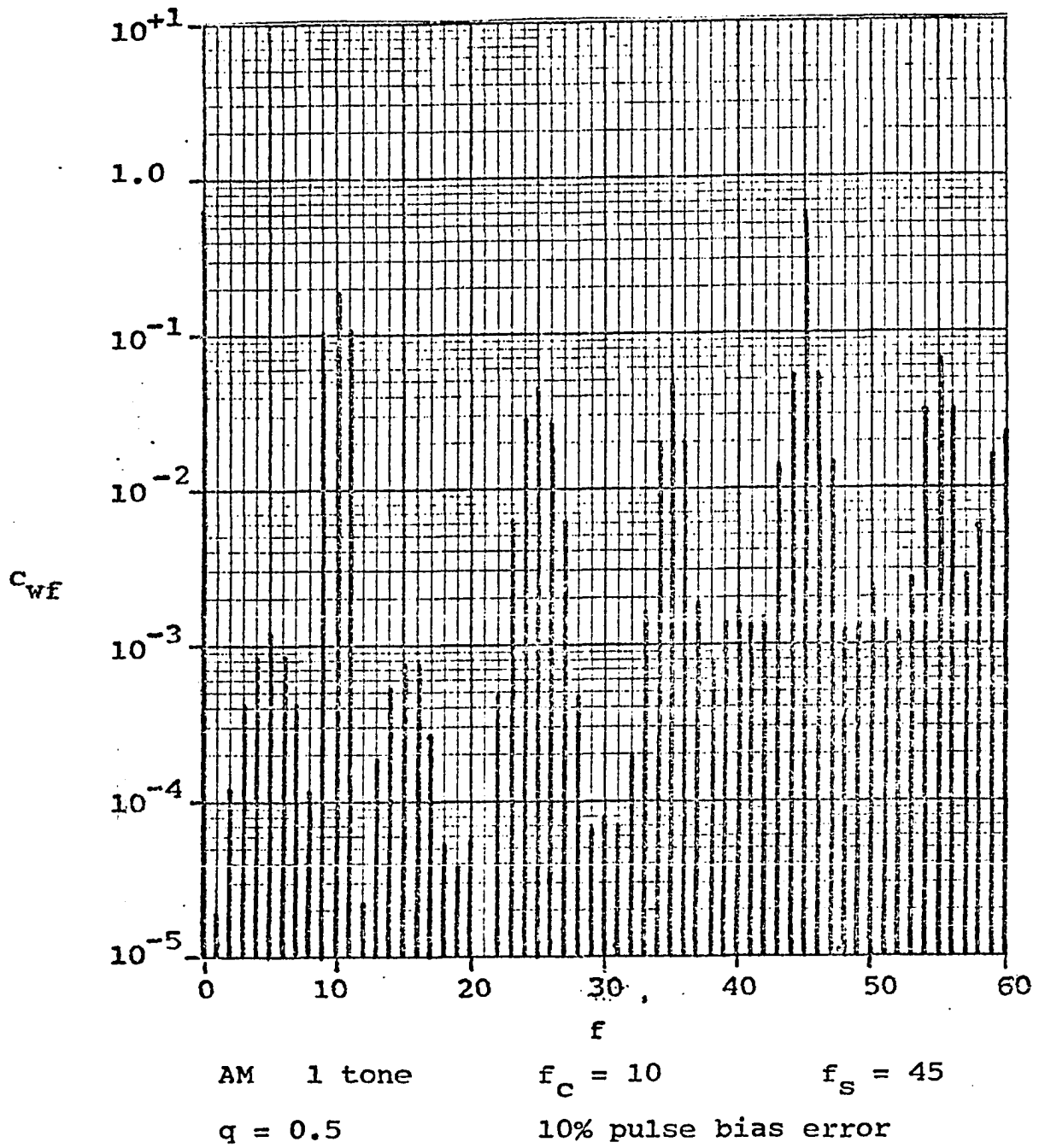


Figure 13.15. Spectrum of a Class AD Amplifier.



pulses. Assuming  $y$  is always negative,

$$\begin{aligned}
 -u_{B-}(t) \approx & \frac{\tau_3 + \tau_4}{2\pi} + \frac{1}{\pi} \sum_{n=1}^{\infty} (-1)^n [(\tau_3 + \tau_4) \cos n|y| \cos n\omega_s t \\
 & + (-\tau_3 + \tau_4) \sin n|y| \sin n\omega_s t] \quad . \quad (13.44)
 \end{aligned}$$

The last two equations can be combined to produce

$$u_B(t) = u_{B+}(t) \left( \frac{\text{sgn } v(t) - 1}{2} \right) + u_{B-}(t) \left( \frac{1 - \text{sgn } v(t)}{2} \right) \quad . (13.45)$$

This results in the addition of further spurious products due to phase shifting. Martin (15) claims that this spreads (flattens) the spectrum and is therefore more useful for an audio amplifier. However, the usefulness of this effect in an RF amplifier is doubtful.

Based on the above theory and the simulations performed, it appears that classes AD and BD would generate little IMD, but would have much stronger spurious product scattered throughout the RF spectrum, which would make broadband operation difficult.

### C. Other Amplifiers

Spurious products generated by amplitude modulation of a class C or constant carrier class D amplifier are essentially those produced by the modulator. However, if the shape of the transistor waveforms changes as a function of modulation, other spurious signals can be generated.

If Kahn's method of generating SSB is used, with external

envelope amplification; harmonics of the carrier will have the form  $E(t) \sin k[\omega_c t + \varphi(\theta)]$ , and will presumably generate the same kind of product as if width and phase modulation of a class D RF amplifier had been used.

## XIV. APPENDIX II: PROTOTYPE

A prototype amplitude-modulated transmitter employing class D RF amplification was built to illustrate the principles of operation.

This transmitter used a carrier frequency of 125 kHz. The rather low frequency for an RF carrier was chosen because of the limitations of the author's oscilloscope and power supplies. Had lower-voltage/higher-current power been available, and an oscilloscope with a smaller rise time, it should have been possible to operate at 1 MHz with the transistors used. The limitation to AM, rather than DSB/SC or SSB was made to simplify the circuitry.

The circuitry follows the block diagram of an AM transmitter given in Figure 3.4. The prototype requires both +12 and -12 Volts input power. Transistor voltage regulators (Q1 - Q4) provide additional voltages of  $\pm 3.3$  and  $\pm 10$  Volts. A 125 kHz sine wave of approximately 5 V p-p is supplied by the oscillator. The audio amplifier provides a high input impedance and voltage gain for demonstrating the amplifier; it can be bypassed for measurements.

Transistors Q9 and Q10, and the associated circuitry, allow an adjustable delay to provide for unequal delays in the two signal paths in the transmitter. Transformer T2 inverts the signal, which is rectified by diodes D5 - D8, to form the reference wave (which is negative). The reference wave is

added to the audio signal and an adjustable bias (carrier level). This sum is applied to a clipping circuit to form pulses whenever the sum is greater than zero.

The output of the oscillator is applied to a clipping circuit to produce a square wave with frequency of 125 kHz. The square wave and the comparator output are applied to an AND circuit (Q20, actually NAND), which provides a pulse when the output should be positive. A similar circuit generates pulses when the output should be negative.

Each of the four output transistors acts as a voltage amplifier, and is driven by one other transistor. The drive to the grounding transistors Q29 and Q30 can be switched to provide monopolar or bipolar operation. The output pulse waveform is switched between +10, 0, and -10 Volts. The load impedance is  $50 \Omega$ . The output tuning coil, L3, consists of 250 turns on a 2.5 cm. form. Maximum output power is 1.62 Watts.

Some observations of the transmitter were made using a Tektronix 564 oscilloscope (10 MHz). A photograph of the pulse train and filtered output are shown in Figure 14.7. The efficiency, determined by comparing the actual output voltage with the ideal output voltage for a 9.5 V power supply, was only approximately 75%. However, saturation voltage was relatively large (1.5 V during grounding, 0.5 V for + or -), and the rise time  $\sigma = 0.1 \cdot 2\pi$ .

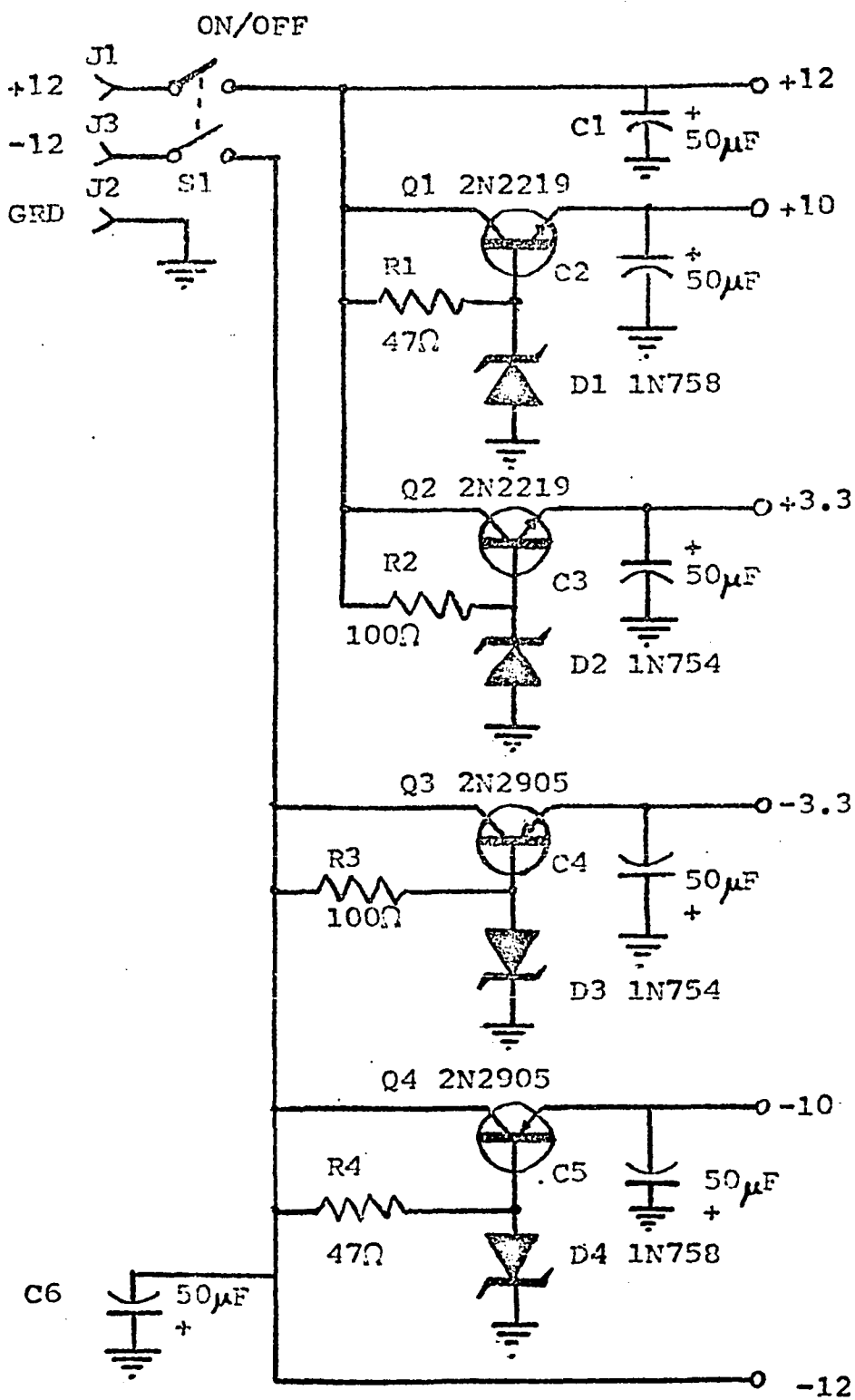
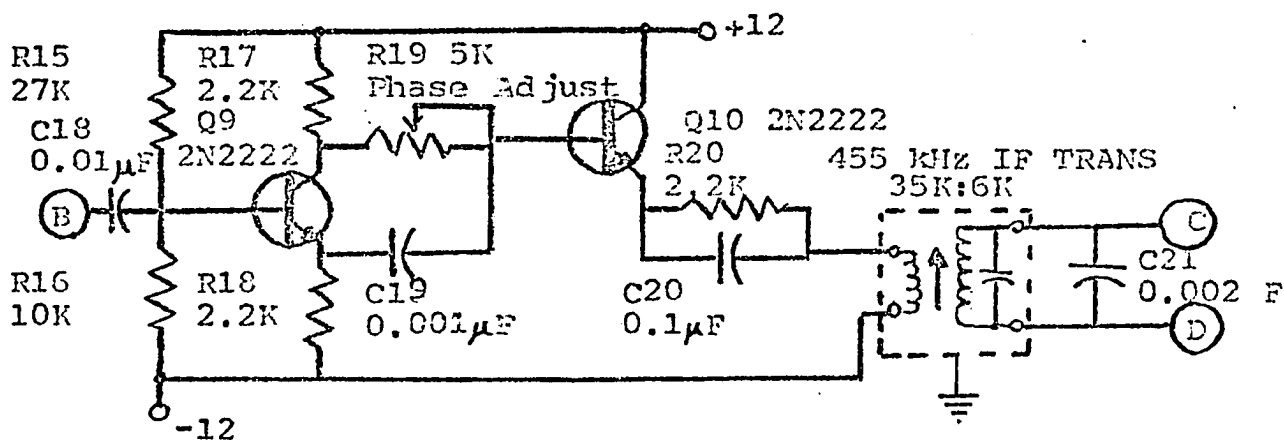


Figure 14.1. Power Supply.



PHASE SHIFTER



REFERENCE WAVE GENERATOR

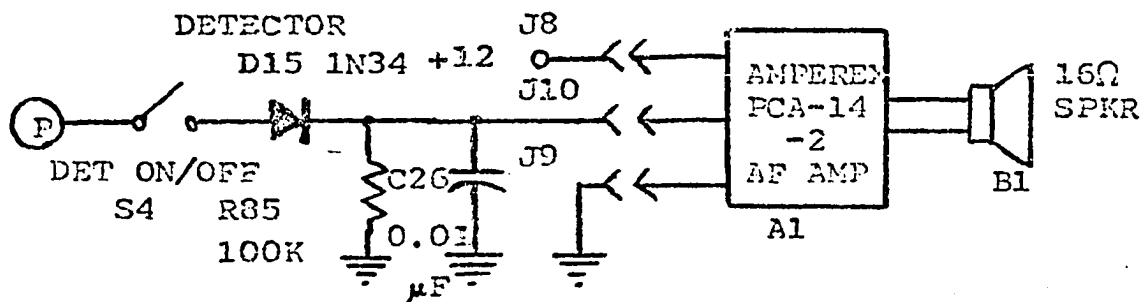
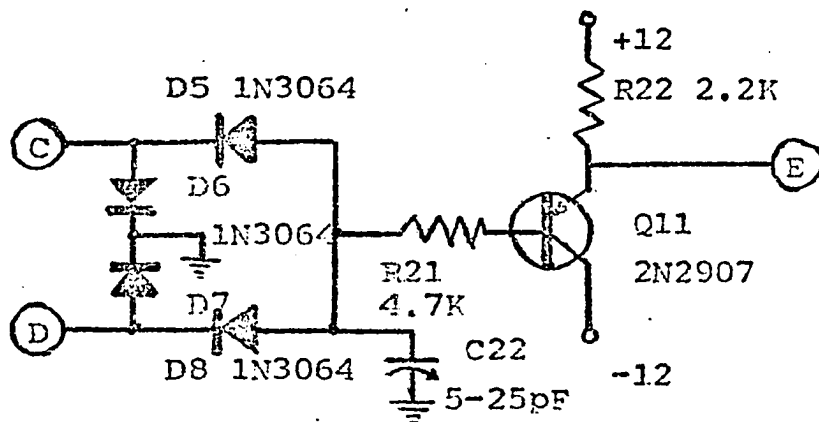
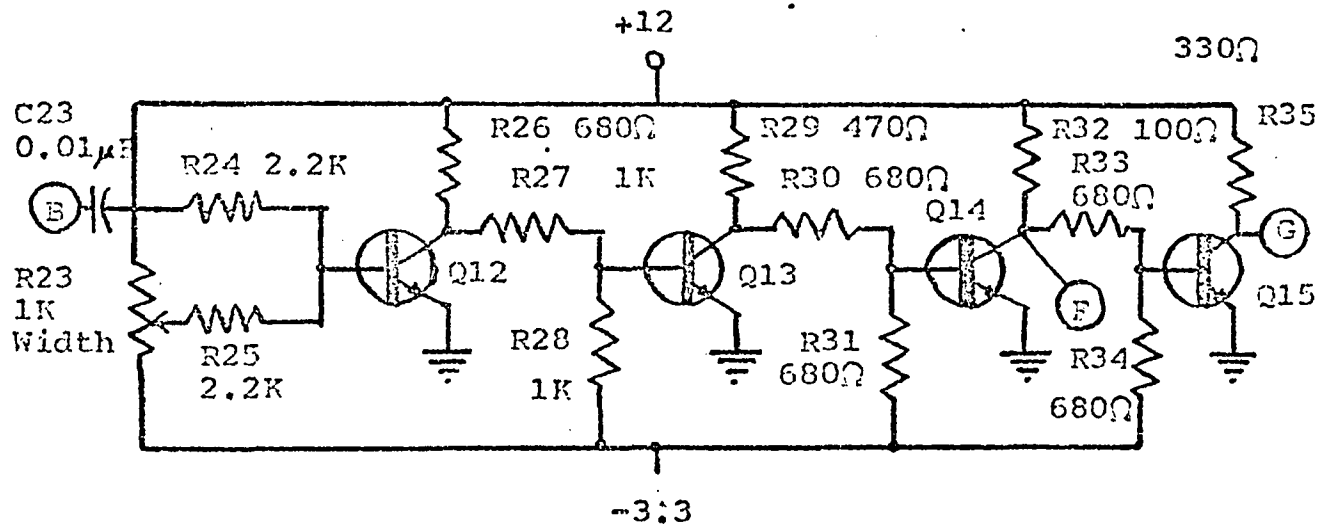
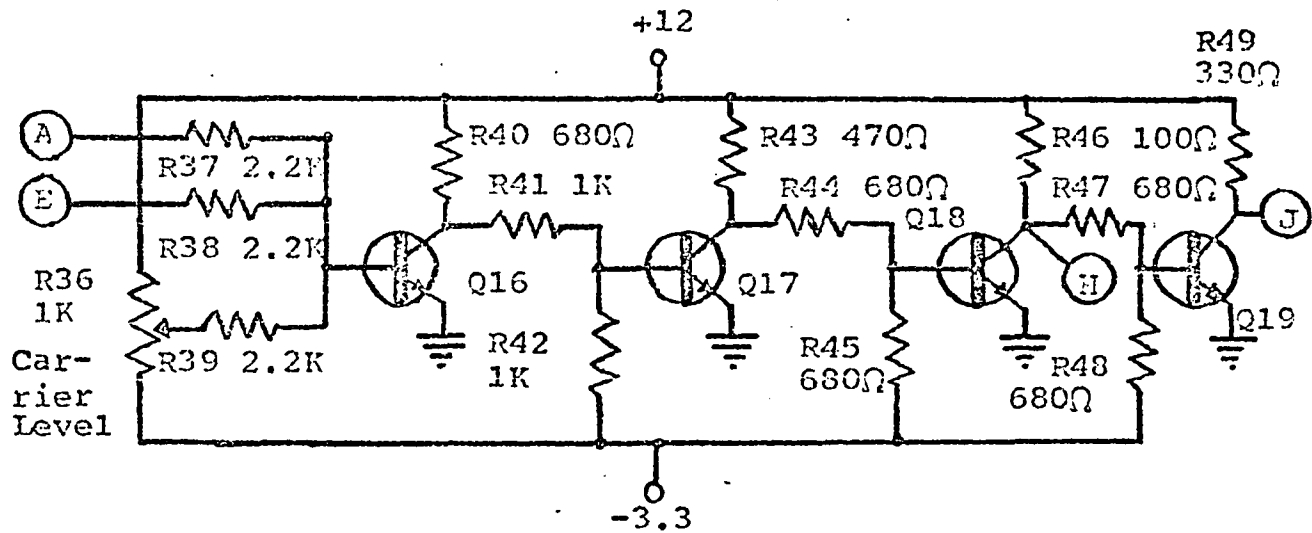


Figure 14.3. Reference Generator and Detector.

## CLIPPER



## COMPARATOR



NOTE: All transistors on this page are 2N2222.

Figure 14.4. Clipper and Comparator.



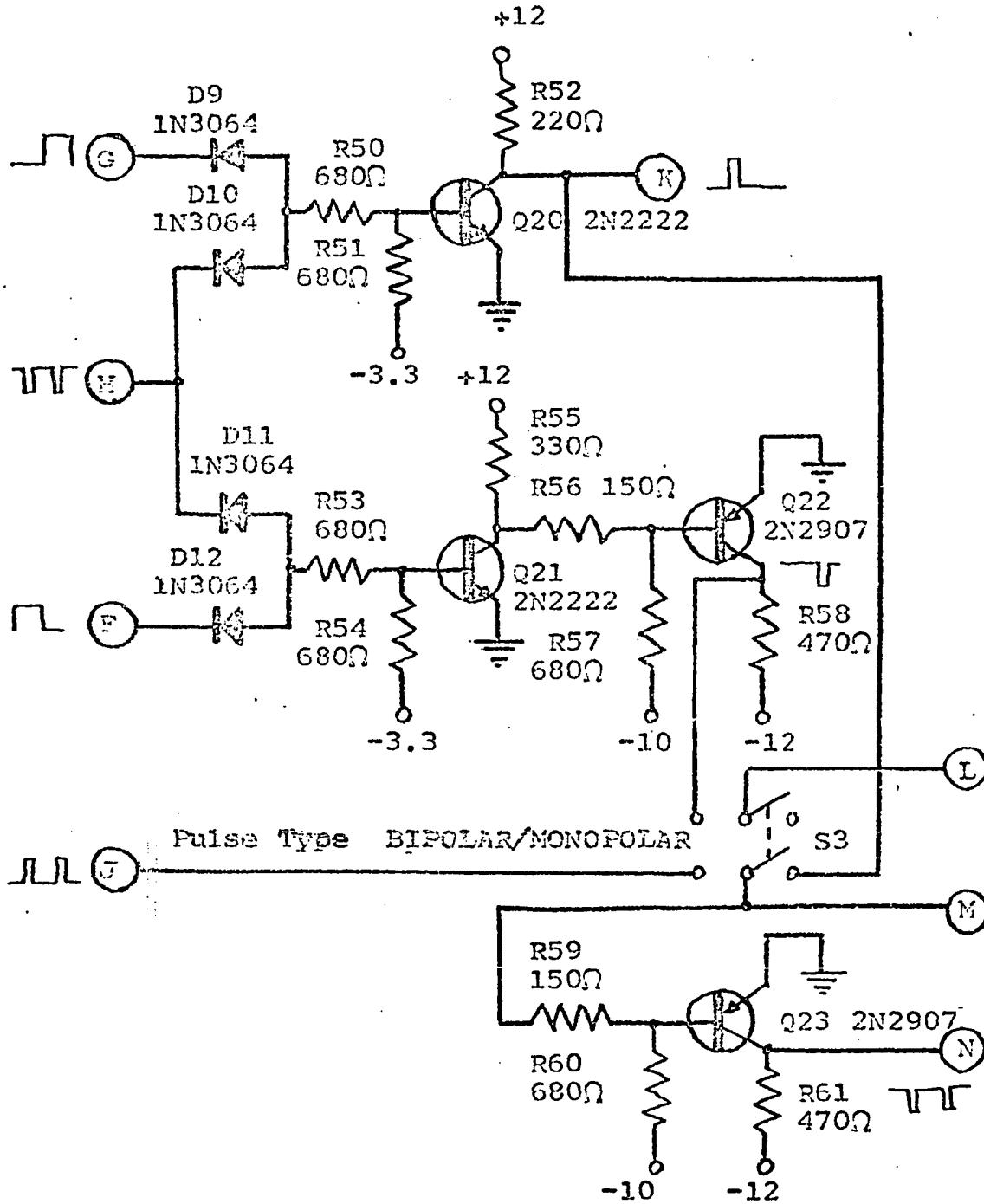
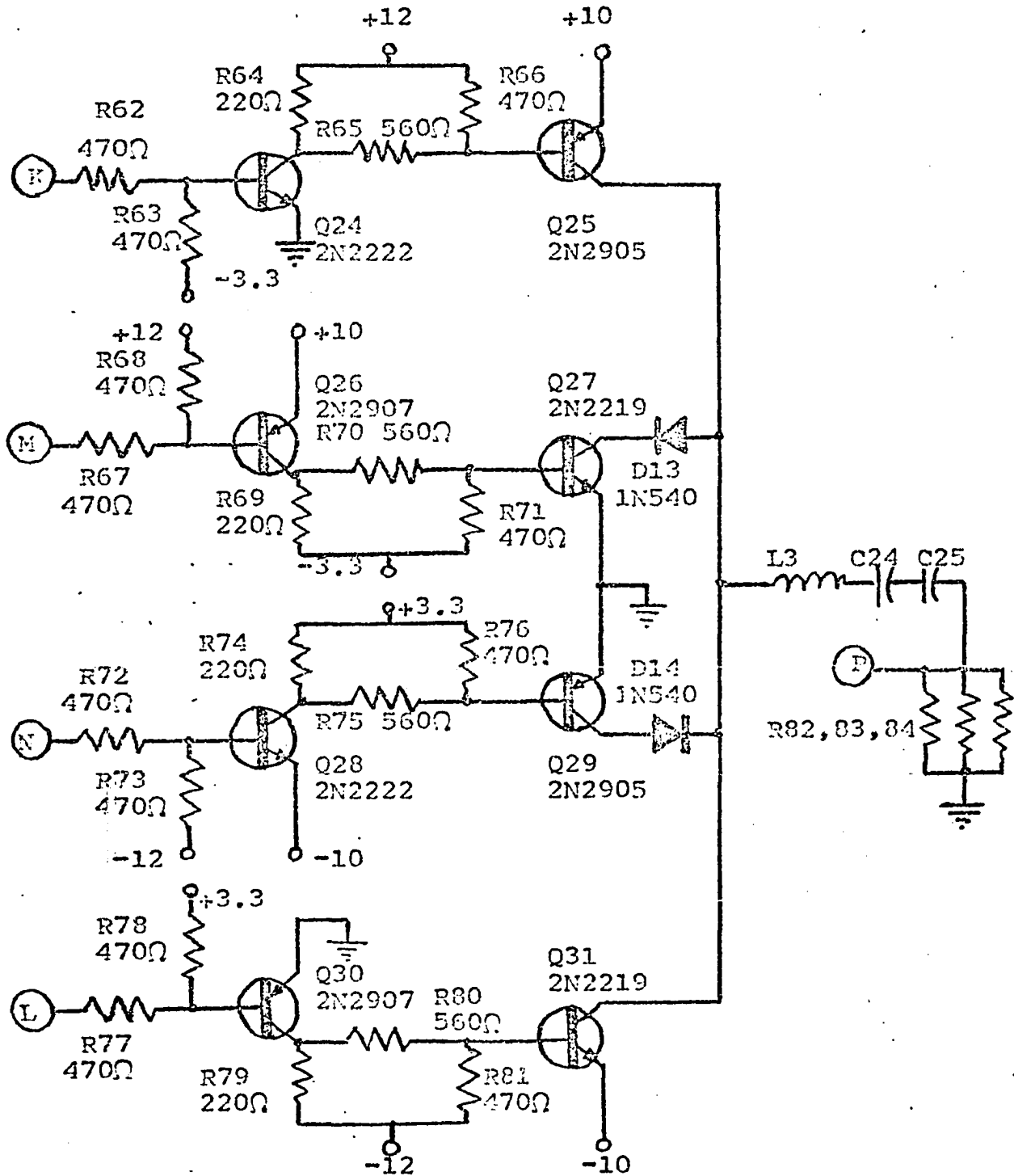


Figure 14.5. Logic.



NOTE: R82, R83, R84 =  $150\Omega$ , 1W.  
 C24, C25 =  $0.005\mu\text{F}$ ; L3 =  $0.7\text{mH}$ .

Figure 14.6. Power Amplifier.

Modulation characteristics were satisfactory, however. The envelope for 90% amplitude modulation is shown in Figure 14.8. The modulator in this type of amplifier is quite broadband, and works as well at 10 kHz as at 1 kHz. The spectrum of the pulse waveform for 10 kHz 90% modulation is shown in Figure 14.9. The concentration of spurious products near the third and fifth harmonics of the carrier can be observed. Assuming that the sidebands are 6 dB below the carrier, the level of the strongest IMD product outside of the desired bandwidth is approximately -27 dB from the sidebands. Rapid decay of IMD and presence of small even harmonics (due to pulse asymmetry) can also be observed. Figure 14.10 shows the inclusion of even harmonics when monopolar PWM is used.

It should be remembered that the purpose of this prototype was to illustrate qualitatively the method of class D RF amplification (or generation). It is neither exemplary of efficiencies that are possible, nor of linearity which is possible. Presumably, with more time, better components, and especially better test equipment, a much better model could be built.

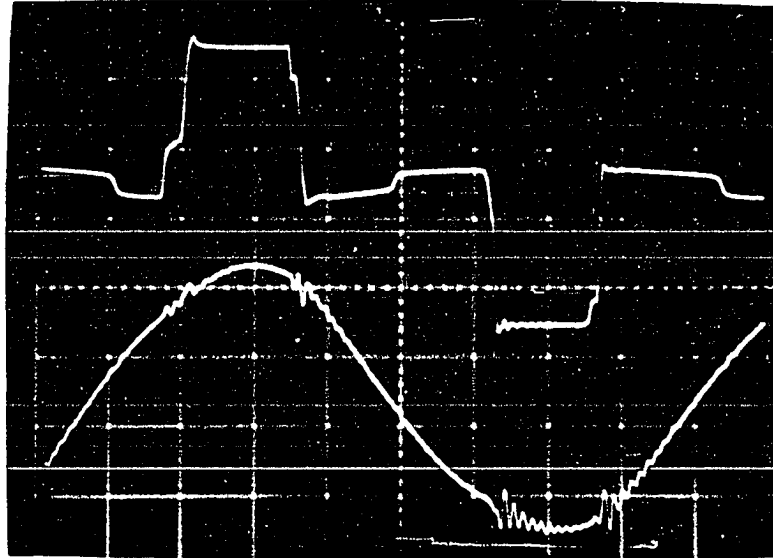


Figure 14.7. Pulse Train and Output Waveform.

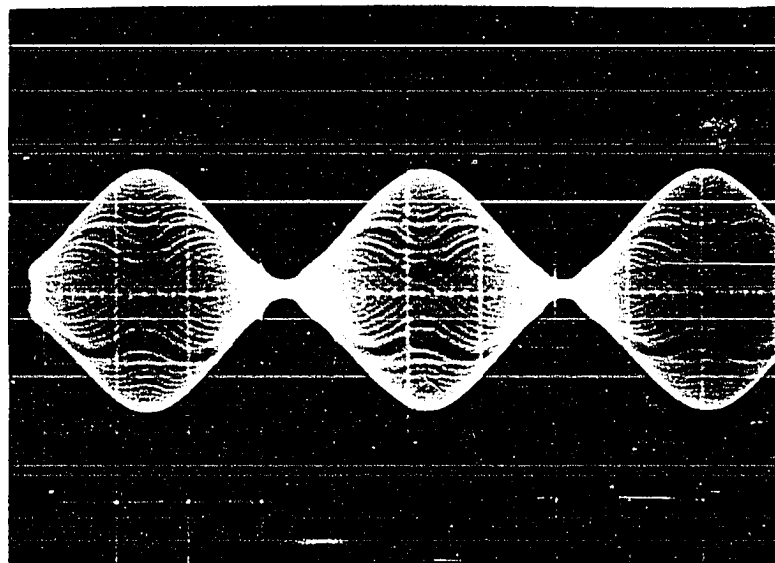


Figure 14.8. Envelope.

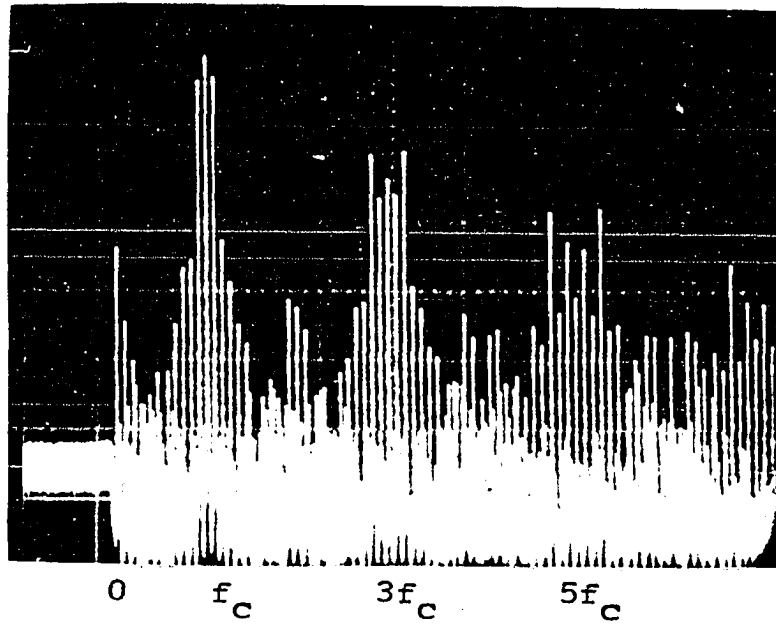


Figure 14.9. Spectrum of Bipolar PWM.

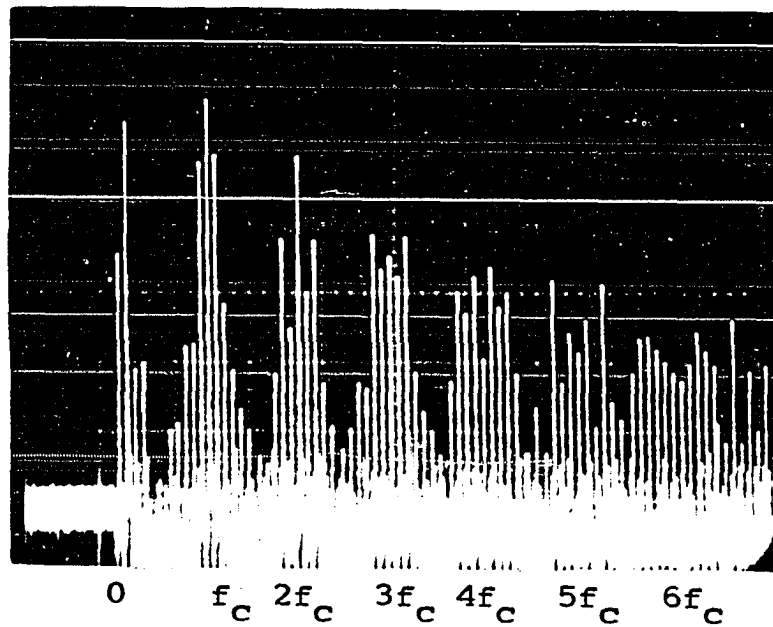


Figure 14.10. Spectrum of Monopolar PWM.

## XV. APPENDIX III: SIMULATION

Digital computer simulations of classes B, AD, BD, and D-RF amplifiers were performed. To minimize programming effort, the programs were constructed in several subroutines, several of which were common to each program. The main program, of which only the version for the class D RF amplifier is included (there are only minor changes in the others), serves the functions of reading parameters, writing some information not written by the subroutines, and calling subroutines in the appropriate order. Only a small amount of trivial computation is done in the main program. Subroutine GRAPH refers to the simplotter at the ISU computation center, which provides a quick graph of the data.

In order to avoid the use of numerical integration, which is either very expensive or inaccurate, all waveforms are defined on the interval

$$0 \leq \theta \leq 2\pi \quad . \quad (15.1)$$

Since there is no memory in the amplifiers, products generated must be harmonics of this basic frequency. For this reason, carrier and switching frequencies are specified as integers. All programs and subroutines were designed for use with the WATFIV compiler.

The first subroutine called is WAVNRM. This is used primarily for adjusting the peak of a given waveform so that overmodulation does not occur. This is achieved by generating

the waveform  $x_u(\theta)$  and accumulating the maximum value. The original unnormalized Fourier coefficients ( $AXU\emptyset$ ,  $AXU(N)$ ,  $BXU(N)$ ) are then multiplied by a constant to produce the normalized coefficients ( $AX\emptyset$ ,  $AX(N)$ ,  $BX(N)$ ). A second function of WAVNRM is to produce Fourier coefficients of the in-phase and quadrature modulating functions  $x_p(\theta)$  and  $x_q(\theta)$ , which are used for SSB waveforms.

The second subroutine, WAVGEN, furnished values of the modulated signal

$$v(\theta) = E(\theta) \sin[f_c \theta + \varphi(\theta)] + q, \quad (15.2)$$

as well as  $E(\theta)$  and  $\varphi(\theta)$ , when furnished with a value of  $\theta$ .

It is not called by the main program, but is called by the amplifier subroutine as needed.

Each amplifier subroutine determines an array of pulse transition times (PSI), and associated arrays for waveform type (MODE) and amplitude (WPL). The maximum number of transitions, IMAX, is also specified. The different MODEs which are possible are:

MODE = 0 , used to skip calculations for that interval,

MODE = 1 , used for linear amplification,

MODE = 2 , used for a constant value on the interval,

MODE = 3 , used for linear rise (or fall), and

MODE = 4 , used for exponential rise or fall.

A diagrammatic description of these is given in Figure 15.1.

Subroutine PLS DST elongates or shortens pulses (MODE = 2),

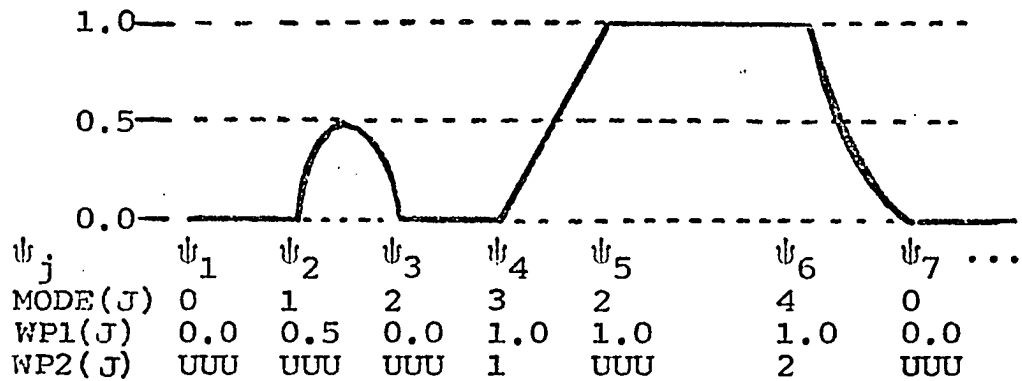


Figure 15.1. Arrays Used in Simulation.

and adds rise or fall times to them. Either linear or exponential characteristics can be used by changing the value of MODERF. The distorted waveform is specified by arrays PSID, MODED, WP1D, AND WP2D. The additional parameter, WP2D(N) indicates the nature of a rise or fall (WP2D = 1 for rise from 0 to 1, = 2 for fall from 1 to 0, etc.). A "null version" of PLS DST is used when no distortion is to be introduced. Basically it copies the undistorted arrays into the distorted arrays, but it has the additional feature of changing MODE to 0 (skip) when WP1 (amplitude) is zero; this results in a saving in time computing the Fourier coefficients. The constants  $\xi$  and  $\gamma_i$  used in the exponential rise/fall are defined in Figure 15.2.

Fourier coefficients are computed by subroutine FTRANS. For each transition, FTRANS goes to the appropriate point in the program and calculates up to 200 coefficients. Programing



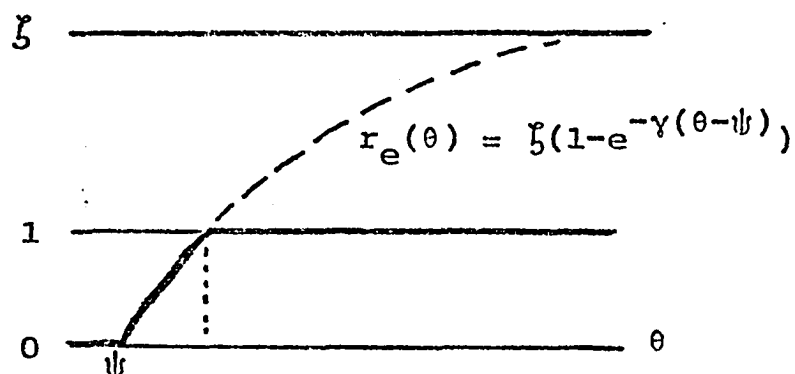


Figure 15.2. Exponential Mode.

simplicity was obtained by the use of functions CINT, SINT, RCINT, RSINT, ECINT, and ESINT, which perform operations such as

$$\text{RCINT}(m, \psi_1, \psi_2) = \int_{\psi_1}^{\psi_2} r(\theta) \cos m\theta \, d\theta \quad . \quad (15.3)$$

Upon completion of calculations, FTRANS prints out a table of the coefficients. AW(N) and BW(N) correspond to the cosinusoidal and sinusoidal Fourier coefficients  $a_{wn}$  and  $b_{wn}$ , respectively. CW(N) and CSQW(N) correspond to absolute voltage and power coefficients, defined by

$$\text{CSQW}(N) = c_{wn}^2 = a_{wn}^2 + b_{wn}^2 \quad . \quad (15.4)$$

Subroutine CLDAMP determines pulse transitions for a class D RF amplifier with double sideband or AM signals. Since the phase of these signals is fixed (excepting shifts of  $\pi$ , which amounts to polarity reversals, one transition must occur in each interval of  $2\pi/4f_c$ . The value of  $E(\theta)$  at the

center of the interval is used as a starting point (Figure 15.3 (a)). The point of intersection with the reference signal is then estimated by using the inverse sine relationship between  $E(\theta)$  and  $r(\theta)$ . Using the new value of  $\theta$  just determined, a new  $E(\theta)$  is determined, and the process is repeated. Seven iterations seems to be sufficient to produce as much accuracy as is possible using single-precision (REAL\*4) numbers. Figure 15.4 shows the spectrum calculated for a pure carrier (square wave). All computer errors are seen to be below  $10^{-5}$ , approximately 110 dB below the carrier.

A second version of CLDAMP was devised for SSB signals. Since the phase of an SSB signal is not fixed, there is no certain interval in which one and only one transition is guaranteed. The program thus must take many small steps, checking each time whether  $r(\theta)$  and  $E(\theta)$  have crossed. When a transition is found (Figure 15.3(b)) an iteration procedure is initiated. A "brute-force" technique is employed, whereby the interval in which the transition occurs is halved, the values  $E(\theta_2)$  and  $r(\theta_2)$  checked at the middle point, and the half of the interval not containing the crossing discarded. Though a crude technique, it avoids some problems with linear interpolation which select a point outside the original interval. Approximately 15 iterations are required to achieve maximum accuracy. This program has two problems, however. When  $r(\theta)$  is small, and  $E(\theta)$  is also small, it was possible to step over both transitions occurring near  $r = 0$ . This problem was elim-

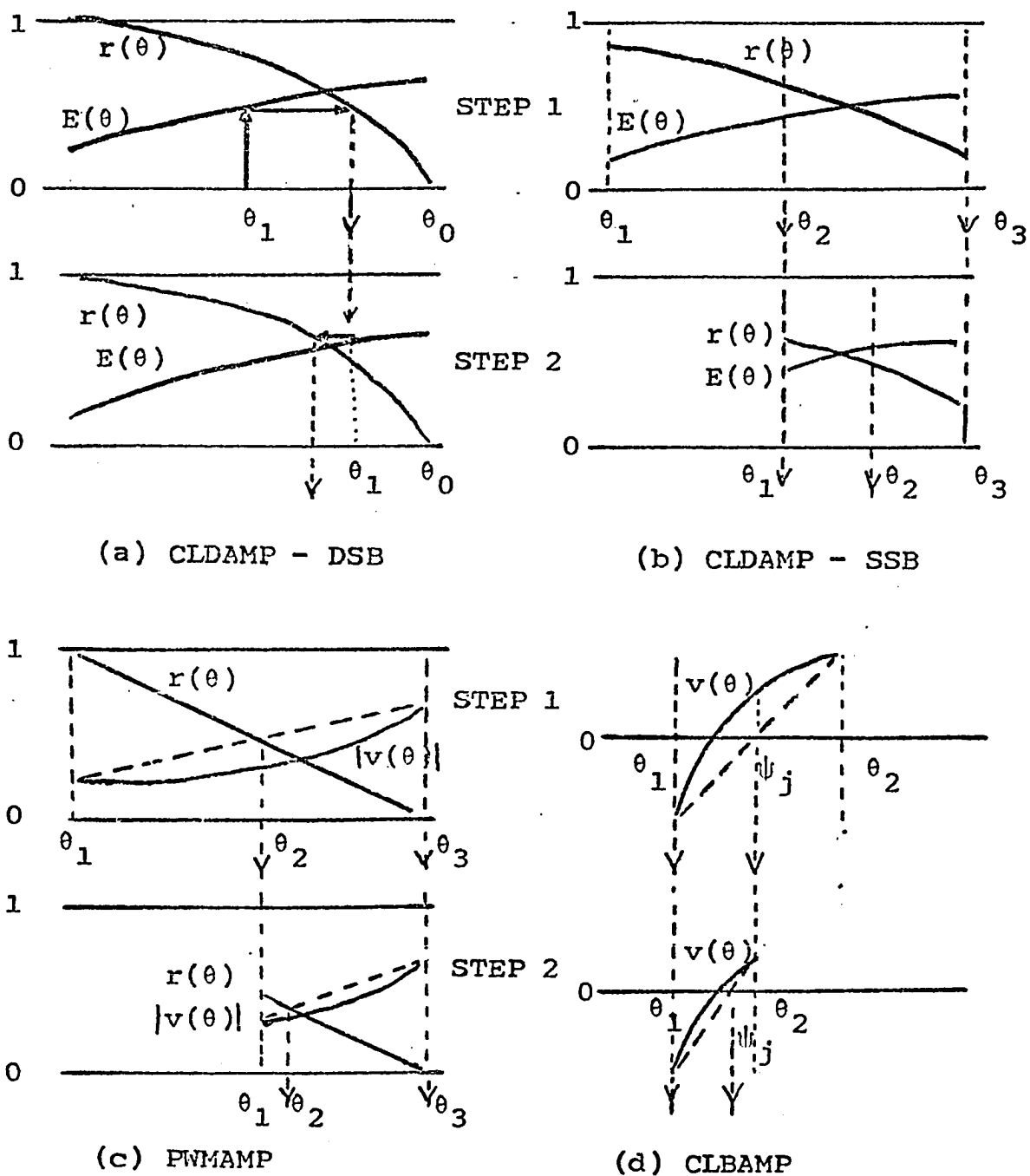


Figure 15.3. Methods of Iteration.

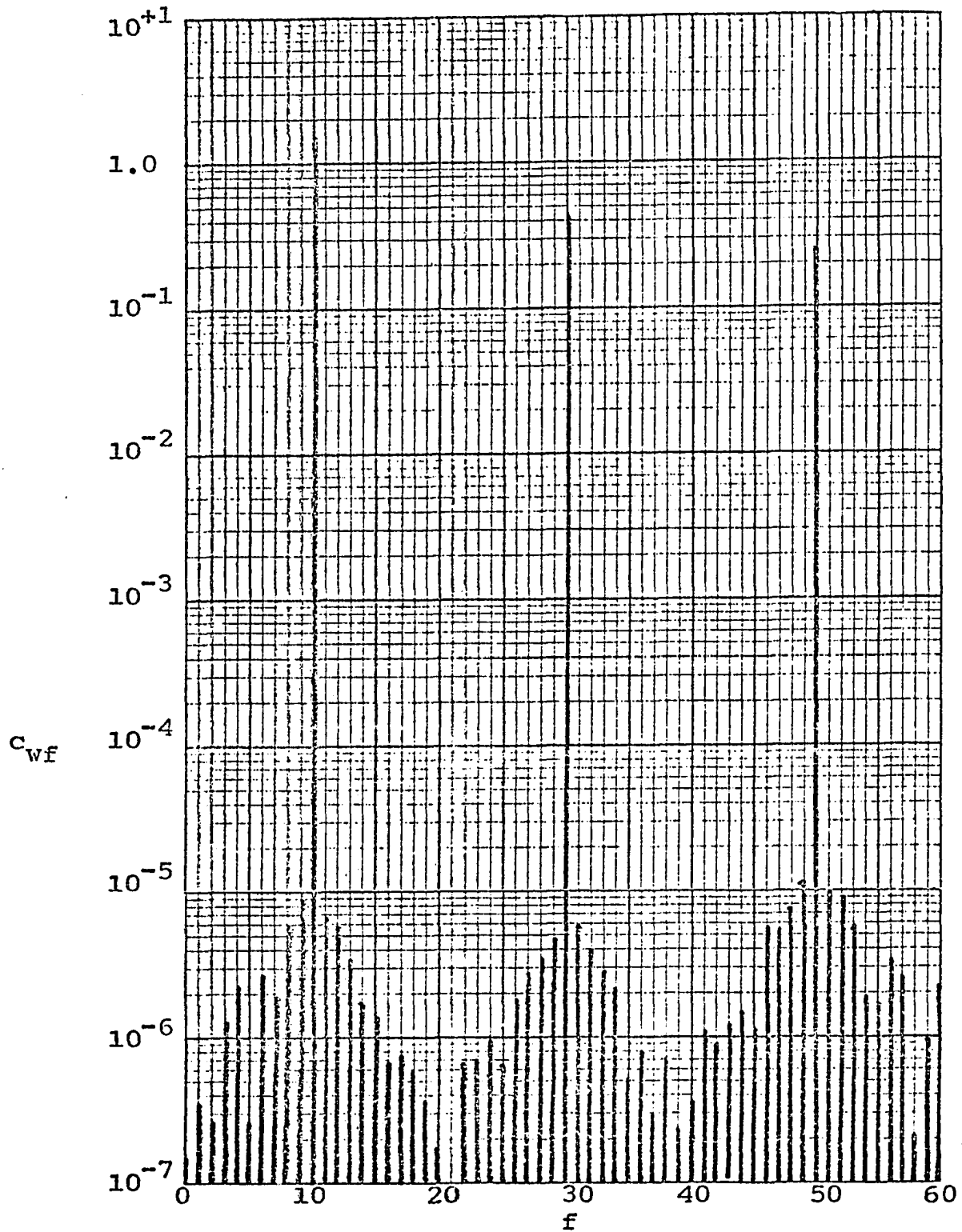


Figure 15.4. Computer Errors in Square-Wave Spectrum.

inated by reducing the step size when both  $r$  and  $E$  are small. The second problem is similar, and occurs when  $r$  and  $E$  are large and nearly tangential. This could be eliminated in the same way, but doing so increases the computation time from 2 seconds to 20. Pulse errors on the order of  $10^{-3}$  can occur, which cause spectral errors on the order of  $5 \cdot 10^{-4}$ .

PWMAMP searches for one transition in every interval of  $2\pi/2f_s$ , and uses linear interpolation (Figure 15.3(c)). Approximately 10 iterations are required. Note that no information is required (other than  $q$ ) to change from class AD to class BD.

CLBAMP uses small steps, as does the SSB version of CLDAMP, and can suffer from the problem of stepping over a small pulse, although this was not encountered in any of the simulations performed using it. Linear interpolation is used (Figure 15.3(d)), and 5 steps is sufficient.

A listing of the one main program and subroutines follows:

```
C      AMPLIFIER SIMULATION PROGRAMS *****

$JOB

C      FOURIER SERIES FOR WIDTH-MODULATED CLASS D RF AMPLIFIER
      INTEGER*4  ALC,SB,TYPE,FC,WP2D(400)
      DIMENSION AXU(10),BXU(10),AX(10),BX(10),CX(10),CSQX(10),
1     AXP(10),BXP(10),AXQ(10),BXQ(10),
2     PSI(200),MODE(200),WP1(200),WP2(200),AW(200),BW(200),
3     CW(200),CSQW(200),PSID(400),MODED(400),WP1D(400),
4     XLAB(5),YLAB(5),GLAB(5),DATLAB(5),X(200),Y(200)
```

```

COMMON/NRM/ AXUO, AXU, BXU
COMMON/WAV1/ Q, AXO, AXP, BXP, AXQ, BXQ
COMMON/WAV2/ FC, NMAX
COMMON/AMP1/ PSI, MODE, WP1, WP2
COMMON/AMP2/ FS, TYPE
COMMON/FTR1/ MMIN, MMAX, AWO, AW, BW, CW, CSQW
COMMON/DST1/ TAU1,TAU2,TAU3,TAU4,TAU5,TAU6,TAU7,TAU8,
1 ZETA,GAMMA5,GAMMA6,GAMMA7,GAMMA8
COMMON/DST2/ PSID, MODED, WP1D, WP2D
Q=0.0
READ(5,1) NMAX, SB, AXUO
DO 10 N=1, NMAX
2 FORMAT(2G10.4)
10 READ(5,2) AXU(N),BXU(N)
READ(5,3) FC, TYPE
READ(5,5) ALC, EMAX
READ(5,6) MMIN, MMAX
READ(5,8) ITMAX
READ(5,8) MODERF
READ(5,9) TAU1,TAU2,TAU3,TAU4
READ(5,9) TAU5,TAU6,TAU7,TAU8
READ(5,11) ZETA, GAMMA5,GAMMA6,GAMMA7,GAMMA8
READ(5,90) XLAB,YLAB,GLAB,DATLAB
1 FORMAT(2I10, G10.4)
3 FORMAT(2I10)
5 FORMAT(I10,G10.4)
6 FORMAT(2I10)
8 FORMAT(I10)
9 FORMAT(4G10.4)
11 FORMAT(5G10.4)
90 FORMAT(20A4)
WRITE(6,20)
20 FORMAT('1',15X,'WIDTH MODULATED CLASS D RF AMPLIFIER',
1 //)
IMAX=4*NMAX*FC
CALL WAVNRM(ALC,SB,NMAX,IMAX,EMAX)
CALL CLDAMP(ITMAX, KMAX)
CALL PLSDST(MODERF, KMAX, KMAXD)
WRITE(6,31)
31 FORMAT(' J',7X,'PSI',7X,'MODE',8X,'WP1',15X,'J',5X,
1 'PSID',7X,'MODED',5X,'WP1D',9X,'WP2D',/)
DO 33 J=1, KMAX
32 FORMAT(' ',I4,2X,G10.4,2X,I5,3X,G10.4,12X,I4,2X,G10.4,
1 2X,I5,3X,G10.4,5X,I5)
33 WRITE(6,32) J,PSI(J),MODE(J),WP1(J),J,PSID(J),MODED(J),
1 WP1D(J), WP2D(J)
KMAXP=KMAX+1
DO 43 J=KMAXP, KMAXD
42 FORMAT(49X,I4,2X,G10.4,2X,I5,3X,G10.4,5X,I5)
43 WRITE(6,42) J,PSID(J),MODED(J),WP1D(J),WP2D(J)
CALL FTRANS(KMAXD)

```

```

JJ=MMIN-1
LMAX=MINO(200,MMAX-JJ)
NPTS=LMAX+1
XMIN=1.0*MMIN-1.0
XSIZE=0.1*NPTS
DO 100 L=1, LMAX
M=L+JJ
X(L)=M*1.0
Y(L)=-6.0
IF(CW(L).GT.0.1E-05) Y(L)=ALOG10(CW(L))
100 CONTINUE
CALL GRAPH(NPTS,X,Y,13,7,XSIZE,-7.0,10.0,XMIN,7.0,-5.0,
1 XLAB,YLAB,GLAB,DATLAB)
STOP; END

```

```

SUBROUTINE WAVNRM(ALC,SB,NMAX,IMAX,EMAX)
INTEGER*4 ALC, SB
DIMENSION AXU(10),BXU(10),AXPU(10),BXP(10),AXQU(10),
1 BXQU(10),AX(10),BX(10),CX(10),CSQX(10),AXP(10),
2 BXP(10),AXQ(10),BXQ(10)
COMMON/NRM/ AXUO, AXU, BXU
COMMON/WAV1/ Q, AXQ, AXP, BXP, AXQ, BXQ
IF(SB.NE.0) GO TO 9
DO 1 N=1, NMAX
AXPU(N)=0.0
BXP(N)=0.0
AXQU(N)=AXU(N)
BXQU(N)=BXU(N)
1 CONTINUE
9 CONTINUE
IF((SB.EQ.3).OR.(SB.EQ.4)) GO TO 20
L=1
IF(SB.EQ.1) L=-1
AXUO=0.5*AXUO
DO 10 N=1, NMAX
AXPU(N)=0.5*BXP(N)
BXP(N)=-0.5*AXU(N)
AXQU(N)=0.5*L*AXU(N)
BXQU(N)=0.5*L*BXP(N)
10 CONTINUE
GO TO 40
20 CONTINUE
DO 30 N=1, NMAX
AXPU(N)=AXU(N)
BXP(N)=BXU(N)
AXQU(N)=0.0
BXQU(N)=0.0
30 CONTINUE
40 CONTINUE
RATIO=1.0

```

```

IF(ALC.EQ.0) GO TO 70
EUMAX=0.0
XPU0=AXU0
XQU0=0.0
IF(SB.NE.4) GO TO 41
XPU0=0.0
XQU0=0.0
41 CONTINUE
DO 60 I=1, IMAX
XPU=XPU0
XQU=XQU0
THETA=6.2831852*I/IMAX
DO 50 N=1, NMAX
ARG=N*THETA
COSARG=COS(ARG)
SINARG=SIN(ARG)
XPU=XPU+AXPU(N)*COSARG+BXPU(N)*SINARG
XQU=XQU+AXQU(N)*COSARG+BXQU(N)*SINARG
50 CONTINUE
EU=SQRT(XPU**2+XQU**2)
IF(EU.GT.EUMAX) EUMAX=EU
60 CONTINUE
RATIO=EUMAX/EUMAX
70 CONTINUE
IF(SB.EQ.4) GO TO 71
AX0=AXU0*RATIO
GO TO 72
71 CONTINUE
AX0=AXU0
72 CONTINUE
CSQX0=AX0**2
CX0=SQRT(CSQX0)
PX=CSQX0
DO 80 N=1, NMAX
AX(N)=AXU(N)*RATIO
BX(N)=BXU(N)*RATIO
CSQX(N)=AX(N)**2+BX(N)**2
CX(N)=SQRT(CSQX(N))
PX=PX+0.5*CSQX(N)
AXP(N)=AXPU(N)*RATIO
BXP(N)=BXPU(N)*RATIO
AXQ(N)=AXQU(N)*RATIO
BXQ(N)=BXQU(N)*RATIO
80 CONTINUE
IF(ALC.EQ.0) WRITE(6,90)
90 FORMAT(/,' WAVEFORM NOT NORMALIZED.',/)
IF(ALC.EQ.1) WRITE(6,91)IMAX, EMAX
91 FORMAT(/,' WAVEFORM NORMALIZED WITH ',I4,' POINTS TO ',
1 'PEAK AT', G10.4,'.',/)
WRITE(6,92) RATIO, PX
92 FORMAT(' NORMALIZATION RATIO = ',G10.4,5X,'PX = ',

```



```

1  G10.4,/)
  IF(SB.EQ.0) WRITE(6,100)
100 FORMAT(' BASEBAND',/)
  IF(SB.EQ.1) WRITE(6,101)
101 FORMAT(' LOWER SIDEBAND',/)
  IF(SB.EQ.2) WRITE(6,102)
102 FORMAT(' UPPER SIDEBAND',/)
  IF(SB.EQ.3) WRITE(6,103)
103 FORMAT(' DOUBLE SIDEBAND',/)
  IF(SB.EQ.4) WRITE(6,104)
104 FORMAT(' AMPLITUDE MODULATION',/)
  WRITE(6,110)
110 FORMAT(35X,'FOURIER COEFFICIENTS OF XU AND X',/)
  WRITE(6,120)
120 FORMAT('  N',8X,'AXU(N)',11X,'BXU(N)',11X,'AX(N)',12X,
1  'BX(N)',12X,'CX(N)',11X,'CSQX(N)',/)
  WRITE(6,130) AXU0, AX0, CX0, CSQX0
130 FORMAT('  0',G17.8,17X,G17.8,17X,2G17.8)
  DO 150 N=1, NMAX
140 FORMAT(' ',I4,6G17.8)
150 WRITE(6,140) N,AXU(N),BXU(N),AX(N),BX(N),CX(N),CSQX(N)
  RETURN; END

```

```

SUBROUTINE WAVGEN(THETA,V,E,PHI)
  INTEGER*4 FC
  DIMENSION AXP(10),BXP(10),AXQ(10),BXQ(10)
  COMMON/WAV1/ Q, AX0, AXP, BXP, AXQ, BXQ
  COMMON/WAV2/ FC, NMAX
  THETAC=FC*THETA
  XP=AX0
  XQ=0.0
  DO 10 N=1, NMAX
  ARG=N*THETA
  COSARG=COS(ARG)
  SINARG=SIN(ARG)
  XP=XP+AXP(N)*COSARG+BXP(N)*SINARG
  XQ=XQ+AXQ(N)*COSARG+BXQ(N)*SINARG
10 CONTINUE
  V=XP*SIN(THETAC)+XQ*COS(THETAC)+Q
  E=SQRT(XP**2+XQ**2)
  IF((XP.EQ.0.0).AND.(XQ.EQ.0.0)) GO TO 20
  PHI=ATAN2(XQ,XP)
  GO TO 30
20 CONTINUE
  PHI=0.0
30 CONTINUE
  RETURN; END

```

```

SUBROUTINE CLDAMP(ITMAX, KMAX)
DSB/AM VERSION
C
INTEGER*4 FC, TYPE, WP2(200)
DIMENSION PSI(200), MODE(200), WP1(200)
COMMON/AMP1/ PSI, MODE, WP1, WP2
COMMON/AMP2/ FS, TYPE
COMMON/WAV2/ FC, NMAX
D1=0.7853981/FC
D2=1.5707963/FC
JMAX=4*FC-1
DO 40 J=1, JMAX, 2
  THETA0=J*D2
  THETA1=THETA0-D1
  THETA2=THETA0+D1
  DO 20 L=1, ITMAX
    CALL WAVGEN(THETA1,V1,E1,PHI1)
    CALL WAVGEN(THETA2,V2,E2,PHI2)
    Y1=ARSIN(E1)/FC
    Y2=ARSIN(E2)/FC
    THETA1=THETA0-Y1
    THETA2=THETA0+Y2
20  CONTINUE
    CALL WAVGEN(THETA0,V0,E0,PHI0)
    PSI(J)=THETA1
    JP=J+1
    PSI(JP)=THETA2
    WP1(J)= SGN(V0)
    IF((TYPE.EQ.1).AND.(WP1(J).EQ.-1.0)) WP1(J)=0.0
    WP1(JP)=0.0
    MODE(J)=2
    MODE(JP)=2
40  CONTINUE
    KMAX=JMAX+2
    PSI(KMAX)=PSI(1) + 6.2831852
    WRITE(6,59) FC
59  FORMAT(/, ' FC = ', I4, /)
    IF(TYPE.EQ.1) WRITE(6,61)
    IF(TYPE.EQ.2) WRITE(6,62)
61  FORMAT(' MONOPOLAR PULSE TRAIN', /)
62  FORMAT(' BIPOLAR PULSE TRAIN', /)
    WRITE(6,70) ITMAX
70  FORMAT(' NATURAL SAMPLING USING ', I2, ' STEP ITERATION', /)
    RETURN; END

```

```

SUBROUTINE PLSDST(MODERF, JMAX, KMAX)
INTEGER*4 WP2D(400)
DIMENSION PSI(200), MODE(200), WP1(200),
1  PSID(400), MODED(400), WP1D(400), WP2(200)
COMMON/DST1/ TAU1,TAU2,TAU3,TAU4,TAU5,TAU6,TAU7,TAU8,
1  ZETA,GAMMA5,GAMMA6,GAMMA7,GAMMA8

```

```

COMMON/DST2/ PSID,MODED,WP1D,WP2D
COMMON/AMP1/ PSI,MODE,WP1,WP2
K=1
JMAXM=JMAX-1
DO 50 J=1, JMAXM
JM=J-1
IF(JM.EQ.0) JM = JMAXM
JP=J+1
KM=K-1
KP=K+1
IF(WP1(JM).EQ.WP1(J)) GO TO 49
IF((WP1(JM).EQ. 0.0).AND.(WP1(J).EQ. 1.0)) GO TO 10
IF((WP1(JM).EQ. 1.0).AND.(WP1(J).EQ. 0.0)) GO TO 20
IF((WP1(JM).EQ. 0.0).AND.(WP1(J).EQ.-1.0)) GO TO 30
IF((WP1(JM).EQ.-1.0).AND.(WP1(J).EQ. 0.0)) GO TO 40
PSID(K)=PSI(J)
MODED(K)=MODE(J)
WP1D(K)=WP1(J)
WP2D(K)=0
GO TO 49
10 CONTINUE
PSID(K)=PSI(J)-TAU1
MODED(K)=MODERF
WP2D(K)=1
PSID(KP)=AMIN1(PSI(JP),PSID(K)+TAU5)
MODED(KP)=2
WP1D(KP)=1.0
K=K+2
GO TO 49
20 CONTINUE
PSID(K)=AMIN1(PSI(J)+TAU2,PSI(JP))
MODED(K)=MODERF
WP2D(K)=2
PSID(KP)=PSID(K)+TAU6
MODED(KP)=0
WP1D(KP)=0.0
K=K+2
GO TO 49
30 CONTINUE
PSID(K)=PSI(J)-TAU3
MODED(K)=MODERF
WP2D(K)=3
PSID(KP)=AMIN1(PSI(JP),PSID(K)+TAU7)
MODED(KP)=2
WP1D(KP)=-1.0
K=K+2
GO TO 49
40 CONTINUE
PSID(K)=AMIN1(PSI(J)+TAU4, PSI(JP))
MODED(K)=MODERF
WP2D(K)=4

```

```

PSID(KP)=PSID(K)+TAU8
MODED(KP)=0
WP1D(KP)=0.0
K=K+2
49 CONTINUE
50 CONTINUE
KMAX=K
PSID(KMAX)=PSID(1)+6.2831852
WRITE(6,60)TAU1,TAU2,TAU3,TAU4,TAU5,TAU6,TAU7,TAU8
60 FORMAT(/,' PULSE DISTORTION PARAMETERS:',/,6X,
1 'BIAS      : TAU1 = ',G11.4,' TAU2 = ',G11.4,
2 ' TAU3 = ',G11.4,' TAU4 = ',G11.4,/,6X,'RISE/FALL:',
3 ' TAU5 = ',G11.4,' TAU6 = ',G11.4,' TAU7 = ',
4 G11.4,' TAU8 = ',G11.4,/)
IF(MODERF.EQ.3) WRITE(6,63)
63 FORMAT(' LINEAR RISE/FALL SHAPE USED',/)
IF(MODERF.EQ.4) WRITE(6,64) ZETA,GAMMA5,GAMMA6,
1 GAMMA7, GAMMA8
64 FORMAT(' EXPONENTIAL RISE/FALL CHARACTERISTIC USED:',
1 ' ZETA = ',G12.4,/,6X,'GAMMA5 = ',G12.4,' GAMMA6 = ',
2 G12.4,' GAMMA7 = ',G12.4,' GAMMA8 = ',G12.4,/)
RETURN; END

```

```

SUBROUTINE FTRANS(KMAX)
INTEGER*4 WP2(400), FC
DIMENSION AW(200), BW(200), CW(200), CSQW(200),
1 AXP(10), BXP(10), AXQ(10), BXQ(10),
2 AVM(10), BVM(10), AVP(10), BVP(10),
3 PSI(400), MODE(400), WP1(400)
COMMON/WAV1/ Q, AXQ, AXP, BXP, AXQ, BXQ
COMMON/DST2/ PSI, MODE, WP1, WP2
COMMON/FTR1/ MMIN, MMAX, AWQ, AW, BW, CW, CSQW
COMMON/WAV2/ FC, NMAX
COMMON/DST1/ TAU1,TAU2,TAU3,TAU4,TAU5,TAU6,TAU7,TAU8,
1 ZETA,GAMMA5,GAMMA6,GAMMA7,GAMMA8
J=MMIN-1
LMAX=MINO(200,MMAX-J)
AWQ=0.0
DO 1 L=1, LMAX
AW(L)=0.0
BW(L)=0.0
1 CONTINUE
AVQ=0.0
BVQ=AXQ
DO 2 N=1, NMAX
AVM(N)=0.5*(BXP(N)+AXQ(N))
BVM(N)=0.5*(AXP(N)-BXQ(N))
AVP(N)=0.5*(-BXP(N)+AXQ(N))
BVP(N)=0.5*(AXP(N)-BXQ(N))
2 CONTINUE

```

```

KMAXM=KMAX-1
DO 90 K=1, KMAXM
  KP=K+1
  IF(MODE(K).EQ.0) GO TO 80
  IF(MODE(K).EQ.1) GO TO 10
  IF(MODE(K).EQ.2) GO TO 20
  IF(MODE(K).EQ.3) GO TO 30
  IF(MODE(K).EQ.4) GO TO 40
  WRITE(6,5) K,MODE(K),PSI(K),PSI(KP)
5  FORMAT(' *** MODE(' ,I3,') = ' ,I2, ' USED FOR ' ,G10.4,
1  ' < PSI < ' ,G10.4, ' IS NOT DEFINED.***',/)
  GO TO 100
10 CONTINUE
  AWO=AWO+Q*(PSI(KP)-PSI(K))+AVO*CINT(FC,PSI(K),PSI(KP))
1  +BVO*SINT(FC ,PSI(K),PSI(KP))
  DO 11 N=1, NMAX
  AWO=AWO+{AVM(N)*CINT(FC -N,PSI(K),PSI(KP))
1      +BVM(N)*SINT(FC -N,PSI(K),PSI(KP))
2      +AVP(N)*CINT(FC +N,PSI(K),PSI(KP))
3      +BVP(N)*SINT(FC +N,PSI(K),PSI(KP))}*WP1(K)
11 CONTINUE
  DO 13 L=1, LMAX
  M=L+J
  AW(L)=AW(L)+Q*CINT(M,PSI(K),PSI(KP))+0.5*WP1(K)*
1  (AVO*(CINT(FC+M,PSI(K),PSI(KP))+CINT(FC-M,PSI(K),
2  PSI(KP)))+BVO*(SINT(FC+M,PSI(K),PSI(KP))
3  +SINT(FC-M,PSI(K),PSI(KP))))
  BW(L)=BW(L)+Q*SINT(M,PSI(K),PSI(KP))+0.5*WP1(K)*
1  (AVO*(SINT(FC+M,PSI(K),PSI(KP))+SINT(FC-M,PSI(K),
2  PSI(KP)))+BVO*(-CINT(FC+M,PSI(K),PSI(KP))+CINT(FC-M,
3  PSI(K),PSI(KP))))
  DO 12 N=1, NMAX
  CINTMM=CINT(FC -N-M,PSI(K),PSI(KP))
  CINTMP=CINT(FC -N+M,PSI(K),PSI(KP))
  CINTPM=CINT(FC +N-M,PSI(K),PSI(KP))
  CINTPP=CINT(FC +N+M,PSI(K),PSI(KP))
  SINTMM=SINT(FC -N-M,PSI(K),PSI(KP))
  SINTMP=SINT(FC -N+M,PSI(K),PSI(KP))
  SINTPM=SINT(FC +N-M,PSI(K),PSI(KP))
  SINTPP=SINT(FC +N+M,PSI(K),PSI(KP))
  AW(L)=AW(L)+0.5*(AVM(N)*(CINTMP+CINTMM)+
1      BVM(N)*(SINTMP+SINTMM)+
2      AVP(N)*(CINTPP+CINTPM)+
3      BVP(N)*(SINTPP+SINTPM))*WP1(K)
  BW(L)=BW(L)+0.5*(AVM(N)*(SINTMP-SINTMM)+
1      BVM(N)*(-CINTMP+CINTMM)+
2      AVP(N)*(SINTPP-SINTPM)+
3      BVP(N)*(-CINTPP+CINTPM))*WP1(K)
12 CONTINUE
13 CONTINUE
  GO TO 80

```

```

20 CONTINUE
   AWO=AWO+WP1(K)*(PSI(KP)-PSI(K))
   DO 21 L=1, LMAX
     M=L+J
     AW(L)=AW(L)+WP1(K)*CINT(M,PSI(K),PSI(KP))
     BW(L)=BW(L)+WP1(K)*SINT(M,PSI(K),PSI(KP))
21 CONTINUE
   GO TO 80
30 CONTINUE
   IF(WP2(K).EQ.1) GO TO 31
   IF(WP2(K).EQ.2) GO TO 32
   IF(WP2(K).EQ.3) GO TO 33
   IF(WP2(K).EQ.4) GO TO 34
31 CONTINUE
   TAU=TAU5
   C=0.0
   GO TO 35
32 CONTINUE
   TAU=-TAU6
   C=1.0
   GO TO 35
33 CONTINUE
   TAU=-TAU7
   C=0.0
   GO TO 35
34 CONTINUE
   TAU=TAU8
   C=-1.0
35 CONTINUE
   IF((TAU.EQ.0.0).OR.(PSI(K).EQ.PSI(KP))) GO TO 39
   AWO=AWO + RCINT(0, PSI(K),PSI(KP))/TAU+(C-PSI(K)/TAU)
1   * CINT(0, PSI(K), PSI(KP))
   DO 36 L=1, LMAX
     M=L+J
     AW(L)=AW(L) + RCINT(M, PSI(K), PSI(KP))/TAU
1   +(C - PSI(K)/TAU)*CINT(M, PSI(K), PSI(KP))
     BW(L)=BW(L) + RSINT(M, PSI(K), PSI(KP))/TAU
1   +(C - PSI(K)/TAU)*SINT(M, PSI(K), PSI(KP))
36 CONTINUE
39 CONTINUE
   GO TO 80
40 CONTINUE
   IF(WP2(K).EQ.1) GO TO 41
   IF(WP2(K).EQ.2) GO TO 42
   IF(WP2(K).EQ.3) GO TO 43
   IF(WP2(K).EQ.4) GO TO 44
   GO TO 49
41 CONTINUE
   C1=+ZETA
   C2=-ZETA
   TAU=TAU5

```

```

      GAMMA=GAMMA5
      GO TO 45
42  CONTINUE
      C1=+1.0-ZETA
      C2=+ZETA
      TAU=TAU6
      GAMMA=GAMMA6
      GO TO 45
43  CONTINUE
      C1=-ZETA
      C2=+ZETA
      TAU=TAU7
      GAMMA=GAMMA7
      GO TO 45
44  CONTINUE
      C1=-1.0+ZETA
      C2=-ZETA
      TAU=TAU8
      GAMMA=GAMMA8
45  CONTINUE
      DELTA=PSI(KP)-PSI(K)
      EXPPSI=EXP(GAMMA*PSI(K))
      IF((TAU.EQ.0.0).OR.(DELTA.EQ.0.0)) GO TO 49
      AWO=AWO +C1*CINT(0, PSI(K), PSI(KP))
      1  +C2*ECINT(0,-GAMMA,PSI(K),PSI(KP))*EXPPSI
      DO 46 L=1, LMAX
      M=L+J
      AW(L)=AW(L)+C1*CINT(M,PSI(K),PSI(KP))
      1  +C2*ECINT(M,-GAMMA,PSI(K),PSI(KP))*EXPPSI
      BW(L)=BW(L)+C1*SINT(M,PSI(K),PSI(KP))
      1  +C2*ESINT(M,-GAMMA,PSI(K),PSI(KP))*EXPPSI
46  CONTINUE
49  CONTINUE
80  CONTINUE
90  CONTINUE
      AWO=AWO/6.2831852
      CWO=ABS(AWO)
      CSQWO=AWO**2
      DO 92 L=1, LMAX
      AW(L)=AW(L)/3.1415926
      BW(L)=BW(L)/3.1415926
      CSQW(L)=AW(L)**2+BW(L)**2
      CW(L)=SQRT(CSQW(L))
92  CONTINUE
      WRITE(6,93)
93  FORMAT(//,25X,'FOURIER COEFFICIENTS OF W',/)
      WRITE(6,94)
94  FORMAT('  M',10X,'AW(M)',12X,'BW(M)',12X,'CW(M)',
      1  12X,'CSQW(M)',/)
      WRITE(6,95) AWO,CWO,CSQWO
95  FORMAT('      0',G17.8,17X,2G17.8)

```

```

      DO 97 L=1, LMAX
      M=L+J
96  FORMAT(' ',I4,4G17.8)
97  WRITE(6,96)M,AW(L),BW(L),CW(L),CSQW(L)
100 CONTINUE
      RETURN; END

```

```

      FUNCTION SGN(V)
      SGN=0.00000000
      IF(V.GT.0.00000000) SGN=+1.0
      IF(V.LT.0.00000000) SGN=-1.0
      RETURN; END

```

```

      FUNCTION CINT(M,PSI1,PSI2)
      CINT=0.0
      IF(PSI1.EQ.PSI2) GO TO 10
      IF(M.EQ.0) CINT=PSI2-PSI1
      IF(M.NE.0) CINT=(SIN(M*PSI2)-SIN(M*PSI1))/M
10  CONTINUE
      RETURN; END

```

```

      FUNCTION SINT(M, PSI1, PSI2)
      SINT=0.0
      IF(PSI1.EQ.PSI2) GO TO 10
      IF(M.NE.0) SINT=(-COS(M*PSI2)+COS(M*PSI1))/M
10  CONTINUE
      RETURN; END

```

```

      FUNCTION RCINT(M, PSI1, PSI2)
      IF(M.NE.0) GO TO 10
      RCINT=(PSI2**2-PSI1**2)/2
      GO TO 20
10  CONTINUE
      ARG1=M*PSI1
      ARG2=M*PSI2
      RCINT=(COS(ARG2)-COS(ARG1)+ARG2*SIN(ARG2)
1  -ARG1*SIN(ARG1))/M**2
20  CONTINUE
      RETURN; END

```

```

      FUNCTION RSINT(M, PSI1, PSI2)
      RSINT=0.0
      IF(M.EQ.0) GO TO 10
      ARG1=M*PSI1
      ARG2=M*PSI2
      RSINT=(SIN(ARG2)-SIN(ARG1)-ARG2*COS(ARG2)

```



```

1   +ARG1*COS(ARG1))/M**2
10  CONTINUE
    RETURN; END

```

```

FUNCTION ECINT(M,P,PSI1,PSI2)
D=M**2+P**2
IF(D.NE.0.0) GO TO 10
ECINT=PSI2-PSI1
GO TO 20
10  CONTINUE
    ARG1=M*PSI1
    ARG2=M*PSI2
    ECINT=(EXP(P*PSI2)*(P*COS(ARG2)+M*SIN(ARG2))
1   -EXP(P*PSI1)*(P*COS(ARG1)+M*SIN(ARG1)))/D
20  CONTINUE
    RETURN; END

```

```

FUNCTION ESINT(M,P,PSI1,PSI2)
D=M**2+P**2
IF(D.NE.0.0) GO TO 10
ESINT=0.0
GO TO 20
10  CONTINUE
    ARG1=M*PSI1
    ARG2=M*PSI2
    ESINT=(EXP(P*PSI2)*(P*SIN(ARG2)-M*COS(ARG2))
1   -EXP(P*PSI1)*(P*SIN(ARG1)-M*COS(ARG1)))/D
20  CONTINUE
    RETURN; END

```

\$ENTRY

C OTHER SUBROUTINES

```

SUBROUTINE PLS DST(MODERF,KMAX,KMAXD)
C  NULL VERSION
    INTEGER*4 WP2D(400)
    DIMENSION PSI(200), MODE(200), WP1(200), WP2(200),
1   PSID(400), MODED(400), WP1D(400)
    COMMON/AMP1/ PSI, MODE, WP1, WP2
    COMMON/DST2/ PSID, MODED, WP1D, WP2D
    KMAXD=KMAX
    KMAXM=KMAX-1
    DO 10 K=1, KMAX
    PSID(K)=PSI(K)
10  CONTINUE

```

```

DO 20 K=1, KMAXM
MODED(K)=MODE(K)
WP1D(K)=WP1(K)
IF(WP1(K).EQ.0.0) MODED(K)=0
20 CONTINUE
RETURN; END

```

```

SUBROUTINE CLDAMP(ITMAX, KMAX)
C   SSB VERSION
C   ERRORS IN PULSE WIDTH MAY OCCUR WHEN E IS NEAR 1.0.
INTEGER*4 FC, TYPE, WP2(200)
DIMENSION PSI(200), MODE(200), WP1(200)
COMMON/AMP1/ PSI, MODE, WP1, WP2
COMMON/AMP2/ FS, TYPE
COMMON/WAV2/ FC, NMAX
THETA1=0.0
CALL WAVGEN(THETA1, V1, E1, PHI1)
R1=ABS(COS(FC*THETA1+PHI1))
W1=0.0
IF(E1.GE.R1) W1=SGN(V1)
J=1
RMIN=6.2831852/50
DELTA=RMIN/FC
5 CONTINUE
D=DELTA
IF(R1.LT.RMIN) D=AMAX1(0.8*R1/FC, 0.628E-05)
THETA4=THETA1+D
IF(J.EQ.1) GO TO 8
IF(J.GT.2) GO TO 6
THETAM=PSI(1)+6.283185
6 CONTINUE
IF(THETA4.LT.THETAM) GO TO 7
THETA4=THETAM
GO TO 40
7 CONTINUE
8 CONTINUE
CALL WAVGEN(THETA4, V4, E4, PHI4)
R4=ABS(COS(FC*THETA4+PHI4))
W4=0.0
IF(E4.GE.R4) W4=SGN(V4)
IF(W4.EQ.W1) GO TO 30
THETA3=THETA4
W3=W4
E3=E4
V3=V4
PHI3=PHI4
R3=R4
DO 20 L=1, ITMAX
DIFF=THETA3-THETA1
IF(DIFF.LT.0.1E-05) GO TO 21

```

```

      THETA2=0.5*(THETA1+THETA3)
      CALL WAVGEN(THETA2,V2,E2,PHI2)
      R2=ABS(COS(FC*THETA2+PHI2))
      W2=0.0
      IF(E2.GE.R2) W2=SGN(V2)
      IF(W1.EQ.W2) GO TO 10
      THETA3=THETA2
      W3=W2
      R3=R2
      E3=E2
      V3=V2
      GO TO 11
10  CONTINUE
      THETA1=THETA2
      R1=R2
      W1=W2
      E1=E2
      V1=V2
11  CONTINUE
20  CONTINUE
21  CONTINUE
      PSI(J)=THETA2
      MODE(J)=2
      WP1(J)=W4
      IF((TYPE.EQ.1).AND.(WP1(J).EQ.-1.0)) WP1(J)=0.0
      J=J+1
      THETA4=THETA4+0.628319E-05
      CALL WAVGEN(THETA4,V4,E4,PHI4)
      R4=ABS(COS(FC*THETA4+PHI4))
      W4=0.0
      IF(E4.GE.R4) W4=SGN(V4)
      JM=J-1
      IF((WP1(JM).NE.0.0).AND.(W4.EQ.0.0)) GO TO 25
      GO TO 29
25  CONTINUE
      PSI(J)=THETA4
      MODE(J)=2
      WP1(J)=W4
      IF((TYPE.EQ.1).AND.(WP1(J).EQ.-1.0)) WP1(J)=0.0
      J=J+1
29  CONTINUE
30  CONTINUE
      THETA1=THETA4
      E1=E4
      W1=W4
      R1=R4
      GO TO 5
40  CONTINUE
      KMAX=J
      PSI(KMAX)=THETAM
      WRITE(6,59) FC

```

```

59 FORMAT(/, ' FC = ', I4, /)
   IF(TYPE.EQ.1) WRITE(6,61)
   IF(TYPE.EQ.2) WRITE(6,62)
61 FORMAT(' MONOPOLAR PULSE TRAIN', /)
62 FORMAT(' BIPOLAR PULSE TRAIN', /)
   WRITE(6,70) ITMAX
70 FORMAT(' NATURAL SAMPLING USING ', I2,
1 ' STEP ITERATION', /)
   RETURN; END

```

```

SUBROUTINE PWM&MP(ITMAX, KMAX, PHIO, Q)
INTEGER*4 SAMPLE, FC, FS, TYPE
DIMENSION PSI(200), MODE(200), WP1(200), WP2(200)
COMMON/WAV2/ FC, NMAX
COMMON/AMP1/ PSI, MODE, WP1, WP2
COMMON/AMP2/ FS, TYPE
TYPE=1
KMAX=2*FS+1
KMAXM=KMAX-1
D=1.5707963/FS
THETA1=PHIO/FS
R1=1.0
CALL WAVGEN(THETA1, V1, E1, PHI1)
V1=ABS(V1)
DO 30 K=1, KMAXM
THETA4=THETA1+2*D
CALL WAVGEN(THETA4, V4, E4, PHI4)
S4=SGN(V4)
V4=ABS(V4)
R4=0.0
IF(R1.EQ.0.0) R4=1.0
THETA3=THETA4
V3=V4
R3=R4
DO 10 L=1, ITMAX
DNM=R3-R1+V1-V3
IF(ABS(DNM).GT.(0.1E-09)) GO TO 1
THETA2=THETA3
R2=R3
GO TO 11
1 CONTINUE
THETA2=THETA1+(V1-R1)*(THETA3-THETA1)/DNM
CALL WAVGEN(THETA2, V2, E2, PHI2)
V2=ABS(V2)
R2=R3
IF(ABS(THETA3-THETA1).LT.0.1E-09) GO TO 11
R2=R1+(R3-R1)*(THETA2-THETA1)/(THETA3-THETA1)
IF(V2.GT.R2) GO TO 2
THETA3=THETA2
R3=R2

```

```

V3=V2
GO TO 3
2 CONTINUE
  THETA1=THETA2
  R1=R2
  V1=V2
3 CONTINUE
10 CONTINUE
11 CONTINUE
  PSI(K)=THETA2
  MODE(K)=2
  WP1(K)=1.0
  IF(K/2*2.EQ.K) WP1(K)=0.0
  IF(WP1(K).EQ.1.0) WP1(K)=S4
  IF(WP1(K).EQ.-1.0) TYPE=2
  PSI(KMAX)=6.2831852
  THETA1=THETA4
  R1=R4
  V1=V4
30 CONTINUE
  IF(TYPE.EQ.1) WRITE(6,31)
  IF(TYPE.EQ.2) WRITE(6,32)
31 FORMAT(/,' CLASS AD AMPLIFIER')
32 FORMAT(/,' CLASS BD AMPLIFIER')
  WRITE(6,40) FC, FS, Q, PHIO
40 FORMAT(/,' FC = ',I3,5X,' FS = ',I3,5X,' Q = ',G12.4,4X,
1 ' PHIO = ',G12.4,/)
  WRITE(6,53) ITMAX
53 FORMAT(' NATURAL SAMPLING BY ',I2,' STEP ITERATION',/)
  RETURN; END

```

```

SUBROUTINE CLBAMP(ITMAX, JMAX)
  INTEGER*4 FC
  DIMENSION PSI(200), MODE(200), WP1(200), WP2(200),
1  AXP(10), BXP(10), AXQ(10), BXQ(10)
  COMMON/WAV1/ Q, AX0, AXP, BXP, AXQ, BXQ
  COMMON/WAV2/ FC, NMAX
  COMMON/AMP1/ PSI, MODE, WP1, WP2
  IMAX=FC*NMAX*10
  THETA1=0.0
  J=1
  CALL WAVGEN(THETA1, V1, E, PHI)
  DO 50 I=1, IMAX
  THETA4=6.2831852*I/IMAX
  CALL WAVGEN(THETA4, V4, E, PHI)
  IF(((V1.GT.1.0).AND.(V4.GT.1.0)).OR.((V1.LT.0.0).AND.
1 (V4.LT.0.0)).OR.((V1.LT.1.0).AND.(V1.GT.0.0)).
2 AND.(V4.LT.1.0).AND.(V4.GT.0.0))) GO TO 40
  THETA2=THETA4
  V2=V4

```

```

P=1.0
IF((V1.LE.0.0).AND.(V2.GE.0.0)) P=0.0
IF((V2.LE.0.0).AND.(V1.GE.0.0)) P=0.0
PSI(J)=(P-V1)*(THETA2-THETA1)/(V2-V1)+THETA1
DO 30 IT=1, ITMAX
CALL WAVGEN(PSI(J),V3,E,PHI)
IF(V3.GT.P) GO TO 10
V1=V3
THETA1=PSI(J)
GO TO 20
10 CONTINUE
V2=V3
THETA2=PSI(J)
20 CONTINUE
IF(ABS(V2-V1).LT.(0.1E-09)) GO TO 31
IF(ABS(THETA2-THETA1).LT.(0.1E-09)) GO TO 31
PSI(J)=(P-V1)*(THETA2-THETA1)/(V2-V1)+THETA1
30 CONTINUE
31 CONTINUE
MODE(J)=1
WP1(J)=1.0
IF((V4.LT.1.0).AND.(V4.GT.0.0)) GO TO 39
MODE(J)=2
IF(V4.LE.0.0) WP1(J)=0.0
39 CONTINUE
J=J+1
40 CONTINUE
THETA1=THETA4
V1=V4
50 CONTINUE
JMAX=J
PSI(JMAX)=PSI(1)+6.2831853
WRITE(6,60) FC, Q
60 FORMAT(/, ' FC = ',I3,5X, ' Q = ',G10.4,/)
RETURN; END

```

## XVI. APPENDIX IV: COMMONLY-USED SYMBOLS

The following symbols are used consistently throughout this dissertation. Listing is alphabetically by Roman and then Greek letters.

$a_{xn}$	$n^{\text{th}}$ cosine Fourier coefficient of wave $x$
A	Ampere
b	magnitude of $\sin \theta$
$b_{xn}$	$n^{\text{th}}$ sine Fourier coefficient of wave $x$
$c_{xn}$	$n^{\text{th}}$ magnitude Fourier coefficient of wave $x$
$c(\theta)$	cosinusoidal switching function
$c_i$	constant used in feedback analysis
$\bar{C}$	matrix of $c_i$
$dc_i$	increment of $c_i$
$d\bar{C}$	vector of $dc_i$
e	$\approx 2.718\dots$
$E(\theta)$	envelope function
f	frequency
$f_c$	carrier frequency
$f_s$	switching frequency
$f_x$	modulation frequency
$f_+(\theta)$	monopolar pulse train
$f_{\pm}(\theta)$	bipolar pulse train

F	Farad
$F(\omega)$	filter
$F_o(\omega)$	output filter
$F_d(\omega)$	detector filter
$g(\sigma)$	saturation function
G	gain
H	Henry
$i, j, k, m, n$	indices
i	current
k	kilo
m	milli
n	nano
o	output
$p(y; \sigma)$	distortion function
$P_o$	output power
$P_i$	input power
$P_{DR}$	power dissipated due to rise/fall times
$P_{DS}$	power due to saturation voltage
q	quiescent voltage or current
$r(\theta; \lambda, \tau)$	ramp waveform
$s(\theta)$	sinusoidal switching function
s	seconds
t	time
$u(\theta)$	distortion waveform



$v(\theta)$	output or modulated waveform
$v_o$	output voltage
$v_s$	saturation voltage
V	Volt
$w(\theta)$	pulse waveform
$w_D(\theta)$	distorted pulse waveform
$x(\theta)$	modulating waveform
$x_p(\theta)$	modulation of $\sin \omega_c t$
$x_q(\theta)$	modulation of $\cos \omega_c t$
$X(\omega)$	spectrum of $x(\theta)$
$y(\theta)$	pulse (half) width
y	integrated distortion function
$z_k(\theta)$	modulation of $k^{\text{th}}$ harmonic of $f_c$ or $f_s$
$\alpha$	ratio of carrier to modulation frequencies
$\beta$	ratio of switching to carrier frequencies
$\gamma$	exponential rise/fall time exponent constant
$\delta$	small change
$\xi$	exponential rise/fall time amplitude constant
$\eta$	efficiency
$\eta_i$	sum of several coefficients in frequency expansion
$\theta$	normalized time (in terms of $2\pi$ )
$\lambda$	ramp location parameter
$\mu$	micro
$\Xi$	coefficient matrix in feedback problem

$\pi$	$\approx 3.14159\dots$
$\Pi$	product
$\sigma$	sum of pulse error
$\Sigma$	sum
$\tau_i$	pulse bias error if $1 \leq i \leq 4$
$\tau_i$	pulse rise/fall error if $5 \leq i \leq 8$
$\varphi(\theta)$	phase shift function
$\varphi_s$	phase of conventional PWM pulse train
$\psi$	$\omega_c t + \varphi$
$\psi_j$	pulse transition time
$\omega$	angular frequency
$\Omega$	Ohm